EPA-650/3-75-007

August 1975

Ecological Research Series

STUDY OF AEROSOL FORMATION IN PHOTOCHEMICAL AIR POLLUTION

U.S. Environmental Protection Agency
Office of Research and Development
Washington, D. C. 20460

EPA-650/3-75-007

STUDY OF AEROSOL FORMATION IN PHOTOCHEMICAL AIR POLLUTION

by

W. C. Kocmond, D. B. Kittelson,
J. Y. Yang, and K. L. Demerjian

Calspan Corporation
4455 Genesee Street
Buffalo, New York 14221

Contract No. 68-01-1231
ROAP No. 21AKB-02
Program Element No. 1A1008

EPA Project Officer: Marijon Bufalini

Chemistry and Physics Laboratory
National Environmental Research Center
Research Triangle Park, North Carolina 27711

Prepared for

COORDINATING RESEARCH COUNCIL, INC.
30 Rockefeller Plaza
New York, New York 10020
CAPA-8-71

and

U.S. ENVIRONMENTAL PROTECTION AGENCY
Office of Research and Development
Washington, D.C. 20460

August 1975

EPA REVIEW NOTICE

This report has been reviewed by the National Environmental Research Center - Research Triangle Park, Office of Research and Development, EPA, and approved for publication. Approval does not ignify that the contents necessarily reflect the views and policies of the Environmental Protection Agency, nor does mention of trade names or commercial products constitute endorsement or recommendation for use.

RESEARCH REPORTING SERIES

Research reports of the Office of Research and Development, U.S. Environmental Protection Agency, have been grouped into series. These broad categories were established to facilitate further development and application of environmental technology. Elimination of traditional grouping was consciously planned to foster technology transfer and maximum interface in related fields. These series are:

1. ENVIRONMENTAL HEALTH EFFECTS RESEARCH
2. ENVIRONMENTAL PROTECTION TECHNOLOGY
3. ECOLOGICAL RESEARCH
4. ENVIRONMENTAL MONITORING
5. SOCIOECONOMIC ENVIRONMENTAL STUDIES
6. SCIENTIFIC AND TECHNICAL ASSESSMENT REPORTS
9. MISCELLANEOUS

This report has been assigned to the ECOLOGICAL RESEARCH series. This series describes research on the effects of pollution on humans, plant and animal species, and materials. Problems are assessed for their long- and short-term influences. Investigations include formation, transport, and pathway studies to determine the fate of pollutants and their effects. This work provides the technical basis for setting standards to minimize undesirable changes in living organisms in the aquatic, terrestrial, and atmospheric environments.

This document is available to the public for sale through the National Technical Information Service, Springfield, Virginia 22161.

Publication No. EPA-650/3-75-007

ABSTRACT

Photochemical aerosol production in several SO_2 + clean air (filtered air), HC + NO and HC + NO + SO_2 systems has been examined using the smog chamber approach. The reaction vessels used in this study were the 20,800 ft^3 Calspan chamber and the 600 ft^3 University of Minnesota chamber. Aerosol formation, growth, and decay mechanisms are described for each of the systems studied. It has been possible in this investigation to characterize system reactivity in terms of aerosol behavior. The most important variables are maximum number concentration, equilibrium surface concentration, and particle volumetric growth rate. Measurements of these variables are made for several systems and are discussed within the text.

Of the hydrocarbons studied, cyclohexene was the most reactive in terms of aerosol production and rate of NO oxidation followed by m-xylene, hexene, and toluene. For the simple HC + NO system, each experiment can be divided into two phases. During the initial phase, NO is converted to NO_2 and some oxidation of hydrocarbon occurs. No appreciable aerosol is formed during this phase, but ozone starts to appear near the end of this period. The second phase, accompanied by substantial aerosol formation, begins as soon as NO is oxidized out of the system and NO_2 reaches a maximum; ozone levels rise rapidly during this phase and approach a maximum. The addition of SO_2 to the HC + NO system leads to some aerosol formation during the first phase and was generally found to exert a synergistic effect on aerosol formation in the second phase. The addition of SO_2 also led to a marked decrease in the diameter of the particles ultimately formed. This results from the formation of very high concentrations of nuclei during the initial stages of the experiment.

For the SO_2 + clean air system, photooxidation rates of a few tenths of a percent per hour are typically observed for a light intensity of 50% noon day sun. In the presence of hydrocarbons and NO, accelerated rates are generally observed.

The data show that aerosol formation rates are enhanced at high relative humidities, probably as a result of the higher water content of the aerosols.

ACKNOWLEDGMENTS

The authors wish to express their thanks to three University of Minnesota graduate students: David Cress, Kui Chiu Kwok, and Ping Auw for performing the experiments in and reducing the data from the University of Minnesota Smog Chamber.

Special thanks are also due Mrs. Joyce Terrano for her skillful typing of this manuscript.

TABLE OF CONTENTS

TABLE OF CONTENTS (Cont'd)

LIST OF TABLES

LIST OF FIGURES

Section 1

INTRODUCTION AND SUMMARY

Calspan Corporation, in collaboration with the Particle Technology Laboratory of the University of Minnesota, has been engaged in a laboratory study of the formation mechanisms and growth processes of photochemical aerosols. The primary objective of the investigation is to improve our understanding of photochemical aerosol behavior in urban environments by conducting studies in carefully controlled environments, simulating those occurring in the real atmosphere.

During the first year program, emphasis was placed on preparing the Calspan 20,800 ft^3 reaction chamber for photochemical aerosol studies and in examining aerosol behavior in SO_2 and propylene-NO_x systems. At the University of Minnesota, studies in 600 ft^3 and 90 ft^3 chambers were conducted to help determine the effects of bag size on aerosol production and also to study the influence of varying relative humidities on aerosol behavior. Results of the first year program have been presented in an earlier report, Kocmond et al. (1973).

During this second year program, greater emphasis was placed on understanding aerosol behavior in representative HC+NO_x+SO_2 systems. Two collaborative workshops were held at Calspan. During the November 1973 workshop, aerosol behavior was studied in SO_2 + clean air, toluene + NO_2, and hexene + NO_2 + SO_2 systems. The data and experience gained from these tests were applied to designing experiments for a second and perhaps more productive workshop held during March 1974. These experiments involved HC-NO_x-SO_2 systems using toluene, hexene, m-xylene, and cyclohexene as representative hydrocarbons. For each of the test series performed in Calspan's 20,800 ft^3 chamber, a comparative set of experiments were conducted in the 600 ft^3 chamber at the University of Minnesota.

A total of 145 smog chamber experiments were performed. For the most part, good agreement was found in the experimental data obtained at Calspan and the University of Minnesota; and a reasonably good understanding of the kinetics of gas to aerosol conversion in the polluted atmosphere was achieved. From the data generated in these experiments, the following points can be made:

(1) SO_2 photooxidation rates of a few tenths of a percent per hour are typically observed in clean, filtered air for a light intensity of about 50% noon day sun. In the presence of hydrocarbon contamination, accelerated rates are generally observed.

(2) Each HC + NO experiment can be divided into two phases. In the first phase, NO is converted to NO_2 and some oxidation of hydrocarbon occurs. Ozone starts to appear near the end of this period. The second phase, accompanied by substantial aerosol formation, begins as soon as NO is oxidized out of the system and NO_2 reaches its maximum; ozone grows rapidly and approaches a maximum.

(3) The addition of SO_2 to the HC + NO system was generally found to exert a synergistic effect on aerosol surface and volume production. At Calspan the effect was greatest for m-xylene, while at the University of Minnesota the largest effect on aerosol behavior was observed in the hexene + NO + SO_2 system. Possible synergistic effects in the cyclohexene system were masked by the explosive growth of aerosol with and without the addition of SO_2.

(4) The addition of SO_2 to the HC + NO system produces a dramatic decrease in the mean particle diameter. This results from the initial formation of very high concentrations of H_2SO_4 nuclei during the initial stages of the experiment. During the second stage of aerosol growth, condensation proceeds on the existing particles. In the HC + NO system alone, fewer but larger particles are produced.

(5) Of the hydrocarbons studied, cyclohexene was the most reactive, both in terms of aerosol and chemical behavior, followed by m-xylene, hexene,

and toluene. The main difference observed in the duplicate experiments at the University of Minnesota was that hexene was the least reactive hydrocarbon.

(6) It is possible to characterize system reactivity in terms of aerosol behavior. The most important variables are maximum number concentration, equilibrium surface concentration, and volumetric growth rate. These aerosol measures of reactivity have been found to correlate well with other conventional parameters, such as time to $[NO_2]_{max}$ and $[O_3]_{max}$.

(7) Increasing relative humidity was found to significantly increase aerosol surface and volume production.

Because of the large body of experimental data generated during the program, graphical presentations of both the chemical conversion and the aerosol growth data for the individual experiments are given in Appendices A and B at the end of this report. Data summations and discussions are provided in Section 4, Results and Discussion. Since detailed descriptions of experimental facilities were provided previously in the first year report, only brief descriptions highlighting some recent facilities improvements are given in Section 2. Detailed discussions of light intensity measurement techniques employed at Calspan and the University of Minnesota are therefore provided in Section 3. Chamber characterization tests designed to assess the effects of chamber contamination and to assure validity of experimental data presented in this report are described in Section 5.

Section 2

EXPERIMENTAL FACILITIES

2.1 Calspan

The smog chambers used at Calspan and the University of Minnesota have been discussed elsewhere (Kocmond et al., 1973; Clark, 1972) and will not be treated in detail here. Briefly, however, the Calspan chamber consists of a cylindrical chamber 30 feet in diameter and 30 feet high, enclosing a volume of 20,800 ft^3. The chamber walls are coated with a specially formulated fluoroepoxy, which has surface adhesion characteristics very similar to those of FEP teflon. Illumination within the chamber is provided by a combination of fluorescent daylight and blacklight lamps installed inside 24 lighting modules and arranged in eight vertical channels attached to the wall of the chamber. Light intensity has been increased to give $k_{d[NO_2]} \sim 0.23\ min^{-1}$ during this second year by installing two 215-watt fluorescent daylight lamps, eight 85-watt high output blacklamps, and two 40-watt sunlamps in each module. (Further modifications have been made since the end of the program to give $k_{d[NO_2]} \sim 0.33\ min^{-1}$). The lighting modules are covered with 1/4" Pyrex glass and are thus sealed from the chamber.

Air purification is provided by a recirculation system which can continuously filter the air through a series of absolute and activated charcoal filters. Experiments show that nearly all gaseous contaminants and particulate matter (<200 nuclei cc^{-1}) can be removed from the chamber air in about four hours of filtration.

2.1.1 Instrumentation

Instrumentation used to monitor aerosol behavior and reactant concentrations within the chamber included the following:

(1) Bendix Model 8002 Ozone Analyzer -- The instrument uses photometric detection of chemiluminescence resulting from the reaction of ozone with ethylene to determine ozone level. The minimum detectable sensitivity is reported to be 0.001 ppm. Good reliability and reproducibility of data was achieved using this instrument.

(2) Bendix Model 8101-B Nitrogen Oxides Analyzer -- Detection is based on chemiluminescent reaction between nitric oxide and ozone. The detection limit for each of the nitrogen oxides is 0.005 ppm. Periodic maintenance, as well as frequent calibration of this instrument, was often necessary.

(3) Bendix Model 8300 Sulfur Analyzer -- Operation of this instrument is based on the photometric detection of sulfur atoms excited in a hydrogen-rich flame. A set of filters is used for selective monitoring of sulfur dioxide and hydrogen sulfide. The minimum detectable sensitivity is 0.005 ppm. This instrument was found to be excessively sensitive to pressure changes within the smog chamber and required frequent adjustments to the sample flow.

(4) Hewlett-Packard Model 5750 Gas Chromatograph -- The chromatograph is equipped with dual column and dual flame ionization detectors. Depending on the column in use, either total hydrocarbon or individual components can be analyzed.

(5) Bendix Model 820 Reactive Hydrocarbon Analyzer -- This instrument uses flame ionization detection to provide quantitative analysis of methane (CH_4), total hydrocarbons (THC), and reactive hydrocarbons (THC-CH_4). The instrument was received late in the contract period and provided only limited use during this program.

In addition to the gas analyzers, a number of aerosol measuring instruments were used on the program. These included the following:

(6) Electrical Aerosol Analyzer (EAA) -- This instrument (described in the next section) was provided by the University of Minnesota during our joint workshops held at Calspan in November 1973 and March 1974. The instrument gives size distribution data of the photochemically-produced aerosols. Calspan obtained a Model 3030 Electrical Aerosol Analyzer of its own during the summer of 1974.

(7) An MRI integrating nephelometer for aerosol light scattering and visual range measurements.

(8) A Gardner Associates Small Particle Detector -- This manually operated instrument is used to measure total particle concentration. It has a range of sensitivity from 200 to 10^7 nuclei/cc and can detect particles as small as 0.002 μm.

(9) An Environment-One Model 100 Condensation Nucleus Monitor -- This instrument is reported to measure particle sizes down to 0.0025 μm and have a range of sensitivity from 50 to 10^7 nuclei/cc . Considerable difficulty was experienced in maintaining continuous operation of this instrument. There also appeared to be some lack in sensitivity to photochemically-produced aerosols during the initial homogeneous nucleation stage. An earlier stage of GE model has been acquired and modified for current usage with more reliable performance.

2.2 University of Minnesota

The University of Minnesota smog chamber is a cylindrical vessel fabricated of 0.01 in. DuPont FEP Teflon and encompassing a volume of 625 ft^3. For a complete description of the chamber and supporting facilities, see Clark (1972). The illumination system consists of 72 GE F40BL fluorescent lamps mounted in vertical pairs on 36 evenly-spaced supports. Aluminum foil has been attached behind the lamps to increase the uniformity and intensity of the light. Light intensity (see next section) is measured to be $k_{d[NO_2]_{avg}}$ ~0.20 min^{-1} for the U of M chamber.

The air purification system consists of an absolute particle filter, an activated charcoal scrubber, silica gel dryer, humidifier, and final filter. Ambient laboratory air is purified by pumping it through the purification system at about 15 CFM. Air passing through the purification system is exposed to only non-reactive metal, glass and Teflon duct surfaces in order to minimize sources of contamination.

2.2.1 Instrumentation

(1) Electrical Aerosol Analyzer -- Two versions of a portable electrical aerosol analyzer were used for the experiments. The "laboratory prototype" analyzer, used for the joint Calspan-University of Minnesota workshops and the first 45 experiments at the University of Minnesota, has been described by Liu et al. (1974). A second version, the "commercial prototype" (Thermo-Systems Model 3030), was used for the remainder of the experiments. A description of this second instrument is in Liu and Pui (1975). Figure 1 shows a schematic of the commerical instrument. This latter instrument requires 4 l/m of aerosol-laden air as a sample and 46 l/m "clean" sheath air. Usually, the entire 50 l/m air supply was taken from the chamber, and the sheath air portion was filtered with an absolute filter. The sheath air then had the same relative humidity and contained the same trace gases as the sample.

Both analyzers are based on the "diffusion charging-mobility analysis" principle described by Whitby and Clark (1966). The aerosol-laden air flows through the charger, a region containing unipolar ions which have been produced by a corona discharge. The aerosol particles emerge from the charger carrying a negative charge and are introduced into the mobility analyzer. In this section, a positive voltage on a collection rod causes all particles with electrical mobilities greater than a certain critical value to be precipitated. Those particles with smaller mobilities flow past this section and are collected by an absolute filter. An electrometer, which is connected to the filter, measures the current carried by the charged particles. The mobility spectrum, and, therefore, the size distribution can be inferred

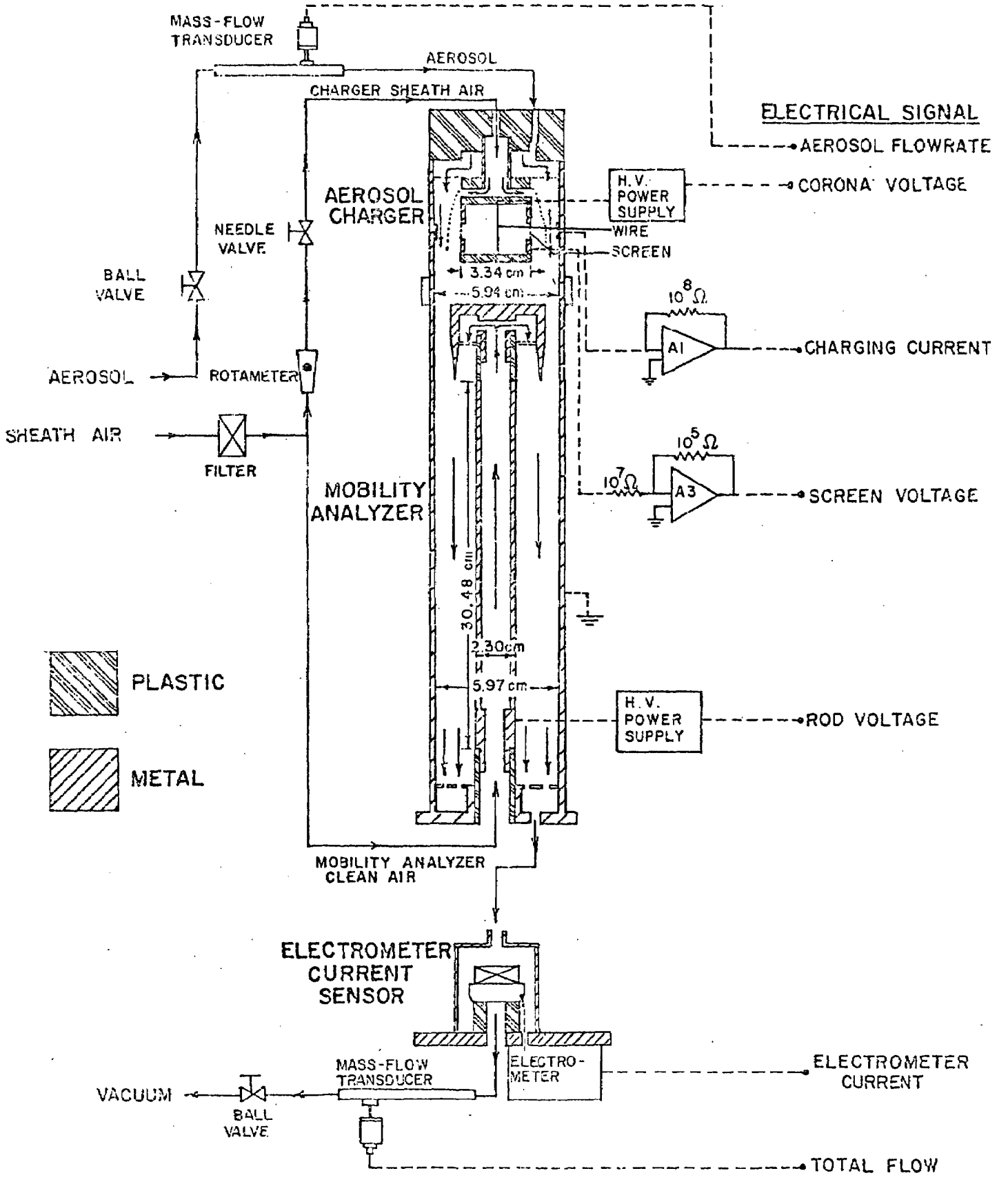

Figure 1 Electrical Aerosol Analyzer

from the electrometer current as a function of collecting rod voltage. A complete set of readings takes about 2 1/2 minutes; each current is measured at a different time. The aerosol is dynamic, however, and the size distribution may change substantially during the course of one set of data. To compensate for the error that this time lag introduces, an interpolation program was used to generate corrected currents for a given time in the experiment. All data were analyzed using the calibration of Liu et al. (1974). These constants are in error when used with the TSI 3030. However, the errors associated with their use should not be large. The use of these constants results in higher measured volume and surface concentrations.

(2) Condensation Nuclei Counter -- A General Electric Condensation Nuclei Counter (CNC) was used to measure total particle concentrations. All particles larger than about 0.002 μm should be detected. Details of the instrument have been given by Skala (1963). It has a range of sensitivity from about 50 to 10^7 particles/cm^3. For this study, the instrument was used primarily on the 100,000 particles/cm^3 scale. This scale was calibrated as described by Liu and Pui (1974). If concentrations greater than 100K were encountered, diluters were used in the sampling line. They could be used to give 394,000 or 1.3 x 10^6 particles/cm^3 full scale deflection. The diluters have been described by Whitby et al. (1972).

(3) Gas Analysis -- SO_2 concentration was measured with a Meloy Model SA 160-2 flame photometric total sulfur analyzer. This instrument was calibrated with a span gas produced with an SO_2 permeation tube. A Bendix Model 8101-B $NO+NO_2+NO_x$ analyzer was used to measure oxides of nitrogen. A span gas for calibrating the NO_2 scale was again produced using a permeation tube, while a commercial 205 ppm NO gas was diluted to provide calibration points for the NO scale. The Bendix instrument was zeroed with "boil off" gas from liquid nitrogen. The gas analysis equipment included an REM Model 612B chemiluminescent ozone analyzer. An ozone generator and wet analysis tests were used for its calibrations. A Cambridge Instrument Model 880 hygrometer indicated the dew point temperature, while chamber temperature was measured with a copper-constantan thermocouple. The chamber air and dew point temperatures were then used to derive relative humidity.

Hydrocarbon concentration was measured with a Hewlett-Packard Model 5700 gas chromatograph. Separation of components was made using a column packed with SE-30 silicon rubber on chromasorb. The column was maintained at 80°C for 1-hexene and cyclohexene, while a temperature of 90°C was used for toluene and m-xylene. The output from the gas chromatograph's flame ionization detector was recorded, and peak areas were measured with a planimeter for quantitative computations. Hydrocarbon span gases were made by evaporating small, measured volumes of the liquid hydrocarbons into known volumes of air.

Section 3

CHAMBER LIGHT INTENSITY MEASUREMENTS

3.1 Calspan Chamber

Light source improvements made in the Calspan chamber were completed by September 1973. The modifications involved the installation of six additional 85-watt blacklights and two 40-watt sunlamps in each of the 24 lighting modules. The two 215-watt fluorescent white lamps in each module remained unchanged. This mix of lamps increased the measured $k_{d[NO_2]}$ from ~0.05 min^{-1} to a new level of ~0.23 min^{-1}. (Since completion of the experiments reported here, all white lamps have been replaced by blacklamps giving rise to a new $k_{d[NO_2]}$ of ~0.33 min^{-1}.)

Initial light intensity measurements were attempted by measuring the rate constant, k_d, for NO_2 photolysis in nitrogen by irradiating a 15 ft^3 nitrogen-filled Teflon bag in the chamber center. The experiments gave results which suggested that the inner surface of the teflon bag was contaminated, since during the experimental period a rise in both the NO and NO_2 was observed suggesting surface absorption and desorption of NO_2.

An alternate scheme was adopted following a method reported by Stedman and Niki (1973) which was found to be fairly repeatable and well suited to a large chamber such as Calspan's. The method gives a measured value of $k_1\phi$ of NO_2 from the ratio of the initial production rates of O_3 or NO by photolysis of NO_2 in clean chamber air. Before reporting the experimental results, however, it is instructive to recognize a few of the inherent errors regarding the method. Some effects of normal background contaminants on the accuracy of the method were studied, as well as the conditions needed for valid interpretation.

A computer model for the NO_x+CO+H_2O-air system was used to assess possible contaminant effects. This model includes all the reactions considered by Stedman and Niki, as well as those reactions due to the presence of CO and H_2O. Several computer runs have been made for varying NO_2, NO, CO, HONO, and $k_1\phi$. The results are reported in Table I. The theoretical k_1's in Table I were calculated from the ratio of the O_3 production rates (modeled) and $[NO_2]_o$ at 6, 10, and 15 seconds. Changes in [CO], $[H_2O]$, and [HONO] have no appreciable effect on the calculated k_1's, but the accuracy of the calculated k_1 is very much dependent on the $[NO]_o/[NO_2]_o$ ratio. The accuracy of the method is also dependent on the response times of the O_3 and NO analytical instruments. For example, commercial ozone chemiluminescent devices have response times of the order of 1 second; therefore, accurate initial rates will require at least 5 seconds to be established and probably more realistically 10 to 15 seconds. The error introduced in $d[O_3]/dt$ (that is, in terms of its representing O-atom production from NO_2 photolysis) is due to ozone loss reactions.

$$NO + O_3 \rightarrow NO_2 + O_2 \qquad (1)$$

$$NO_2 + O_3 \rightarrow NO_3 + O_2 \qquad (2)$$

A simple calculation is sufficient to illustrate the error involved in the method due to ozone loss reactions. Assume we are using the method to measure a $k_1\phi$ of .15 min^{-1}, and that the initial concentrations are $[NO_2]$ = 5.0 ppm and [NO] = 0.0. In a five-second photolysis period, the following will have happened.

First, .0625 ppm NO_2 will be lost and .0625 ppm of NO and O_3 will be formed. Assuming a mean concentration of .0312 ppm for NO and O_3 in this 5 sec period, ozone loss due to reactions (1) and (2) is then given by,

$$.0625 \text{ ppm} - (.0312 \text{ ppm})(5 \text{ ppm})(.078 \text{ ppm}^{-1} \text{ min}^{-1}) \frac{5}{60} \text{ min}$$
$$- (.0312 \text{ ppm})(.0312 \text{ ppm})(23 \text{ ppm}^{-1} \text{ min}^{-1}) \frac{5}{60} \text{ min}$$
$$= - .00101 - .00187 = -.00288 \text{ ppm}$$

Table I.

MODELED RESULTS FOR NO_2 PHOTOLYSIS IN AIR WITH H_2O AND CO PRESENT

NO_2	NO	H_2O	CO	HONO	k_1 actual	k_1 theoretical			Percentage ERROR
						5 sec	10 sec	15 sec	
ppm	ppm	ppm	ppm	ppm	min^{-1}	min^{-1}	min^{-1}	min^{-1}	@ 5 sec
5.0	.01	$1.5x10^4$	0	0	.15	.136	.120	.103	9.3%
5.0	.01	$1.5x10^4$	2.0	0	.15	.136	.120	.103	9.3%
5.0	.01	$1.5x10^4$	10.0	0	.15	.136	.120	.103	9.3%
5.0	.01	$1.5x10^4$	10.0	0.1	.15	.135	.119	.102	10.0%
5.0	.01	$1.5x10^2$	10.0	0	.15	.136	.120	.103	9.3%
5.0	.01	$1.5x10^2$	10.0	0.1	.15	.135	.119	.102	10.0%
5.0	0.1	$1.5x10^2$	0	0	.15	.123	.103	.086	18.0%
5.0	0.1	$1.5x10^2$	10.0	0	.15	.123	.103	.086	18.0%
5.0	.01	$1.5x10^4$	10.0	0	.27	.233	.220	.196	13.7%
5.0	.01	$1.5x10^4$	10.0	0.1	.27	.233	.195	.158	13.7%
2.45	.01	$1.5x10^4$	0	0	.27	.245	.220	.192	9.3%
2.45	.01	$1.5x10^4$	2.0	0	.27	.245	.220	.192	9.3%
2.45	.01	$1.5x10^4$	10.0	0	.27	.245	.220	.192	9.3%
2.45	0.1	$1.5x10^4$	0	0	.27	.226	.192	.161	16.3%
2.45	0.1	$1.5x10^4$	2.0	0	.27	.226	.192	.161	16.3%
2.45	0.1	$1.5x10^4$	10.0	0	.27	.226	.192	.161	16.3%
2.45	.01	$1.5x10^4$	10.0	0	.15	.141	.131	.119	6.0%
2.45	0.1	$1.5x10^4$	0	0	.15	.119	.112	.098	20.7%
3.00	.01	$1.5x10^4$	0	0	.15	.139	.130	.118	8.0%
1.00	.01	$1.5x10^4$	0	0	.15	.146	.139	.132	2.7%
1.00	0.1	$1.5x10^4$	0	0	.15	.134	.116	.105	10.7%

which represents a 5% error. If there were 1% NO initially present, the error becomes 10%. A similar calculation as above except with a 10 second interval for initial rate determination gives an inherent error of 20%. For any given time period at which an initial rate is determined, the inherent error will therefore be directly related to the $k_1 \times (NO_2)$ and the initial NO present. It should be noted that in all cases the error introduced in calculating k_1 represents a lower value than actually present.

The experimental results for NO_2 photolysis in air carried out in the Calspan chamber are shown in Table II. The samples were taken from a distance of about 2 meters from the chamber wall so that the data represent approximate average light intensity levels in the smog chamber. The initial ozone production rates were determined in the first five seconds of the run after switching on the lights. The lights were not temperature stabilized prior to a run. The simple calculation mentioned above would suggest that the experimental k's are ~7% too low.

Table II. CALSPAN CHAMBER - NO_2 PHOTOLYSIS IN AIR

$[NO_2]$ ppm	[NO] ppm	$d[O_3]/dt$ ppm/min	k_1 min^{-1}	k_d min^{-1}
3.70	.04	.528	.143	.220
3.70	.04	.552	.149	.230

Although it has been shown that there are a number of possible errors inherent in the use of this method, the results obtained are in close agreement with the calculated k_d expected from the number and type of lights that are now used in the Calspan chamber.

3.2 University of Minnesota Chamber Light Intensity Measurements

For the University of Minnesota smog chamber, a slightly different procedure was followed using the Stedman and Niki (1973) method. After admitting approximately 5 ppm NO_2 into the chamber, the 72 F40BL blacklights were turned on, and the NO and O_3 concentrations were recorded as a function of time. Very early (during the first few seconds) in such an experiment, the only important reactions are:

$$NO_2 + h\nu \rightarrow NO + O \qquad (1)$$

$$M + O + O_2 \rightarrow O_3 + M \qquad (2)$$

where M is any third body. The O quickly achieves a stationary state so that

$$\frac{d[NO]}{dt} = \frac{d[O_3]}{dt} = k_1[NO_2]$$

Hence, the initial rate of production of either NO or O_3 may be used along with $[NO_2]$ to determine k_1. Later in the experiment, reactions (3) and (4) become important in removing O_3.

$$NO + O_3 \rightarrow NO_2 + O_2 \qquad (3)$$

$$NO_2 + O_3 \rightarrow NO_3 + O_2 \qquad (4)$$

When $[O_3]$ reaches the maximum

$$k_1[NO_2] = k_3[NO][O_3] + k_4[NO_2][O_3].$$

This is called the photostationary state; and under these conditions, k_1 can be calculated from measurements of $[NO]$, $[NO_2]$, and $[O_3]$, provided k_3 and k_4 are known.

Reactions (3) and (4) are fast enough to cause significant losses of NO and O_3 as they pass from the chamber to the measuring instruments. Consequently, a correction for losses in the sampling lines had to be made. The residence times in the sampling lines were 0.108 and 0.159 min for the ozone and NO instruments, respectively. Corrections for line losses were made using the following expressions:

$$[O_3]_{chamber} = [O_3]_{measured} + [O_3]_{line}(k_3[NO]_{line} + k_4[NO_2]_{line})\tau_{O_3}$$

$$[NO]_{chamber} = [NO]_{measured} + k_3[NO]_{line}[O_3]_{line}\tau_{NO}$$

The average values of [NO] and $[O_3]$ in the lines are not known and were determined by an iterative procedure. The NO and O_3 data obtained were all corrected using this method.

Values of k_1 were determined using both the initial rate of NO formation and measurements of photostationary state. Measurements of k_1 were made at the beginning and end of our entire experimental program in order to determine if deterioration of the lights was significant. The results of these measurements are listed in Table III. It may be seen that the two methods are in good agreement, and that the light intensity fell by about 20% during the course of this program. In order to make data comparisons with results reported in a large body of smog chamber experiments which have already been performed, light intensities are also expressed in terms of k_d values, where k_d is the first order NO_2 photolysis rate which would be observed if NO_2 were photolyzed in N_2 under the same lights. Under such conditions, the reactions

$$O + NO_2 \rightarrow NO + O_2 \qquad (5)$$

$$O + NO_2 + M \rightarrow NO_3 + M \qquad (6)$$

are also important and k_d becomes:

$$k_d = d(\ln[NO_2])/dt = k_1k_5/(k_5 + k_6[M]).$$

Inserting the rate constants given by Stedman and Niki gives

$$k_d = k_1/0.64$$

This relationship and the average value of k_1 for each experiment has been used to calculate the k_d values given in Table III.

TABLE III. LIGHT INTENSITY MEASUREMENTS

Run	k_1 (min^{-1})		k_d (min^{-1})	Comments
	NO_{slope}	stationary state		
A	0.087	0.084	0.13	Before November Workshop
B	0.094	0.097	0.15	
C	0.073	0.074	0.12	After March Workshop

The method used above gives local values of light intensity at the point of sampling from within the chamber which is on the chamber centerline. Clark (1972) measured the variation of light intensity with radial position in the chamber with a chemical actinometer utilizing the photoisomerization of o-nitrobenzaldehyde to o-nitrobenzoic acid. He found that the light intensity increased significantly as the walls were approached. His results have been used to calculate the ratio of chamber volume average light intensity to centerline intensity. This ratio is 1.04 for the small bag and 1.45 for the large bag. Volume average values of k_d have been calculated by multiplying these ratios by the measured values on the chamber axis. The results are presented in Table IV. Note that the average light intensity in the large bag is about 40% greater than in the small bag because the small bag only contains volume near the chamber centerline where the low light intensity is lowest. From these data, $k_{d[NO_2]_{avg}}$ for the large U of M bag is 0.20 min^{-1}.

Table IV. VOLUME AVERAGE LIGHT INTENSITIES

$k_d(min^{-1})$

Run	Centerline	Averages Large Bag	Small Bag
A	0.13	0.19	0.14
B	0.15	0.21	0.16
C	0.11	0.15	0.12

Section 4

RESULTS AND DISCUSSION

In this section, results of the Calspan and University of Minnesota experiments are discussed in the order the experiments were performed. Two joint workshops were held at Calspan during the project year--one in November 1973 and another in March 1974. The purpose in performing the experiments cooperatively was to take advantage of the additional aerosol measuring capability at the University of Minnesota. (Calspan did not acquire its own electrical aerosol analyzer until the summer of 1974.) In addition to the joint experiments at Calspan, more tests were matched as closely as possible at the University of Minnesota in order to allow additional interchamber comparisons of the aerosol and chemistry data.

In the discussion which follows, results of the workshop data are first summarized in tables and then treated individually when it is instructive to do so. Because of the large number of experiments performed during the year, graphs of the aerosol and chemical data have been combined and placed in an appropriate appendix. Wherever possible, data from duplicate experiments performed at the University of Minnesota are matched with the corresponding Calspan experiment. Within the text, however, only representative cases from each of the test systems are compared and discussed in detail.

4.1 November Workshop

During the first joint workshop, the experimental schedule was divided into three phases: (1) SO_2 experiments, (2) toluene, toluene + NO_2 and toluene + NO_2 + SO_2 tests, and (3) hexene, hexene + NO_2 and hexene + NO_2 + SO_2 experiments. The initial SO_2 experiments were performed to compare the effects of light intensity and chamber contamination on aerosol production and SO_2 photooxidation rates in the SO_2-clean air system. The experiments included irradiations of SO_2 using the old lighting configuration (k_d~0.05 min^{-1}) in a "dirty" chamber (contamination on the walls due to auto exhaust

irradiations performed on another contract was not cleaned prior to the first test) followed by several experiments after washing the chamber with distilled water. A summary of all experiments performed during the workshop is given in Table V. Graphs of the aerosol and chemistry data are shown in Appendix A and matched with the comparable University of Minnesota test where possible.

As in the past, computations of SO_2 oxidation rate were made from the aerosol volume data generated by the EAA. The procedure is described by Clark (1972); briefly, however, the rate of production of sulfuric acid aerosol, corrected for molecular weight change, and water concentration is assumed to be equal to the rate of photooxidation of SO_2 which is constant for the linear growth portion of the experiment. Thus, the slope of the straight line volume growth curve may be related directly to the rate of photooxidation of SO_2. The governing equation is:

$$-\frac{d[SO_2]}{dt} = \frac{dv}{dt}(\rho)(P)\left(\frac{MW_1}{MW_2}\right) \qquad (7)$$

where ρ is the density of the sulfuric acid droplet, P is the weight fraction of H_2SO_4 in the droplet, MW_1 is the molecular weight of SO_2, and MW_2 is the molecular weight of H_2SO_4. The quantities ρ and P can be determined from data given by Bray (1970) assuming that water vapor in the gas phase is in equilibrium with water in the aerosol droplets.

- SO_2 Experiments

The first six experiments at Calspan were SO_2 irradiations under either partial lighting or full light intensity. After experiment 2, the chamber walls were cleaned using a triplicate rinsing with distilled water. The water washing did not appear to have affected the SO_2 photooxidation rate as shown by the data in Table V. Note that an initial and final photooxidation rate has been computed for some cases based on the form of the volumetric growth curve (i.e., for the first 30 to 60 min, a slower initial rate was often observed followed by somewhat faster growth, probably due to

Table V. SUMMARY OF DATA FROM NOVEMBER 1973 WORKSHOP

Run No.	System	RH %	HC ppm by volume	NO_2 ppm	SO_2 ppm	N_{max} $\times 10^{-3}$ cc^{-1}	S_L μm^2-cc^{-1}-hr^{-1}	$\frac{dv}{dt}$ (SO_2) μm^3-cc^{-1}-hr^{-1}	SO_2 photox. %-hr^{-1}
1	SO_2*	--	b***	b	0.63	560	470	1.71	.03
2	SO_2	30	b	b	0.70	700	not reached	6.15i** / 13.75f**	.17 / .37
3	SO_2*	33	b	b	0.58	525	>600	1.60i / 3.60f	.05 / .11
4	SO_2*	34	b	b	0.55	570	>600	1.20i / 2.83f	.04 / .09
5	SO_2	31	b	b	0.52	960	>1100	7.33	.27
6	SO_2	32	b	b	0.55	750	1600	6.0 i / 16.7 f	.21 / .57
7	toluene	35	0.8	b	---	NO AEROSOL			
8	toluene + NO_2	37	0.8	5.0	---				
9	toluene + NO_2	34	0.8	3.3	---				
10	toluene + NO_2 + SO_2	45	0.8	1.95	.19	1000	1000 then less	7.50i / 1.90f	.64 / .18
11	toluene + NO_2 + SO_2	36	0.8	3.55	.07	800	700 then less	5.00i / 0.41f	1.30 / 0.10
12	toluene + NO_2 + SO_2	33	0.8	1.45	.01	500	280 then less	0.88i / 0.28f	1.65 / .53
13	hexene	38	0.6	b	---	95	>50	---	---
14	hexene + NO_2	34	0.6	3.35	---	46	---	---	---
15	hexene + NO_2 + SO_2	32	0.6	1.64	.01	580	400	2.4 i / 0.9 f	4.57 / 1.71

*partial lights used on experiments 1, 3 and 4 to duplicate previous year's light intensity, i.e., $k_{d[NO_2]} \sim 0.05$ min^{-1}.

**i and f refer to initial (usually first 30 min) and final growth rates.

***b = background

contributions from contaminants). It is interesting to note that the average initial SO_2 photooxidation rate for the two lighting configurations reflects very nearly the measured k_d ratio:

$$\frac{k_d \text{ new lights}}{k_d \text{ old lights}} = \frac{0.22}{0.05} = 4.6 \qquad \frac{SO_2 \text{ ox. rate (av. new)}}{SO_2 \text{ ox. rate (av. old)}} = \frac{0.22}{0.04} = 5.4$$

This relation is also true when comparing the average final SO_2 oxidation rates for the two light intensities.

Figures 2 and 3 show typical SO_2 aerosol behavior for linear growth and also for a system in which there is upward curvature in the volumetric growth rate. Number concentration grows rapidly after the lights are switched on as a result of homogeneous nucleation processes. As the experiment progresses, the rate of nucleation drops until the production of particles by nucleation is balanced by the removal of particles by coagulation. The surface concentration grows rapidly initially as surface is formed by the nucleation of new particles and growth of existing particles. The rate of growth of surface concentration slowly decreases as the nucleation rate drops and the removal of surface by coagulation becomes more important. The surface concentration then slowly tends toward a steady-state value where the rate of production of new surface by nucleation and condensation is exactly balanced by the rate of removal of surface by coagulation. The volume concentration frequently grows slowly at first and then grows linearly. This results from a constant rate of oxidation of SO_2 which leads to a constant rate of production of sulfuric acid mist. On occasion, there is upward curvature to the volumetric growth rate probably due to trace contaminants within the chamber air which contribute to aerosol formation. Substantial contamination (due mainly to inadequate filtration or the previous history of experiments) manifests itself in the form of a very pronounced increase in the conversion rate or large upward curvature or both. This behavior can be seen by comparing the data shown in Figures 2 and 3.

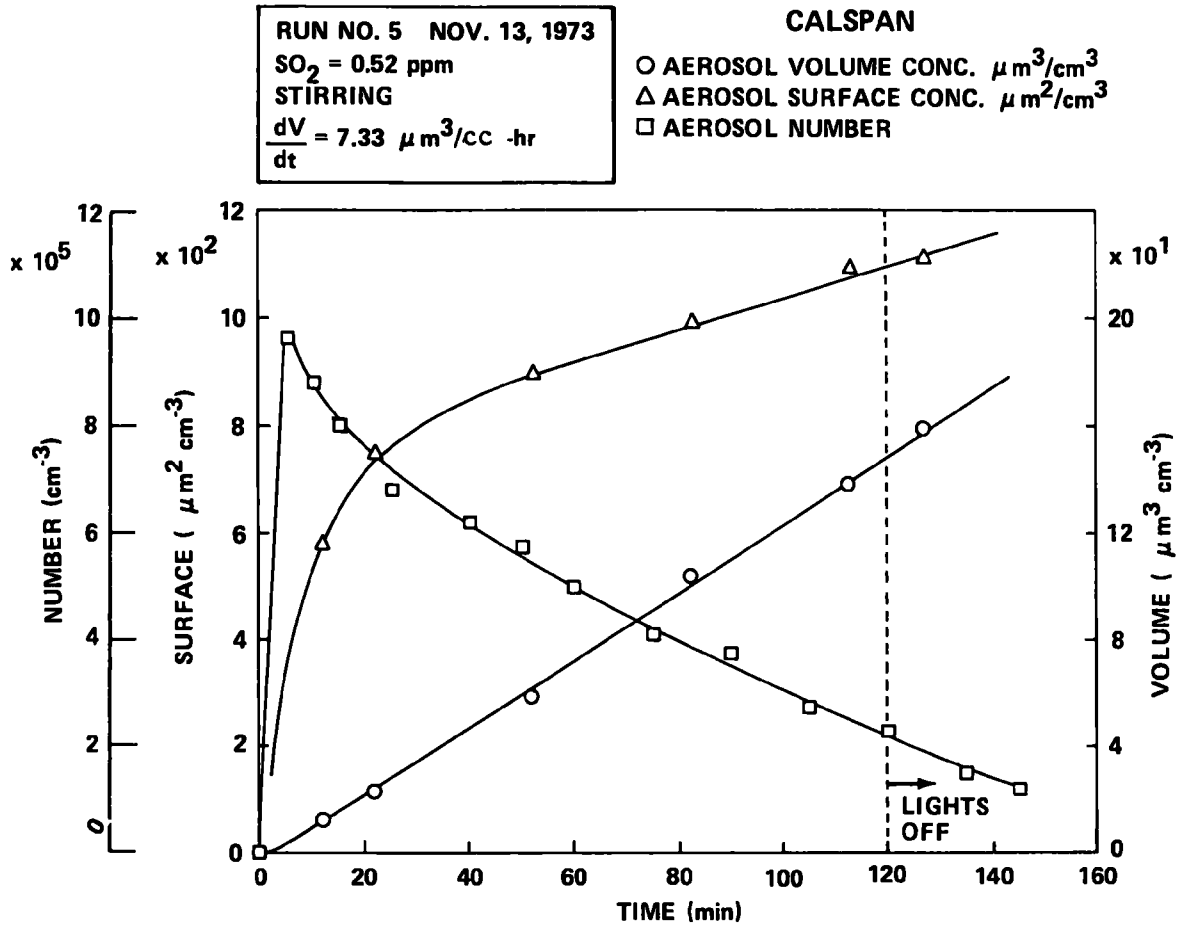

FIGURE 2. SO_2 EXPERIMENT SHOWING LINEAR VOLUMETRIC GROWTH.

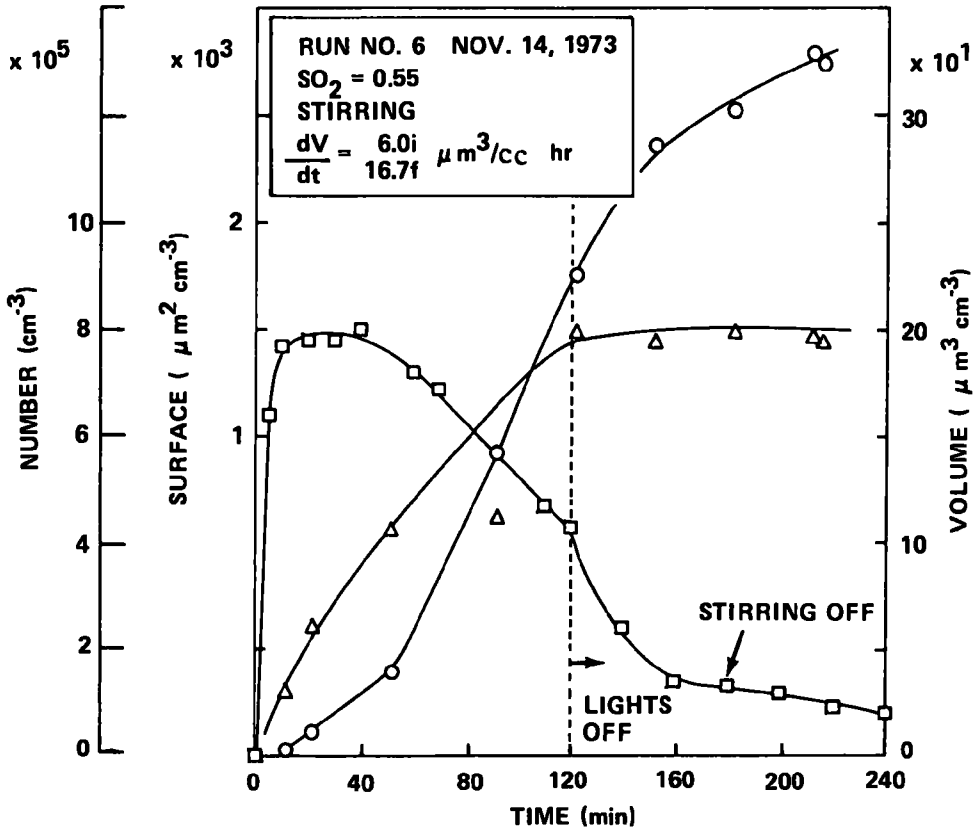

FIGURE 3. SO_2 EXPERIMENT SHOWING UPWARD CURVATURE OF AEROSOL VOLUME.

- HC + NO_2 Experiments

Experiments 7-15 were carried out to study the effects of toluene and hexene on aerosol formation. The irradiation of these hydrocarbons with background levels of NO_x does not lead to appreciable aerosol formation, a fact that was also observed in the comparable U of M experiments for toluene. The toluene and hexene systems with added NO_2 also showed very little aerosol formation; however, the ratios of HC:NO_2 were always much less than one, and complete domination of the chemistry by the excess NO_2 present has resulted. The relatively small concentration of toluene present in these runs had only a minor effect in converting NO to NO_2. Some additional discussion relative to the mechanisms at work in the HC+NO_2 system during the photolysis period is given below.

The photolysis of NO_2 in clean air proceeds through a rather complex reaction mechanism, the most important steps of which are given below.

$$NO_2 + h\nu \rightarrow NO + O$$

$$O + O_2 + M \rightarrow O_3 + M$$

$$O_3 + NO \rightarrow O_2 + NO_2$$

$$O_3 + NO_2 \rightarrow NO_3 + O_2$$

$$NO_3 + NO_2 \rightarrow NO + NO_2 + O_2$$

$$NO_3 + NO_2 \leftrightarrows N_2O_5$$

$$N_2O_5 + H_2O \rightarrow 2HONO_2$$

It has been observed, both experimentally and theoretically, through modeling techniques that during NO_2 photolysis a gradual formation of NO occurs. The rate of NO production is a function of light intensity, initial NO_2 concentration and relative humidity.

The addition of hydrocarbon to the NO_2 system introduces free radical species formed as a result of the hydrocarbon photooxidation. The major hydrocarbon photooxidation processes are thought to proceed via attack by one or more of the following species: O-atom, O_3, HO, HO_2, NO_3, and CH_3O. The first three species are thought to contribute most significantly, though their order of importance will vary with respect to the structure of the hydrocarbon being oxidized. Peroxy radicals, a transient species formed in the hydrocarbon oxidation process, are of major importance in the nitric oxide oxidation process. Reactivity scales have been formulated based on the rate at which hydrocarbons catalyze the oxidation of nitric oxide, but unfortunately these scales can be ambiguous. For instance, in any given light condition, the rate of nitric oxide oxidation is dependent upon the hydrocarbon to nitric oxide ratio, the initial NO_2 concentration, as well as the experimental system itself. Table VI contains reactivities for several hydrocarbons and their reaction rate constants with O-atom, O_3, and HO.

It appears from the toluene-NO_2 experiments, runs 8 through 12, that the toluene-NO_2 ratios chosen were such that the rate of NO oxidation, due to the oxidation of toluene, was too slow to compensate for the NO formation rate resulting from the NO_2 photolysis mechanism mentioned earlier. Therefore, in all of the toluene studies, NO was never oxidized out of the system. Also, any observable loss of toluene was within the experimental error of the analytical system.

In the hexene-NO_2 studies, run 14 (see Appendix A) shows an effect similar to that observed in the toluene system, while run 15 with a higher HC/NO_x ratio shows oxidation of virtually all the hexene-1 and conversion of all the NO formed in the system to NO_2. For the comparable toluene experiment, oxidation of the HC was very slow and incomplete. These results suggest a greater difference in reactivity between toluene and hexene-1 than Table VI would indicate. One possible explanation is that aromatics may vary in reactivity with respect to the HC/NO ratio much differently than the olefins. For example, toluene's reactivity is mostly dependent on the HO-toluene

reaction, while hexene-1 reactivity receives comparable contributions from O-atom, O_3, and HO reactions. Under the NO_2-toluene conditions in these experiments, the HO-NO_2 reaction dominates, virtually eliminating a HO-toluene chain mechanism and thus exhibiting the very low reactivity observed.

In the cases of the hexene-NO_2 studies, the results suggest that the conditions for short and long chain length reactions involving HO were achieved respectively in Runs 14 and 15.

Table VI. HYDROCARBON REACTIVITY

Compound	k in ppm^{-1} min^{-1}			Reactivity[4]
	O-atom[1]	O_3[2]	HO[3]	
ethylene	7.7×10^{2}	3.8×10^{-3}	2.5×10^{3}	1.7[*]
propylene	4.4×10^{3}	1.6×10^{-2}	2.5×10^{4}	3.5
hexene-1	5.0×10^{3}	1.5×10^{-2}	6.0×10^{4}[**]	1.7
toluene	1.7×10^{2}	1.8×10^{-5}[5]	2.0×10^{4}[***]	1.3
NO_2	8.1×10^{3}[6]	7.8×10^{-2}[6]	1.5×10^{4}[6]	---

[1]Cvetanovic, R.J., Adv. in Photochemistry 1, 115 (1963).

[2]Wei, Y.K. and Cvetanovic, R.J., Can. J. Chem. 41, 913 (1963).

[3]Morris, E.D., Jr. and Niki, H., J. Phys. Chem. 75, 3640 (1971).

[4]Glasson, W.A. and Tuesday, C.S., Environ. Sci. Technol. 4, 916 (1970).

[5]Stedman, D.H. and Niki, H., Environ. Letters, 4, 303 (1973).

[6]Demerjian, K.L., Kerr, J.A. and Calvert, J.G., Adv. in Environ. Sci. Technol. Vol. 3, Wiley-Interscience, New York (1973).

*Based on the average rate of NO photooxidation (ppb/min); $k_d = 0.29$ min^{-1} and HC to NO ratio of 2.5.

**Rate constant based on reaction of HO with pentene-1.

***Upper limit based on rate constant of HO-xylene reaction.

- HC + NO_2 + SO_2 Experiments

The addition of SO_2 to the HC-NO_2 systems had a profound effect on aerosol formation. In reviewing the data in Table V, the toluene + NO_2 + SO_2 systems (runs 10, 11, and 12) and the hexene + NO_2 + SO_2 experiment (run 15), show rapid initial aerosol growth followed by somewhat slower volume production. Similar characteristics were found in the U of M experiments. The apparent SO_2 oxidation rates for these systems were quite high, initially up to several percent per hour, followed by a slower final rate that is very similar to that of SO_2 alone. Matched aerosol and chemistry data from a representative Calspan and U of M experiment for the toluene + NO_2 + SO_2 system can be seen in Figures 4 and 5.

In view of the chemical profiles for these experiments, we believe the following processes can account for the observed aerosol behavior. In the early stages of the HC+NO_2+SO_2 runs, there are two major sources of aerosol formation, that resulting from SO_2 oxidation and the other from the reaction of O_3 with the hydrocarbon. Rapid volumetric growth occurs and, therefore, the apparent initial SO_2 photooxidation rate is quite high. As irradiation continues, ozone levels quickly decline (see Figure 4) resulting in the loss of one important source of aerosol. This, in turn, causes a change in the observed volumetric aerosol growth rate of the system. In the absence of SO_2, the HC+NO_2 system shows only one growth mode which is consistent with the above explanation of aerosol behavior.

4.2 Duplicate Experiments to the November Workshop - University of Minnesota

After completing the joint workshop at Calspan during November, a similar set of experiments was performed at the U of M. Some additional SO_2 irradiations were performed after HC-NO_2 experiments in order to observe the effect of possible chamber contamination on the SO_2 oxidation rate. The results of the Minnesota experiments are summarized in Tables VII and VIII. Three systems were investigated: SO_2, toluene + NO_2, and toluene + NO_2 + SO_2.

FIGURE 4

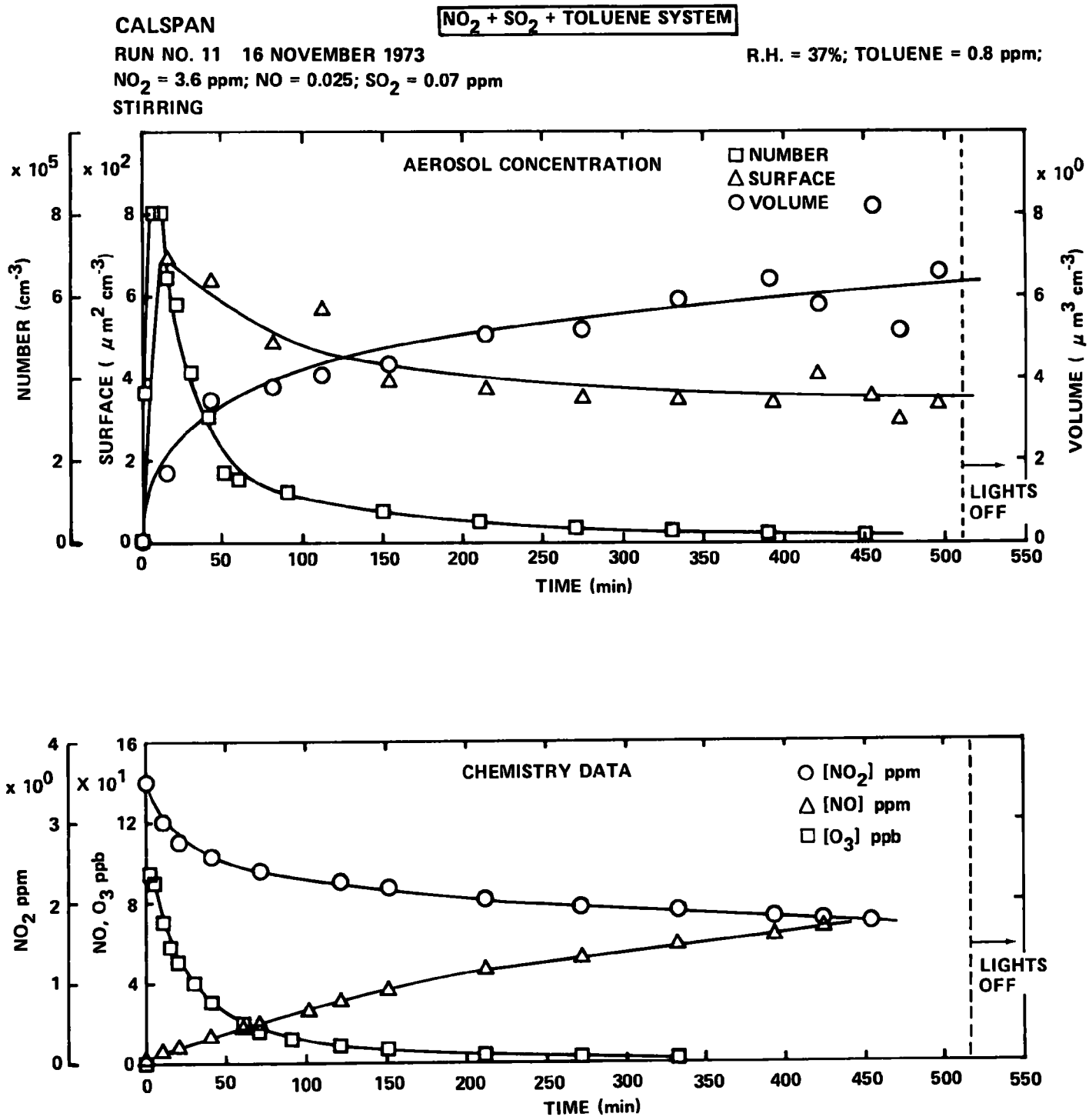
CALSPAN
NO_2 + SO_2 + TOLUENE SYSTEM
RUN NO. 11 16 NOVEMBER 1973
R.H. = 37%; TOLUENE = 0.8 ppm;
NO_2 = 3.6 ppm; NO = 0.025; SO_2 = 0.07 ppm
STIRRING
AEROSOL CONCENTRATION
NUMBER
SURFACE
VOLUME
NUMBER (cm^{-3})
SURFACE ($\mu m^2 cm^{-3}$)
VOLUME ($\mu m^3 cm^{-3}$)
LIGHTS OFF
TIME (min)
CHEMISTRY DATA
[NO_2] ppm
[NO] ppm
[O_3] ppb
NO_2 ppm
NO, O_3 ppb
LIGHTS OFF
TIME (min)

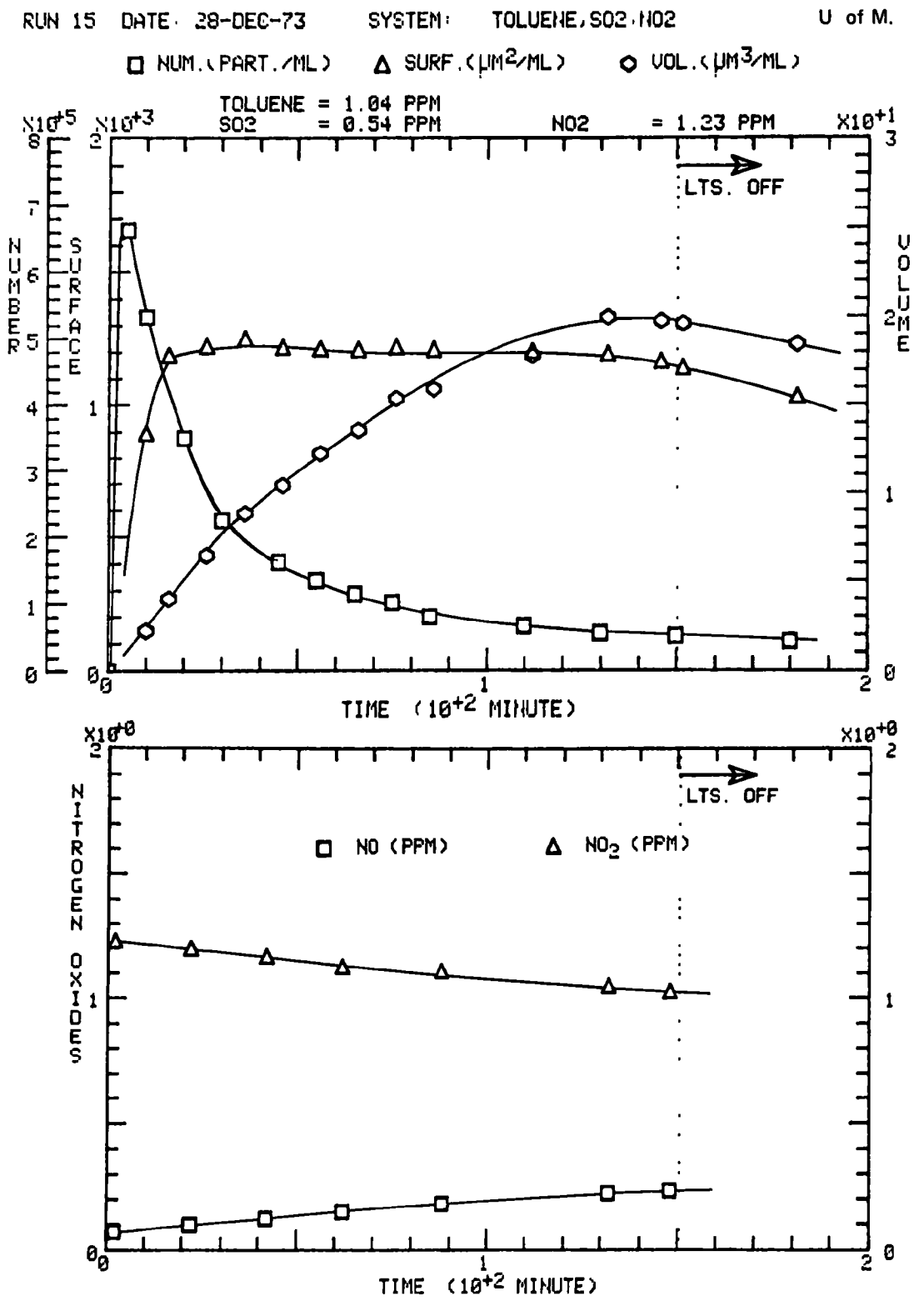
RUN 15 DATE: 28-DEC-73 SYSTEM: TOLUENE/SO2/NO2 U of M.
NUM.(PART./ML) SURF.(μM²/ML) VOL.(μM³/ML)
TOLUENE = 1.04 PPM
SO2 = 0.54 PPM
NO2 = 1.23 PPM
X10+5
X10+3
X10+1
LTS. OFF
NUMBER
SURFACE
VOLUME
TIME (10+2 MINUTE)
X10+0
NITROGEN OXIDES
NO (PPM)
NO2 (PPM)
LTS. OFF
TIME (10+2 MINUTE)

FIGURE 5

TABLE VII. UNIVERSITY OF MINNESOTA DUPLICATE TESTS SUBSEQUENT TO NOVEMBER WORKSHOP:

SUMMARY OF SO_2 EXPERIMENTS

Run No.	Concentration ppm	RH %	N_{max} #-cc^{-1}	SE μm^2-cc^{-1}	$\frac{dv}{dt}_3$ SO_2 μm^3-cc^{-1}-hr^{-1}	$\frac{1}{SO_2}\frac{dv}{dt}$ μm^3-cc^{-1}-hr^{-1}-ppm^{-1}	SO_2 photox %-hr^{-1}
1	.51	13	90 K	420*	2.3	4.5	.12
2	.53	9	150 K	420*	2.6	4.9	.13
3	.64	64	320 K	660	3.1	4.8	.057
4	.59	36	170 K	340	.98	1.7	.030
5	.55	35	160 K	380*	.93	1.7	.032
6	.55	29	110 K	210	.49	.89	.018
11	.55	30	600 K	1300	12.0	22	.42
12	.47	49	330 K	1400	9.8	21	.35
17	.54	27	220 K	420	1.1	2.0	.041
18	.012	17	54 K	72*	.12	10	.23
19	.012	36	35 K	25*	---	---	---
20	.54	29	280 K	620*	2.2	4.1	.079

*Equilibrium surface not reached.

have been responsible for the observation because number concentration continued to decay normally, and also a second phase of growth was not apparent in the comparable Calspan experiment. For Run 14, the EAA data proved to be unreliable and only number against time data were obtained. Following EAA repair, a complete set of aerosol data was obtained for the remainder of the experiments in the series. Runs 14 and 16 were made with the toluene + NO_2 + SO_2 system. The aerosol growth behavior of these systems is different from the SO_2-pure air system in that two distinct growth phases are evident: rapid initial volume production for about the first hour, as observed in the Calspan experiments, followed by a slower but essentially linear increase with time. The volume production rates during the linear rate periods are tabulated in Table VII, as well as the corresponding apparent SO_2 photooxidation rates. Comparison of these results with Calspan's for the same chemical system reveals very similar behavior. The shapes of the plots of N, S, and V against time, shown in Figures 4 and 5 and also Appendix A, are the same except that the surface concentration obtained in the Calspan experiments is not as constant as in the Minnesota tests. The Calspan and Minnesota experiments were performed at different SO_2 concentrations and, consequently, the resulting aerosol concentrations were different. However, when the volumetric production rates during the linear growth phase are normalized by converting them into apparent SO_2 photooxidation rates, good qualitative agreement is obtained between the two sets of experiments. Thus, on the average, Calspan SO_2 oxidation rates with full light intensity are about 0.2%/hr, while in the U of M chamber, values less than 0.1%/hr are usually noted.

The last group of experiments in these series, 17-20, were all SO_2 experiments. The usual SO_2 photooxidation behavior is evident. Apparent photooxidation rates in these experiments are nearly a factor of two higher than before the toluene experiments were performed. This suggests that some chamber contamination was produced in the toluene experiments.

4.3 Conclusions from the November Workshop

From a complete review of the Calspan and University of Minnesota duplicate experiments involving SO_2 + clean air, HC + NO_2, and HC + NO_2 + SO_2 system, the following points emerge:

(1) SO_2 photooxidation rates of ~0.2%/hr are typically observed in the Calspan chamber and rates generally less than ~0.1%/hr and occasionally a few hundreths of a percent hr^{-1} are found in the U of M chamber.

(2) A conditioning effect in which each subsequent SO_2 irradiation produces slightly less aerosol is normal in both chambers. The effect is more pronounced in University of Minnesota tests. Generally, the history of previous experiments does not appear to have as large an effect on the SO_2 oxidation rates in the Calspan chamber as it does in the U of M chamber. This could be due to the very large size of the Calspan chamber and also to the method of air purification (i.e., recirculation through charcoal filters until the desired level of cleanliness is achieved).

(3) Irradiations of toluene or hexene + clean air produce no aerosol in either the Calspan or U of M chambers. The addition of excess NO_2 does not cause appreciable additional aerosol formation in either chamber.

(4) The addition of even small amounts of SO_2 (~0.01 ppm) to the HC + NO_2 systems had a profound effect on aerosol production. Rapid initial aerosol formation appears to be due to a combination of SO_2 oxidation (and subsequent formation of H_2SO_4 particles) and ozone reaction with HC. As the ozone levels decline, only the SO_2 photooxidation mechanism remains which leads to final volume production rates similar to that for SO_2 alone.

4.4 March 1974 Workshop

A second joint workshop was held for a three-week period in March 1974. The test series was designed to investigate chemical conversion and aerosol behavior of various HC+NO and HC+NO+SO_2 systems using realistic concentrations of reactants. The hydrocarbons chosen for study were toluene, hexene-1, m-xylene, and cyclohexene. NO was used in place of NO_2 in order to more closely simulate photochemical processes responsible for aerosol formation in an urban environment. The normal concentrations of reactants used in the experiments were ~0.35 ppm HC, 0.15 ppm NO, and 0.05 ppm SO_2. As in the November workshop, a number of SO_2 + clean air experiments were performed as part of normal chamber characterization and contaminant monitoring procedures.

Two series of experiments are reported in this section. The first represents data obtained during the joint Calspan/University of Minnesota workshop held at Calspan in March 1974, and the other consists of duplicate experiments performed at the U of M following the workshop. Since Calspan did not yet have its own aerosol analyzer at the time of the March workshop, there was no opportunity to repeat any of the experiments once the workshop was over. In several instances, it would have been instructive to do so. In spite of this limitation, there is generally very good agreement of the data in both a qualitative and quantitative sense.

A total of 31 experiments were performed during the workshop using various HC, HC+SO_2, HC+NO, and HC+NO+SO_2 mixtures. Following the workshop, additional experiments were performed at the U of M. Many extra SO_2 experiments were performed to study the effects of chamber contamination on SO_2 oxidation rate. All chemical and aerosol conversion data for these experiments are presented in Appendix B, together with the duplicate U of M experiments. Several specific examples are discussed within the text. In order to preserve continuity, the experiments are discussed in the following sequence: SO_2 experiments, HC+NO tests, HC + SO_2, and HC+NO+SO_2 experiments. Four experiments were also performed at Calspan using various concentrations of

NaCl particles. The aerosol and chemistry data are shown in Appendix B but not discussed in the text, since the NaCl aerosol generally masked the important features of the aerosol surface and volume behavior.

4.4.1 SO_2 Experiments and Influence of Bag Size on Aerosol Production

In order to allow direct comparison of the pertinent chemical and aerosol data, summary tables from both the Calspan workshop and U of M experiments are shown in Tables IX through XIII. At the beginning of the joint workshop, four SO_2 experiments were performed using concentrations of either 0.50 ppm or 0.05 ppm SO_2. The data are consistent in that each experiment shows an initial SO_2 photooxidation rate of approximately 0.2% hr^{-1}, followed by a somewhat accelerated rate. As previously discussed, the accelerated or 'final' rate is thought to be the result of contributions to aerosol growth by background contamination in the chamber air. Note that the final photooxidation rate for the lower concentration runs (numbers 2 and 3) is somewhat elevated compared to the high concentration experiments. It appears that when the SO_2 concentration is fairly high, i.e., 0.50 ppm, the contributions to aerosol growth from trace contaminants, is quite small. Thus, for a slightly contaminated chamber, the higher the SO_2 concentration the more nearly the data represent SO_2 photooxidation alone. From the large number of SO_2 irradiations performed in the Calspan chamber over the past two years, it appears that the normal oxidation rate of SO_2 in filtered air is approximately 0.2% hr^{-1}.

A substantial number of additional experiments were performed by the U of M to test the effects of bag size and condition. The dimensions of the smog chamber bags used in these experiments are as follows:

Dimensions of Smog Chamber Bags

	Large Bags	Small Bags
Diameter	3.05 m	1.16 m
Height	2.44 m	2.16 m
Volume	17.8 m^3	2.28 m^3
Surface/Volume	2.13 m^{-1}	4.38 m^{-1}

The results of the experiments are presented in plots of aerosol number, surface and volume concentrations in Appendix B and summarized in Table XIII. The first experiments, numbers 45, 46, and 49, were performed in large bag #3. This bag was fabricated shortly after the November workshop was completed and had been used for a number of SO_2 oxidation and NO photolysis experiments. It proved to be impossible to eliminate dark reactions in this bag, and consequently, it was only used for system characterization studies.

The SO_2 photooxidation rates calculated from the aerosol volume production rates are 0.07, 0.06, and 0.10 per hour for runs 45, 46, and 49, respectively. The latter rate is believed to be higher because chamber contamination was produced by runs 47 and 48, which were NO photolysis experiments. These rates of SO_2 photooxidation do not relate directly to that expected in a clean SO_2-air system but rather give a measure of the contamination present in a particular experiment.

The next group of SO_2 experiments 52, 53, 54, 57, and 66 were performed in the small bag. Data showing the influence of bag size on aerosol production are shown in Table XIV. Only seven experiments were performed in the small bag because its volume was inadequate to allow a complete set of data to be obtained during long experiments. The SO_2 photooxidation rates with pure SO_2 and in the early phases of the SO_2 + NO + HC experiments were found to be about a factor of two lower in the small bag compared to the large bag. This is believed to be due to three factors:

(a) The average light intensity in the U of M small bag is lower because it is located at the center of the chamber and contains none of the high intensity regions near the walls,

(b) The chamber itself is less contaminated, and

(c) The walls of the small bag may act as a sink for photochemically-produced species.

TABLE IX. SUMMARY OF AEROSOL DATA FROM MARCH WORKSHOP

Run No.	System	RH %	N_{max} #-cc^{-1}	SE μm^2-cc^{-1}	$\frac{dv}{dt}(SO_2)$ μm^3-cc^{-1}-hr^{-1}	$\frac{dv}{dt}$[max] μm^3-cc^{-1}-hr^{-1}	SO_2 Photox %-hr^{-1}	Comments
6	toluene + NO	30	3.1×10^4	640	--	2.2	--	no vol. first 4 hrs
30	toluene + NO	20	1.3×10^4	750	--	2.6	--	no vol. first 4 hrs
29	toluene + NO + SO_2	30	1.6×10^5	>750	0.78	1.5	0.32	1st 4 hrs*
7	toluene + SO_2	20	2.1×10^5	800	1.17	3.2	0.45	1st 50 min*
5	hexene + NO	40	1.4×10^5	610	--	2.1	--	no vol. first 5 hrs
21	hexene + NO	37	1.2×10^5	215	--	0.5	--	no vol. first 6 hrs
18	hexene + NO + SO_2	37	1.4×10^5	>1500	0.61	5.8	0.16	1st 6 hrs*
20	hexene + SO_2	35	3.6×10^5	950	0.75	3.2	0.25	1st 60 min*
15	m-xylene + NO	38	8.4×10^4	1150	--	14.1	--	no vol. first 60 min.
14	m-xylene + NO + SO_2	29	2.6×10^5	2700	0.92	25.0	0.32	1st 60 min*
17	m-xylene + SO_2	35	2.8×10^5	384	0.84	1.6	0.23	1st 60 min*
10	cyclohexene + NO	38	3.6×10^4	3500	--	110	--	no vol. first 90 min
12	cyclohexene + NO	30	4.2×10^4	2450	--	75	--	no vol. first 3 hrs
9	cyclohexene + NO + SO_2	30	1.7×10^5	4200	0.74	105	0.28	first 2 hrs
13	cyclohexene + SO_2	35	2.7×10^5	1300	1.20	10	0.49	first 30 min
1	0.52 ppm SO_2	25	5.5×10^5	>1450	5.61 10.60	--	0.21 0.39	1st 30 min* 1st 2 hrs
4	0.55 ppm SO_2	30	3.9×10^5	4400	4.49 13.60	--	0.16 0.48	1st 30 min* 1st 2 hrs
2	0.05 SO_2	37	2.3×10^5	>575	0.65 2.35	--	0.23 0.79	1st 30 min* 1st 2 hrs
3	0.05 SO_2	40	2.9×10^5	>675	1.04 2.31	--	0.36 0.79	1st 40 min* 1st 2 hrs

*Time over which aerosol growth rate was used in computing SO_2 photooxidation.

Table X . UNIVERSITY OF MINNESOTA DUPLICATE TESTS SUBSEQUENT TO THE MARCH WORKSHOP:

SUMMARY OF AEROSOL DATA FOR HYDROCARBON EXPERIMENTS

Run No.	System	RH %	N_{max} $\#\text{-cc}^{-1}$	SE $\mu m^2\text{-cc}^{-1}$	$\frac{dv}{dt}$ SO_2 $\mu m^3\text{-cc}^{-1}\text{-hr}^{-1}$	$\frac{1}{SO_2}\frac{dv}{dt}$ $\mu m^3\text{-cc}^{-1}\text{-hr}^{-1}\text{-ppm}^{-1}$	$\frac{dv}{dt}$ [max] $\mu m^3\text{-cc}^{-1}\text{-hr}^{-1}$	SO_2 photo oxidation $\%\text{-hr}^{-1}$
65	toluene + NO + SO_2	28	185 K	330*	1.23	11.3	same	.23
76	toluene + NO	47	4.2 K	550*	--	--	24.5	---
77	toluene + NO + SO_2	57	170 K	1850	1.17	29.9	27.4	.39
87	toluene + NO	30	10 K	340	--	--	8.6	---
88	toluene + NO + SO_2	24	160 K	1600*	1.22	30.5	16.6	.67
60	hexene + NO + SO_2	28	74 K	1200*	.40	5.7	21.2	.12
78	hexene + NO + SO_2	55	230 K	1530	.53	13.9	19.1	.18
92	hexene + NO	33	8.8 K	31	--	--	.09	---
93	hexene + NO + SO_2	32	150 K	1300	.29	8.5	18.0	.16
81	m-xylene + NO	75	23 K	1600	--	--	73	---
82	m-xylene + NO + SO_2	54	230 K	2800	.49	10.4	67	.14
89	m-xylene + NO	26	21 K	1000*	--	--	38	---
91	m-xylene + NO + SO_2	26	230 K	1600	.46	10.0	31	.21
83	cyclohexene + NO	51	.9 K	320	--	--	50	---
94	cyclohexene + NO	31	2.7 K	510	--	--	65	---
95	cyclohexene + NO	29	1.9 K	620	--	--	190	---
96	cyclohexene + NO + SO_2	28	280 K	5400	.43	9.7	250	.20

*Equilibrium surface not reached.

TABLE XI. SUMMARY OF CHEMISTRY DATA FROM MARCH WORKSHOP

Run No.	System	RH %	HC ppm	SO_{2i} ppm	NO_i ppm	$t(NO_2)_{max}$ min	O_{3max} ppm
6	toluene + NO	30	0.35	--	0.170	400	0.285
30	toluene + NO	20	1.17	--	0.530	480	0.380
29	toluene + NO + SO_2	30	0.35	0.05	0.146	330	> 0.225
7	toluene + SO_2	20	0.35	0.05	b	b	0.047
5	hexene + NO	40	0.33	--	0.150	420	> 0.200
21	hexene + NO	37	0.33	--	0.180	420	0.275
18	hexene + NO + SO_2	37	0.33	0.07	0.178	430	--
20	hexene + SO_2	35	0.33	0.055	b	b	0.052
15	m-xylene + NO	38	0.34	--	0.150	100	0.222
14	m-xylene + NO + SO_2	29	0.34	0.055	0.150	105	0.305
17	m-xylene + SO_2	35	0.34	0.07	b	b	0.030
10	cyclohexene + NO	38	0.33	--	0.138	120	0.190
12	cyclohexene + NO	30	0.33	--	0.140	190	0.192
9	cyclohexene + NO + SO_2	30	0.33	0.05	0.220	180	0.325
13	cyclohexene + SO_2	35	0.33	0.06	b	b	0.011

Table XII. UNIVERSITY OF MINNESOTA DUPLICATE TESTS SUBSEQUENT TO THE MARCH WORKSHOP:

SUMMARY OF CHEMICAL DATA FOR HYDROCARBON EXPERIMENTS

Run No.	System	RH %	HC ppm	SO_{2i} ppm	NO_i ppm	$[NO_2]_{max}$ ppm	$t[NO_2]_{max}$ min	$[O_3]_{max}$ ppm
65	toluene + NO + SO_2	28	.35	.108	.30	.145*	460	.2*
76	toluene + NO	47	.35	--	.152	.095	210	.30
77	toluene + NO + SO_2	57	.38	.039	.155	.115	160	.362
87	toluene + NO	30	.35	--	.155	.140	130	.402
88	toluene + NO + SO_2	24	.35	.040	.17	.122	155	.315*
60	hexene + NO + SO_2	28	.35	.07	.16	.123	395	.162*
78	hexene + NO + SO_2	55	.35	.038	.165	.130	255	.438
92	hexene + NO	33	.35	--	.12	.104	280	.290
93	hexene + NO + SO_2	32	.35	.034	.122	.125	350	.302*
81	m-xylene + NO	75	.35	--	.155	.144	80	.343
82	m-xylene + NO + SO_2	54	.35	.047	.151	.130	94	.361
89	m-xylene + NO	26	.35	--	.132	.142	68	.379
91	m-xylene + NO + SO_2	26	.35	.046	.117	.115	70	.262
83	cyclohexene + NO	51	.35	--	.13	.101	90	.32*
94	cyclohexene + NO	31	.35	--	.103	.108	60	.20
95	cyclohexene + NO	29	.35	--	.124	.128	103	.254
96	cyclohexene + NO + SO_2	28	.35	.045	.133	.130	85	.241

*max not reached by end of irradiation period.

TABLE XIII. UNIVERSITY OF MINNESOTA DUPLICATE TESTS SUBSEQUENT TO THE MARCH WORKSHOP: SUMMARY OF SO_2 EXPERIMENTS

Run No.	Concentration ppm	RH %	N_{max} #-cc^{-1}	SE μm^2-cc^{-1}	$\frac{dv}{dt}$ SO_2 μm^3-cc^{-1}-hr^{-1}	$\frac{1}{SO_2}\frac{dv}{dt}$ μm^3-cc^{-1}-hr^{-1}-ppm^{-1}	SO_2 photox %-hr^{-1}
45	.59	28	260 K	470	1.9	3.2	.07
46	.59	40	340 K	570	2.2	3.8	.065
49	.59	67	590 K	800	5.6	9.4	.10
52	.56	36	90 K	190	.46	.83	.015
53	.56	30	670 K	2100	20	3.7	.07
54	.56	25	100 K	190	.28	.50	.01
57	.56	12	39 K	210	.78	1.4	.04
66	.61	27	100 K	680*	2.7	4.5	.10
68	.62	39	94 K	310	1.1	1.8	.03
69	.053	40	280 K	270	.84	16	.27
70	.54	57	210 K	400*	1.2	2.2	.03
71	.048	55	95 K	200*	.32	6.6	.09
72	.50	54	220 K	840*	4.2	8.5	.12
79	.038	70	68 K	110*	.21	5.6	.06
80	.40	78	250 K	550	2.2	5.5	.05
85	.38	34	245 K	640	2.5	6.6	.13
86	.051	27	82 K	190	.35	6.8	.14
97	.035	27	100 K	270*	1.1	30	.63

*Equilibrium surface not reached, maximum surface.

If (c) is indeed an important factor, it may help to explain the slightly higher (~0.2%) SO_2 oxidation rates noted in the Calspan chamber under clean conditions and similar lighting intensities. No clear trend is apparent when the maximum volumetric aerosol production rates observed with SO_2 + NO + HC in large and small bags are compared. In the systems studied, the growth phase corresponding to the most rapid rate of aerosol production came so late in the experiment that the bag was nearly collapsed, and so it is difficult to point to any clear-cut effects. Additional experiments should be performed with more reactive hydrocarbons in order that the times to $NO_{2[max]}$ and $O_{3[max]}$ are achieved earlier in the experiment.

TABLE XIV. INFLUENCE OF BAG SIZE ON AEROSOL PRODUCTION

System	Small Bag Run No.	Small Bag $\frac{dv}{dt}$ [max] μm^3-cc^{-1}-hr^{-1}	Small Bag Apparent SO_2 Photooxidation Rate %-hr^{-1}	Large Bags Run No.	Large Bags $\frac{dv}{dt}$ [max] μm^3-cc^{-1} hr^{-1}	Large Bags Apparent SO_2 Photooxidation Rate %-hr^{-1}
SO_2+clean air	(52,53, 54,57, 60)	--	0.05	11 runs		0.10
SO_2+NO+Hexene	(69)	21.2	0.12	78	19.1	0.18
SO_2+NO+toluene	(65)	1.4	0.23	77, 88	22.0	0.53

In reviewing the data in Table XIII, U of M experiments 52 and 54 show low apparent SO_2 photooxidation rates of 0.015 and 0.01% hr^{-1}, respectively. Experiment 57 was performed after two NO photolysis experiments and shows only slight contamination in its higher SO_2 photooxidation rate of 0.04%/hr. Experiment 66 shows more evidence of contamination with an apparent SO_2 photooxidation rate of 0.1% hr^{-1}. Since run 65 was a toluene + NO + SO_2 experiment, the higher rate of photooxidation in run 66 is possibly a result of contaminants remaining on the bag surface after the previous run.

The remaining SO_2 experiments in this series were performed in a new large bag (LB-4). Run 68 was the first SO_2 experiment in the large bag; no dark growth was observed, and the apparent rate of SO_2 photooxidation was 0.03%/hr. Runs 69-72 were all SO_2 experiments and showed a considerable variation in the apparent SO_2 photooxidation rate. This type of variation has been observed previously with new bags and is believed to be related to a conditioning process in the chamber. (The SO_2 oxidation rate tends toward lower values but will vary in both directions depending on the purity of the chamber air.) After run 72, a series of hydrocarbon experiments were started. The next SO_2 experiments were runs 79 and 80 which immediately followed a 1-hexene + NO + SO_2 experiment. The apparent SO_2 photooxidation rates in these experiments are fairly low, 0.06 and 0.05%/hr, respectively, but higher than the lowest levels attained in the first large bag (0.02%/hr in run 6) used after the November workshop. It is of interest to note that the apparent photooxidation rates in runs 79 and 80 are nearly equal, despite the fact that the SO_2 concentration in run 79 is 0.038 ppm, whereas in run 80 it is 0.40 ppm. This suggests that either all or a constant fraction of the aerosol formed in these experiments results from SO_2 photooxidation.

Runs 85 and 86 are another pair of SO_2 photooxidation experiments at high and low SO_2 levels. These runs followed another series of experiments involving hydrocarbons and NO. The presence of contamination is indicated by the rather high apparent photooxidation rates, 0.13 and 0.14%/hr for these runs. The last SO_2 experiment in this series, run 97, shows even more contamination with an apparent photooxidation rate of 0.63%/hr.

It is evident from these results that the apparent SO_2 photooxidation rate, based on measurements of aerosol formation in the SO_2 pure air system, is quite dependent upon the experiments performed prior to making a run. This is especially true in the U of M system. Previous exposure of the bag to hydrocarbons and NO leads to enhanced aerosol formation. Apparently,

reactive materials are either adsorbed or absorbed by the Teflon bag and only slowly desorb when the bag is flushed with clean air.

In the Calspan chamber, there is somewhat less of a conditioning effect on SO_2 oxidation and also less influence from the history of previous experiments. It is possible that this is due to the very low surface-to-volume ratio of the Calspan chamber and the fact that the walls are less of an influence on the behavior of aerosol and gaseous species.

4.4.2 Hydrocarbon Experiments

Several types of hydrocarbon experiments were performed at the workshop and later at the University of Minnesota. At Calspan the three main systems studied were: HC + NO, HC + SO_2, and HC + NO + SO_2. Two basic types of experiments were performed at the U of M: HC + NO and HC + NO + SO_2. Initial reactant concentrations in each case were set as closely as possible to 0.35 ppm (volume) HC, 0.15 ppm NO, and 0.05 ppm SO_2. Again, the main experimental conditions and results are listed in Tables IX through XII.

Plots of aerosol number, surface and volume concentrations against time and NO, NO_2, O_3, and hydrocarbon concentrations against time are given in Appendix B. The plots are grouped together according to hydrocarbon type and are in the same order as the runs listed in Tables IX through XI. The chemical reactivity of these systems is characterized by listing the time to the NO_2 peak and the maximum ozone concentration produced. In the U of M tests, considerable lack of reproducibility existed in the ozone measurements, apparently as a result of day-to-day variations in the sensitivity of the ozone instrument. Some run-to-run variation is also evident in the NO-NO_2 results; however, this variation is believed to be real because both NO-NO_2 analyzers were stable and readily calibrated. Consequently, the main measure of chemical reactivity of both the hydrocarbon + NO and the hydrocarbon + NO + SO_2 will be taken as the time to maximum NO_2 concentration, $t[NO_2]_{max}$. A shorter time implies a more reactive system.

In addition to these conventional measures, HC reactivity can also be described in terms of aerosol behavior. The parameters used are: maximum number concentration, maximum surface concentration, and two rates of volume production. These parameters were chosen for the following reasons:

(1) Some description of number concentration was considered necessary because CNC data are easily obtained and other investigators have presented such data for various photochemical systems.

(2) Maximum surface concentration, S_M, is listed because many photochemical systems tend to establish an equilibrium surface concentration (Clark & Whitby, 1975) which is related to the rate of aerosol volume (or mass) production.

(3) The volume of aerosol formed multiplied by its density gives the mass of aerosol formed. The density of these particles should not be very different from unity. (Most organic acids and H_2SO_4 lie in the range of 0.8 to 1.2 gm/cm^3.) Consequently, the aerosol volume is nearly proportional to aerosol mass. Since mass is a conserved quantity, the rate of mass formation in the aerosol phase must equal the rate of mass removal from the gas phase. The rate of volume production is, therefore, directly proportional to the rate of condensation of slightly volatile species formed by photochemical reactions. Volume against time plots for these experiments have a rather complex shape. Consequently, two volumetric production rates are defined and tabulated in Tables IX and X, namely $(dv/dt)SO_2$, the slope of the essentially linear volume against time curve which is established early in HC + NO + SO_2 or HC + SO_2 experiments and $(dv/dt)_{max}$, the maximum rate of volume production.

4.4.3 Hydrocarbon + NO Experiments

The HC + NO systems were found to behave quite differently from the simple SO_2 + clean air experiments. Each hydrocarbon + NO experiment can be divided into two phases. In the first phase, NO is converted to NO_2, and some oxidation of the hydrocarbon occurs. O_3 starts to appear near the end

of this phase as NO concentrations become very low. The second phase begins as soon as the initial NO has been oxidized out of the system and NO_2 reaches its maximum concentration. During this phase [NO] remains low, and [NO_2] gradually decreases as NO_2 is converted to higher oxides, acids, peroxyacyl nitrates, and other nitrogen compounds; ozone grows rapidly and approaches a maximum; and aerosol formation takes place.

Typical examples of this two-phase behavior is shown in Figures 6 and 7 in which Calspan and U of M hexene-1 + NO experiments are compared. It may be seen from the data that the NO disappears and NO_2 maximizes in about 420 minutes in the Calspan experiment and about 280 minutes in the U of M test. These times are considered as the duration of the first phase for each case. The plots also show that by the end of this phase some ozone has started to appear and the hydrocarbon concentration has started to decrease rapidly. The aerosol data show no measurable aerosol production during this phase in the U of M experiment, but some particles in the Calspan experiment can be noted. The particles are so small, however, that the EAA does not detect their presence.*

Early in the second phase, growth proceeds rapidly. The same physical mechanisms control aerosol formation in this system as in the SO_2 + clean air system, i.e., nucleation, condensation, and coagulation. In the Calspan experiment, note the sharp inflection at this point as the concentration increases and in the corresponding U of M test the sudden appearance of aerosol. In both experiments, there is a corresponding increase in the surface and volume concentration of aerosol. For all of the hydrocarbon + NO systems studied, the number of particles formed was less then in the SO_2 + clean air case, but in every case (except for hexene + NO) the volume was always

---

* This is a particularly useful illustration in that it shows the various detection limits of CN counters used in these tests. For this experiment the Environment-One CN counter did not detect particles early in the first phase of the Calspan test, even though the more sensitive Gardner small particle detector measured the concentrations shown. This situation was found to occur frequently in other experiments.

CALSPAN
RUN NO. 5 22 FEBRUARY 1974 HEXENE-1 - NO-FILTERED AIR SYSTEM R.H. = 41%; HEXENE-1 = 0.33 ppm;
NO = 0.152 ppm; NO_2 = 0.014 ppm

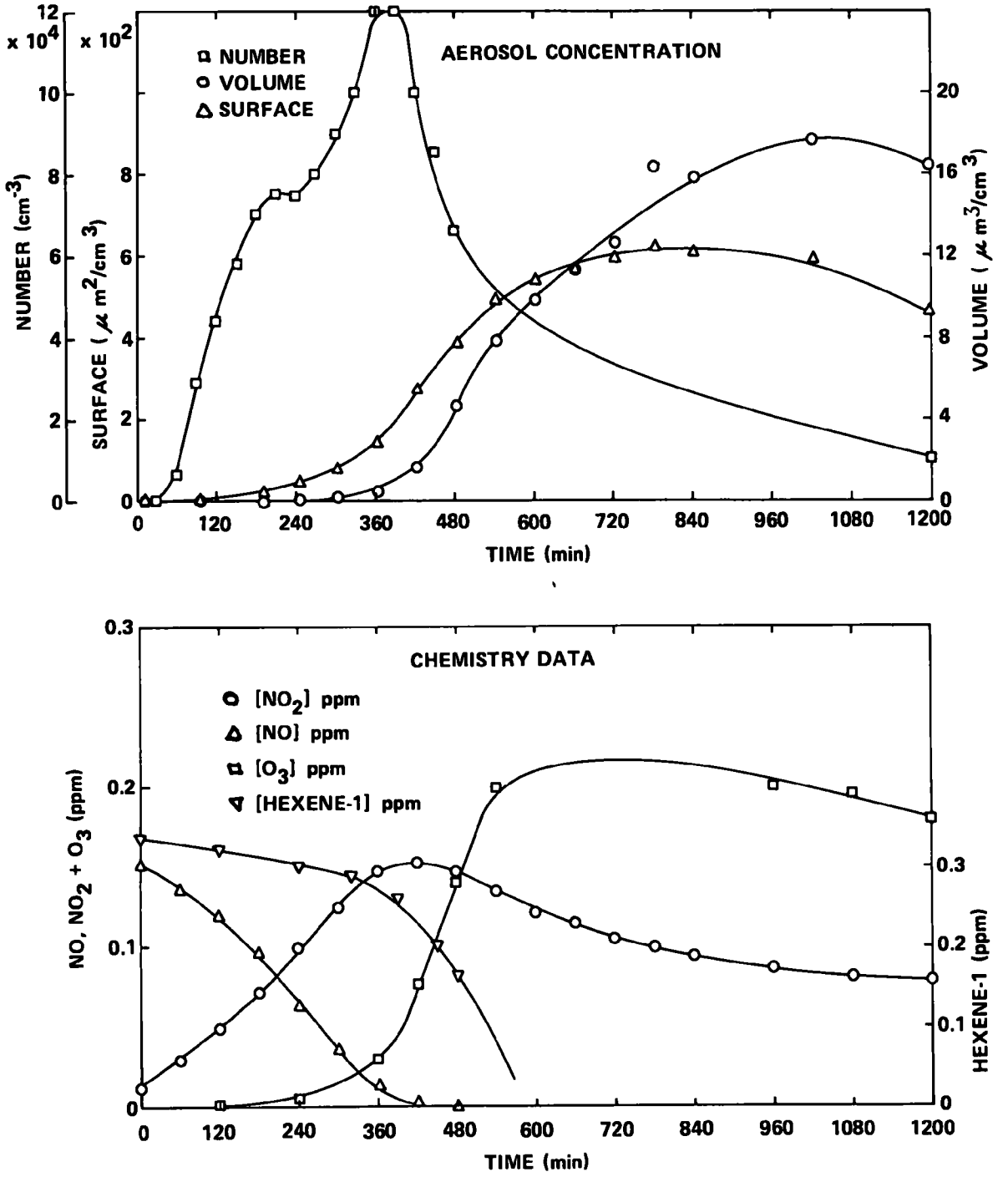

FIGURE 6

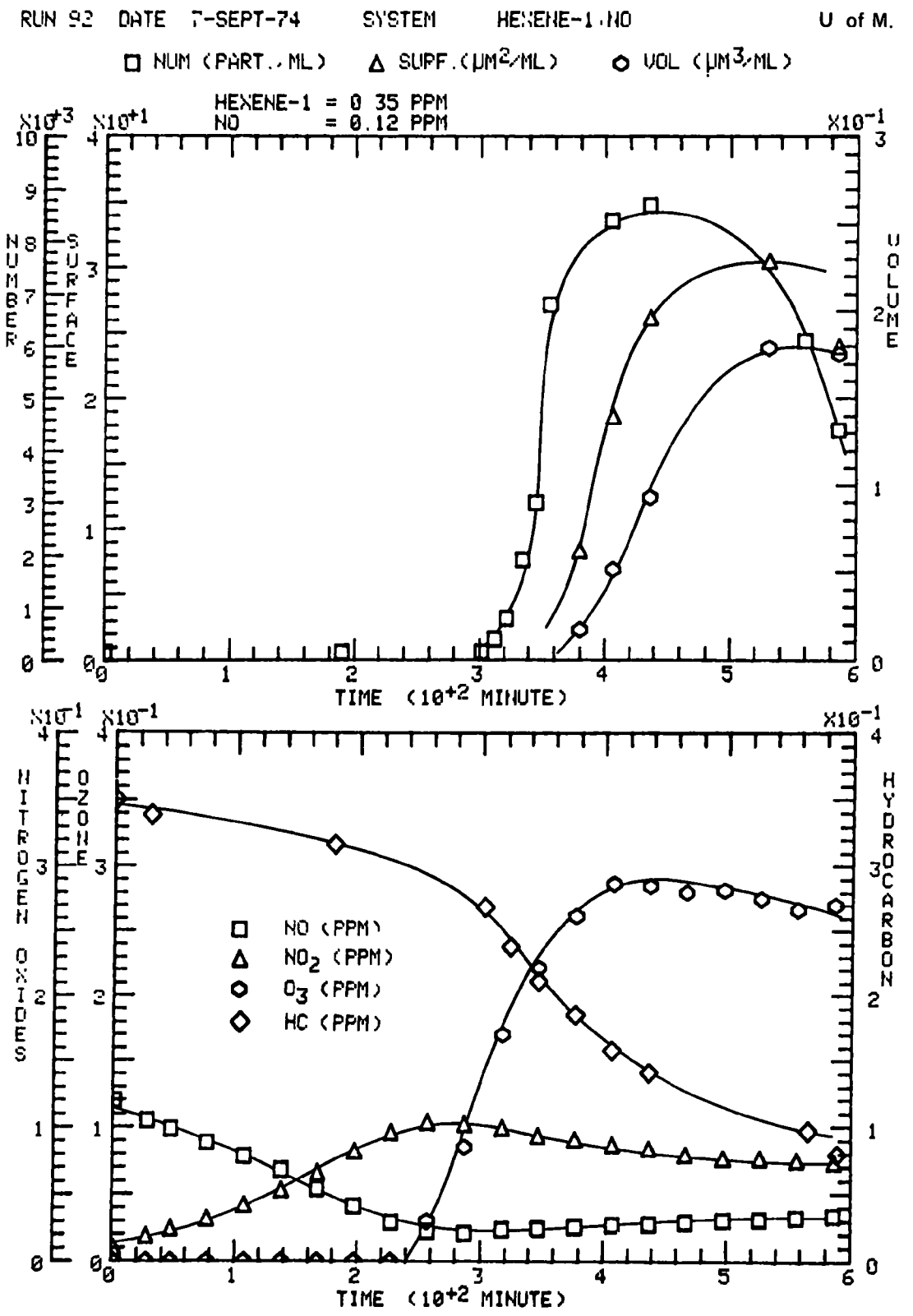
RUN 92 DATE 7-SEPT-74 SYSTEM HEXENE-1/NO U of M.
NUM (PART./ML) SURF.(μM²/ML) VOL (μM³/ML)
HEXENE-1 = 0.35 PPM
NO = 0.12 PPM
X10+3
X10+1
X10-1
NUMBER
SURFACE
VOLUME
TIME (10+2 MINUTE)
X10-1
X10-1
X10-1
NITROGEN OXIDES
OZONE
HYDROCARBON
NO (PPM)
NO2 (PPM)
O3 (PPM)
HC (PPM)
TIME (10+2 MINUTE)

FIGURE 7

larger, implying the production of fewer but larger particles. Another important difference between the aerosol behavior of the hydrocarbon + NO systems studied and that of the SO_2 + clean air systems is the shape of the volume against time curves. They are no longer linear. Volume grows rapidly early in the second phase; later the rate decreases and eventually volume becomes essentially constant or even drops as the largest particles are lost from sedimentation and fall out. In these cases, the species driving aerosol growth becomes depleted and, consequently, new aerosol volume production stops.

The chemical behavior of the system in the second growth phase is also shown in Figures 6 and 7. Production of ozone proceeds rapidly and ozone concentration maximizes at about the same time that the aerosol volume curve reaches its plateau; NO_2 decreases continuously while hexene is oxidized out of the system more rapidly as the ozone concentration increases. In the Calspan experiment, the ozone monitor was set for 0.2 ppm full scale so that the ozone max was not observed. Another nearly identical case, however, (run no. 21) produced an ozone max of 0.275 ppm.

The aerosol and chemical behavior shown in Figures 6 and 7 is quite typical of all HC + NO experiments performed. The most pronounced difference between the four hydrocarbons studied was in the rates of NO oxidation and the rates of aerosol formation. Each of the systems are individually characterized below.

In terms of NO oxidation and aerosol formation rates, toluene was found to be the least reactive hydrocarbon in the Calspan chamber, followed closely by hexene. This is, perhaps, the most significant difference between the sets of data generated by Calspan and the U of M. In the Minnesota studies, 1-hexene proved to be less reactive than toluene. For example, in the 1-hexene + NO experiment shown in Figure 7, the maximum aerosol volumetric production rate $(dv/dt)_{max}$ was only 0.09 $\mu m^3/cc^{-1}hr^{-1}$ and the maximum aerosol surface area S_M was 3 $\mu m^2/cc$, both lower than any other hydrocarbon system investigated. By contrast, in the toluene + NO case (run #76), a

volumetric rate of $(dv/dt)_{max}$= 24.5 $\mu m^3/cc\text{-}hr^{-1}$ was measured with a maximum surface area of 550 $\mu m^2/cc$. The effect of relative humidity on aerosol behavior in the toluene + NO system can be seen by comparing runs 76 and 87 in Table X. In run 87, the relative humidity was lower and aerosol was formed less rapidly with $(dv/dt)_{max}$= 8.6 $\mu m^3/cc\text{-}hr^{-1}$ and S_{MAX} = 340 $\mu m^2/cc$. The change in relative humidity produces no change in the observed chemical behavior of the system, however. The large difference in aerosol production would then seem to be due solely to the formation of particles having a higher water content. Evidently, rather hygroscopic products were being formed even in the toluene + NO case, since the relative humidity was only 50%.

The m-xylene + NO data generated by Calspan and the U of M compare very favorably. Both aerosol and chemical measurements showed the m-xylene + NO systems to be considerably more reactive than either 1-hexene + NO or toluene + NO. Times for NO_2max were only 80 and 68 minutes for the U of M experiments and 100 minutes for the Calspan experiment (see Tables XI and XII). Aerosol and chemistry data for these experiments are shown in Figures 8 and 9. The data show similar results: No aerosol is produced until approximately the time of NO disappearance and rapid formation of ozone. The U of M data show a slight (10 min) lag between disappearance of NO and the onset of aerosol formation. The volume and surface concentration for these tests is substantially higher than for the toluene + NO and hexene + NO cases. An expected humidity effect was noted in the U of M experiments; run 81 @ 75% RH produced about twice as much aerosol volume as run 89 performed at 26% RH.

Three cyclohexene + NO runs were performed at the U of M and two at Calspan during the March workshop. The data compare very well showing cyclohexene to have about the same reactivity as m-xylene in terms of NO oxidation rate but much greater reactivity than any of the other hydrocarbons tested in terms of aerosol production. In the cyclohexene cases, the aerosol growth was almost explosive once oxidation of NO was complete. Both the

FIGURE 8

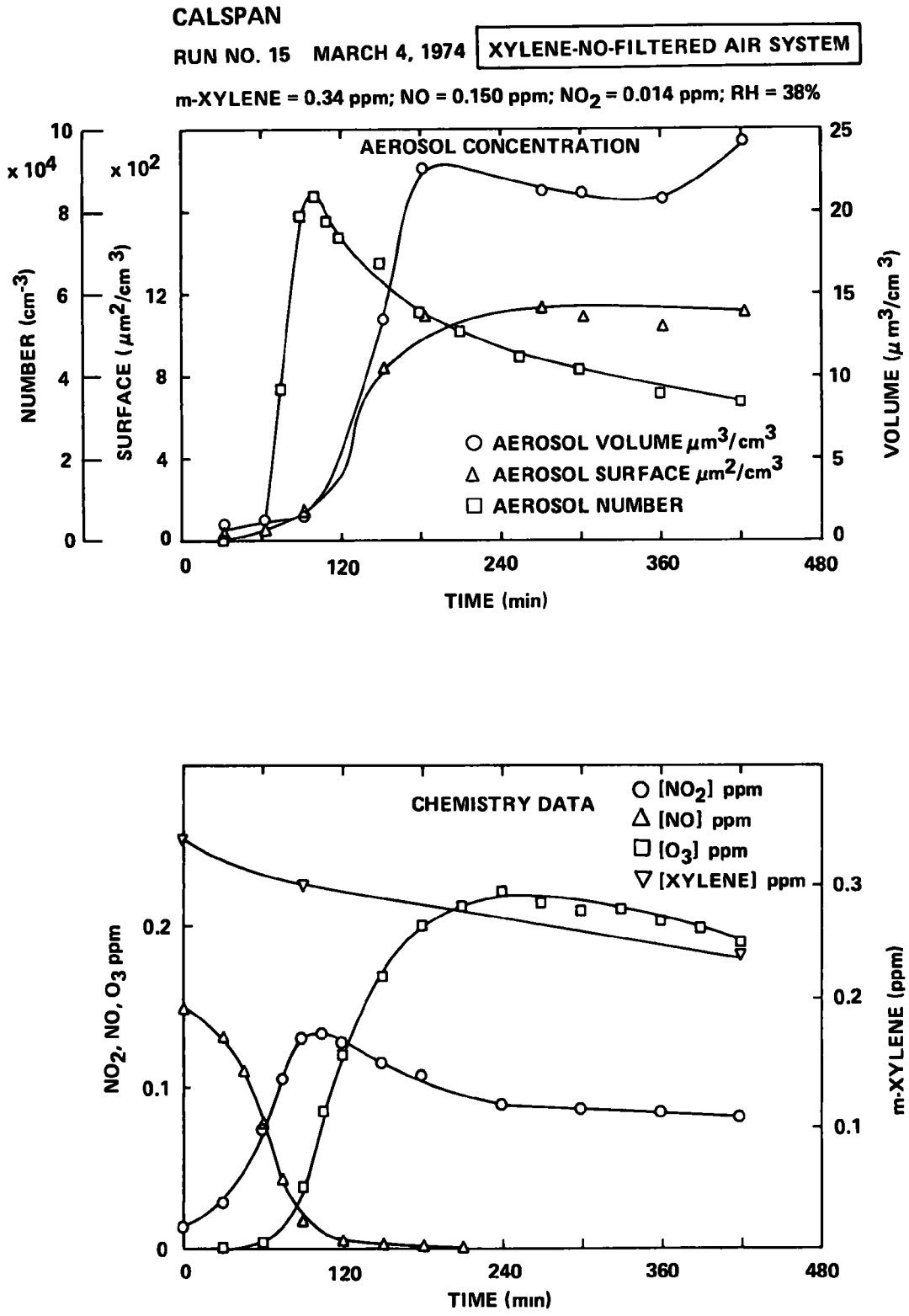
CALSPAN
RUN NO. 15 MARCH 4, 1974
XYLENE-NO-FILTERED AIR SYSTEM
m-XYLENE = 0.34 ppm; NO = 0.150 ppm; NO_2 = 0.014 ppm; RH = 38%
AEROSOL CONCENTRATION
x 10^4
x 10^2
NUMBER (cm^{-3})
SURFACE ($\mu m^2/cm^3$)
VOLUME ($\mu m^3/cm^3$)
AEROSOL VOLUME $\mu m^3/cm^3$
AEROSOL SURFACE $\mu m^2/cm^3$
AEROSOL NUMBER
TIME (min)
CHEMISTRY DATA
[NO_2] ppm
[NO] ppm
[O_3] ppm
[XYLENE] ppm
NO_2, NO, O_3 ppm
m-XYLENE (ppm)
TIME (min)

FIGURE 9

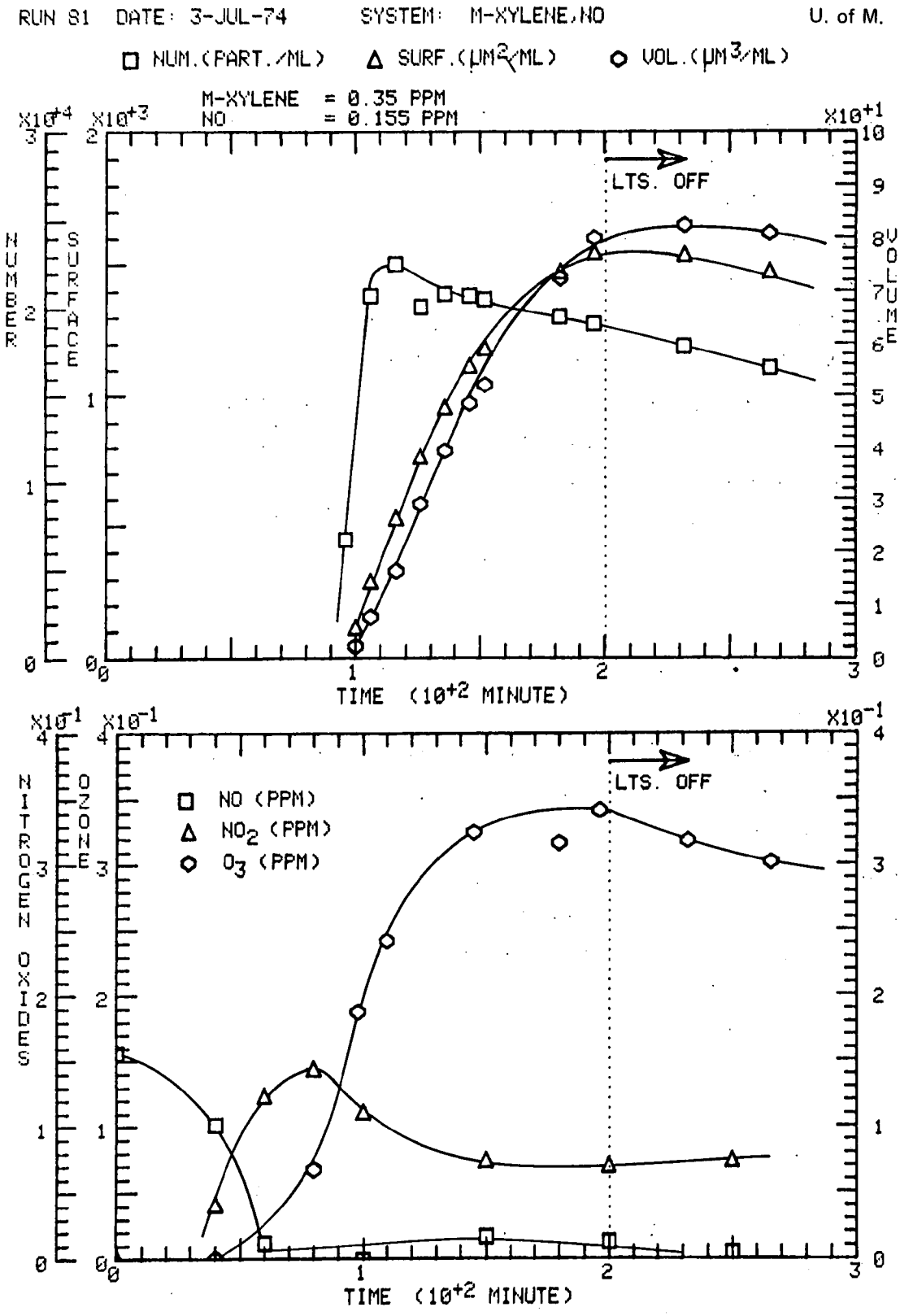
RUN S1 DATE: 3-JUL-74 SYSTEM: M-XYLENE/NO U. of M.
NUM.(PART./ML) SURF.(μM²/ML) VOL.(μM³/ML)
M-XYLENE = 0.35 PPM
NO = 0.155 PPM
X10+4
X10+3
X10+1
NUMBER
SURFACE
VOLUME
LTS. OFF
TIME (10+2 MINUTE)
X10-1
X10-1
X10-1
NITROGEN OXIDES
OZONE
NO (PPM)
NO2 (PPM)
O3 (PPM)
LTS. OFF
TIME (10+2 MINUTE)

surface and volume concentrations of aerosol were much higher than any other system, even though the number of particles was actually less. This implies the presence of extremely large particles and, indeed, this is the case, as in the Calspan experiments where nephelometer measurements were made, and substantial visibility losses were noted after only 2.5 hours of irradiation. Aerosol and chemistry plots from a Calspan and U of M experiment are shown in Figures 10 and 11. The volume production rates $(dv/dt)_{max}$ of 75 to 110 $\mu m^3/cc\text{-}hr^{-1}$ for the Calspan chamber and between 50 and 190 $\mu m^3/cc\text{-}hr^{-1}$ for the U of M are the highest we have measured and substantially higher than that observed in typical urban polluted atmospheres. As well as oxidizing NO quickly and leading to rapid aerosol formation, the cyclohexene itself was quickly oxidized out of the system, as the data in Figures 10 and 11 show.

From the chemistry data for all the hydrocarbon experiments, a family effect is apparent. Cyclohexene and hexene, both olefins, have curves of basically the same shape: a gradual decrease with time until after the NO is oxidized out of the system, followed by rapid decay as ozone builds and aerosol forms. Toluene and m-xylene, both aromatics, have a different shape. In both cases, hydrocarbon concentration decays gradually and at a more or less constant rate. No change is evident in the decay curve once ozone appears and aerosol formation begins.

4.4.4 Hydrocarbon + SO_2 Experiments

During the March workshop, four hydrocarbon + SO_2 experiments were performed at Calspan. The purpose of these experiments was to examine SO_2 oxidation and subsequent aerosol behavior in the presence of hydrocarbons, but without the addition of any NO beyond that normally found in clean country air (i.e., NO <0.01 ppm). As in the other experiments from the March workshop, the chemistry and aerosol data for these tests are summarized in Tables IX and X. Time histories of the data are shown in Appendix B.

By-and-large the data show that the SO_2 oxidation rate for the first hour or so is similar to that for SO_2 alone, followed by a period of accelerated growth. The accelerated growth portion of the experiment is listed as $(dv/dt)_{max}$ in Table IX. Note from the table that, even in the SO_2 + clean air experiments, an initial and final volumetric growth rate was observed; however, the difference in rates was not nearly as large as in the hydrocarbon-polluted SO_2 systems. For example, the average initial rate of SO_2 oxidation for the two Calspan experiments using a 0.05 ppm SO_2 + clean air (runs 2 and 3) was about 0.29% hr^{-1} with a final rate of approximately 0.79% hr^{-1}. For the four hydrocarbon-polluted systems, the average initial SO_2 oxidation rate was ~0.35% hr^{-1} with a final rate, based on $(dv/dt)_{max}$ of about 1.6% hr^{-1}. Since the shape of the aerosol curves for the HC + SO_2 systems is so similar to the SO_2 + clean air systems, specific data plots are not presented here. Very little chemical changes occurred since only background levels of NO_x were present and only modest levels of ozone were produced. The main differences were in the amount of aerosol produced by the hydrocarbon contaminant, and this can be seen from the data in Table IX.

Toluene and hexene were found to have about the same effect on accelerating apparent SO_2 oxidation rate, while cyclohexene was observed to have a much greater impact on aerosol behavior. In the cyclohexene + SO_2 experiment, run 13, volume production $(dv/dt)_{SO_2}$ was 1.20 $\mu m^3/cc\text{-}hr^{-1}$ for the first 30 min, followed by an increased rate of 10 $\mu m^3/cc\text{-}hr^{-1}$ for the remainder of the experiment (an additional two hours). In the toluene and hexene + SO_2 runs, the final volumetric production rates were three to four times greater than the initial rate. M-xylene, on the other hand, was found to have the smallest effect with a final rate only about twice as great as the initial growth stage. Since only one experiment of each type could be run during the workshop, the magnitude of the increase cannot be considered conclusive yet. It seems apparent, however, that the presence of hydrocarbon contamination during SO_2 irradiations, even in the absence of appreciable NO, substantially increases the overall production of aerosol.

FIGURE 10

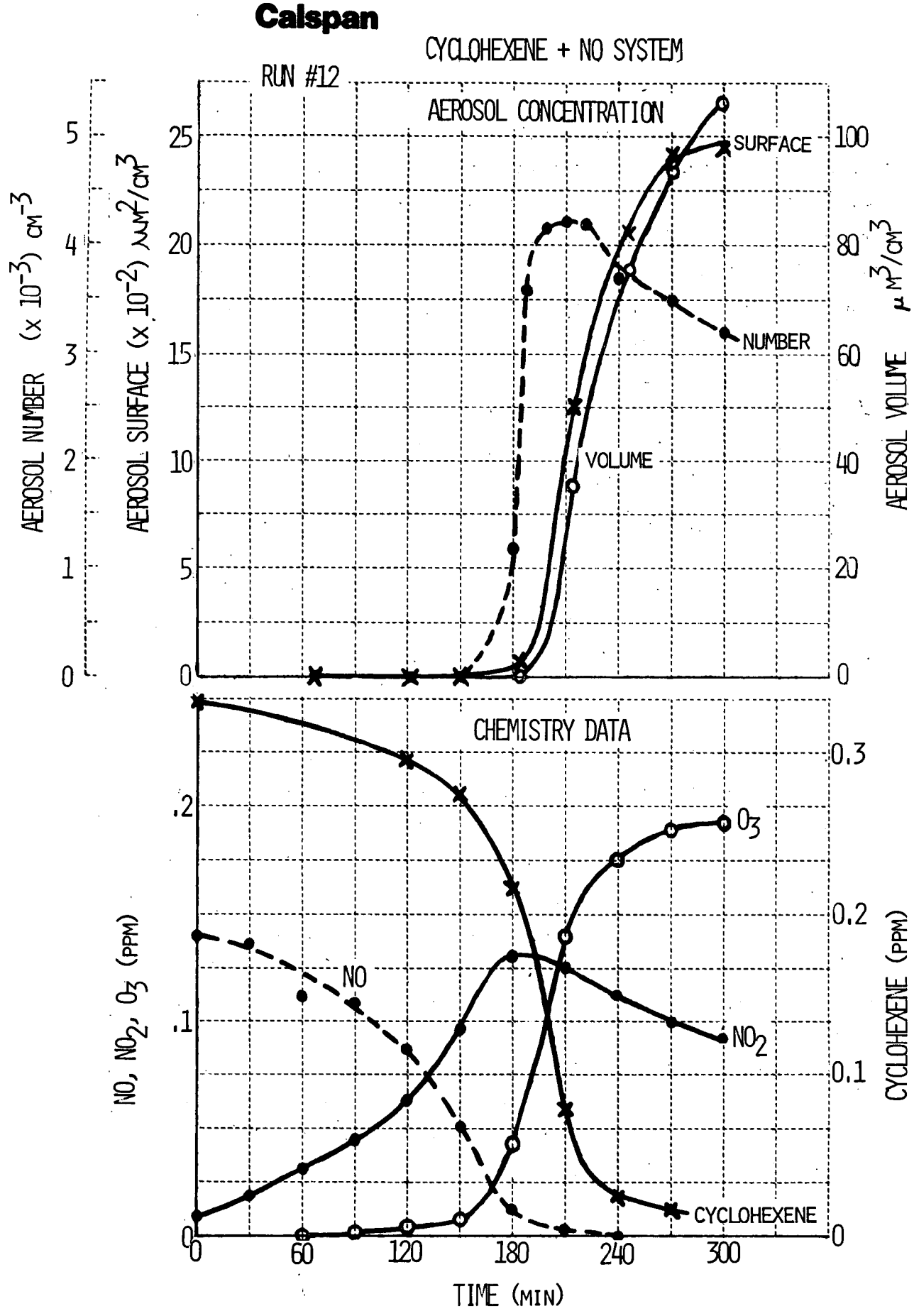
Calspan
CYCLOHEXENE + NO SYSTEM
RUN #12
AEROSOL CONCENTRATION
AEROSOL NUMBER (x 10⁻³) cm⁻³
AEROSOL SURFACE (x 10⁻²) μM²/cm³
AEROSOL VOLUME μM³/cm³
SURFACE
NUMBER
VOLUME
CHEMISTRY DATA
NO, NO₂, O₃ (PPM)
CYCLOHEXENE (PPM)
O₃
NO
NO₂
CYCLOHEXENE
TIME (MIN)

FIGURE 11

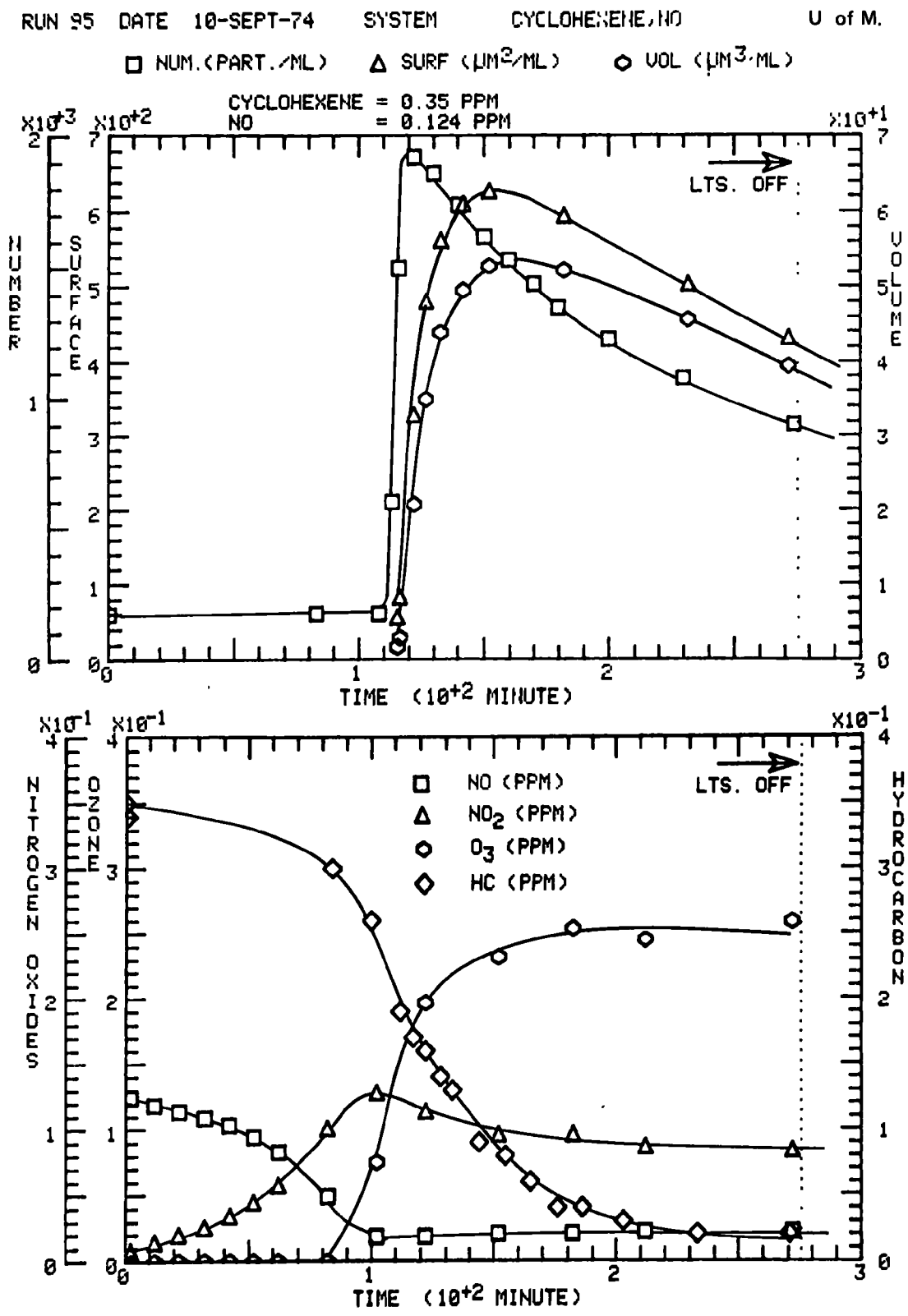
RUN 95 DATE 10-SEPT-74 SYSTEM CYCLOHEXENE/NO U of M.
NUM.(PART./ML) SURF (μM²/ML) VOL (μM³/ML)
CYCLOHEXENE = 0.35 PPM
NO = 0.124 PPM
LTS. OFF
NUMBER
SURFACE
VOLUME
TIME (10+2 MINUTE)
NO (PPM)
NO2 (PPM)
O3 (PPM)
HC (PPM)
NITROGEN OXIDES
OZONE
HYDROCARBON

4.4.5 Hydrocarbon + NO + SO_2 Experiments

An additional degree of complexity is introduced when SO_2 is added to the HC + NO_x system. In terms of the chemical species which we monitor, NO, NO_2, O_3, and hydrocarbon, the experiments with and without SO_2 are virtually identical. The aerosol behavior, however, is quite different when SO_2 is added. During the first phase of the experiment, aerosol growth occurs in a manner very similar to that of a simple SO_2 + clean air experiment; i.e., an essentially linear curve of volume against time. As the second phase of the experiment begins, the rate of volume production increases markedly. During this phase the growth curves are more like the hydrocarbon + NO experiments, except that the aerosol number concentrations are higher. In terms of qualitative behavior, a hydrocarbon + NO + SO_2 experiment behaves almost as though it resulted from a linear combination of the hydrocarbon + NO system and the SO_2 + clean air system. Quantitatively, however, this is not the case. In both growth phases, more aerosol is usually formed than would be predicted by a simple linear combination of the hydrocarbon + NO system and the SO_2 + clean air system. The details of these interactions are discussed more fully below as each hydrocarbon system is treated individually.

As previously stated, the greatest differences between the Calspan and U of M data were found in the toluene systems. At the U of M, toluene was observed to be substantially more reactive (in terms of aerosol behavior) than hexene but less than m-xylene or cyclohexene. At Calspan toluene was the least reactive, followed by hexene, m-xylene and cyclohexene.

For the toluene + NO + SO_2 system, Calspan experiment #29, very little effect was observed over that produced by toluene + NO alone. There was, of course, initial aerosol growth soon after the start of irradiation due to SO_2 oxidation and the formation of H_2SO_4 particles. However, once oxidation of NO was complete, more than six hours later, only a slight increase in aerosol production was detected. Chemical and aerosol data for this experiment are shown in Appendix B and compared with the U of M experiments.

At the U of M the initial phase of aerosol growth in the toluene + NO + SO_2 system was very similar to Calspan's; i.e., before the oxidation of NO was complete, aerosol growth was like that of a SO_2 + clean air system, but higher. Apparent SO_2 oxidation rates for the first 70-100 minutes ranged from 0.23 to 0.67% hr^{-1} at the U of M, compared to a rate of 0.32% hr^{-1} for the first 240 minutes of the Calspan experiment. Compared to all of the other computed SO_2 oxidation rates for the U of M tests the toluene + NO + SO_2 system was the highest. This is rather surprising because toluene is not normally believed to be a highly reactive hydrocarbon.

During the second stage of aerosol growth, appreciably greater volumetric production rates, $(dv/dt)'_{max}$ were observed in the U of M tests, compared to the corresponding Calspan experiment. The values of $(dv/dt)'_{max}$ in U of M runs 77 and 88 were 27.4 and 16.6 $\mu m^3/cc\text{-}hr^{-1}$, respectively, compared to about 1.5 $\mu m^3/cc\text{-}hr^{-1}$ in the Calspan experiment. The rates in both cases are similar to those observed in the corresponding hexene + NO + SO_2 experiments.

In comparing the toluene + NO + SO_2 experiments with toluene + NO, it can be seen that the nature of aerosol growth is quite different in the second phase. Especially in the U of M cases (e.g., runs 76 and 77 and 87 and 88), the experiments reveal that, although aerosol volume production in the second growth phase is similar with and without the addition of SO_2, much larger surface and number concentrations are produced when SO_2 is present. Thus, the particle diameters must be much smaller. (This effect is discussed in more detail in the next section.) Similarly in the Calspan experiment, the number concentration in the SO_2 case is more than an order of magnitude greater than in the toluene + NO case. The surface, however, is not any greater, but this is deceiving since the surface concentration was still increasing at the end of the experiment (No. 29).

Run 65, the only toluene experiment performed in the small bag at the U of M, shows much slower aerosol and chemistry progress than the other

toluene + NO + SO_2 experiments. This probably results from two factors: lower mean light intensity in the small bag and the inadvertent high NO concentration (0.30 ppm) used in this experiment. Bag loss effects could also be involved, but it is impossible to separate the factors leading to the observed behavior, and the two reasons given above are believed to be the most likely explanations for the decreased reactivity of the system.

Three hexene + NO + SO_2 experiments were run at the U of M (runs 60, 78, and 93) and one at Calspan during the March workshop (run 18). The addition of SO_2 was found to appreciably increase aerosol formation in both the Calspan and U of M tests but, as expected, had little effect on the chemical changes. Aerosol and chemistry data for the two sets of data are compared in Figures 12 and 13. Two distinct aerosol growth phases are apparent. During the initial phase, while NO is being converted to NO_2, there is a rise in number concentration due to SO_2 oxidation and H_2SO_4 aerosol formation, but the surface and volume production is quite low and proceeds almost as if only SO_2 were present. For the Calspan and U of M experiments, the apparent SO_2 oxidation rates during this period were 0.16 and 0.18% hr^{-1}, respectively. This is higher than that typically observed in the U of M tests for SO_2 alone, but about the same as the initial rate of SO_2 oxidation in other Calspan experiments with SO_2 + filtered air. The slightly increased rate of aerosol volume production in the U of M case possibly results from an acceleration of the SO_2 photooxidation process by reactive intermediates formed by the NO to NO_2 conversion and 1-hexene photooxidation. However, in the absence of data on aerosol chemical composition, the mechanisms for increased aerosol production cannot be verified.

During the second phase of growth, at about the same time that ozone begins to appear, the rate of aerosol production again increases. Number concentration begins to grow and the rates of surface and volume production are greatly enhanced. The shapes of the surface and volume concentration curves in this growth phase are quite similar to those obtained in the pure 1-hexene + NO system, but the actual concentrations are higher (see Tables IX and X for comparisons). The increases, especially in the

U of M data, are larger than would be expected from a simple linear combination of the aerosol formed by the SO_2 pure air system (for comparable SO_2 concentrations) and that from the hexene + NO system. Synergistic interactions must take place which lead to enhanced aerosol formation in the combined system. Again, chemical composition data would be particularly useful in helping to explain these results. In the absence of these data, some possible explanation may be:

1. The sulfuric acid aerosol formed during the first growth phase might act to catalyze the formation of aerosol from 1-hexene + NO reaction products.

2. Gas phase products of SO_2 photooxidation might act to accelerate the formation of aerosol from 1-hexene + NO reaction products.

3. Gas phase 1-hexene + NO products might act to greatly increase the rate of SO_2 oxidation and thus aerosol formation.

Schemes 1 and 2 both depend upon the interaction of SO_2 photooxidation products with the 1-hexene + NO system. The interaction could lead to an acceleration of the rate of formation of whatever hydrocarbon-related species condensed in the second growth phase or to an alteration of the gas phase reaction paths leading to the formation of a nonvolatile, more readily condensible species. A combination of these two effects could also occur. Only a tiny fraction of the 1-hexene which is oxidized would have to be converted to nonvolatile species to produce a significant aerosol yield. In the first 500 min of U of M experiment 92, about .24 ppm or 890 $\mu g/m^3$ of 1-hexene disappeared from the gas phase, during the same period about 0.18 $\mu m^3/cc$, or assuming an aerosol density of unity, 0.18 $\mu g/m^3$ of aerosol is formed. This represents only about 0.02% of the mass of 1-hexene removed.

FIGURE 12

CALSPAN

RUN NO. 18 MARCH 6, 1974 HEXENE-1-SO_2-NO SYSTEM
HEXENE-1 = 0.33 ppm; NO = 0.178 ppm; NO_2 = 0.008 ppm; SO_2 = 0.07 ppm
RH = 37%

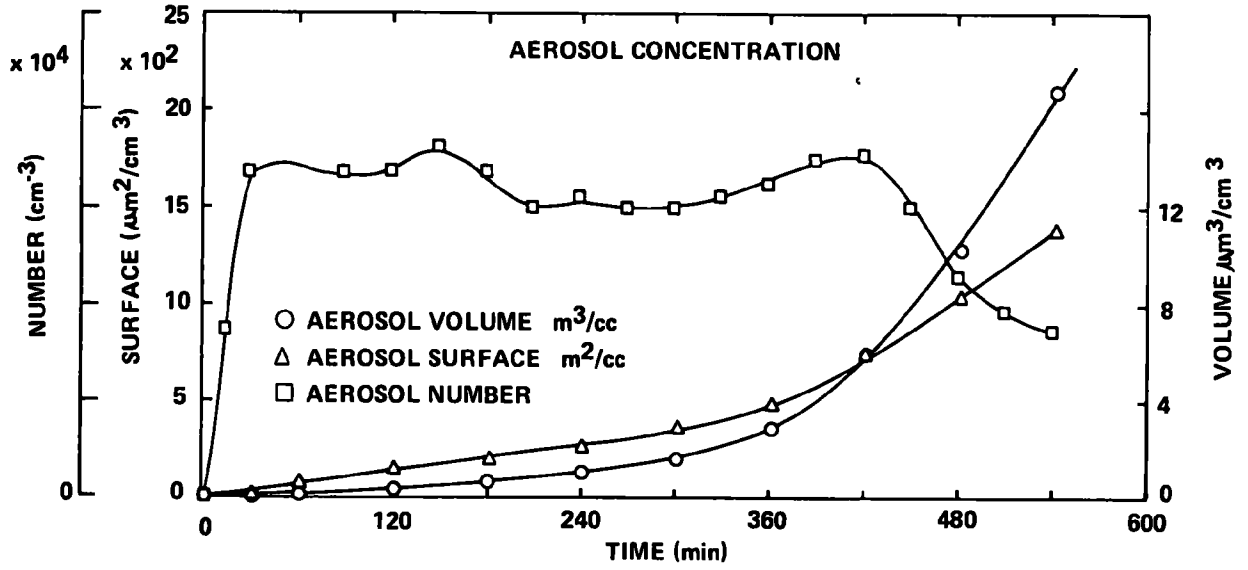

HEXENE-1-SO_2-NO-FILTERED AIR SYSTEM

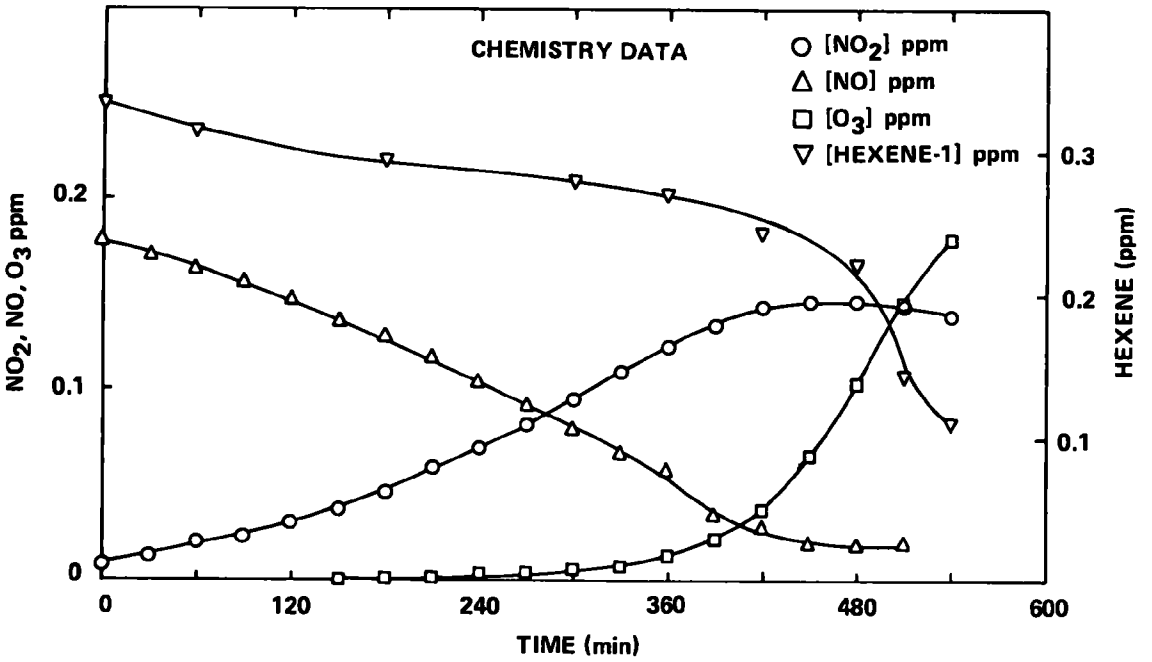

FIGURE 13

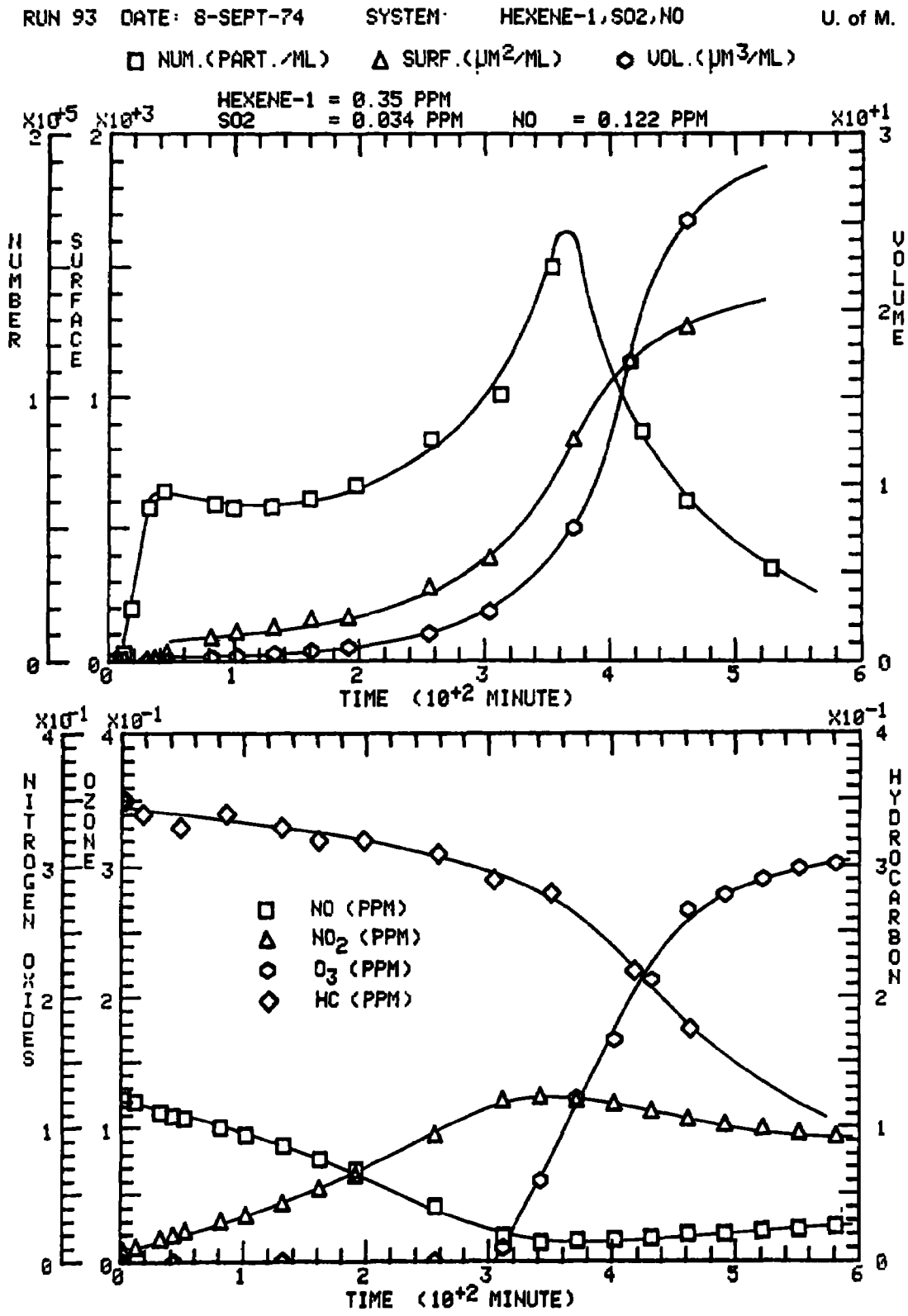
RUN 93 DATE: 8-SEPT-74 SYSTEM: HEXENE-1,SO2,NO U. of M.
NUM.(PART./ML) SURF.(μM²/ML) VOL.(μM³/ML)
HEXENE-1 = 0.35 PPM
SO2 = 0.034 PPM NO = 0.122 PPM
X10+5
X10+3
X10+1
NUMBER
SURFACE
VOLUME
TIME (10+2 MINUTE)
X10-1
NITROGEN OXIDES
OZONE
HYDROCARBON
NO (PPM)
NO2 (PPM)
O3 (PPM)
HC (PPM)
TIME (10+2 MINUTE)

In run 93 with SO_2 present, the aerosol yield is raised to about 3.6% of the mass of 1-hexene removed. Such a change could easily occur as a result of either scheme 1 or 2. If scheme 3 is important, it should be easy to verify experimentally, because in order to explain the observed aerosol formation, a significant fraction, i.e., more than 20% of the SO_2 initially present would have to be removed from the gas phase. This quantity could be detected by gas phase sulfur monitoring. Analysis of aerosol sulfate content would provide more definitive results.

Before concluding the discussion of the 1-hexene system, two other experimental variables must be mentioned: humidity and bag size. The effect of humidity may be seen by comparing U of M experiments 78 and 93. Both of these experiments were for the 1-hexene + NO + SO_2 system; however, 78 was at 55% relative humidity and 93 at 32%. As in the case of the SO_2 + clean air system, aerosol formation is enhanced by increased humidity. In the first phase of growth, the volume production rates are .53 and .29 $\mu m^3/cc\text{-}hr^{-1}$ for the high and low humidity cases, respectively. In the second growth phase, the effect is less apparent but still present with volume production rates of 19.1 and 18 $\mu m^3/cc\text{-}hr^{-1}$ for the high and low humidity cases, respectively. The difference between the two cases during the second growth phase is more apparent when the maximum aerosol surface areas of 1530 and 1300 $\mu m^2/cc$ for the high and low humidity cases are considered.

Run 60 was a 1-hexene + NO + SO_2 experiment done in the small bag. The qualitative behavior of the system is exactly like the large bag with two-phase growth observed. Quantitatively, however, evertyhing seems to take place more slowly in the small bag; the times to NO_2 peak, to the onset of ozone formation, and to the onset of rapid aerosol growth are longer. As previously suggested, the slowing effect on the chemistry in this and other systems in the small bag may be due to lower average light intensity, since the bag is mounted in the center of the cylindrical illumination housing where the light intensity is lowest. It is not yet clear whether wall effects also play a role in the observed results.

The m-xylene + NO + SO_2 systems investigated at Calspan and the U of M were very reactive in terms of chemical and aerosol behavior. The times to reach $[NO_2]_{max}$ were shorter in every case than the analogous toluene or hexene experiments. As is the case of the other hydrocarbons, two phases of aerosol growth are evident. Comparisons between a Calspan and U of M test are shown in Figures 14 and 15 . For the U of M test, the SO_2 photooxidation rates during the initial growth phase were 0.14 and 0.21% hr^{-1}. The Calspan experiment produced a slightly higher rate of 0.32% hr^{-1}. These rates are about the same as for the other hydrocarbons and also for a slightly contaminated SO_2 + clean air system but lower than the U of M toluene + NO + SO_2 cases. In both the Calspan and U of M tests, m-xylene appeared to interact only weakly during the initial phase of aerosol growth.

By contrast, during the second growth phase, very rapid aerosol production was observed as the data in Figures 14 and 15 show. The synergistic interaction of the hydrocarbon + NO and SO_2 + clean air system is more obvious in the Calspan experiments. Here the addition of SO_2 to the m-xylene + NO produces a great deal more aerosol surface and substantial additional volume. For the corresponding U of M experiment, the large increase in surface area takes place at essentially the same volume concentration. The excess surface area produced for the measured volume increase implies the presence of many small particles (compared to m-xylene + NO) and, indeed, this is the case as the data in other HC + NO vs. HC + NO + SO_2 systems show. Smaller particles are present with the added SO_2, since the SO_2 generates a large concentration of tiny nuclei early in the experiment. These particles then serve as sites for subsequent condensation in the second growth phase.

A final feature of the m-xylene + NO and m-xylene + NO + SO_2 experiments investigated is the relative humidity effect. U of M runs 81 and 82 were run at high humidity and runs 89 and 91 at low humidity. As usual, the change in humidity leads to no change in the chemical data but produces significant changes in the aerosol data. Both surface and volume concentration

FIGURE 14

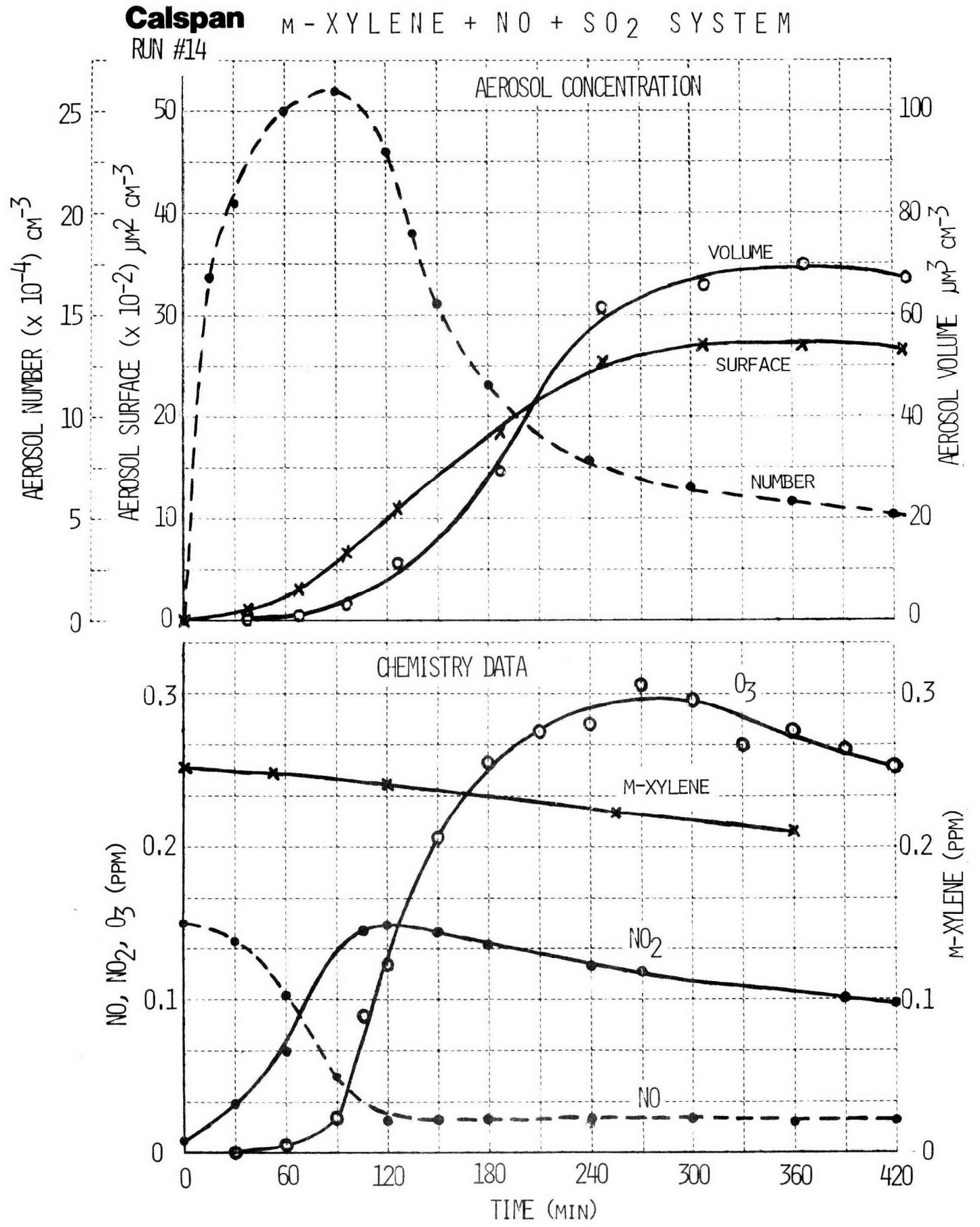
Calspan
M-XYLENE + NO + SO2 SYSTEM
RUN #14
AEROSOL CONCENTRATION
AEROSOL NUMBER (x 10-4) cm-3
AEROSOL SURFACE (x 10-2) µm2 cm-3
AEROSOL VOLUME µm3 cm-3
VOLUME
SURFACE
NUMBER
CHEMISTRY DATA
O3
M-XYLENE
NO2
NO
NO, NO2, O3 (PPM)
M-XYLENE (PPM)
TIME (MIN)

FIGURE 15

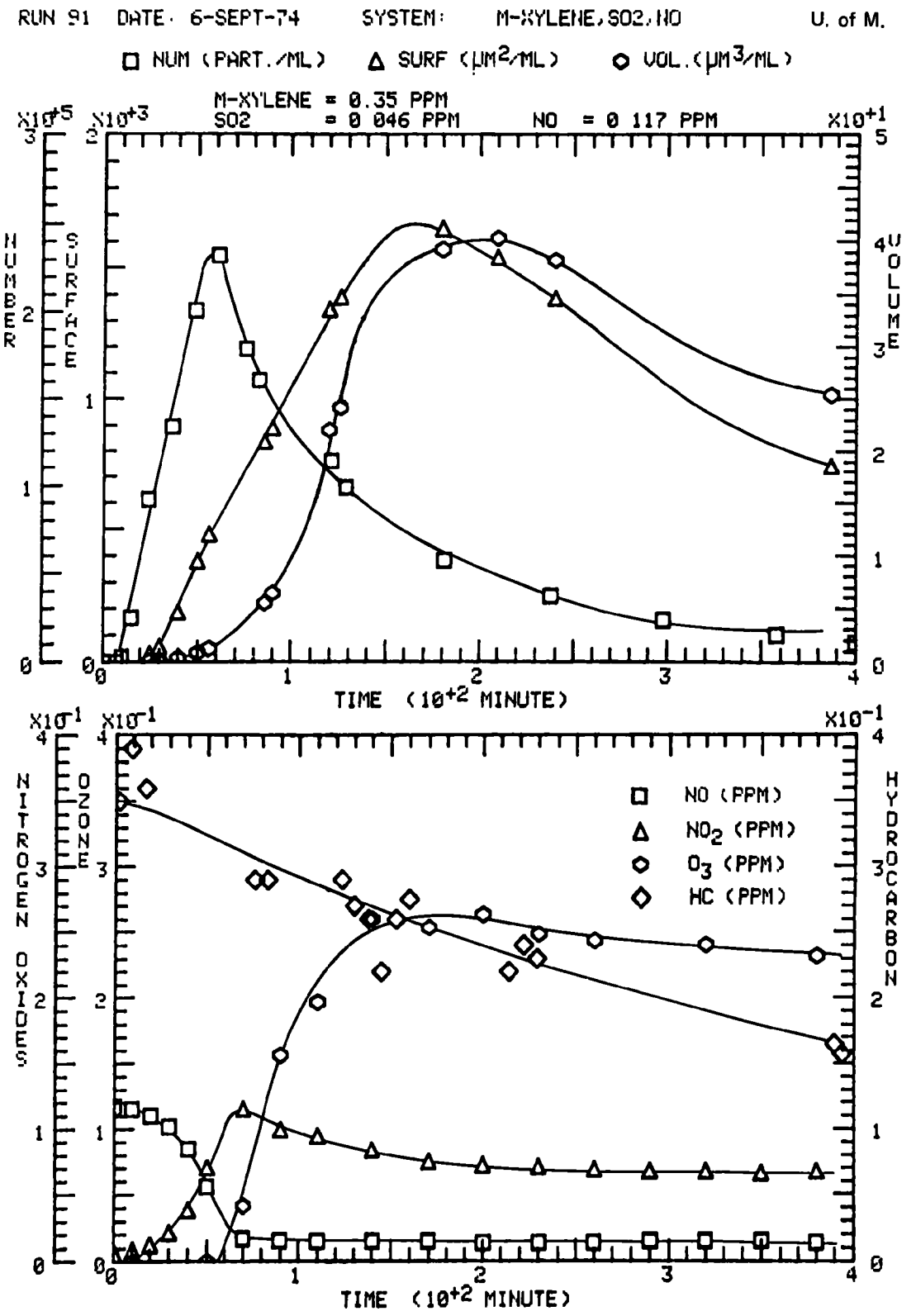
RUN 91 DATE: 6-SEPT-74 SYSTEM: M-XYLENE/SO2/NO U. of M.
NUM (PART./ML) SURF (μM²/ML) VOL.(μM³/ML)
M-XYLENE = 0.35 PPM
SO2 = 0.046 PPM NO = 0.117 PPM
X10+5
X10+3
X10+1
NUMBER
SURFACE
VOLUME
TIME (10+2 MINUTE)
X10-1
NITROGEN OXIDES
OZONE
HYDROCARBON
NO (PPM)
NO2 (PPM)
O3 (PPM)
HC (PPM)
TIME (10+2 MINUTE)

markedly increase with relative humidity, implying deliquescence of the hygroscopic fraction of the aerosol.

One cyclohexene + NO + SO_2 system was investigated at Calspan (run 9) and one at the U of M (run 96). The Calspan and U of M data for this system are very similar and are shown in Figures 16 and 17 . The addition of SO_2 to the cyclohexene + NO system produced effects qualitatively similar to those produced by addition of SO_2 to the other hydrocarbon + NO systems studied. Thus, the NO, NO_2, O_3, and hydrocarbon profiles were essentially unchanged by SO_2 addition. At the same time, aerosol behavior was markedly changed, with two-phase aerosol growth resulting.

The changes in aerosol behavior produced by SO_2 addition to this system were dramatic and informative. During the first phase of growth, aerosol production occurred as though a slightly contaminated SO_2 + clean air system was being irradiated. The apparent SO_2 photooxidation rate was 0.20%/hr in the U of M case and 0.28%/hr in the Calspan experiment, about the same as that observed for other hydrocarbon + NO + SO_2 systems. With this system, evidence of the second phase of aerosol growth appears before NO has been completely oxidized out of the system. Especially in the U of M case, the volume against time data becomes nonlinear with marked upward curvature appearing as early as 50 minutes after lights on. However, in both cases, rapid aerosol volume production does not occur until about the time of complete NO oxidation and rapid formation of ozone.

In terms of volume production, the second phase growth is quite similar to the cyclohexene + NO system in the absence of SO_2. The differences that are observed are not considered significant because of the difficulties associated in measuring $(dv/dt)_{max}$ for the cyclohexene + NO system, i.e., rapid growth beyond the upper particle size limit of the EAA. The change in surface and number concentrations associated with the addition of SO_2, however, are very significant. Both number and maximum surface concentration are much larger. However, since the total aerosol volumes produced in all

cyclohexene cases are about the same, the addition of SO_2 must lead to a dramatic decrease in particle size.

The effect of SO_2 on particle size can be seen in Figure 18 , in which mean surface diameter has been plotted as a function of time for several HC + NO and HC + NO + SO_2 systems studied at the U of M. Data for a typical SO_2 irradiation are also shown in the figure. The almost explosive growth in the cyclohexene + NO case occurs at about the time of complete oxidation of NO and appearance of appreciable ozone. In the case shown, particle diameters of nearly 0.5 μm were produced in less than an hour from the time of initial nucleation. With SO_2 in the system, the particle sizes are much smaller. Under these conditions, initial nuclei formation results from SO_2 oxidation followed by additional condensation on existing particles during the second phase of growth. Although the particles are smaller, the number concentration is higher.

m-Xylene + NO behaves like the cyclohexene + NO system but to a lesser extent. The addition of SO_2 results in the same effect; initial particle formation and growth at a rate similar to that for SO_2 alone, followed by accelerated growth during the second phase.

By comparison, the much less reactive hexene + NO + SO_2 system was observed to essentially follow the SO_2 particle growth curve for the duration of the experiment.

The implications of these data relative to the production of light scattering aerosol can be seen in Figure 19. In the figure the light scattering function b(SCAT) is plotted as a function of time for several HC + NO, HC + NO + SO_2 systems in the Calspan chamber. The production of very large particles in the cyclohexene + NO case results in the rapid formation of light scattering aerosol. Although the particle diameters are much larger than in the comparable cyclohexene + NO + SO_2 experiment, b(SCAT) is nearly the same because fewer particles are produced. The addition of SO_2 results

FIGURE 16

CALSPAN

RUN NO. 9 27 FEBRUARY 1974 CYCLOHEXENE-NO-SO_2-FILTERED AIR SYSTEM R.H. = 36%;

CYCLOHEXENE = 0.33 ppm; NO = 0.220 ppm; NO_2 = 0.020 ppm; SO_2 = 0.05 ppm

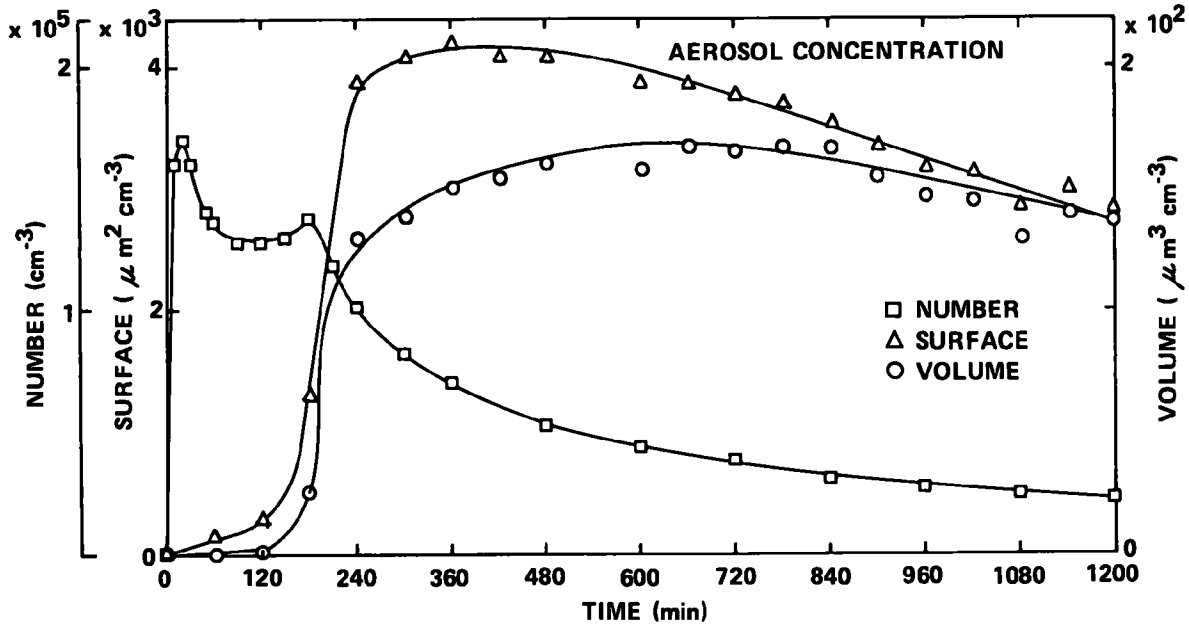

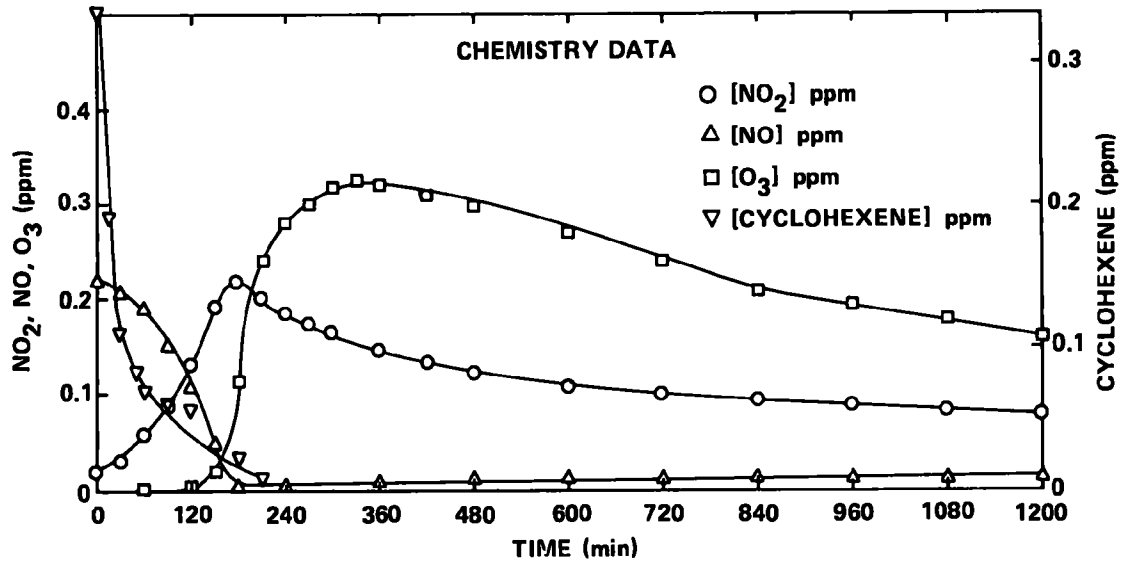

FIGURE 17

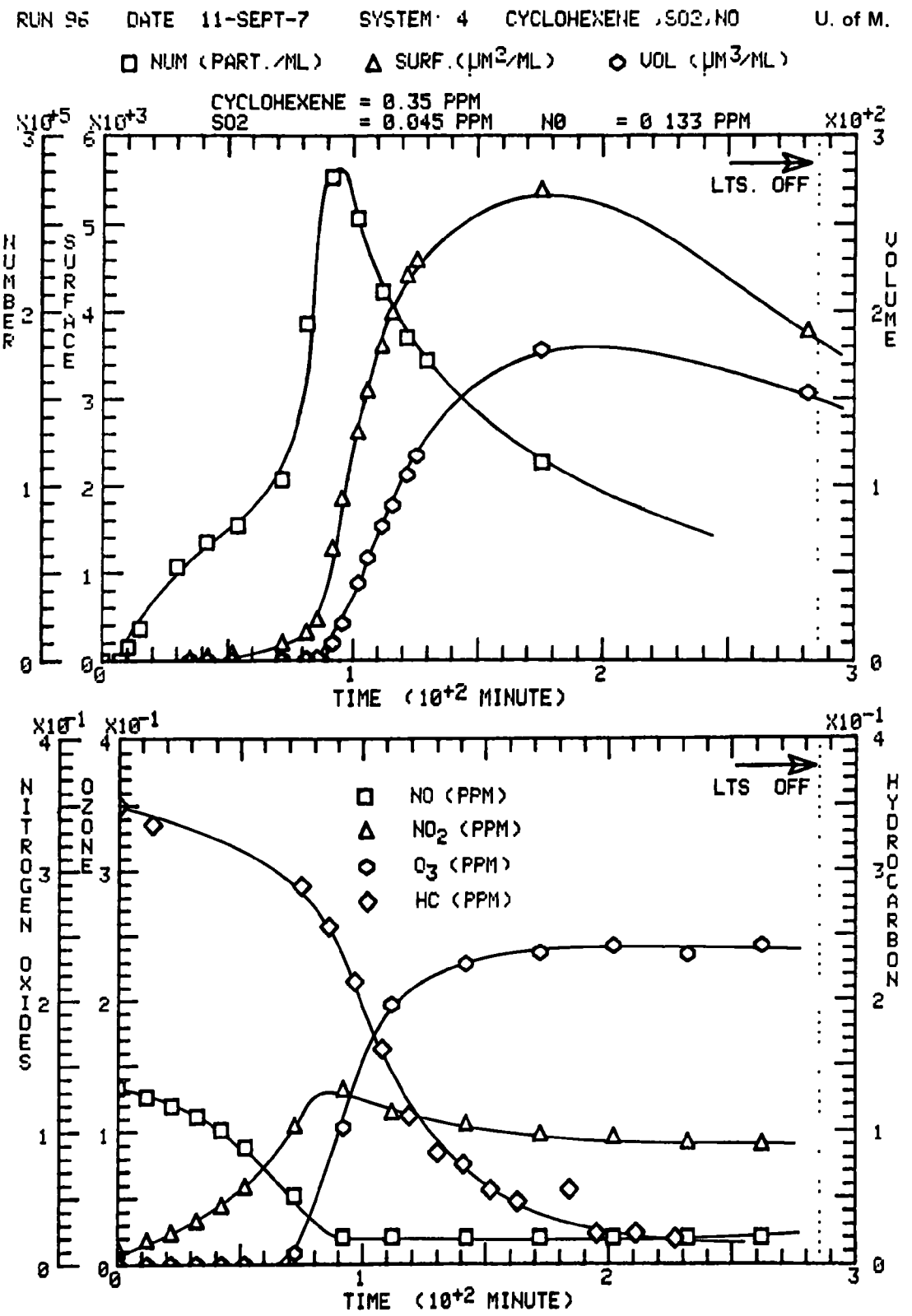
RUN 96 DATE 11-SEPT-7 SYSTEM 4 CYCLOHEXENE ,SO2,NO U. of M.
NUM (PART./ML)
SURF.(μM²/ML)
VOL (μM³/ML)
CYCLOHEXENE = 0.35 PPM
SO2 = 0.045 PPM
NO = 0.133 PPM
LTS. OFF
NUMBER
SURFACE
VOLUME
TIME (10+2 MINUTE)
NO (PPM)
NO2 (PPM)
O3 (PPM)
HC (PPM)
LTS OFF
NITROGEN OXIDES
OZONE
HYDROCARBON
TIME (10+2 MINUTE)

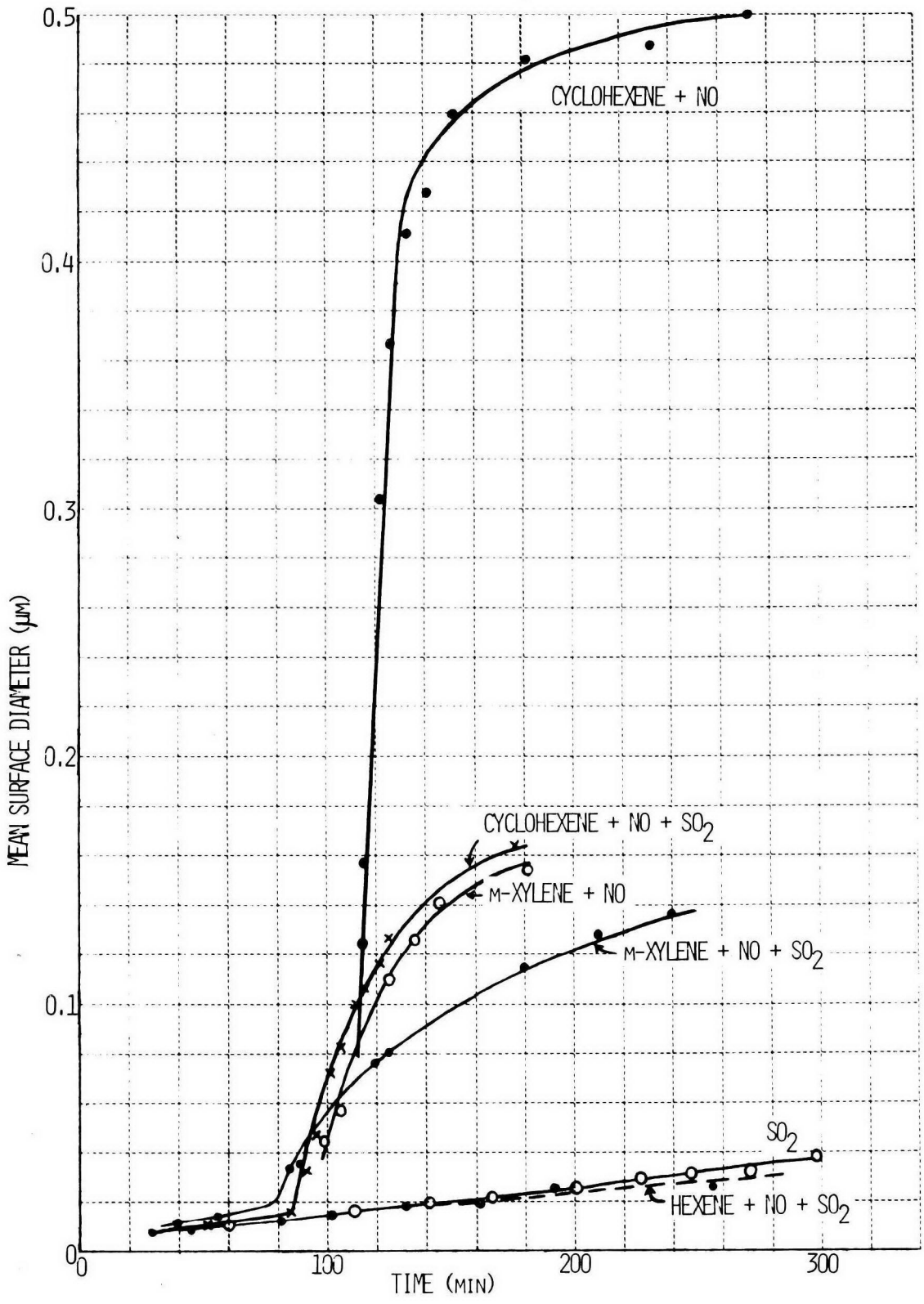

FIGURE 18. MEAN SURFACE DIAMETER VS TIME FOR SEVERAL HC+ NO, HC + NO + SO_2, AND SO_2 EXPERIMENTS.

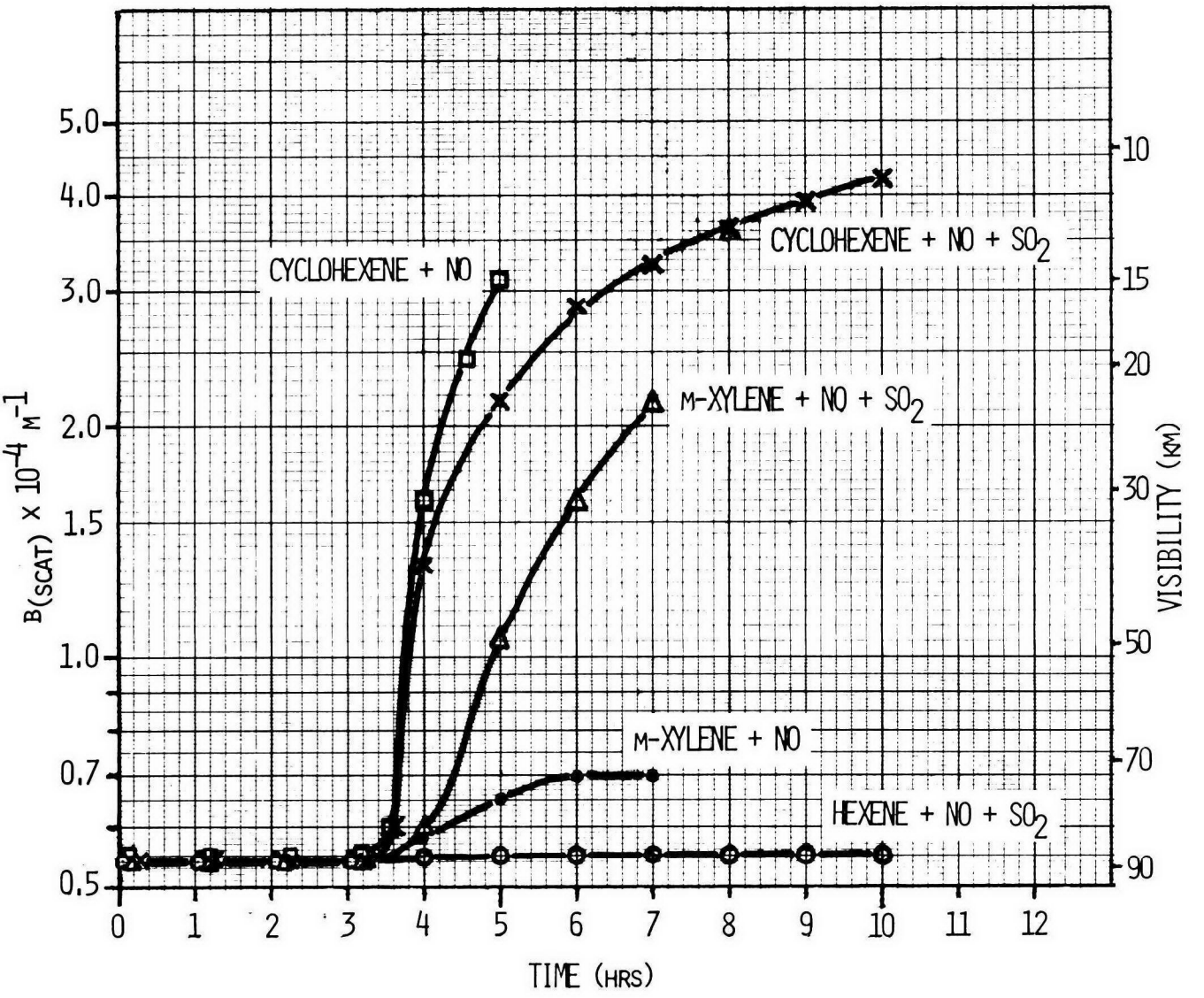

FIGURE 19. LIGHT SCATTERING COEFFICIENT (B_{SCAT}) OF PHOTOCHEMICAL AEROSOLS VS TIME.

in smaller but more numerous particles whose effect on light scattering is about the same.

The addition of SO_2 to the m-xylene + NO case can also be seen to produce substantial light scattering aerosol during the second phase of aerosol growth. For several hours there is no effect, but once NO oxidation is complete and second stage growth begins, large visibility losses are observed. The fact that the concentration of particles is much smaller in the m-xylene + NO case (compared to m-xylene + NO + SO_2) accounts for the lack of appreciable light scattering aerosol.

By contrast, the hexene system, even in the presence of SO_2, did not produce significant light scattering aerosol or visibility losses. The same result was obtained in the Calspan tests for the toluene + NO + SO_2 system. The somewhat accelerated particle growth observed in the U of M tests may have resulted in light scattering aerosol; however, there was no opportunity to make this measurement in their chamber. Finally, the SO_2 alone, while producing very large concentrations of particles, did not produce significant light scattering aerosol over the duration of these tests.

4.5 Conclusions from the March Workshop

From the data generated during the March workshop and the duplicate experiments performed at the University of Minnesota, the following points can be made:

(1) Each HC + NO experiment can be divided into two phases. In the first phase, NO is converted to NO_2 and some oxidation of hydrocarbon occurs. Ozone starts to appear near the end of this period. The second phase, accompanied by substantial aerosol formation, begins as soon as NO is completely oxidized and NO_2 reaches its maximum; ozone increases rapidly and approaches a maximum.

(2) Qualitatively the HC + SO_2 system behaves in a manner similar to SO_2 alone. Quantitatively, the presence of hydrocarbon contamination, even in the absence of appreciable NO, substantially increases the overall production of aerosol. Average apparent SO_2 oxidation rates exceeding 1.6% hr^{-1} were observed for the final stage of growth in the HC-enriched atmospheres in the Calspan experiments.

(3) The addition of SO_2 to the HC + NO system was generally found to exert a synergistic effect on aerosol surface and volume formation. At Calspan the effect on aerosol behavior was greatest for m-xylene, while at the U of M the largest effect was observed in the hexene + NO + SO_2 system. Possible synergistic effects in the cyclohexene system were masked by the explosive growth of aerosol with and without the addition of SO_2.

(4) The addition of SO_2 to the HC + NO system produces a dramatic decrease in the mean particle diameter. This results from the initial formation of very high concentrations of nuclei in the presence of SO_2. During the second stage of aerosol growth, condensation proceeds on the existing particles rather than forming fewer but larger particles typical of the HC + NO system.

(5) Of the hydrocarbons studied, cyclohexene was the most reactive, both in terms of aerosol and chemical behavior, followed by m-xylene, hexene, and toluene. The main difference observed in the duplicate experiments at the U of M was that hexene was the least reactive hydrocarbon.

(6) It has been possible from these tests to characterize system reactivity in terms of aerosol behavior. The most important variables are maximum number concentration, equilibrium surface concentration, and volumetric growth rate. These aerosol measures of reactivity have been found to correlate well with other conventional parameters, such as time to $[NO_2]_{max}$ and $[O_3]_{max}$.

(7) Aerosol formation rates were enhanced at high relative humidities, probably as a result of the higher water content in the aerosols.

(8) The data generated in these experiments in chambers of widely different physical dimensions show a high degree of correlation. The main difference in the results is indicated in the significantly greater aerosol and chemical reactivity of toluene found in the U of M chamber. The reasons for this difference have not been resolved.

Section 5

CHAMBER CHARACTERIZATION TESTS

During the November and March workshops, a number of experiments were performed to characterize chamber performance and test for contamination. The photooxidation of SO_2 in clean air was one common test of chamber condition that has already been described. In addition to these experiments, however, were a number of dark reaction tests at the University of Minnesota and also NO photolysis experiments and aerosol coagulation tests performed both at Calspan and the U of M. Although the importance of chamber testing is recognized, there has not yet been an established format for intercomparing chamber performance. In retrospect, it may well be that the similarity in test results at Calspan and the U of M during the past year provides the best indicator of comparable chamber performance.

5.1 Dark Reaction Tests -- University of Minnesota

After the November workshop, a number of aerosol experiments were performed to determine the degree of chamber contamination in the U of M chamber. The experiments are summarized in Table XV. Runs 21-24 were SO_2 photooxidation and decay experiments. Note that the peak CNC is lower for run 22 than for run 21 and lower for run 24 than for run 23. This suggests that gradual conditioning of the smog chamber is occurring as a result of performing SO_2 photooxidation experiments. The same type of conditioning effect was observed in the November workshop after several SO_2 photooxidation experiments were performed in a given bag.

Conditioning effects show up in another way in runs 21-24. Figures 20 and 21 show plots of CNC and 1/CNC against time for these four experiments. It is assumed that nucleation of new particles ceases after the lights are turned off, plots of 1/CNC against time during this decay period should be essentially straight lines with a slope equal to the coagulation coefficient. Upward

TABLE XV. AEROSOL REACTIVITY EXPERIMENTS

Run No.	SO_2 Conc. (ppm)	Relative Humidity %	Time Dark (min)	N_{max} dark (part/ml)	Time Light (min)	N_{max} light (part/ml)	Coagulation Rate Constant (x 10^{10} ml/sec)	Comments
21	0.49	25	180*	---	30	241K	21	
22	0.53	29	180*	---	30	112K	27	
23	0.54	29	180*	---	15	90K	26	
24	0.54	25	180*	---	15	66K	21	
27	0.54	52	97**	Not measured	--	--	--	
28	0.54	55	42**	Not measured	--	--	--	New charcoal
30	0.59	55	300	52K	--	--	--	New bag (LB-3)
31	0.59	50	240	53K	120	280K	--	
32	0.59	52	180	30K	70	330K	--	
33	0.59	55	11	---	960	240K	--	Lights on before
34	0.59	55	45	48K	945	220K	--	N_{max} dark obtained
35	0.59	48	100	30K	18	--	--	Very high peak CNC
36	b	41	---	---	820	8.1K	--	
37	b	52	---	---	250	b	--	
38	b	50	---	---	265	b	--	
39	0.59	37	120	14K	---	--	--	
40	b	45	---	---	328	b	--	
43	0.59	16	---	6.2K	---	--	--	

*Dark decay time after lights turned off.

**Time to onset of aerosol growth.

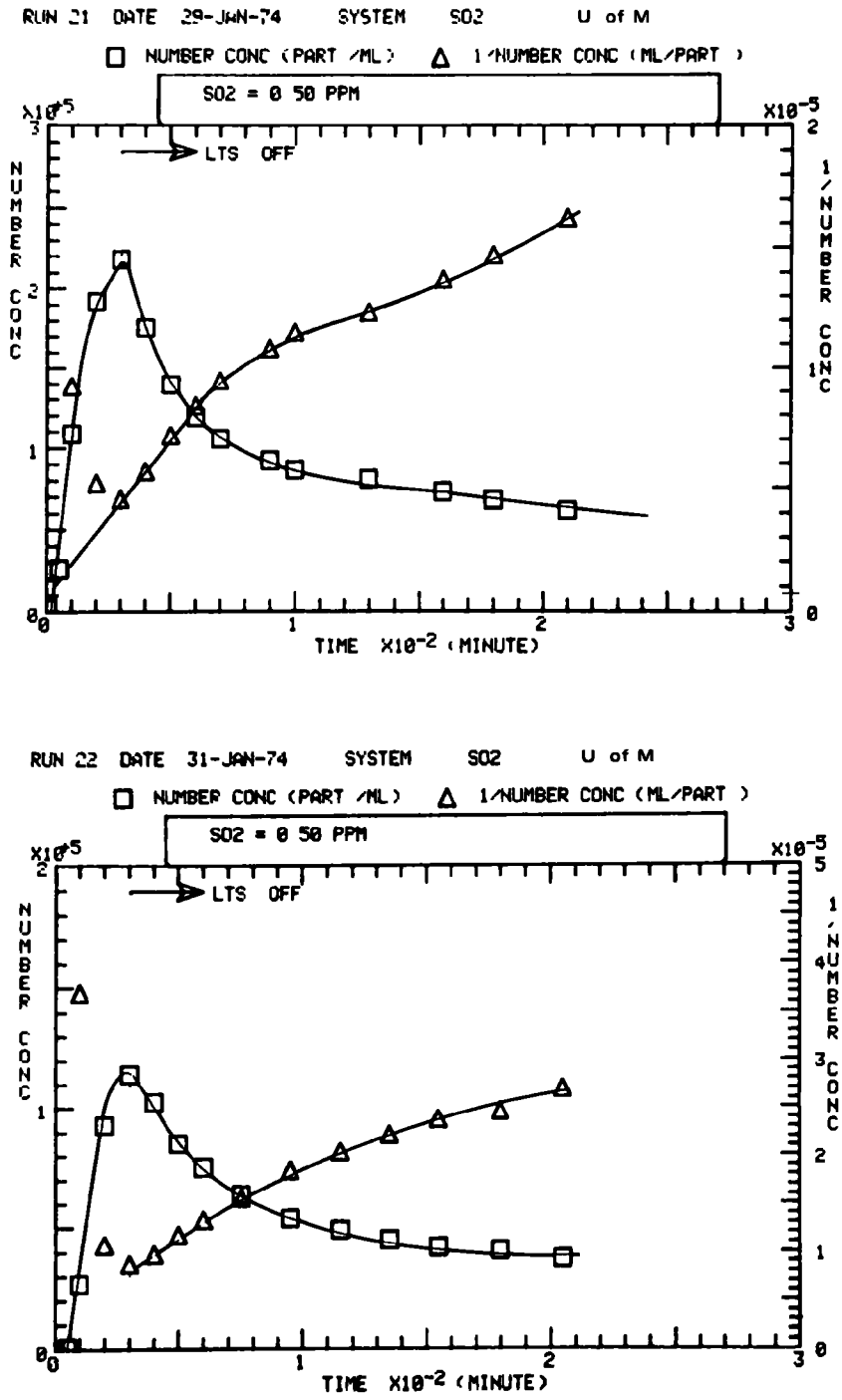

FIGURE 20. TIME HISTORIES OF AEROSOL COAGULATION.

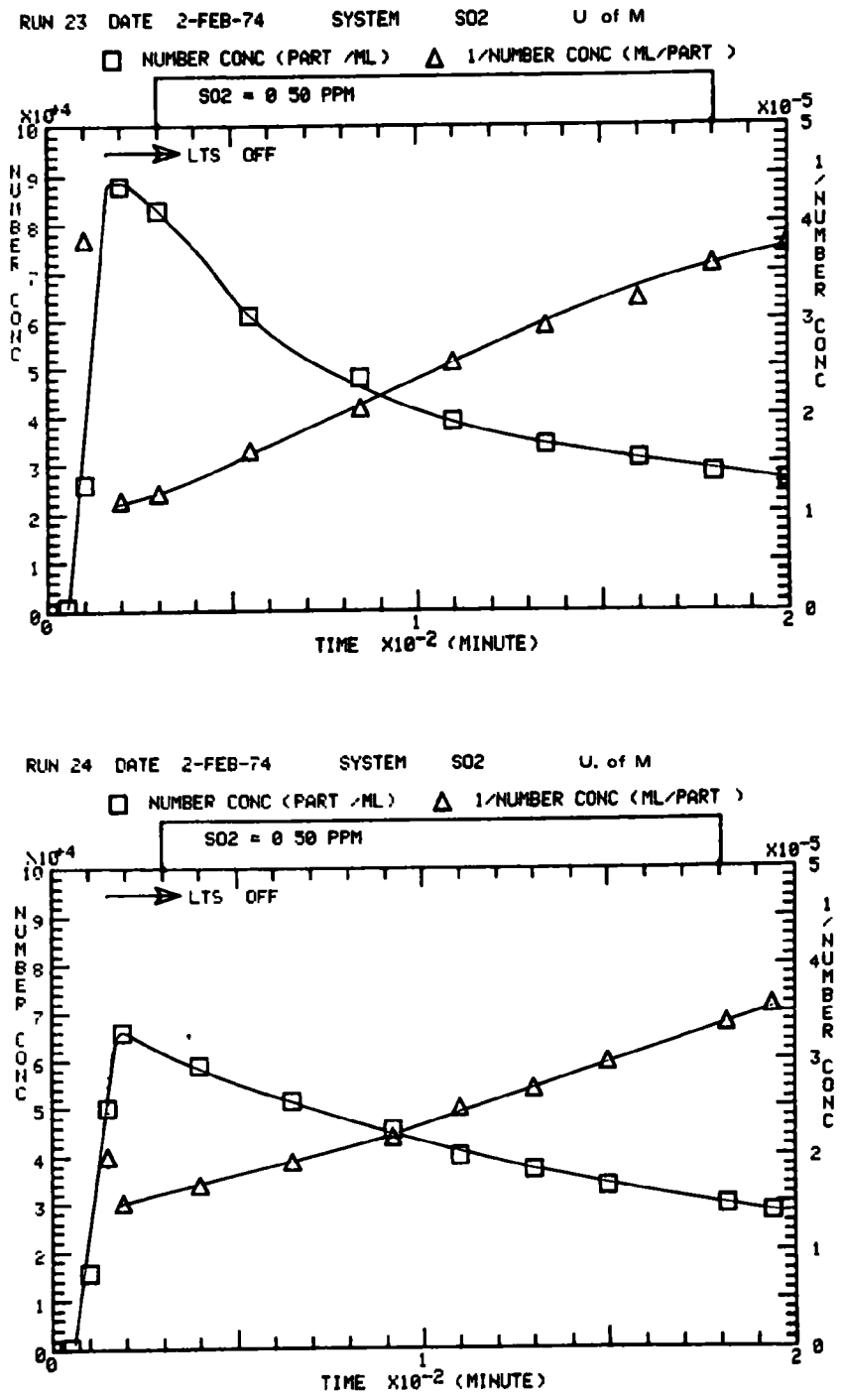

FIGURE 21. TIME HISTORIES OF AEROSOL COAGULATION.

curvature of this line suggests wall losses; downward curvature suggests particle generation. The plot of 1/CNC against time presented in Figure 20a is not a simple straight line but rather two straight line segments. The slope of the line during the first 60 minutes after lights off is 2.1×10^{-9} cm^3/sec, only slightly greater than the 1.5×10^{-9} cm^3/sec predicted by theory for a monodisperse system having the same mean particle size. The theoretical monodisperse coagulation rate would be expected to be lower than the observed coefficient for two reasons: (1) Polydisperse aerosols should have higher coagulation rates than monodisperse aerosols of the same mean size, and (2) losses to the wall of the chamber can only act to increase the rate of particle disappearance and thus raise the apparent coagulation coefficient. The difference between theory and experiment is thus in the correct direction. For the second portion of the curve, however, this is not true. Here the slope is about 0.7×10^{-9} cm^3/sec which is significantly less than predicted by theory. The only reasonable explanation for such a low slope is the generation of new particles through a dark reaction mechanism. Secondary particle production is, therefore, taken as evidence of contamination. Run 22 also shows this type of behavior; however, in this case the difference in slope between the apparently uncontaminated and the contaminated decay period is less pronounced. In runs 23 and 24, Figure 21, evidence of contamination has disappeared altogether, and only simple second order aerosol decay is evident. The series of SO_2 experiments has, therefore, led to a conditioning of the chamber and the disappearance of effects which could only be attributed to contamination.

The coagulation coefficients measured in runs 21 through 24 varied from 2.1 to 2.7×10^{-9} cm^3/sec with an average value of $2.4 \pm 0.3 \times 10^{-9}$ cm^3/sec.

Dark reaction experiments were also performed in order to measure chamber contamination. In these experiments the bag was filled with clean air and humidified to 50%. About 0.5 ppm of SO_2 was then added to the system. The bag was left in the dark and the CNC was monitored. In experiments 27

and 28 the time to onset of aerosol growth in the dark was measured to be 97 and 42 minutes, respectively. Dark growth in the SO_2 system is considered an indication of chamber contamination. The short time to the onset of dark growth in run 28 possibly indicates more chamber contamination. This seems rather surprising because as is noted in Table XV, the charcoal in the air purification scrubbers was changed before run 28.

The persistence of dark reactions, even after the charcoal was changed, was taken as evidence of chamber contamination. A new large bag (LB-3) was, therefore, constructed. Run 30 was the first dark reactivity test performed in this bag. Aerosol growth began almost immediately after SO_2 was introduced, and eventually a peak CNC of 52,000 particles/cm^3 was attained. This significant dark growth was not unexpected, because past experience has indicated that new Teflon bags require a conditioning period to remove or deactivate contaminants on the bag surface.

Consequently, several experiments to condition the bag were performed. In these experiments the normal procedure used in dark reactivity tests were followed, and the aerosol was allowed to grow in the dark until a maximum CNC, (N_{max}) was obtained. The lights were then turned on and the chamber was irradiated for up to 16 hours to condition the chamber. Runs 31-35 were of this type. Table XV shows the light and dark times and values of N_{max} obtained. The steady reduction of N_{max} achieved both in the dark and during irradiation suggests a conditioning effect. However, even after 5 runs, dark reactions were still very important. Several clean air irradiations, runs 36-38, were then performed to further condition the bag. Run 36 showed slight aerosol growth with N reaching 8100 particles/cm^3, whereas runs 37 and 38 resulted in no aerosol formation. The aerosol produced in run 36 probably resulted from residual SO_2 which remained attached to the walls of the smog chamber after the previous SO_2 experiments.

When SO_2 was again added in run 39, dark reaction occurred, although N_{max} was only 14K. Run 40 was another clean air irradiation and showed no aerosol formation. The last simple dark growth experiment was run 43; here N_{max} was only 6200 particles/cm^3, but this run was performed at a low relative humidity of 16% due to a failure of the humidification system. This fairly low value of N_{max} is at least partly due to the decrease in relative humidity.

5.2 Coagulation Experiments -- Calspan

A good opportunity for studying Calspan chamber performance was provided by data generated from a series of auto exhaust irradiations completed on another EPA-sponsored program.* Coagulation data were analyzed from the tests to try to establish information about wall losses in the large chamber. As previously stated, if wall losses are not important, a plot of $\frac{1}{N}$ (where N is the particle concentration) vs time should give a straight line of slope k. On the other hand, as wall losses begin to dominate, the apparent value of k will increase as the particle concentration decreases.

Plots of particle decay for seven exhaust emissions tests are shown in Figure 22. The data show a break in the 1/N vs time plot at 13 hours in each case. The average k for the seven experiments was 2.65×10^{-9} cm^3/sec which is in good agreement with theory for a polydisperse aerosol in the size range of 0.0075 μm to 0.133 μm. After 13 hours, there is upward curvature in each of the auto exhaust coagulation tests, indicating that wall losses or settling or both are beginning to influence the results. These data suggest that working times of at least 13 hours are possible in the large Calspan Chamber.

Longer working times are likely with photochemical aerosols of smaller size since sedimentation is less of a factor. These tests, however, have not yet been performed.

*Contract No. 68-02-1231

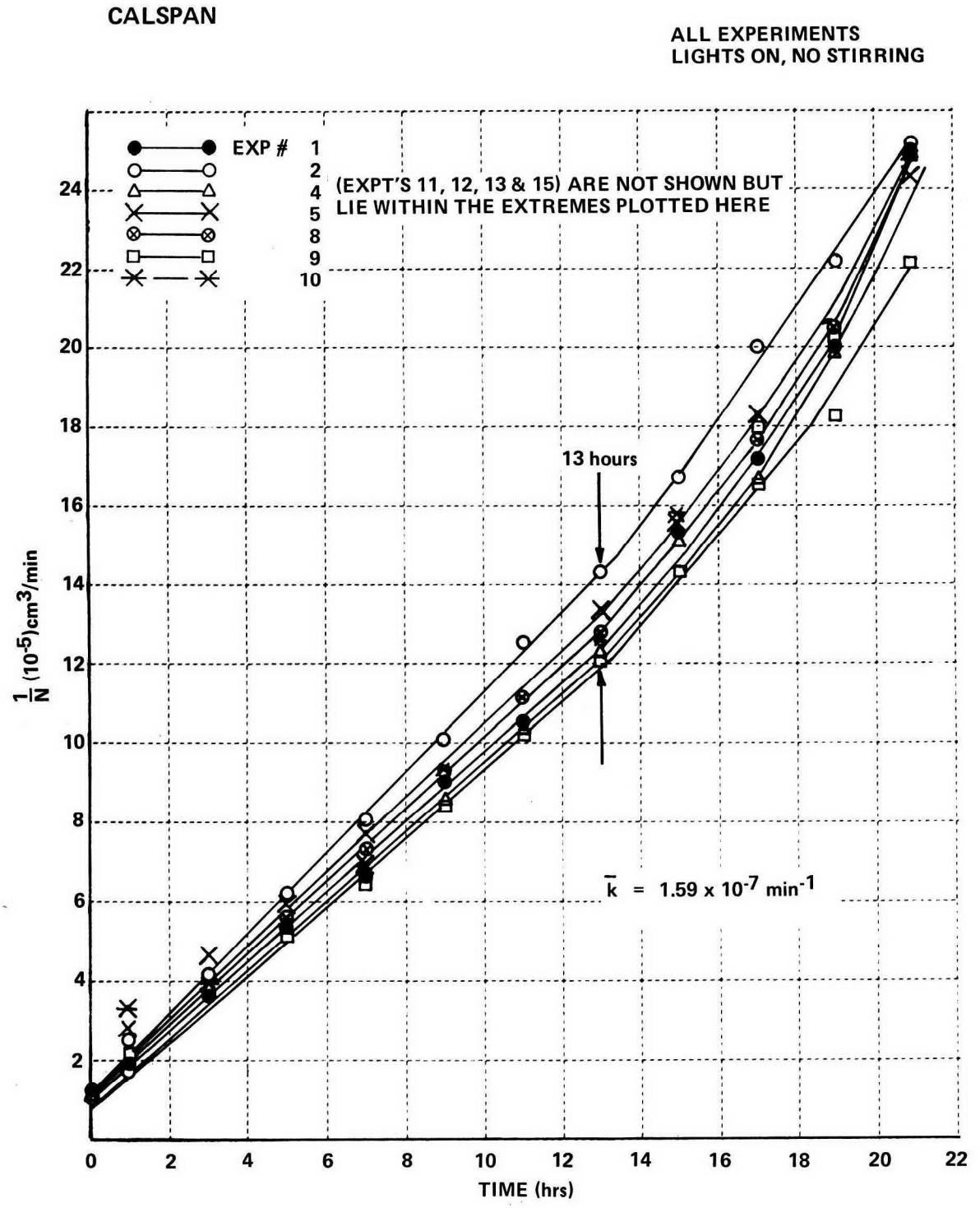

FIGURE 22. AEROSOL COAGULATION DATA - AUTO EMISSION TEST SERIES

5.3 NO Photolysis Experiments -- Calspan and University of Minnesota

The measurement of NO photolysis rates has been suggested as a means of measuring smog chamber contamination (Bufalini, 1972). Consequently, a number of NO photolysis experiments were performed at Calspan and the University of Minnesota in order to compare chamber performance.

The thermal oxidation of NO in clean air occurs by the overall reaction

$$NO + NO + O_2 \rightarrow 2NO_2 \ . \qquad (7)$$

The rate of this reaction is proportional to $[NO]^2$. If contaminants are present, irradiation of the NO + air system will result in the formation of addition species which react with NO and produce much more rapid removal of NO than predicted by reaction (7). Comparison of the NO removal rate, calculated from kinetic data available for reaction (7) and the experimentally determined removal rate, gives a measure of chamber contamination.

Table XVI summarizes the NO photolysis experiments performed in the Calspan and Minnesota chambers. Here, initial NO and NO_2 concentrations, theoretical and experimental NO disappearance rates, ratio of experimental to theoretical NO removal rates, and the percent NO loss per hour are presented. Before further discussion of these results, it should be noted that NO photolysis experiments are more sensitive to contamination if the initial NO concentration is low. This is because at high NO concentrations the rate of reaction (7), which is second order in NO, is large enough to mask any contamination effects. Another important factor lies in the fact that any hydrocarbon contamination effect would be more pronounced at higher HC/NO ratios.

It is probable that reactions between nitrogen oxide and contaminants present in the chamber are first order in NO. The apparent first order dissociation rate, expressed in terms of percent NO removal per hour, provides a useful measure for intercomparing experiments and is also shown in Table XVI.

TABLE XVI. NO OXIDATION EXPERIMENTS

COMMENT	EXP	NO_I PPM	NO_{2I} PPM	THEORY (A) PPM/HR	EXPERIMENTAL PPM/HR	RATIO	%NO/HR
CALSPAN							
(LARGE CHAMBER)							
DEC. 15, 1973	1	0.610	0.08	6.3×10^{-3}	1.5×10^{-2}	2.4	9.3
FEB. 28, 1974	11	0.471	0.07	3.7×10^{-3}	1.4×10^{-2}	3.7	6.1
MAR. 6, 1974	19	0.150	0.01	3.8×10^{-4}	1.9×10^{-2}	50	12.6
MAR. 15, 1974	27	0.147	0.01	3.6×10^{-4}	1.2×10^{-2}	33	8.2
MAR. 16, 1974	28	0.145	0.050	3.6×10^{-4}	2.7×10^{-2}	75	18.6
MAR. 21, 1974	31	0.498	0.08	4.2×10^{-3}	1.1×10^{-2}	2.6	2.2
UNIVERSITY OF MINNESOTA							
LARGE BAG #2	25	0.56	0.01	5.4×10^{-3}	5.2×10^{-2}	9.6	9.3
"	29	0.56	--	5.4×10^{-3}	3.4×10^{-2}	6.3	6.1
LARGE BAG #3	47	0.305	0.02	1.6×10^{-3}	1.6×10^{-2}	10	5.3
"	48	0.67	0.02	7.5×10^{-3}	1.7×10^{-2}	2.2	2.5
SMALL BAG #1	54B	0.11	0.01	2.0×10^{-4}	4.1×10^{-3}	21	3.7
"	55	0.36	0.04	2.2×10^{-3}	5.6×10^{-2}	25	15.6
"	56	0.575	0.012	5.6×10^{-3}	9.6×10^{-3}	1.7	1.7
"	58	0.51	0.01	4.4×10^{-3}	7.6×10^{-3}	1.7	1.5

(A) BUFALINI, J.J. AND STEPHENS, E.R., 1965: "THE THERMAL OXIDATION OF NITRIC OXIDE IN THE PRESENCE OF ULTRAVIOLET LIGHT", INTL. J. AIR WAT. POLL., VOL. 9, PP. 123-128.

The initial Calspan NO photolysis experiment was conducted after the November workshop using an initial NO concentration of 0.61 ppm. As shown, the observed oxidation rate is only 2.4 times greater than theory, suggesting that at higher concentrations of NO the presence of wall contaminants in the large chamber do not greatly affect the NO photolysis rate. The experiments performed during the March workshop showed greater variation depending on the NO concentration used. Generally the lower the concentration the larger the effect of contamination on test results. The very high rate for run no. 28 is largely due to the initial conditions of the experiment. In this run, a substantial amount of NO_2 was inadvertently introduced into the chamber along with the NO resulting in accelerated disappearance of the nitrogen oxide. At the completion of the March test series, another NO photolysis experiment was performed using a higher concentration of NO (0.498 ppm). As before, the presence of wall contamination (based on the history of previous experiments without cleaning of the chamber walls) did not appreciably affect the oxidation rate at these higher concentrations of NO.

In the U of M tests, the first two NO photolysis experiments, runs 25 and 29, were performed in LB-2 after a long series of photochemical aerosol experiments. The main difference is in the 30-40% lower oxidation rate in run 29 compared to run 25. The reduced rate probably resulted from a reduction of background contamination when the charcoal in the scrubbers was changed between runs 28 and 29. As was noted above, however, this new charcoal actually led to more rapid formation of an aerosol by dark reactions.

Runs 47 and 48 were done in large bag 3 after it had been subjected to a long series of conditioning experiments, including two SO_2 photooxidation experiments performed as part of the duplicate March workshop. Both of these experiments showed dark growth and, thus, contamination was indicated. Run 47 showed NO oxidation rates well above theoretical, but run 48 was only 2.2 times as great. Thus, the larger concentration of NO used in the latter experiment helped mask the effects of contamination.

Runs 54b, 55, 56, and 58 were all done in the small bag. Prior to these runs, the small bag had only been used for SO_2 photooxidation experiments. Only one of these experiments, run 53, showed any dark growth and that resulted primarily from the extremely high (5.6 ppm) SO_2 concentration used. The low reactivity of the small bag as indicated by lack of dark growth was partly supported by the low NO photolysis rates observed in runs 54b, 56, and 58. Run 55, however, exhibited greater NO photolysis. The reason for anomalous behavior in run 55 is not clear; however, it is possible that a contaminant may have been present for this experiment only, since the other rates of NO disappearance for the small bag were much lower.

Chamber contamination can thus be monitored using either dark reactivity tests or NO photolysis experiments. The results discussed above indicate a qualitative correlation exists between the two methods. Thus, dark growth and high NO photolysis rates, in general, occur together. It would appear, however, that in order to provide a sensitive measure of chamber contamination using the NO photolysis method that relatively low initial concentrations of NO must be used. While such experiments may be used to give an indication of chamber contamination, they are neither the only nor necessarily the best experiments for this purpose. More work on this problem area is necessary.

Section 6

REFERENCES

Bray, W.H., 1970: "Water Vapor Pressure Control at Aqueous Solutions of Sulfuric Acid, J. of Materials,"Vol. 5, No. 1, p. 233-248.

Bufalini, J.J., S.L. Kopczynski, and M.C. Dodge, 1972: "Contaminated Smog Chambers in Air Pollution Research", Environmental Letters, Vol. 3, No. 2, pp. 101-109.

Bufalini, J.J. and E.R. Stephens, 1965: "The Thermal Oxidation of Nitric Oxide in the Presence of Ultraviolet Light", Intl. J. Air Wat. Poll., Vol. 9, pp. 123-128.

Clark, W.E., 1972 Ph.D. thesis, University of Minnesota, Measurement of Aerosol Produced by the Photooxidation of SO_2 in Air.

Clark, W.E. and K.T. Whitby, 1972: "Measurement of Aerosols Produced by the Photochemical Oxidation of SO_2 in Air", J. Coll. Interface Sci., Vol. 51, No. 3, p. 477.

Cvetanovic, R.J., 1963: Adv. in Photochemistry, Vol. 1, p. 115.

Demerjian, K.L., J.A. Kerr, and J.G. Calvert, 1973: Adv. in Environ. Sci. Technol., Vol. 3, Wiley-Interscience, New York.

Glasson, W.A. and C.S. Tuesday, 1970: Environ. Sci. Technol., Vol. 4, p. 916.

Kocmond, W.C., D.B. Kittelson, J.Y. Yang, and K.L. Demerjian, 1973: "Determination of the Formation Mechanisms and Composition of Photochemical Aerosols", First Annual Summary Report, Calspan Report No. NA-5365-M-1, Calspan Corporation, Buffalo, New York 14221.

Liu, B.Y.H. and D.Y.H. Pui, 1975: "On the Performance of the Electrical Aerosol Analyzer", to be published in J. Aerosol Science.

Liu, B.Y.H. and D.Y.H. Pui, 1974: "A Submicron Aerosol Standard and the Primary, Absolute Calibration of the Condensation Nuclei Counter", J. Colloid and Interface Science, Vol. 47, p. 155.

Liu, B.Y.H., K.T. Whitby, and D.Y.H. Pui, 1974: "Size Distribution Measurement of Submicron Aerosols by a Portable Electrical Aerosol Analyzer", J. of the Air Poll. Control Assoc., Vol. 24, p. 1067.

Morris, E.D., Jr. and H. Niki, 1971: J. Phys. Chem., Vol. 75, p. 3640.

Skala, G.F., 1963: "A New Instrument for the Continuous Measurement of Condensation Nuclei", Anal. Chem., Vol. 35, p. 702.

Stedman, D.H. and H. Niki, 1973: Environ. Letters, Vol. 4, p. 303.

Wei, Y.K. and R.J. Cvetanovic, 1963: Can. J. Chem., Vol. 41, p. 913.

Whitby, K.T. and W.E. Clark, 1966: "Electrical Aerosol Particle Counting and Size Distribution Measuring System for the 0.015 to 1 μm Size Range", Tellus, Vol. 18, p. 573.

Whitby, K.T., B Y.H. Liu, R.B. Husar, and N.J. Barsic, 1972: "The Minnesota Aerosol Analyzing System Used in the Los Angeles Smog Project", J. Coll. and Interface Science, Vol. 39, p. 136.

TECHNICAL REPORT DATA
(Please read Instructions on the reverse before completing)

1. REPORT NO.	2.	3. RECIPIENT'S ACCESSION NO.
EPA-650/3-75-007		

4. TITLE AND SUBTITLE
STUDY OF AEROSOL FORMATION IN PHOTOCHEMICAL AIR POLLUTION

5. REPORT DATE
August 1975

6. PERFORMING ORGANIZATION CODE

7. AUTHOR(S)
W.C. Kocmond, D.B. Kittelson, J.Y. Yang, and K.L. Demerjian

8. PERFORMING ORGANIZATION REPORT NO.
NA-5365-M-2

9. PERFORMING ORGANIZATION NAME AND ADDRESS
Calspan Corporation
P. O. Box 235
Buffalo, New York 14221

10. PROGRAM ELEMENT NO.
1A1008

11. CONTRACT/GRANT NO.
68-01-1231

12. SPONSORING AGENCY NAME AND ADDRESS
Coordinating Research Council, Inc./Environmental Protection Agency
30 Rockefeller Plaza — Office of Res. & Devel.
New York, New York 10020 — Washington, D.C. 20460
CAPA-8-71

13. TYPE OF REPORT AND PERIOD COVERED
Annual

14. SPONSORING AGENCY CODE

15. SUPPLEMENTARY NOTES
Prepared in cooperation with the Particle Technology Laboratory, University of Minnesota

16. ABSTRACT

Photochemical aerosol production in several SO_2 + clean air (filtered air), HC+NO and HC+NO+SO_2 systems has been examined using the smog chamber approach. The reaction vessels used in this study were the 20,800 ft^3 Calspan chamber and the 600 ft^3 University of Minnesota chamber. Aerosol formation, growth, and decay mechanisms are described for each of the systems studied. It has been possible in this investigation to characterize system reactivity in terms of aerosol behavior. The most important variables are maximum number concentration, equilibrium surface concentration, and particle volumetric growth rate. Measurements of these variables are made for several systems and are discussed within the text.

Of the hydrocarbons studied, cyclohexene was the most reactive in terms of aerosol production and rate of NO oxidation followed by m-xylene, hexene, and toluene. For the simple HC+NO system, each experiment can be divided into two phases. During the initial phase, NO is converted to NO_2 and some oxidation of hydrocarbon occurs. No appreciable aerosol is formed during this phase, but ozone starts to appear near the end of this period. The second phase, accompanied by substantial aerosol formation, begins as soon as NO is oxidized out of the system and NO_2 reaches a maximum; ozone levels rise rapidly during this phase and approach a maximum. The addition of SO_2 to the HC+NO system leads to some aerosol formation during the first phase and was generally found to exert a synergistic effect on aerosol formation in the second phase. The addition of SO_2 also led to a marked decrease in the diameter of the particles ultimately formed. This results from the formation of very high concentrations

17. KEY WORDS AND DOCUMENT ANALYSIS

a. DESCRIPTORS	b. IDENTIFIERS/OPEN ENDED TERMS	c. COSATI Field/Group
Photochemistry Photochemical Air Pollution Aerosol Formation Smog Chamber		

18. DISTRIBUTION STATEMENT	19. SECURITY CLASS *(This Report)*	21. NO. OF PAGES
Unlimited Distribution	Unclassified	185
	20 SECURITY CLASS *(This page)*	22. PRICE
	Unclassified	

EPA Form 2220-1 (9-73)

16.

of nuclei during the initial stages of the experiment.

For the SO_2 + clean air system, photooxidation rates of a few tenths of a percent per hour are typically observed for a light intensity of 50% noon day sun. In the presence of hydrocarbons and NO, accelerated rates are generally observed.

The data show that aerosol formation rates are enhanced at high relative humidities, probably as a result of the higher water content of the aerosols.

APPENDIX A

AEROSOL AND CHEMISTRY DATA FROM NOVEMBER 1973 WORKSHOP WITH DUPLICATE UNIVERSITY OF MINNESOTA EXPERIMENTS

ORDER OF PRESENTATION:

(1) SO_2 Experiments

(2) Toluene, Toluene + NO_2, Toluene + NO_2 + SO_2

(3) Hexene, Hexene + NO_2, Hexene + NO_2 + SO_2

Table V. SUMMARY OF DATA FROM NOVEMBER 1973 WORKSHOP

Run No.	System	RH %	HC ppm	NO_2 ppm	SO_2 ppm	N_{max} $x10^{-3}cm^{-3}$	S_E $\mu^2/cc/hr$	$\frac{dv}{dt}(SO_2)$ $\mu m^3/cc/hr$	SO_2 photox. $\%hr^{-1}$
1	SO_2*	--	b*	b	0.63	560	470	1.71	.03
2	SO_2	30	b	b	0.70	700	not reached	6.15i** / 13.75f**	.17 / .37
3	SO_2*	33	b	b	0.58	525	>600	1.60i / 3.60f	.05 / .11
4	SO_2*	34	b	b	0.55	570	>600	1.20i / 2.83f	.04 / .09
5	SO_2	31	b	b	0.52	960	>1100	7.33	.27
6	SO_2	32	b	b	0.55	750	1600	6.0 i / 16.7 f	.21 / .57
7	toluene	35	0.8	b	---	NO AEROSOL			
8	toluene + NO_2	37	0.8	5.0	---				
9	toluene + NO_2	34	0.8	3.3	---				
10	toluene + NO_2 + SO_2	45	0.8	1.95	.19	1000	1000 then less	7.50i / 1.90f	.64 / .18
11	toluene + NO_2 + SO_2	36	0.8	3.55	.07	800	700 then less	5.00i / 0.41f	1.30 / 0.10
12	toluene + NO_2 + SO_2	33	0.8	1.45	.01	500	280 then less	0.88i / 0.28f	1.65 / .53
13	hexene	38	0.6	b	---	95	>50	---	---
14	hexene + NO_2	34	0.6	3.35	---	46	---	---	---
15	hexene + NO_2 + SO_2	32	0.6	1.64	.01	580	400	2.4 i / 0.9 f	4.57 / 1.71

*partial lights used on experiments 1, 3 and 4 to duplicate previous year's light intensity, i.e., $k_d[NO_2]$~0.05 min^{-1}.

**i and f refer to initial (usually first 30 min) and final growth rates.

b = background

TABLE VII. UNIVERSITY OF MINNESOTA DUPLICATE TESTS SUBSEQUENT TO NOVEMBER WORKSHOP:

SUMMARY OF SO_2 EXPERIMENTS

Run No.	Concentration ppm	RH %	N_{max} $\#\text{-cc}^{-1}$	SE $\mu m^2\text{-cc}^{-1}$	$\frac{dv}{dt}_3$ SO_2 $\mu m^3\text{-cc}^{-1}\text{-hr}^{-1}$	$\frac{1}{SO_2}\frac{dv}{dt}_3$ $\mu m^3\text{-cc}^{-1}\text{-hr}^{-1}\text{-ppm}^{-1}$	SO_2 photox $\%\ hr^{-1}$
1	.51	13	90 K	420*	2.3	4.5	.12
2	.53	9	150 K	420*	2.6	4.9	.13
3	.64	64	320 K	660	3.1	4.8	.057
4	.59	36	170 K	340	.98	1.7	.030
5	.55	35	160 K	380*	.93	1.7	.032
6	.55	29	110 K	210	.49	.89	.018
11	.55	30	600 K	1300	12.0	22	.42
12	.47	49	330 K	1400	9.8	21	.35
17	.54	27	220 K	420	1.1	2.0	.041
18	.012	17	54 K	72*	.12	10	.23
19	.012	36	35 K	25*	---	---	---
20	.54	29	280 K	620*	2.2	4.1	.079

*Equilibrium surface not reached.

TABLE VIII . UNIVERSITY OF MINNESOTA DUPLICATE TESTS SUBSEQUENT TO NOVEMBER WORKSHOP: SUMMARY OF CHEMICAL AND AEROSOL DATA FOR TOLUENE EXPERIMENTS

Run No.	System	RH %	HC ppm	NO_2 ppm	SO_2 ppm	N_{max} #-cc^{-1}	S_E μm^2-cc^{-1}	$\frac{dv}{dt}$ SO_2 μm^3-cc^{-1}-hr^{-1}	SO_2 photox %-hr^{-1}
7	Toluene	24	2.0	b	---	---	---	---	---
8	Toluene	24	2.0	b	---	---	---	---	---
9	Toluene + NO_2	33	1.5	3.90	---	2.2 K	NO AEROSOL ---	---	---
10	Toluene + NO_2	32	1.0	3.34	---	.25K	---	---	---
13	Toluene + NO_2 + SO_2	27	1.0	.26	.01	250 K	1200*	---	---
14	Toluene + NO_2 + SO_2	36	1.0	4.19	.01	50 K	---	---	---
15	Toluene + NO_2 + SO_2	25	1.0	1.23	.54	660 K	1200	4.7	.35
16	Toluene + NO_2 + SO_2	26	1.0	1.95	.54	740 K	1300	3.6	.28

*Equilibrium surface not reached.

(1) SO_2 EXPERIMENTS

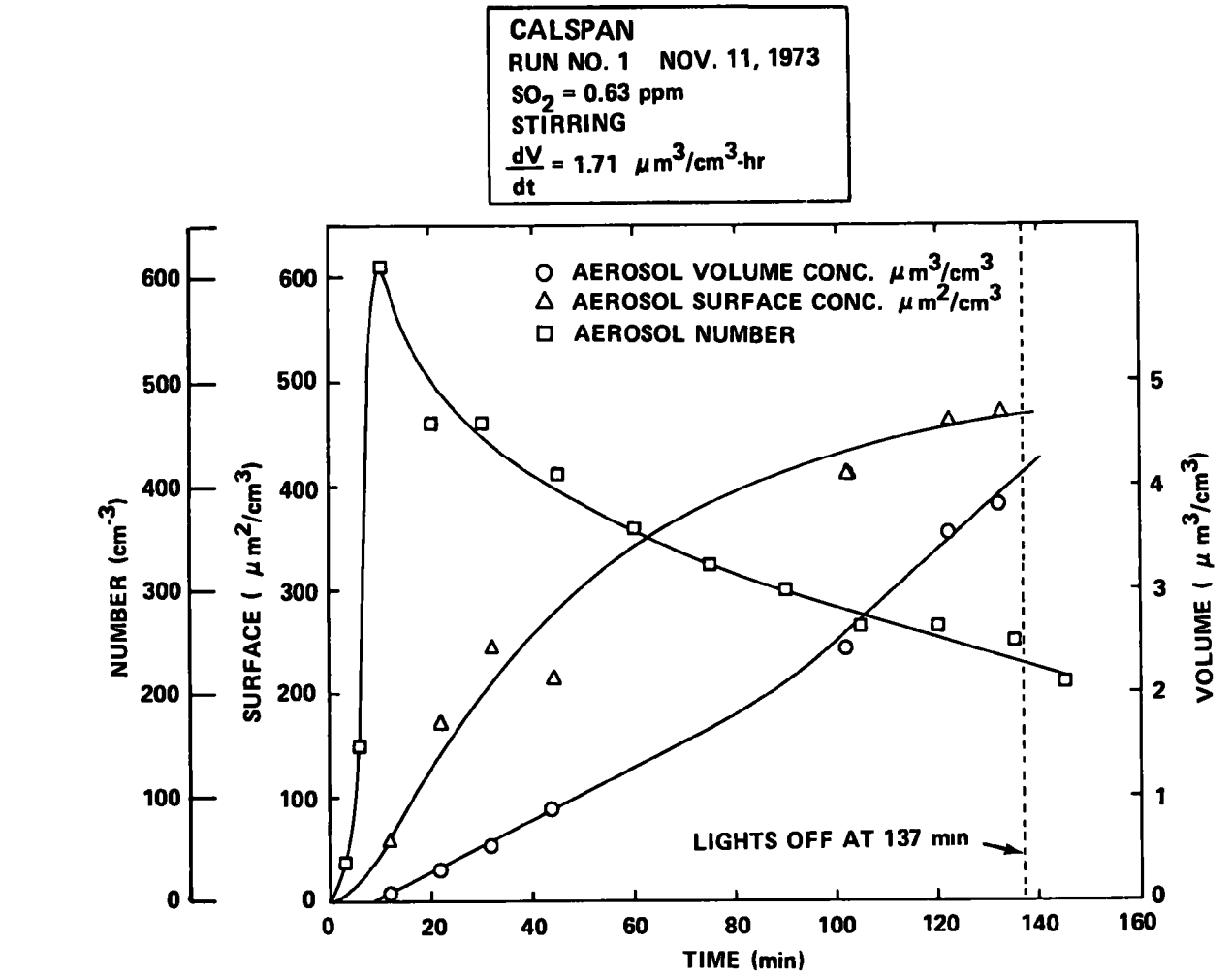
CALSPAN
RUN NO. 1 NOV. 11, 1973
SO_2 = 0.63 ppm
STIRRING
$\frac{dV}{dt}$ = 1.71 $\mu m^3/cm^3$-hr
O AEROSOL VOLUME CONC. $\mu m^3/cm^3$
Δ AEROSOL SURFACE CONC. $\mu m^2/cm^3$
□ AEROSOL NUMBER
NUMBER (cm^{-3})
SURFACE ($\mu m^2/cm^3$)
VOLUME ($\mu m^3/cm^3$)
LIGHTS OFF AT 137 min
TIME (min)

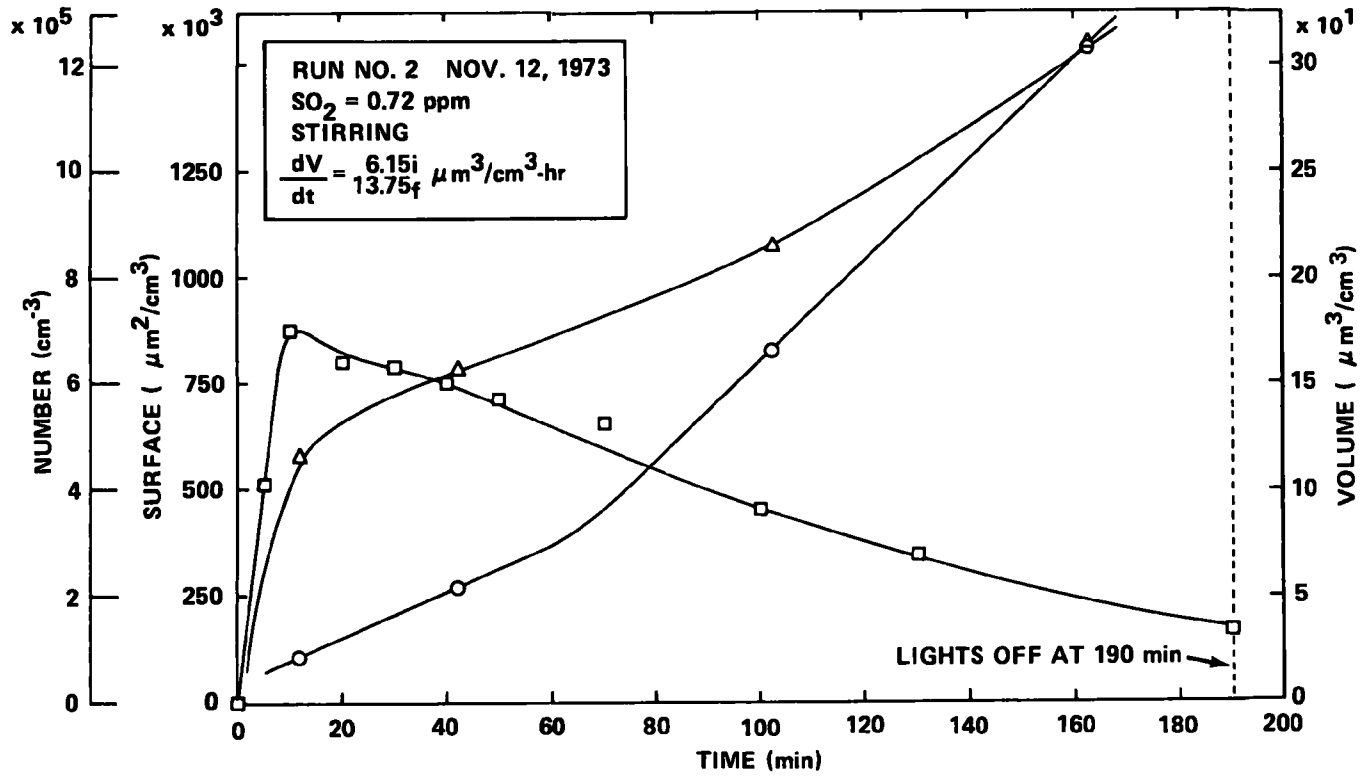
RUN NO. 2 NOV. 12, 1973
SO_2 = 0.72 ppm
STIRRING
$\frac{dV}{dt} = \frac{6.15i}{13.75_f}$ $\mu m^3/cm^3$-hr
x 10^5
x 10^3
x 10^1
NUMBER (cm^{-3})
SURFACE ($\mu m^2/cm^3$)
VOLUME ($\mu m^3/cm^3$)
LIGHTS OFF AT 190 min
TIME (min)

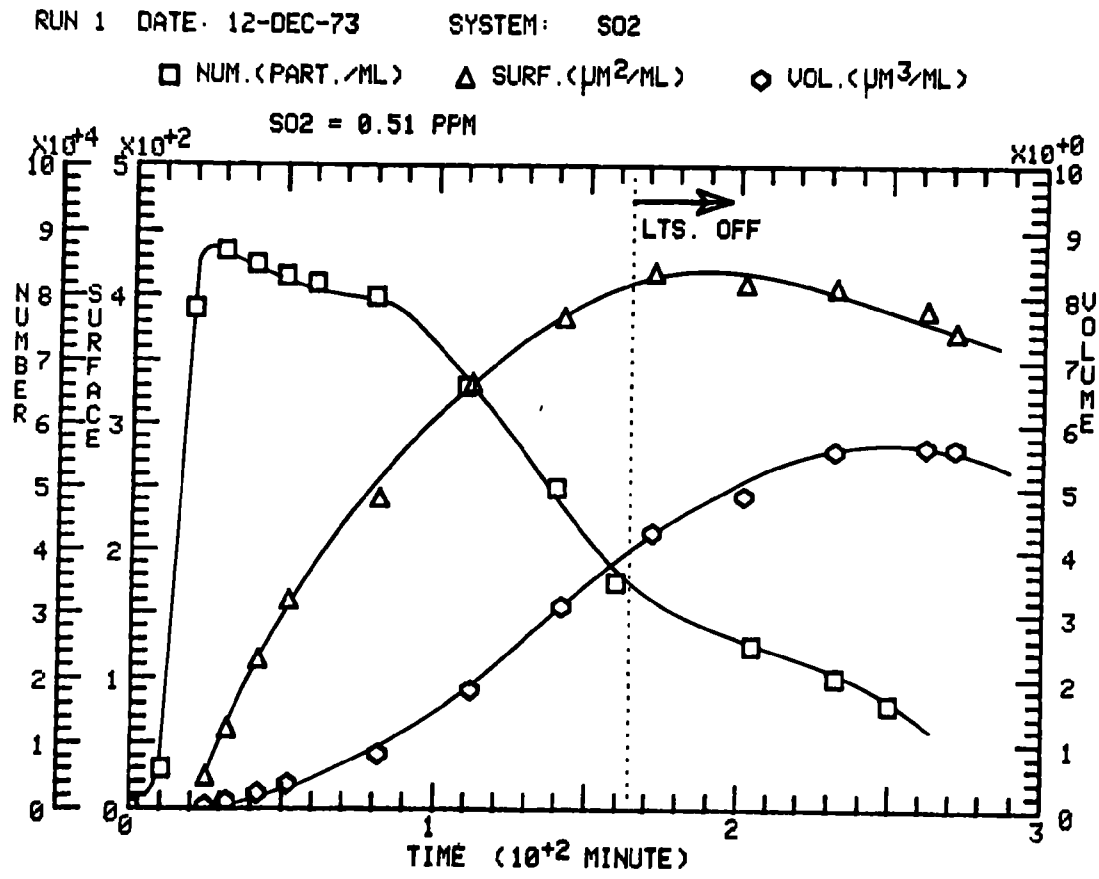
RUN 1 DATE· 12-DEC-73 SYSTEM: SO2
NUM.(PART./ML) SURF.(μM²/ML) VOL.(μM³/ML)
SO2 = 0.51 PPM
X10+4
X10+2
X10+0
LTS. OFF
NUMBER
SURFACE
VOLUME
TIME (10+2 MINUTE)

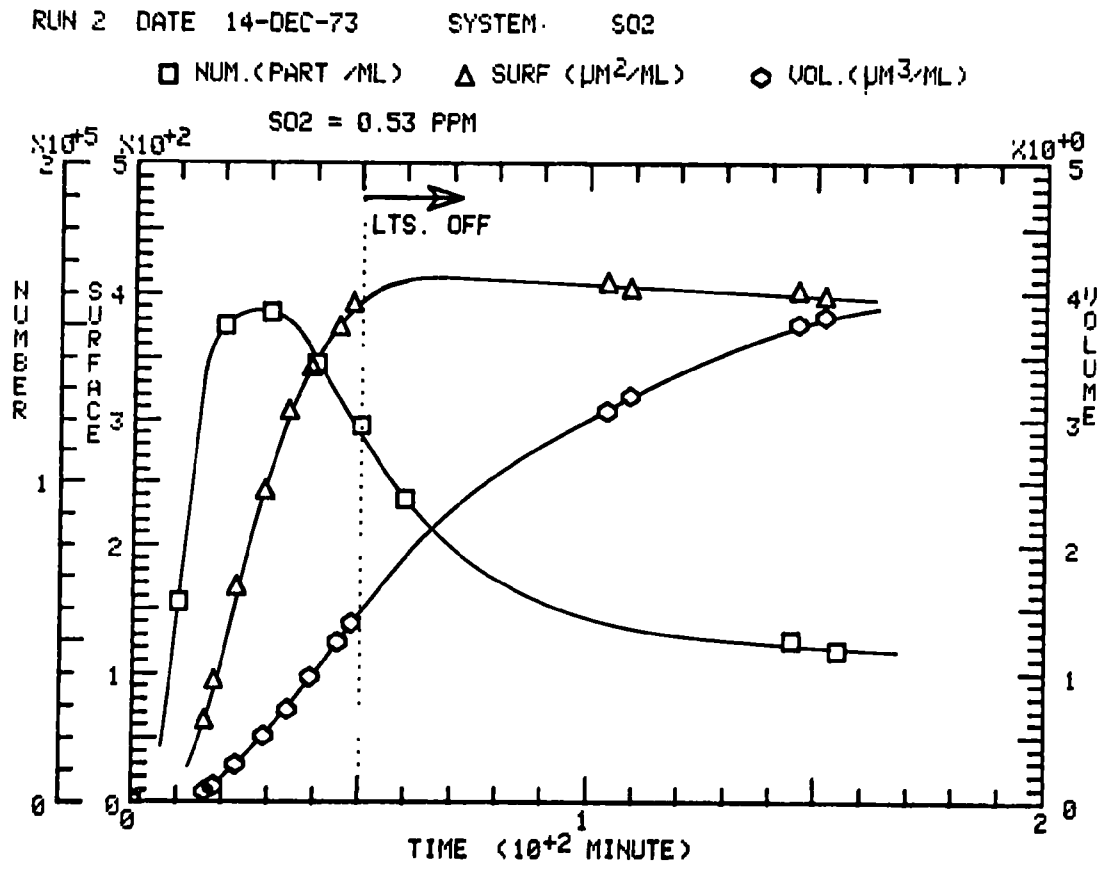
RUN 2 DATE 14-DEC-73 SYSTEM· SO2
NUM.(PART./ML) SURF (μM²/ML) VOL.(μM³/ML)
SO2 = 0.53 PPM
X10+5
X10+2
X10+0
LTS. OFF
NUMBER
SURFACE
VOLUME
TIME (10+2 MINUTE)

RUN NO. 3 NOV. 13, 1973
SO_2 = 0.58 ppm
STIRRING
$\frac{dV}{dT} = \frac{1.60i}{3.60f}$ $\mu m^3/cm^3$-hr

CALSPAN

○ AEROSOL VOLUME CONC. $\mu m^3/cm^3$
△ AEROSOL SURFACE CONC. $\mu m^2/cm^3$
□ AEROSOL NUMBER

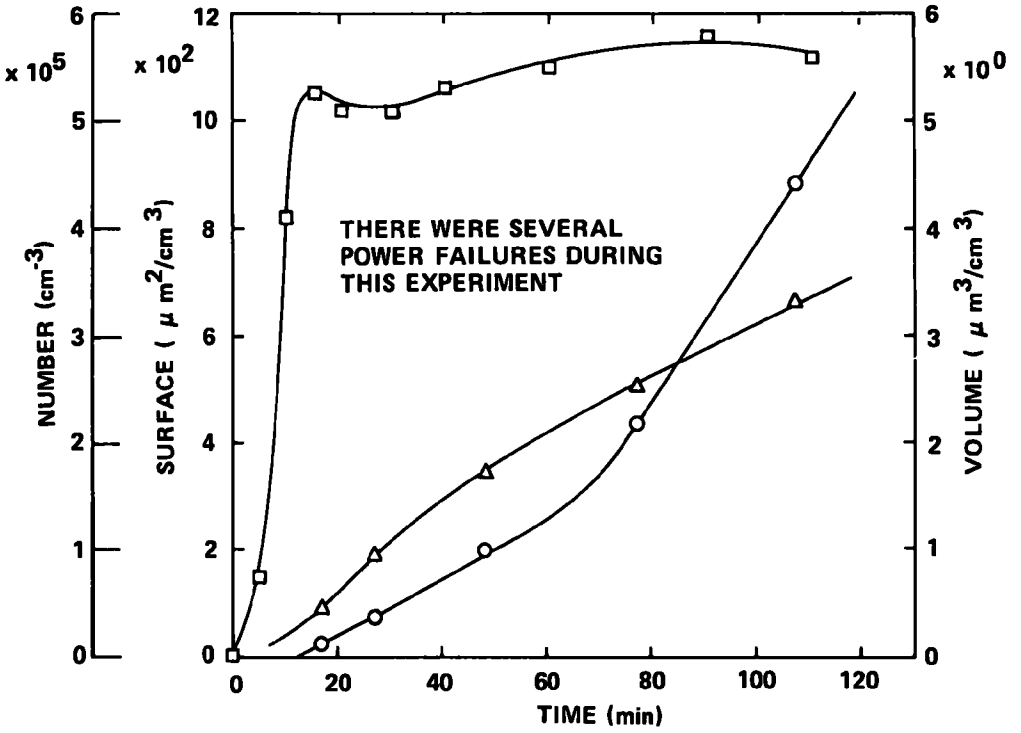

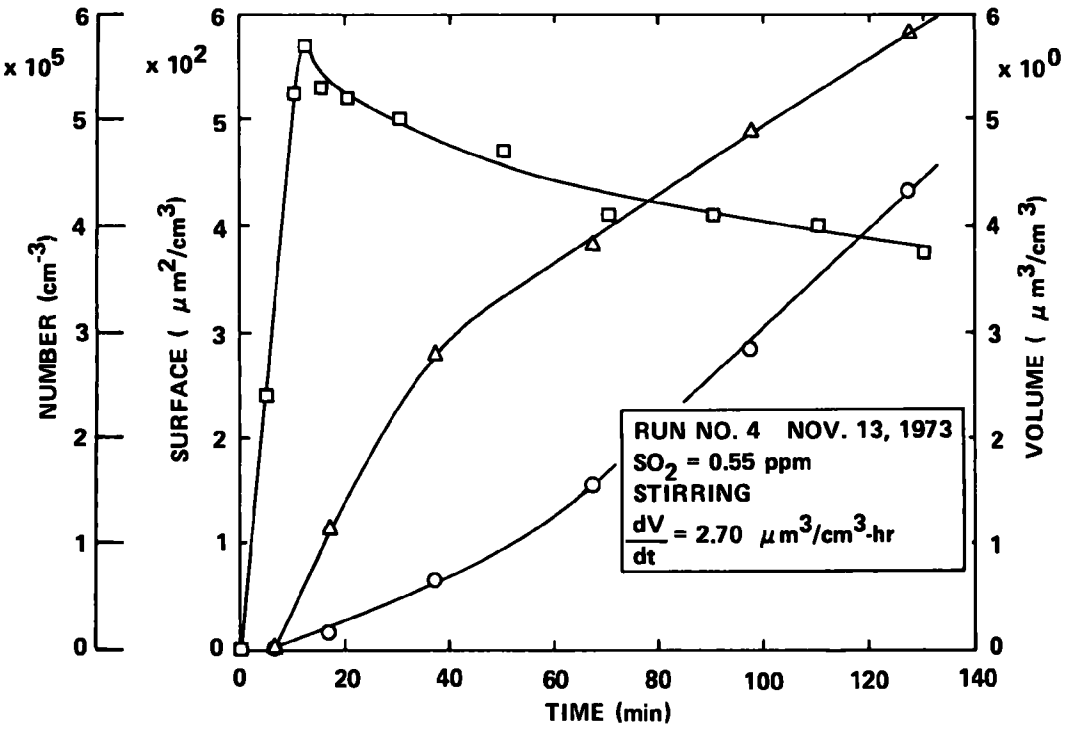

RUN 3 DATE: 18-DEC-74 SYSTEM: SO2

□ NUM.(PART./ML) △ SURF.(μM²/ML) ◇ VOL.(μM³/ML)

SO2 = 0.64 PPM

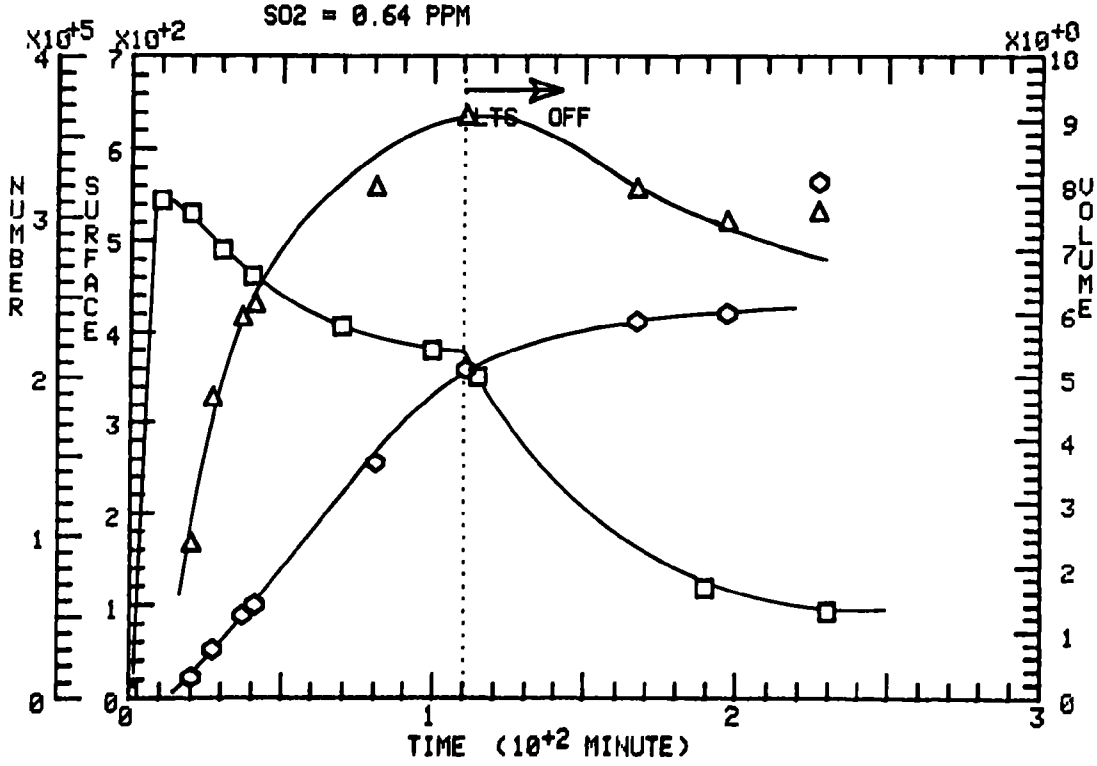

RUN 4 DATE: 18-DEC-73 SYSTEM: SO2

□ NUM (PART./ML) △ SURF.(μM²/ML) ◇ VOL.(μM³/ML)

SO2 = 0.59 PPM

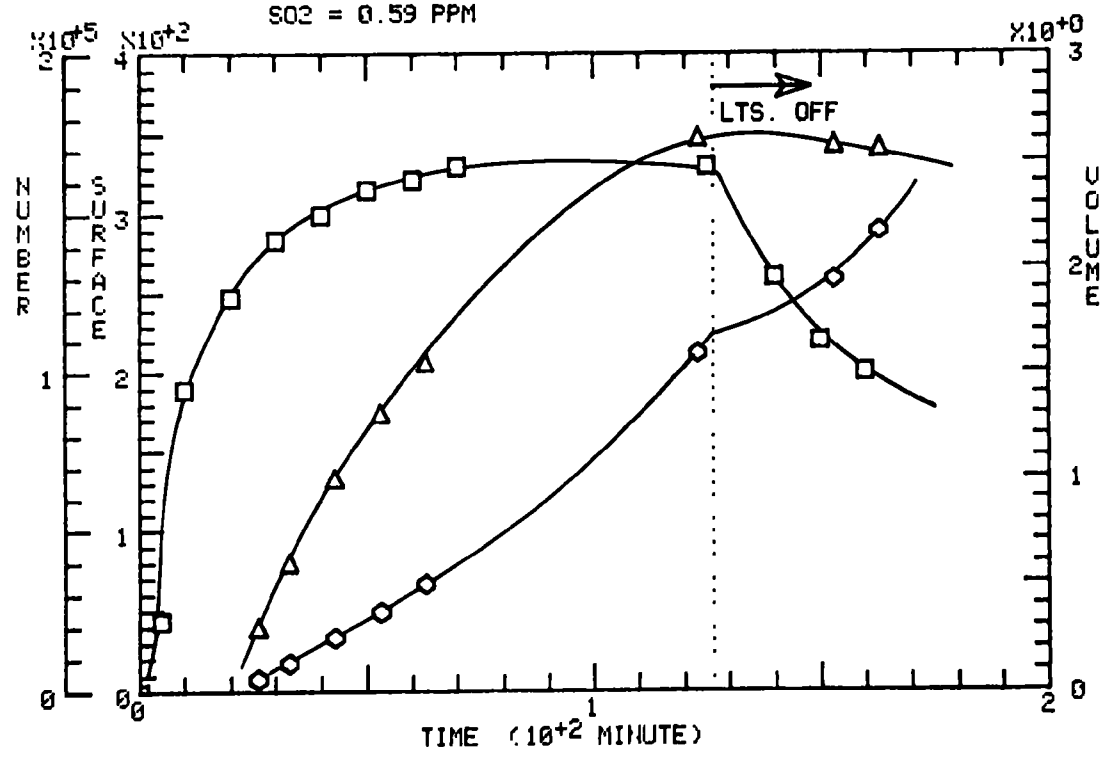

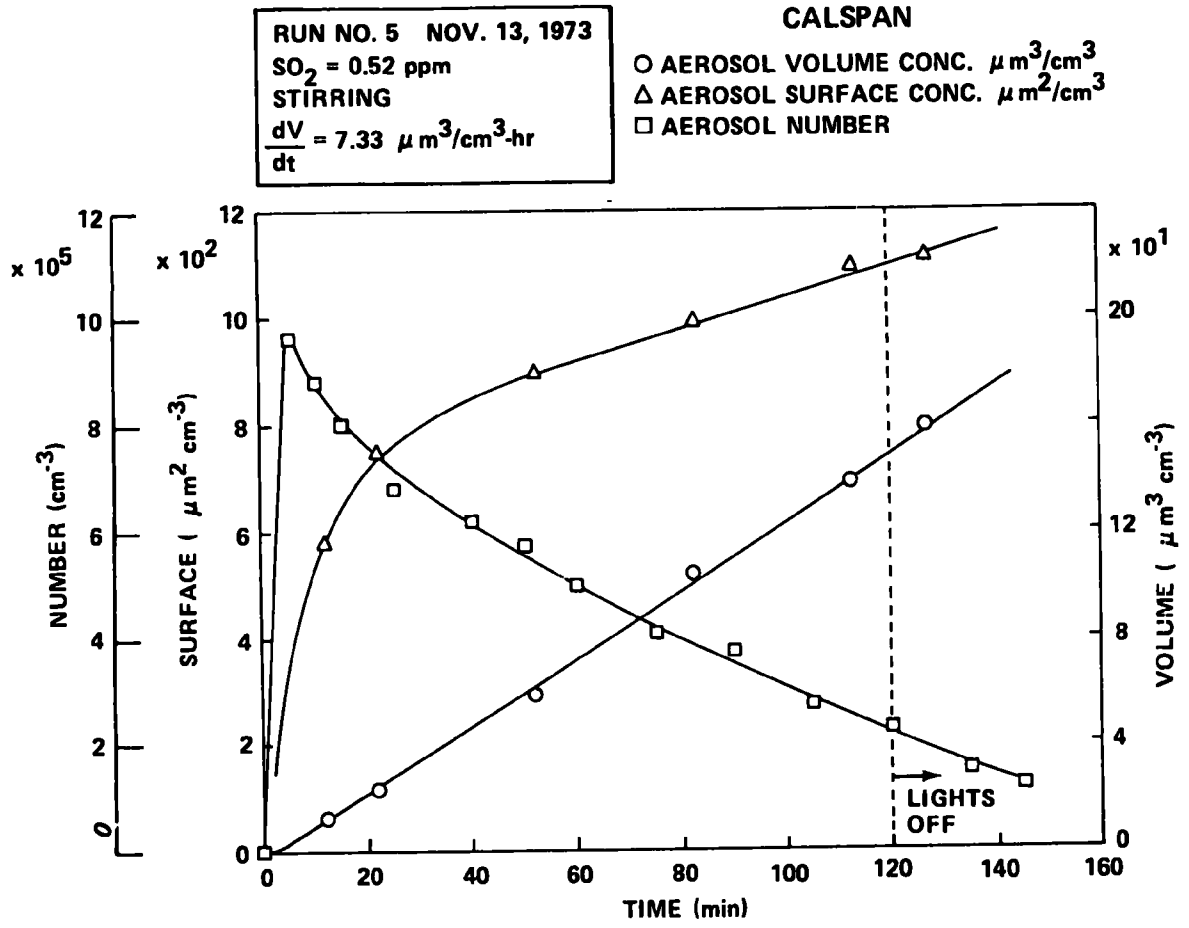
RUN NO. 5 NOV. 13, 1973
SO_2 = 0.52 ppm
STIRRING
$\frac{dV}{dt}$ = 7.33 $\mu m^3/cm^3$-hr
CALSPAN
O AEROSOL VOLUME CONC. $\mu m^3/cm^3$
Δ AEROSOL SURFACE CONC. $\mu m^2/cm^3$
□ AEROSOL NUMBER
NUMBER (cm^{-3})
SURFACE (μm^2 cm^{-3})
VOLUME (μm^3 cm^{-3})
x 10^5
x 10^2
x 10^1
LIGHTS OFF
TIME (min)

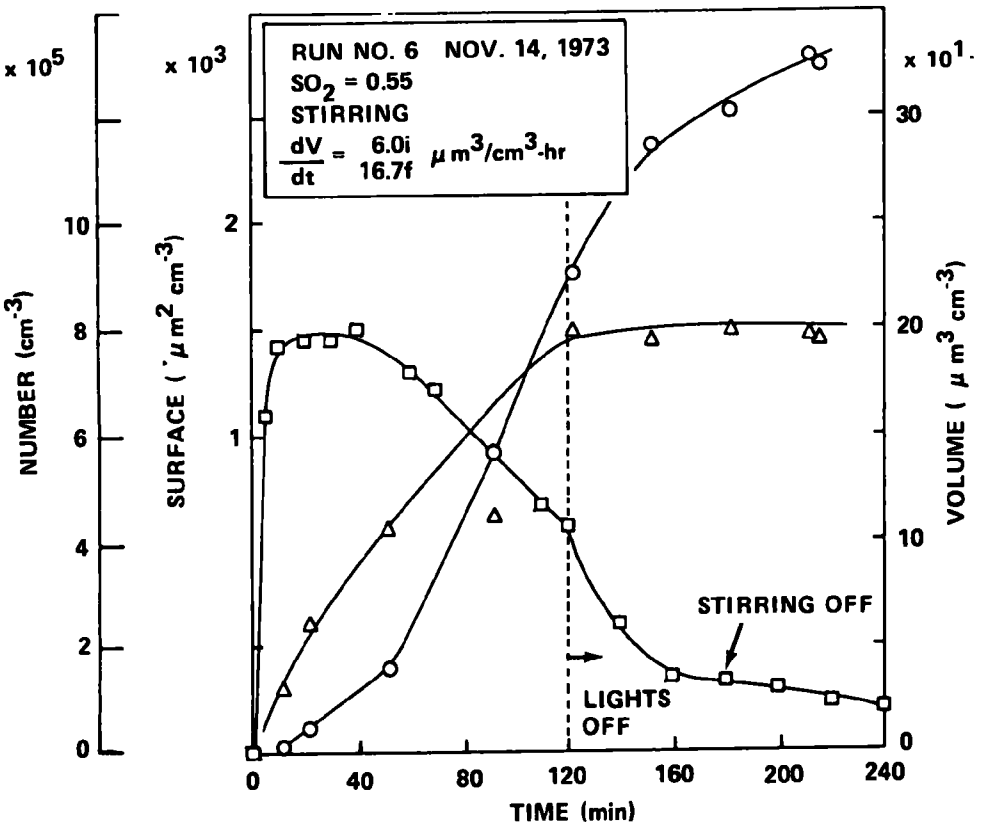
RUN NO. 6 NOV. 14, 1973
SO_2 = 0.55
STIRRING
$\frac{dV}{dt}$ = 6.0i / 16.7f $\mu m^3/cm^3$-hr
NUMBER (cm^{-3})
SURFACE (μm^2 cm^{-3})
VOLUME (μm^3 cm^{-3})
x 10^5
x 10^3
x 10^1
STIRRING OFF
LIGHTS OFF
TIME (min)

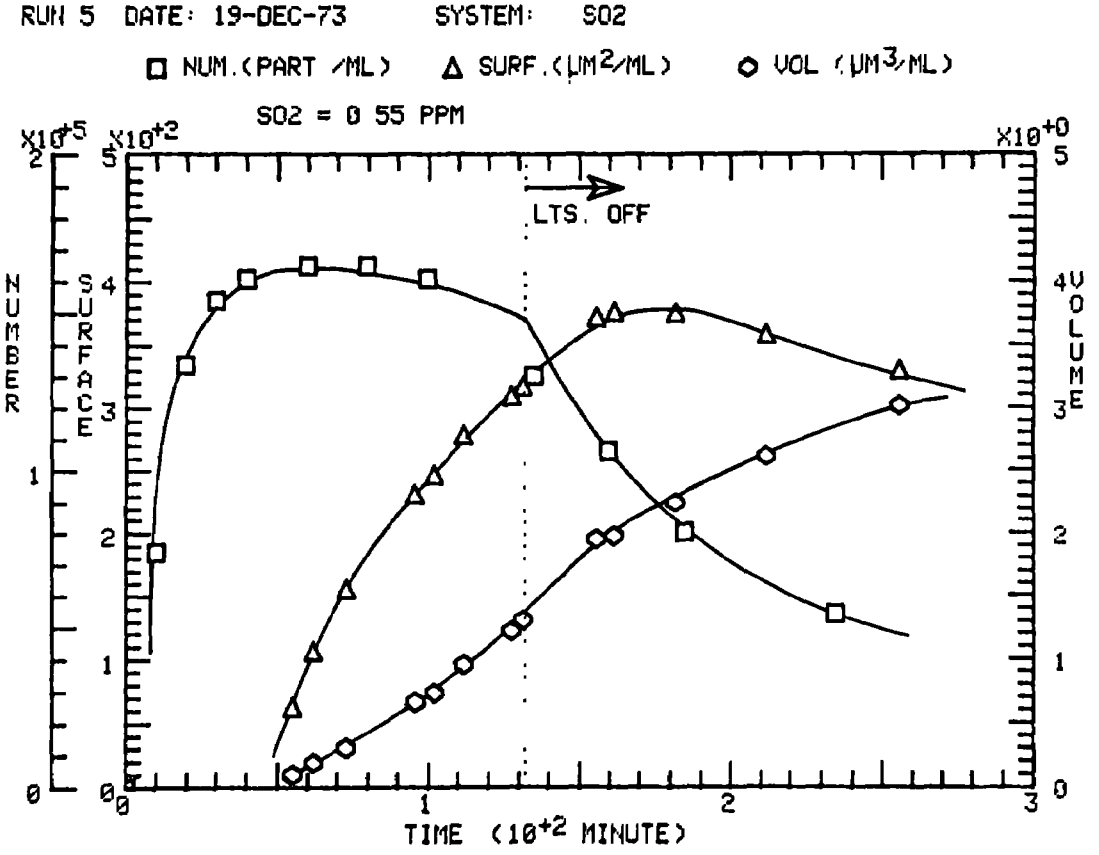
RUN 5 DATE: 19-DEC-73 SYSTEM: SO2
NUM.(PART /ML)
SURF.(μM²/ML)
VOL (μM³/ML)
SO2 = 0 55 PPM
X10+5
X10+2
X10+0
LTS. OFF
NUMBER
SURFACE
VOLUME
TIME (10+2 MINUTE)

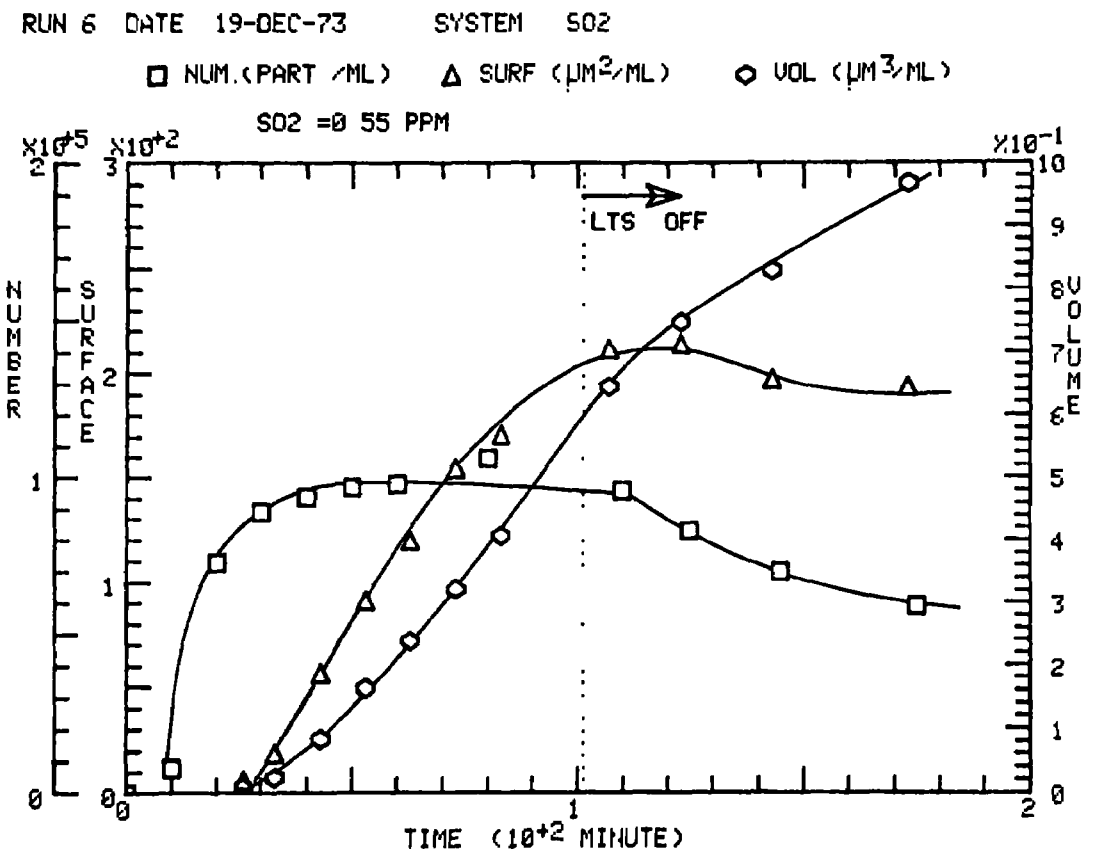
RUN 6 DATE 19-DEC-73 SYSTEM SO2
NUM.(PART /ML)
SURF (μM²/ML)
VOL (μM³/ML)
SO2 =0 55 PPM
X10+5
X10+2
X10-1
LTS OFF
NUMBER
SURFACE
VOLUME
TIME (10+2 MINUTE)

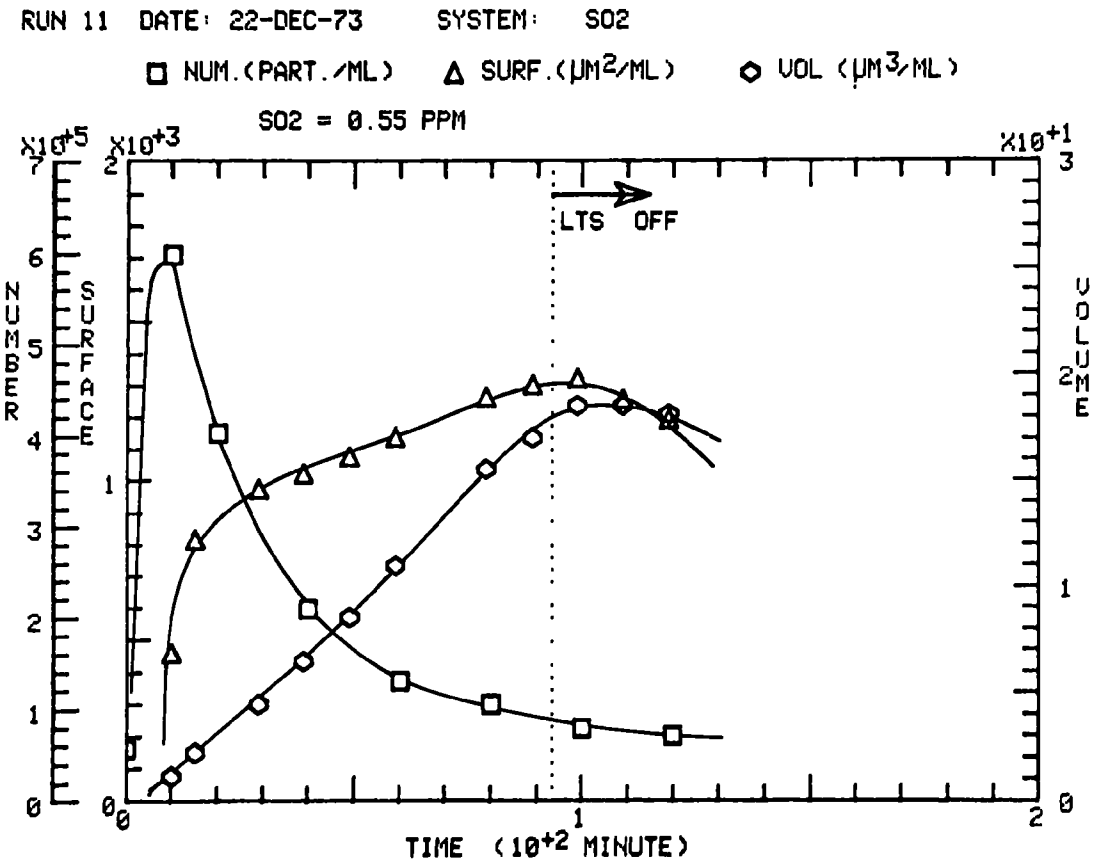
RUN 11 DATE: 22-DEC-73 SYSTEM: SO2
NUM.(PART./ML) SURF.(μM²/ML) VOL (μM³/ML)
SO2 = 0.55 PPM
X10+5
X10+3
X10+1
LTS OFF
NUMBER
SURFACE
VOLUME
TIME (10+2 MINUTE)

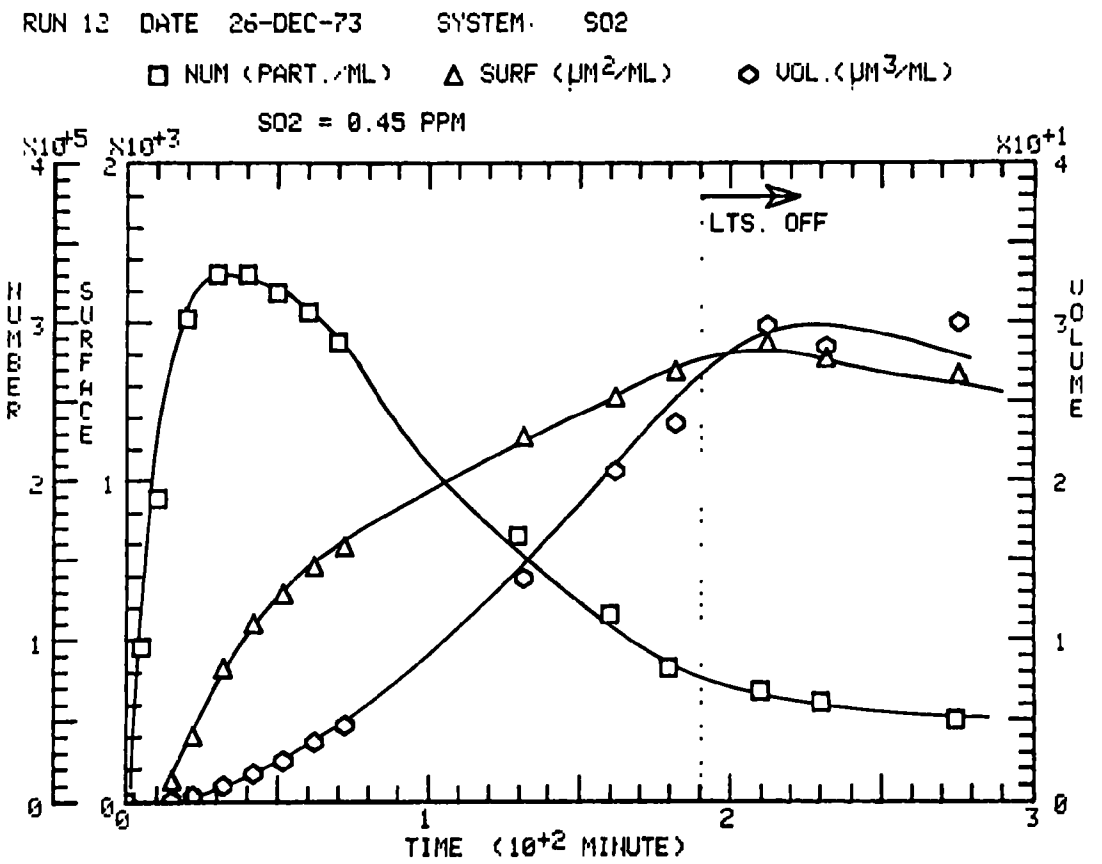
RUN 12 DATE 26-DEC-73 SYSTEM: SO2
NUM (PART./ML) SURF (μM²/ML) VOL.(μM³/ML)
SO2 = 0.45 PPM
X10+5
X10+3
X10+1
LTS. OFF
NUMBER
SURFACE
VOLUME
TIME (10+2 MINUTE)

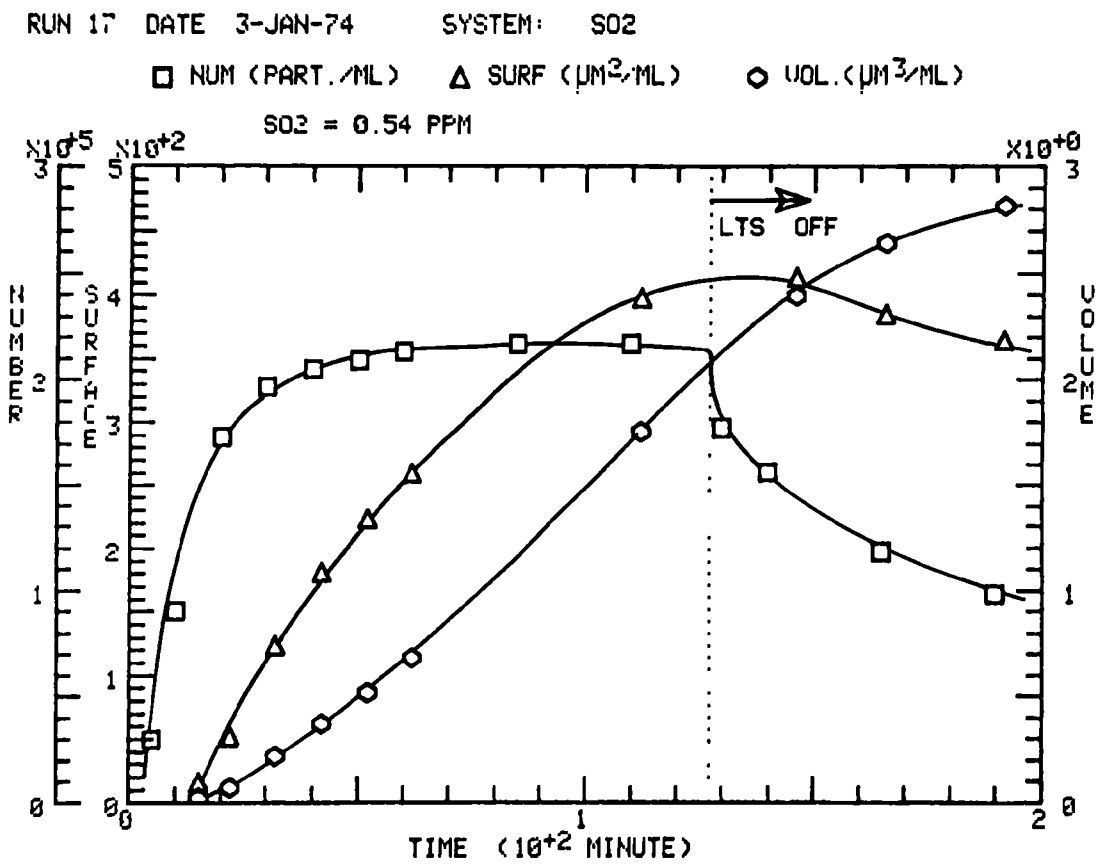
RUN 17 DATE 3-JAN-74 SYSTEM: SO2
NUM (PART./ML) SURF (μM²/ML) VOL.(μM³/ML)
SO2 = 0.54 PPM
X10+5
X10+2
X10+0
LTS OFF
NUMBER
SURFACE
VOLUME
TIME (10+2 MINUTE)

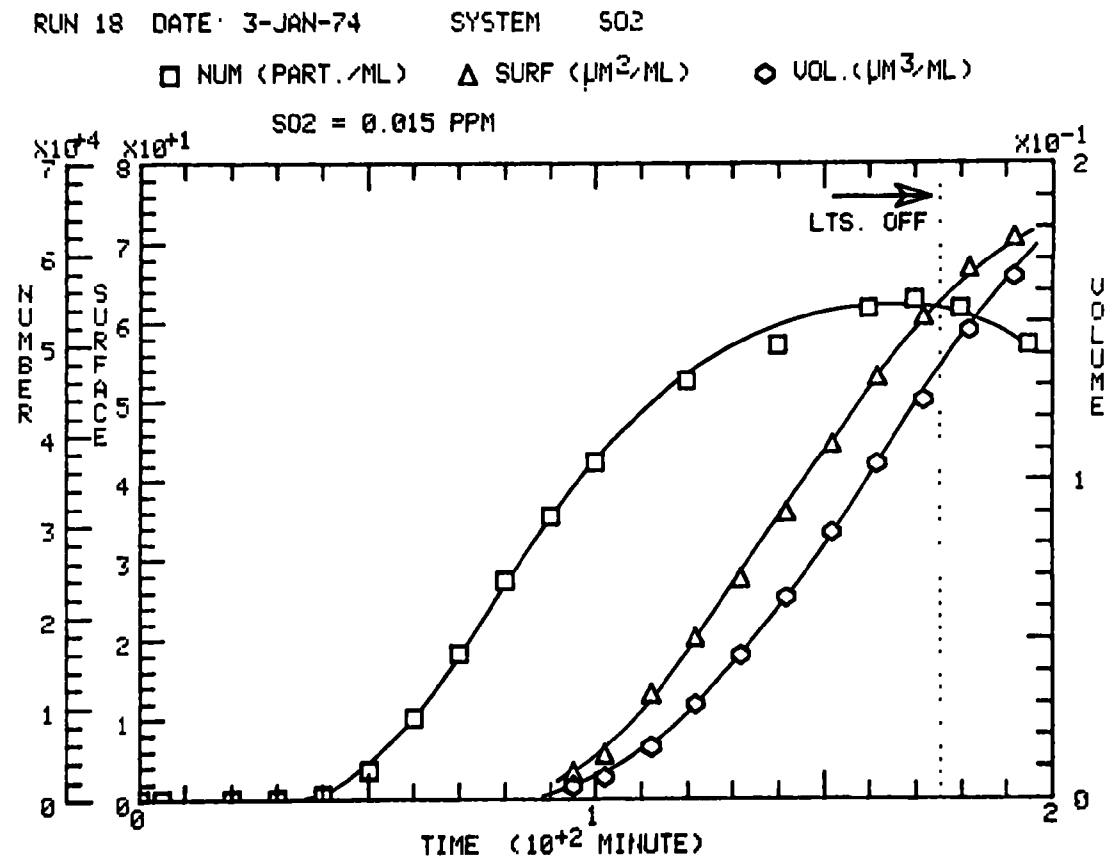
RUN 18 DATE 3-JAN-74 SYSTEM SO2
NUM (PART./ML) SURF (μM²/ML) VOL.(μM³/ML)
SO2 = 0.015 PPM
X10+4
X10+1
X10-1
LTS. OFF
NUMBER
SURFACE
VOLUME
TIME (10+2 MINUTE)

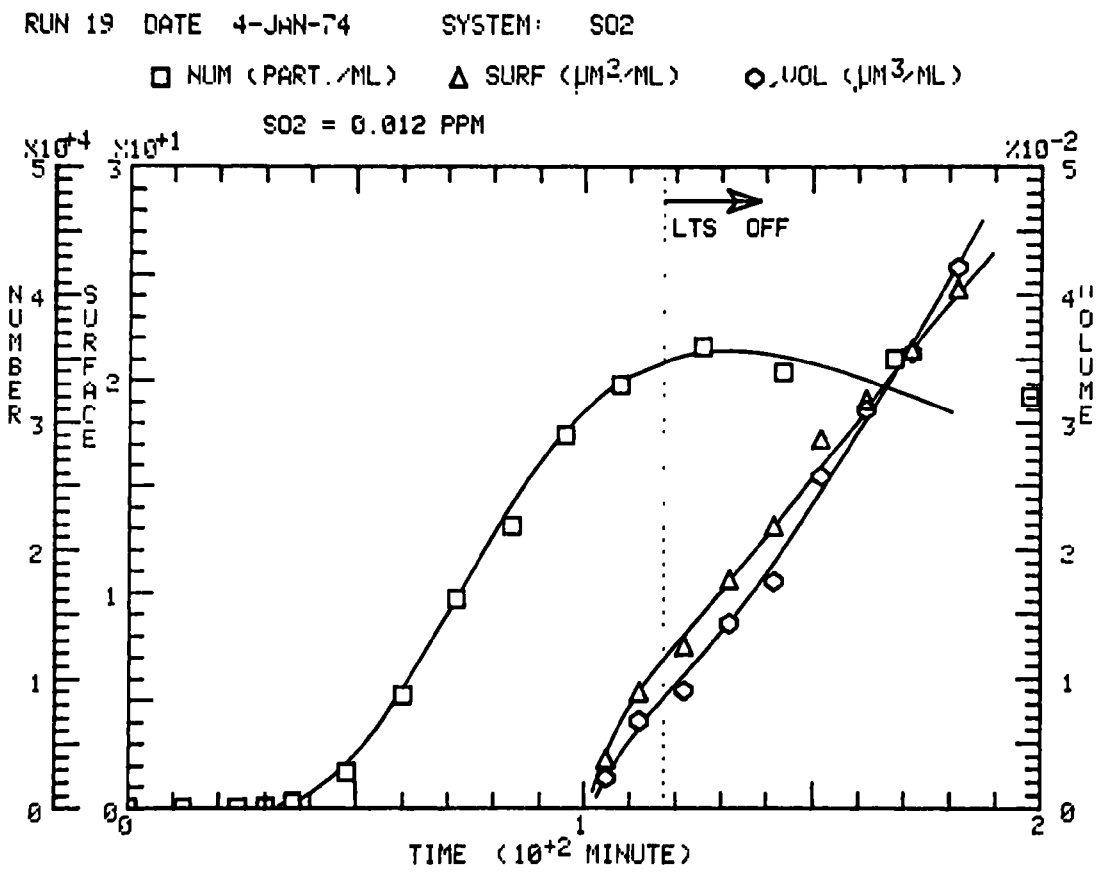
RUN 19 DATE 4-JAN-74 SYSTEM: SO2
NUM (PART./ML) SURF (μM²/ML) VOL (μM³/ML)
SO2 = 0.012 PPM
X10+4
X10+1
X10-2
LTS OFF
NUMBER
SURFACE
VOLUME
TIME (10+2 MINUTE)

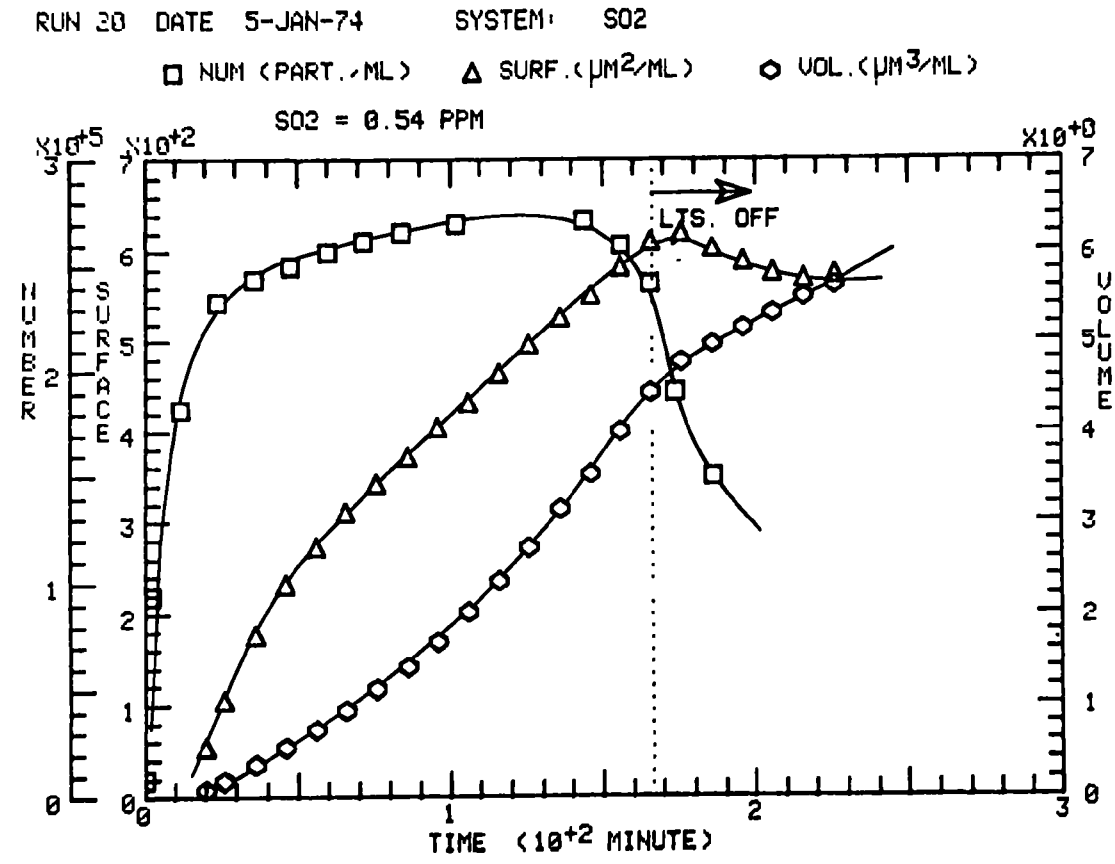
RUN 20 DATE 5-JAN-74 SYSTEM: SO2
NUM (PART./ML) SURF.(μM²/ML) VOL.(μM³/ML)
SO2 = 0.54 PPM
X10+5
X10+2
X10+0
LTS. OFF
NUMBER
SURFACE
VOLUME
TIME (10+2 MINUTE)

(2) TOLUENE, TOLUENE + NO_2, TOLUENE + NO_2 + SO_2 EXPERIMENTS

CALSPAN
RUN NO. 7 14 NOVEMBER 1973 TOLUENE + BACKGROUND NO_x SYSTEM R.H. = 35%;
TOLUENE = 0.8 ppm; NO_2 = 0.00 ppm; NO = 0.004 ppm

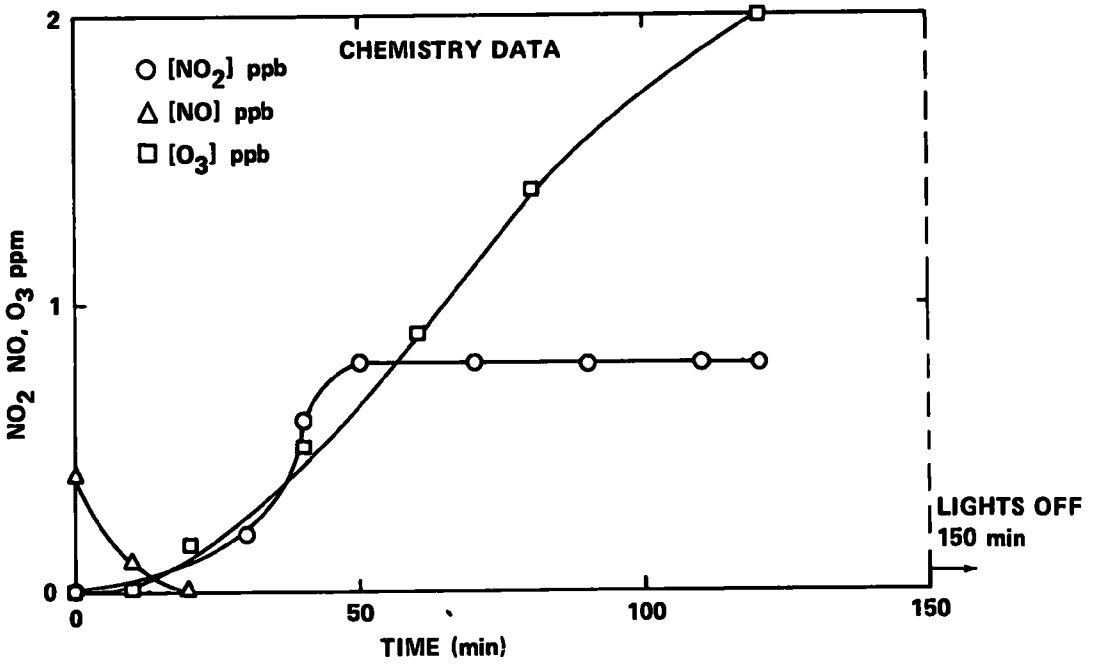

CALSPAN

RUN NO. 8 14 NOVEMBER 1973 TOLUENE + NO_2 SYSTEM R.H. = 37%; TOLUENE = 0.98 ppm; NO_2 = 5.0 ppm; NO = 0.03 ppb

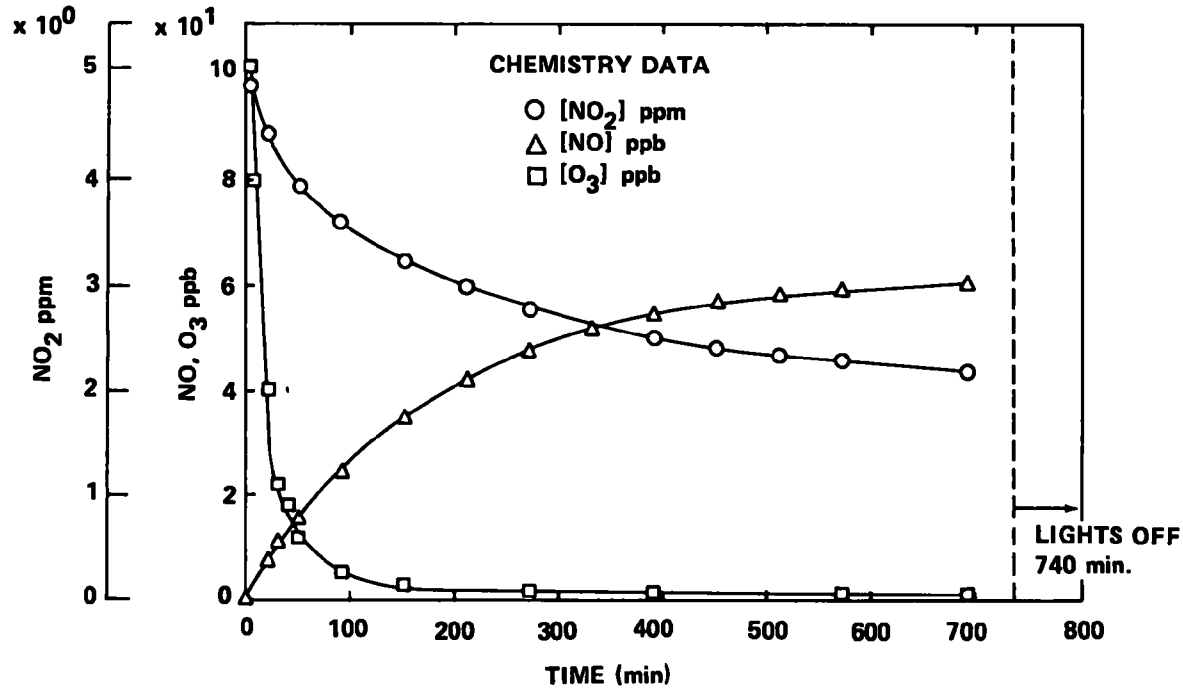

CALSPAN
RUN NO. 9 15 NOVEMBER 1973 TOLUENE + NO_2 SYSTEM R.H. = 34%;
TOLUENE = 0.8 ppm; NO_2 = 3.30 ppm; NO = 0.03 ppm

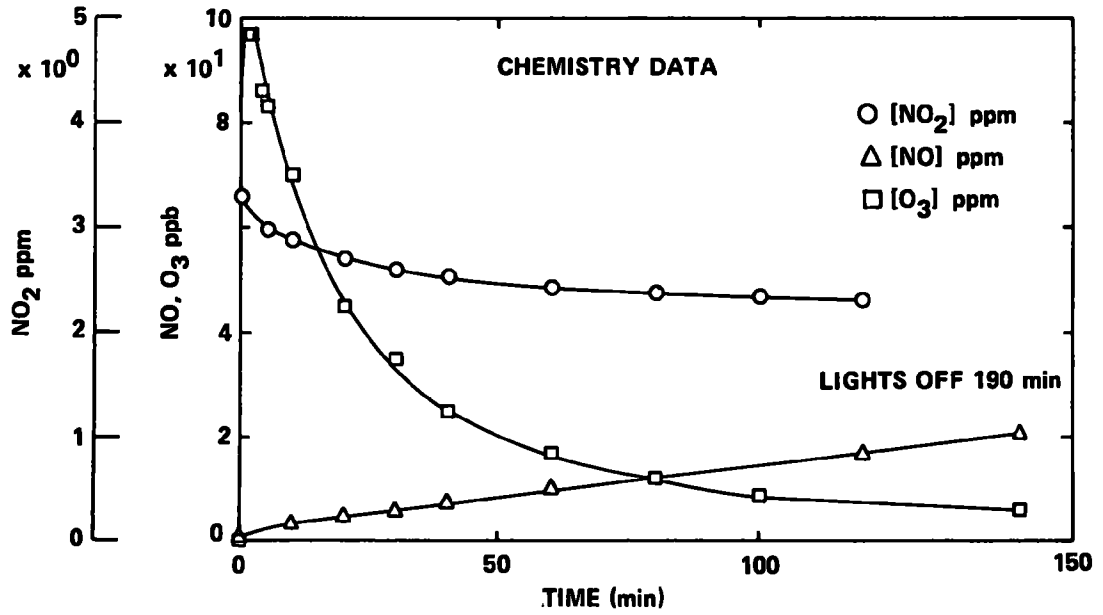

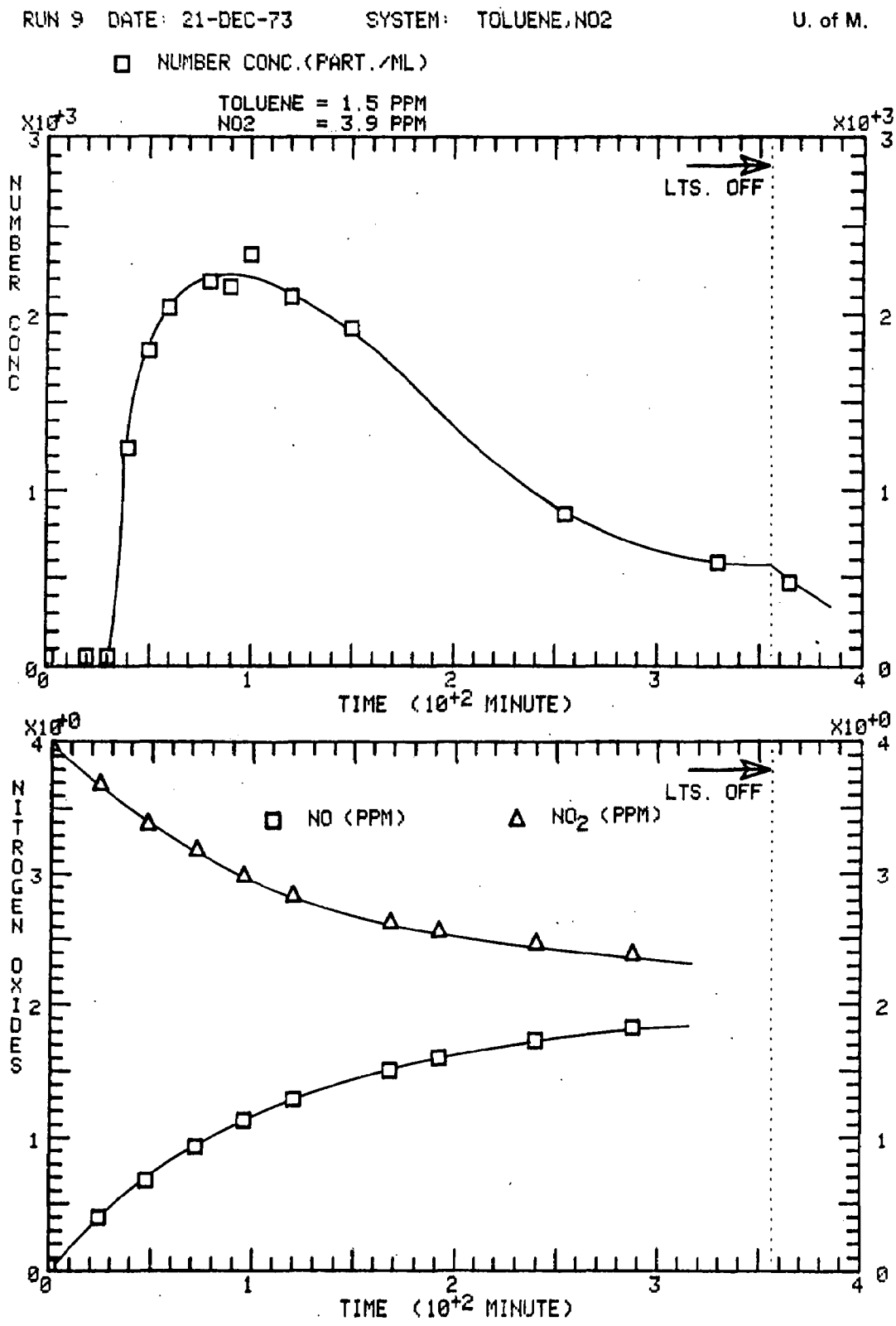
RUN 9 DATE: 21-DEC-73 SYSTEM: TOLUENE/NO2 U. of M.
NUMBER CONC.(PART./ML)
TOLUENE = 1.5 PPM
NO2 = 3.9 PPM
X10+3
NUMBER CONC
LTS. OFF
TIME (10+2 MINUTE)
X10+0
NITROGEN OXIDES
NO (PPM)
NO2 (PPM)
LTS. OFF
TIME (10+2 MINUTE)

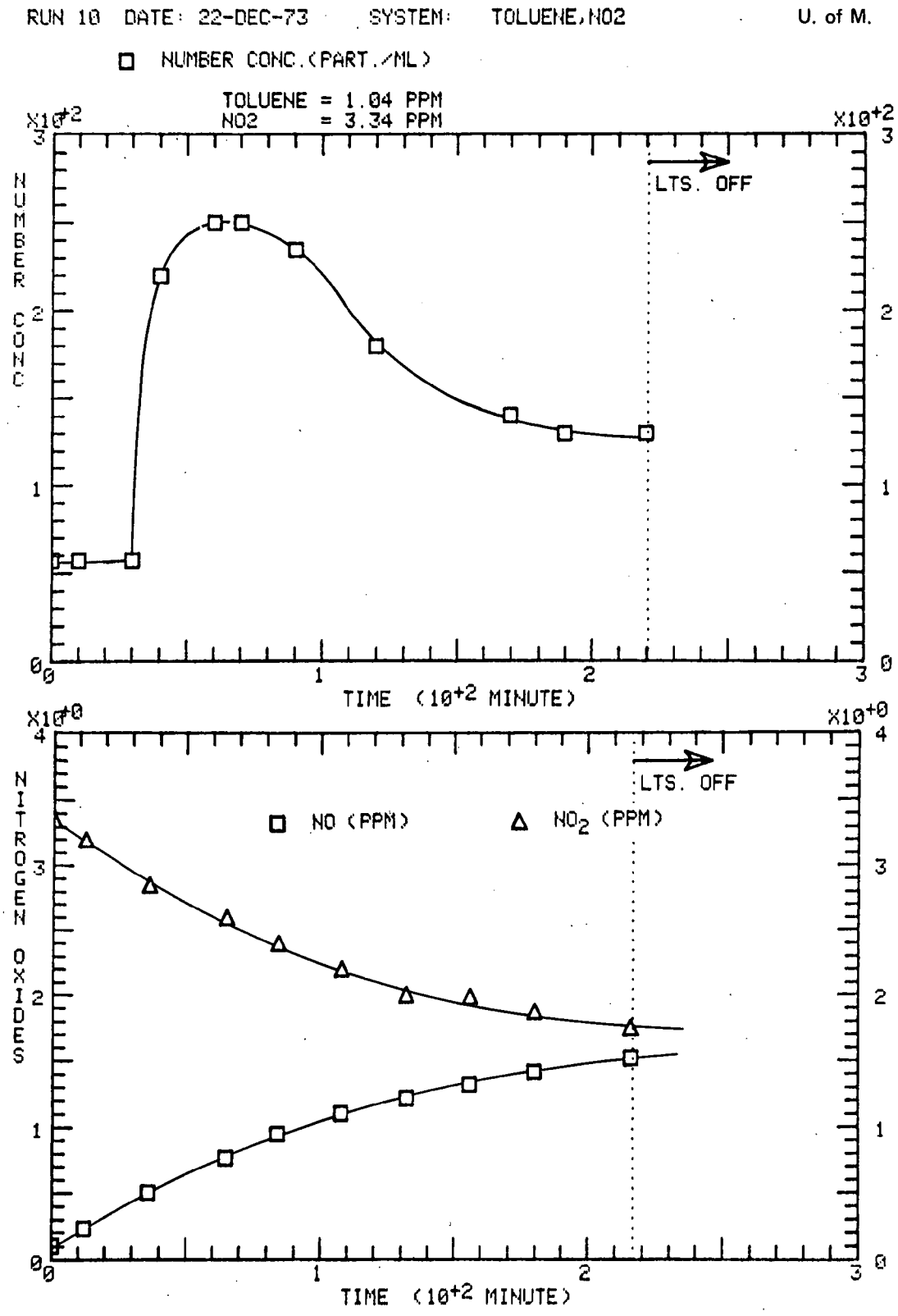
RUN 10 DATE: 22-DEC-73 SYSTEM: TOLUENE,NO2 U. of M.
NUMBER CONC.(PART./ML)
TOLUENE = 1.04 PPM
NO2 = 3.34 PPM
X10+2
NUMBER CONC
LTS. OFF
TIME (10+2 MINUTE)
X10+0
NITROGEN OXIDES
NO (PPM)
NO2 (PPM)
LTS. OFF
TIME (10+2 MINUTE)

CALSPAN

RUN NO. 10 15 NOVEMBER 1973 NO_2 + SO_2 + TOLUENE SYSTEM R.H. = 45%; TOLUENE = 0.8 ppm;
NO_2 = 1.95 ppm; NO = 0.022 ppm; SO_2 = 0,19 ppm
STIRRING

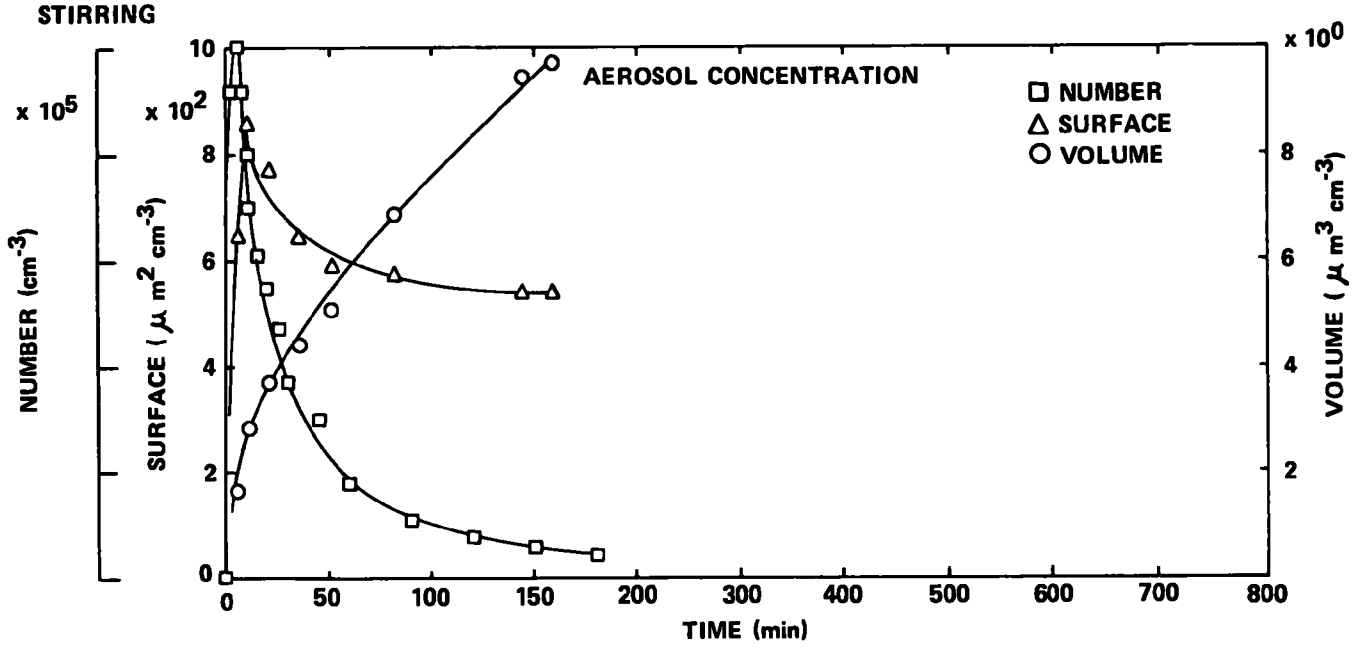

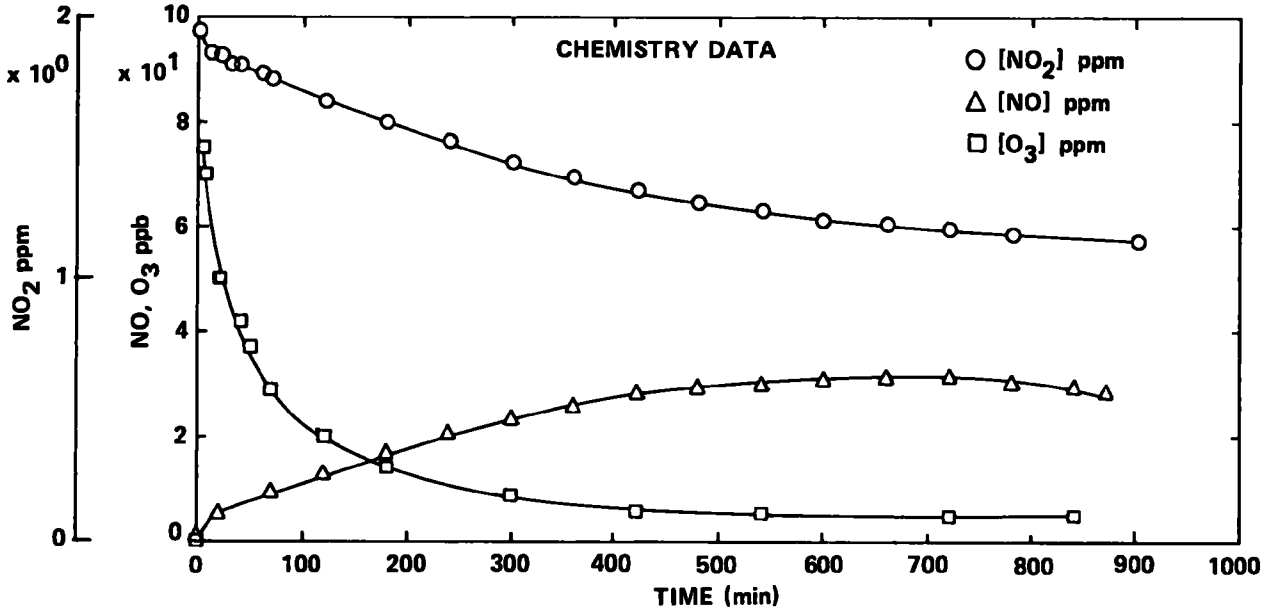

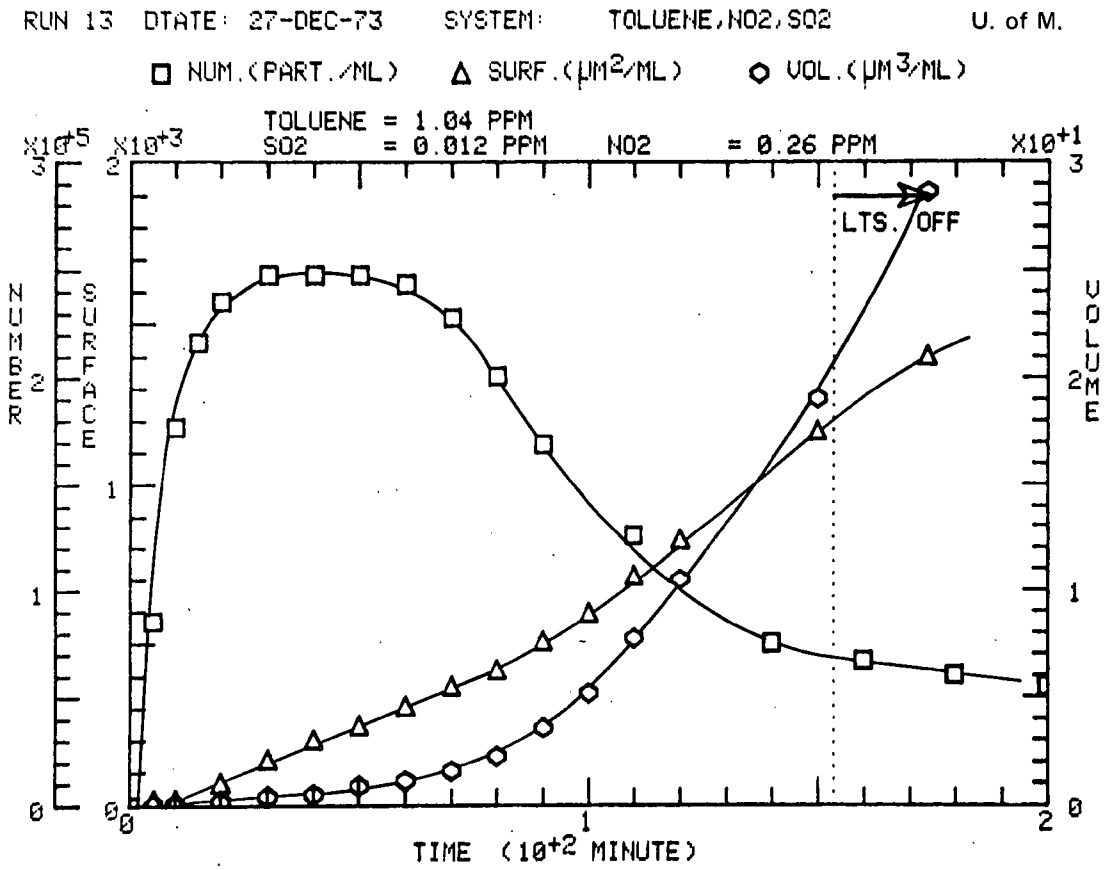
RUN 13 DTATE: 27-DEC-73 SYSTEM: TOLUENE,NO2,SO2 U. of M.
NUM.(PART./ML)
SURF.(μM2/ML)
VOL.(μM3/ML)
TOLUENE = 1.04 PPM
SO2 = 0.012 PPM
NO2 = 0.26 PPM
X10+5
X10+3
X10+1
LTS. OFF
NUMBER
SURFACE
VOLUME
TIME (10+2 MINUTE)

CALSPAN

NO_2 + SO_2 + TOLUENE SYSTEM

RUN NO. 11 16 NOVEMBER 1973

R.H. = 37%; TOLUENE = 0.8 ppm;

NO_2 = 3.6 ppm; NO = 0.025; SO_2 = 0.07 ppm

STIRRING

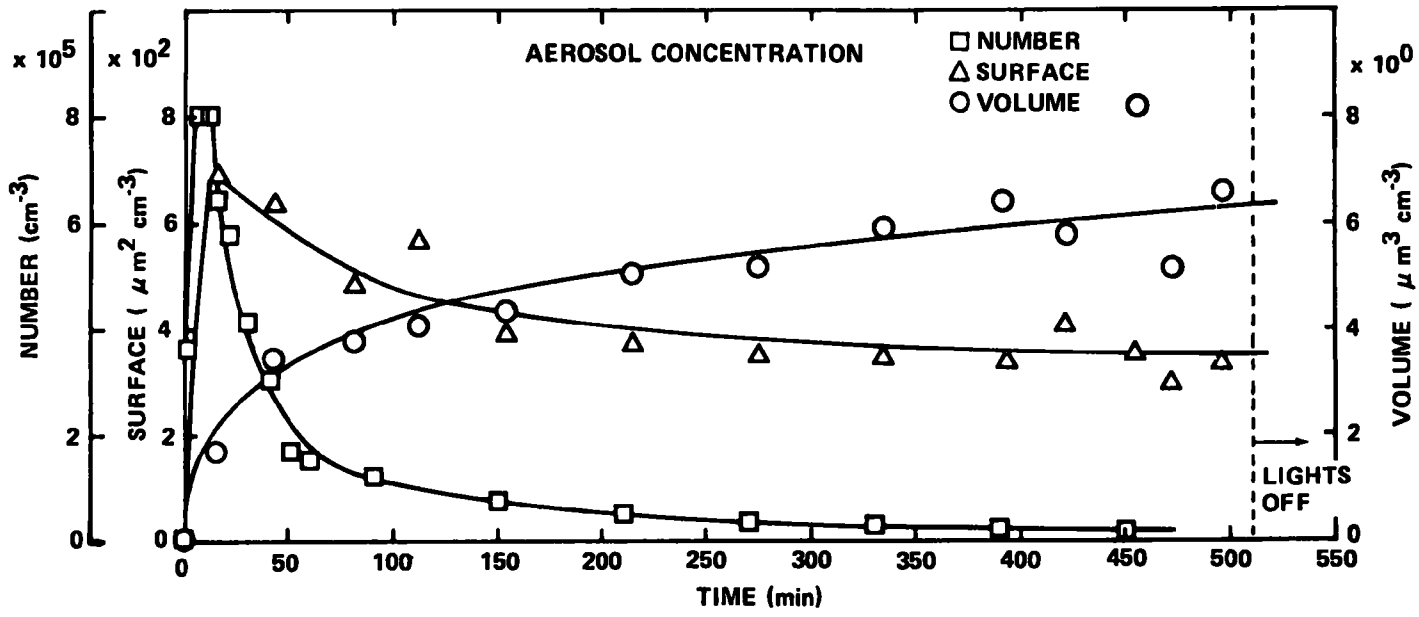

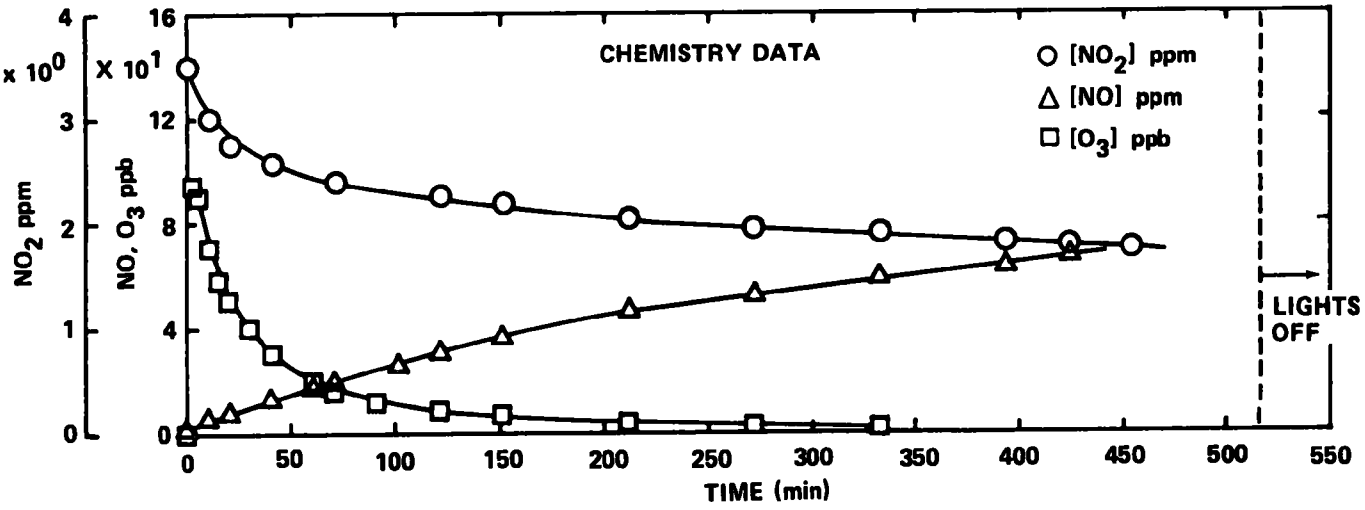

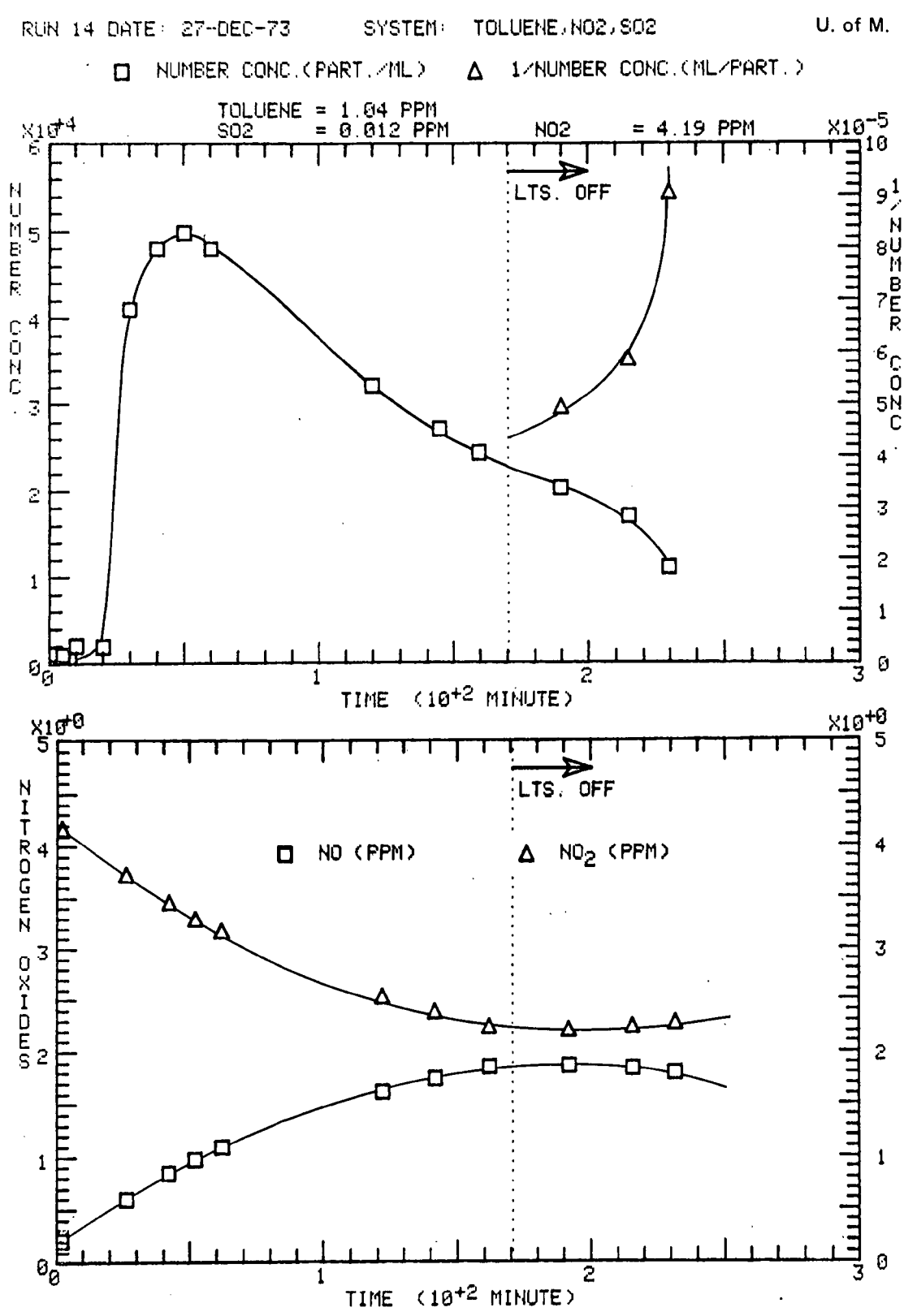
RUN 14 DATE: 27-DEC-73
SYSTEM: TOLUENE,NO2,SO2
U. of M.
□ NUMBER CONC.(PART./ML)
Δ 1/NUMBER CONC.(ML/PART.)
TOLUENE = 1.04 PPM
SO2 = 0.012 PPM
NO2 = 4.19 PPM
X10+4
X10-5
LTS. OFF
NUMBER CONC
1/NUMBER CONC
TIME (10+2 MINUTE)
X10+0
NITROGEN OXIDES
□ NO (PPM)
Δ NO2 (PPM)
TIME (10+2 MINUTE)

CALSPAN

RUN NO. 12 17 NOVEMBER 1973 NO_2 + TOLUENE SYSTEM R.H. = 33%; TOLUENE = 0.8 ppm; NO_2 = 1.45; NO = 0.01 ppm; SO_2 = 0.01 ppm

STIRRING

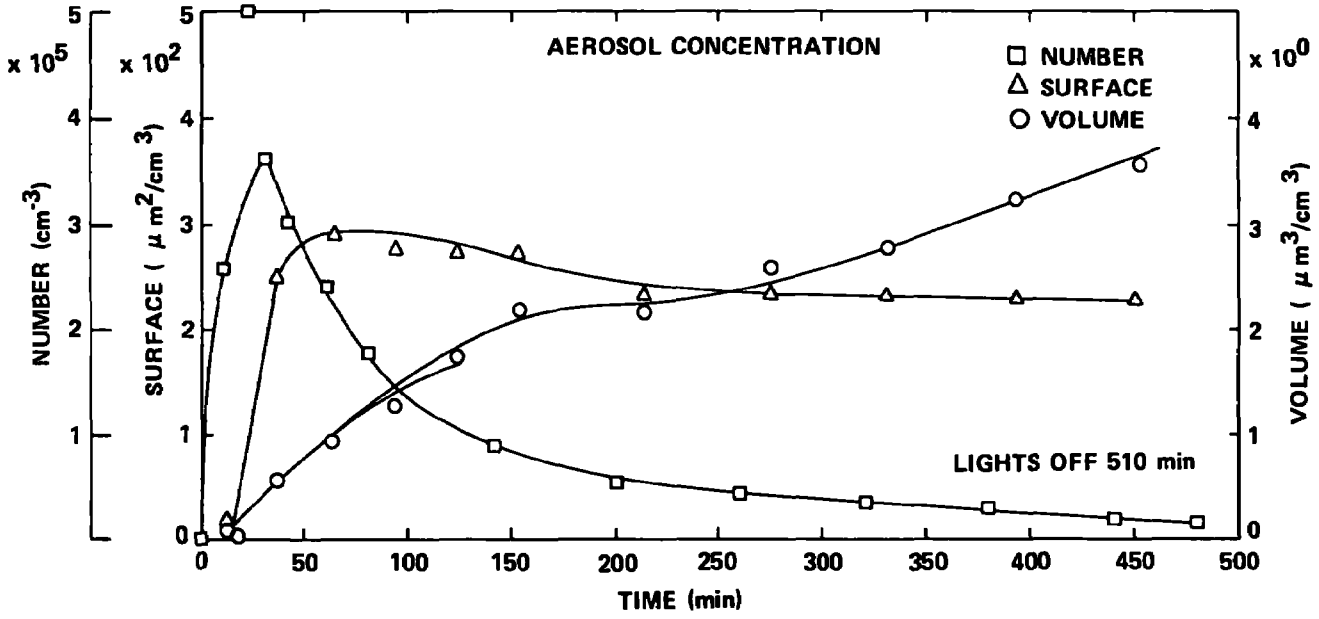

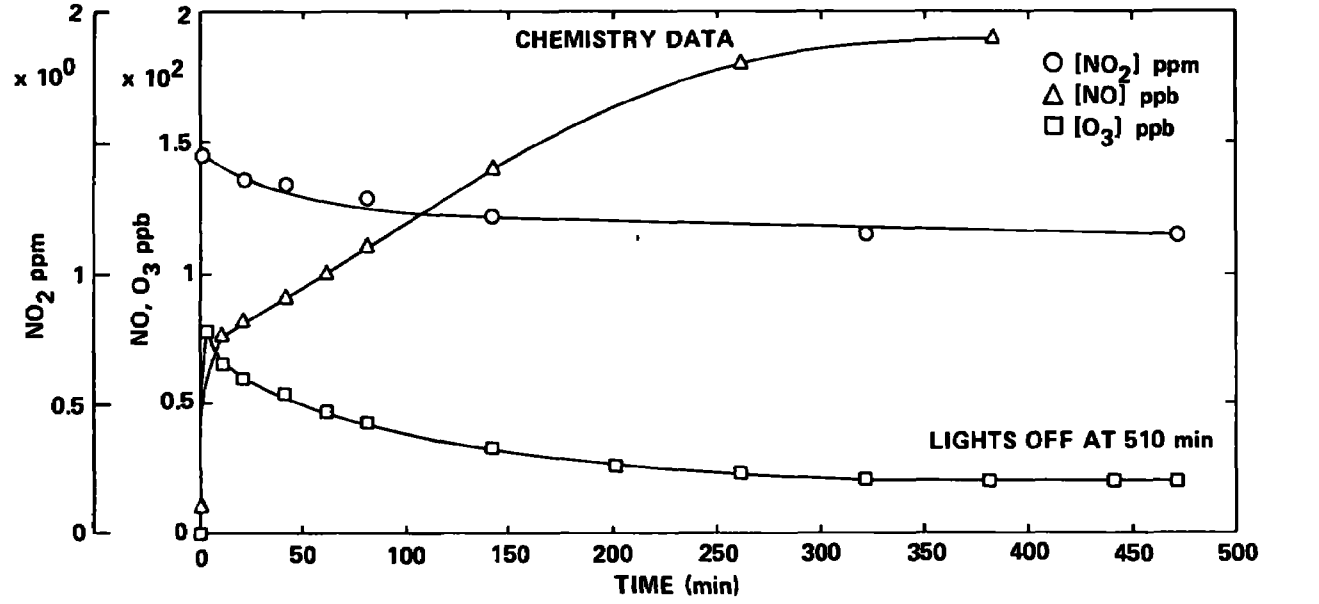

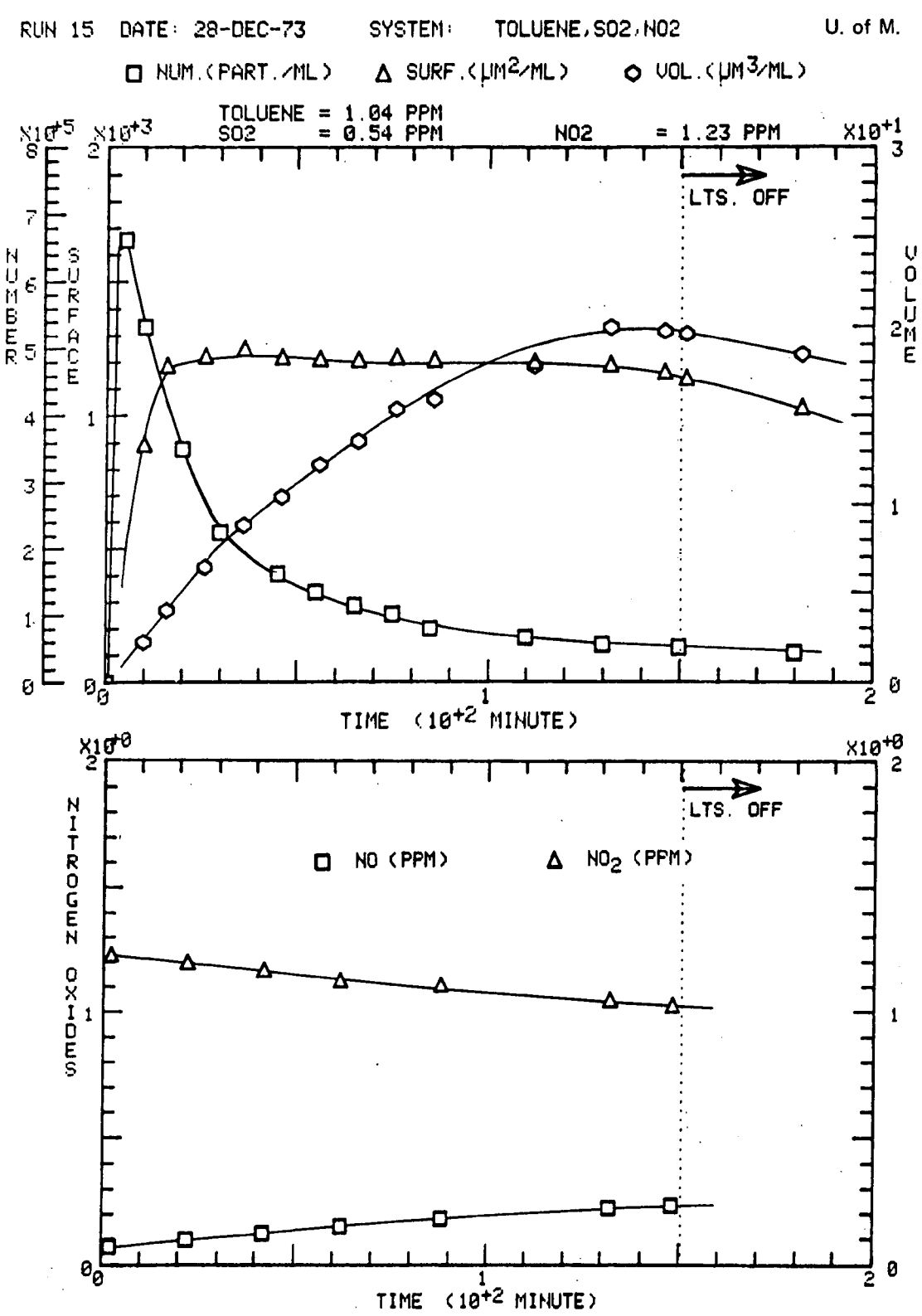
RUN 15 DATE: 28-DEC-73 SYSTEM: TOLUENE, SO2, NO2 U. of M.
□ NUM. (PART./ML) △ SURF. (μM²/ML) ◇ VOL. (μM³/ML)
TOLUENE = 1.04 PPM
SO2 = 0.54 PPM
NO2 = 1.23 PPM
X10+5
X10+3
X10+1
LTS. OFF
NUMBER
SURFACE
VOLUME
TIME (10+2 MINUTE)
X10+0
NITROGEN OXIDES
□ NO (PPM)
△ NO2 (PPM)
TIME (10+2 MINUTE)

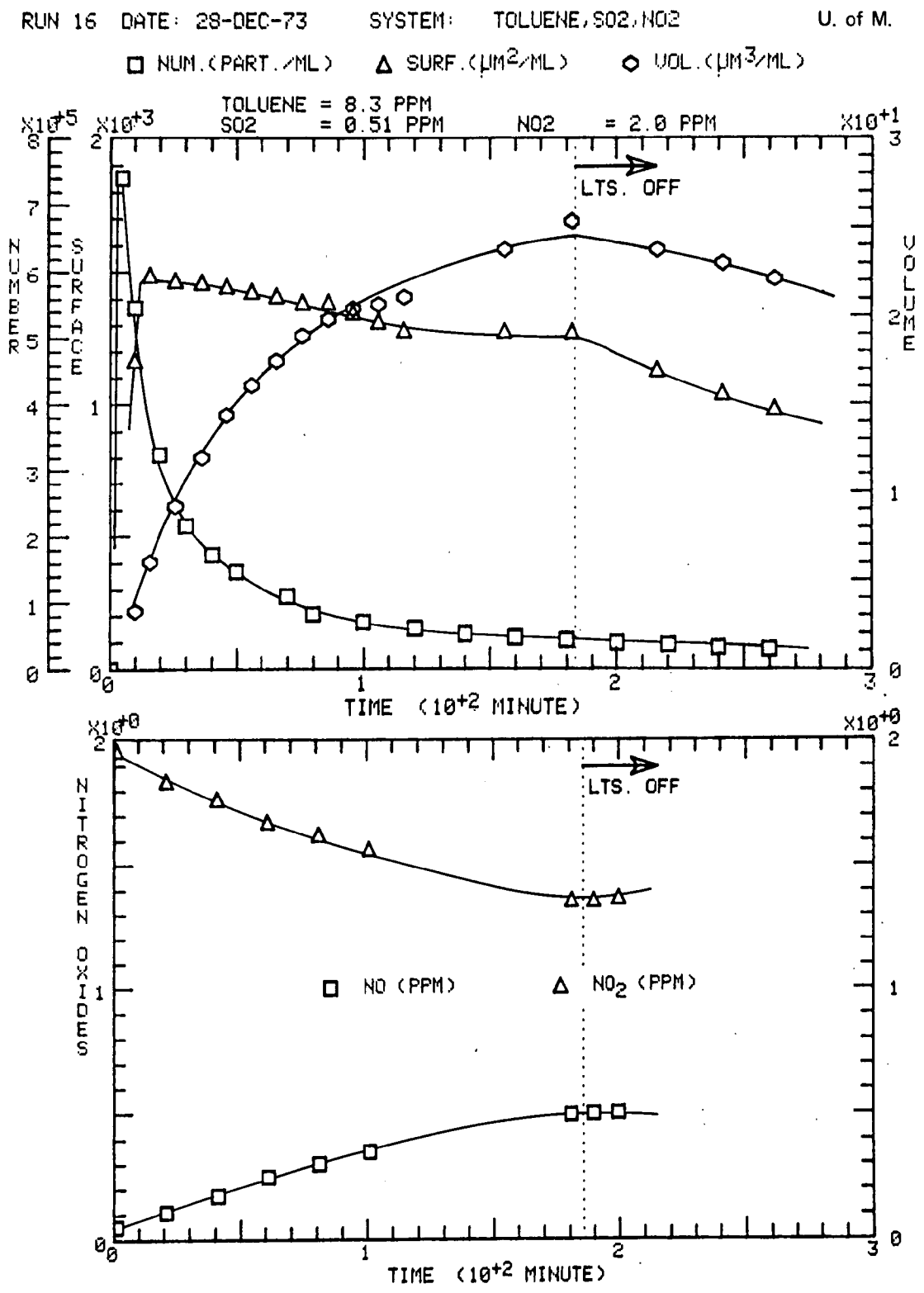
RUN 16 DATE: 28-DEC-73 SYSTEM: TOLUENE/SO2/NO2 U. of M.
NUM.(PART./ML) SURF.(μM²/ML) VOL.(μM³/ML)
TOLUENE = 8.3 PPM
SO2 = 0.51 PPM NO2 = 2.0 PPM
X10+5
X10+3
X10+1
LTS. OFF
NUMBER
SURFACE
VOLUME
TIME (10+2 MINUTE)
X10+0
X10+0
LTS. OFF
NITROGEN OXIDES
NO (PPM)
NO2 (PPM)
TIME (10+2 MINUTE)

(3) HEXENE, HEXENE + NO_2, HEXENE + NO_2 +SO_2 EXPERIMENTS

CALSPAN
RUN NO. 14 19 NOVEMBER 1973 HEXENE-1 + NO_2 SYSTEM R.H. = 34%; HEXENE-1 = 0.6 ppm;
NO_2 = 3.35 ppm; NO = 0.012 ppm

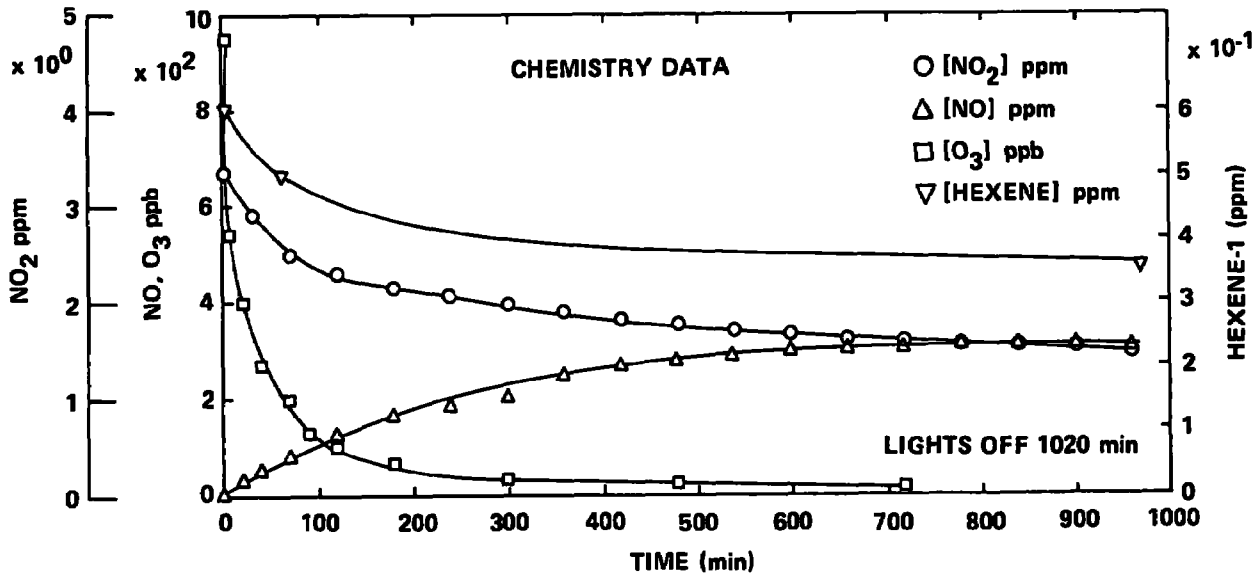

CALSPAN
RUN NO. 13 19 NOVEMBER 1973 HEXENE-1 = 0.6 ppm R.H. = 38%; NO_2 = 0.006 ppm; NO = 0.011 ppm
STIRRING

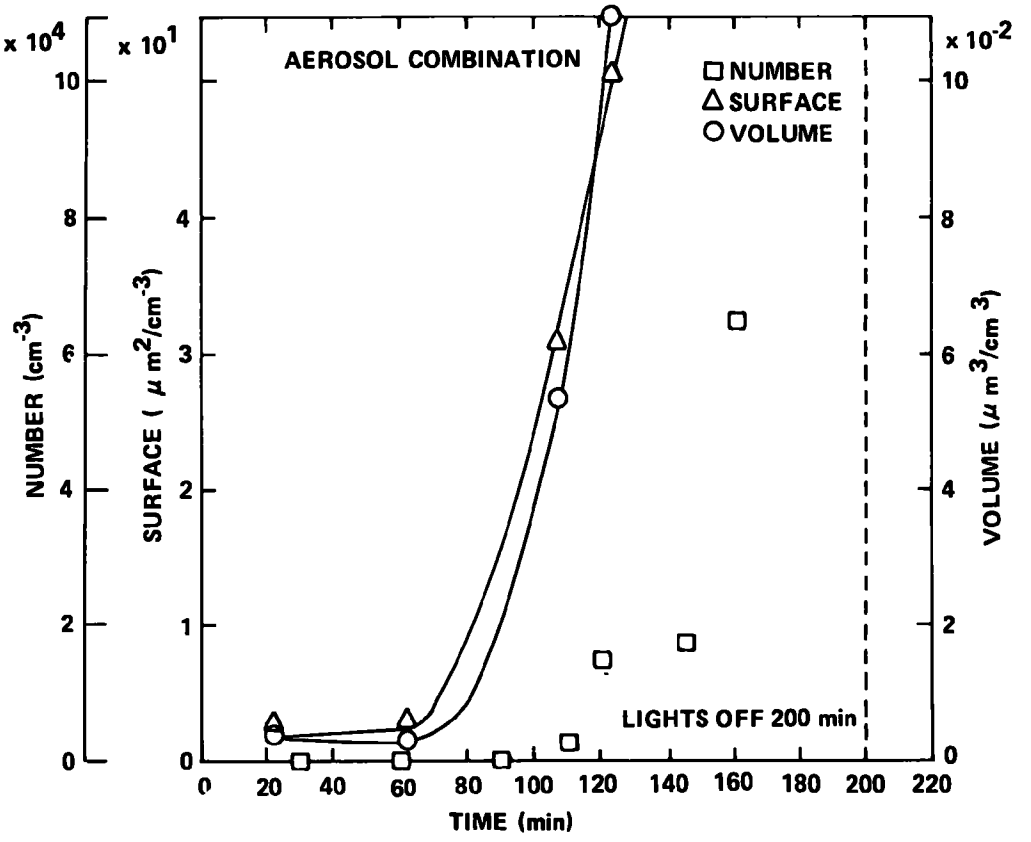

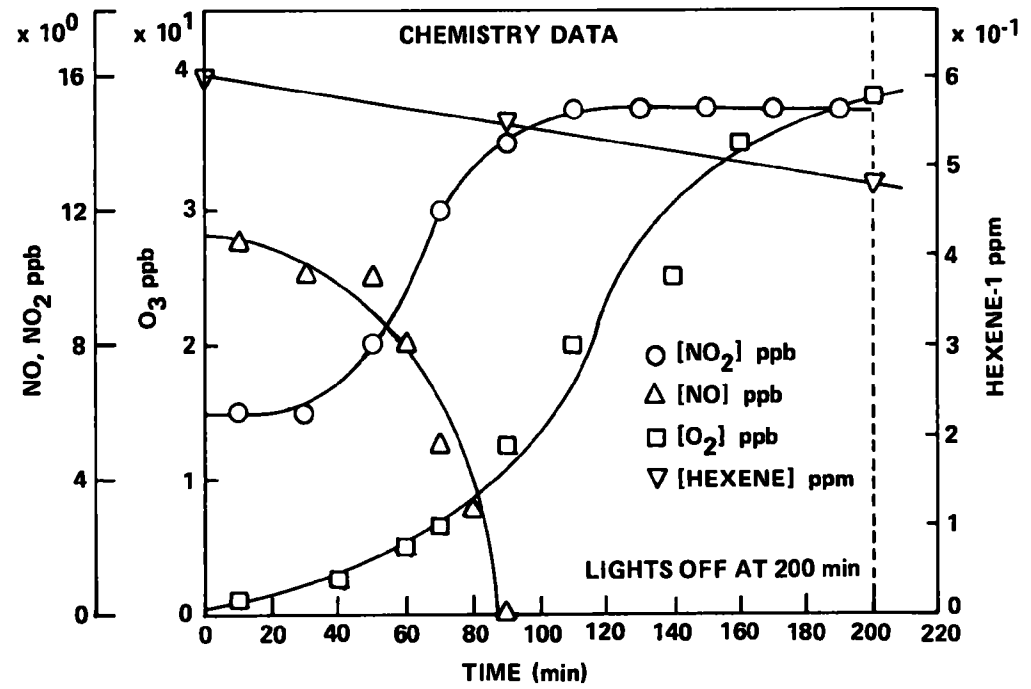

HEXENE-1 + SO_2 + NO_2 SYSTEM

CALSPAN

RUN NO. 15 20 NOVEMBER 1973 R.H. = 32%; HEXENE-1 = 0.6 ppm;

NO_2 = 1.64 ppm; NO = 0.018 ppm; SO_2 = 0.01 ppm

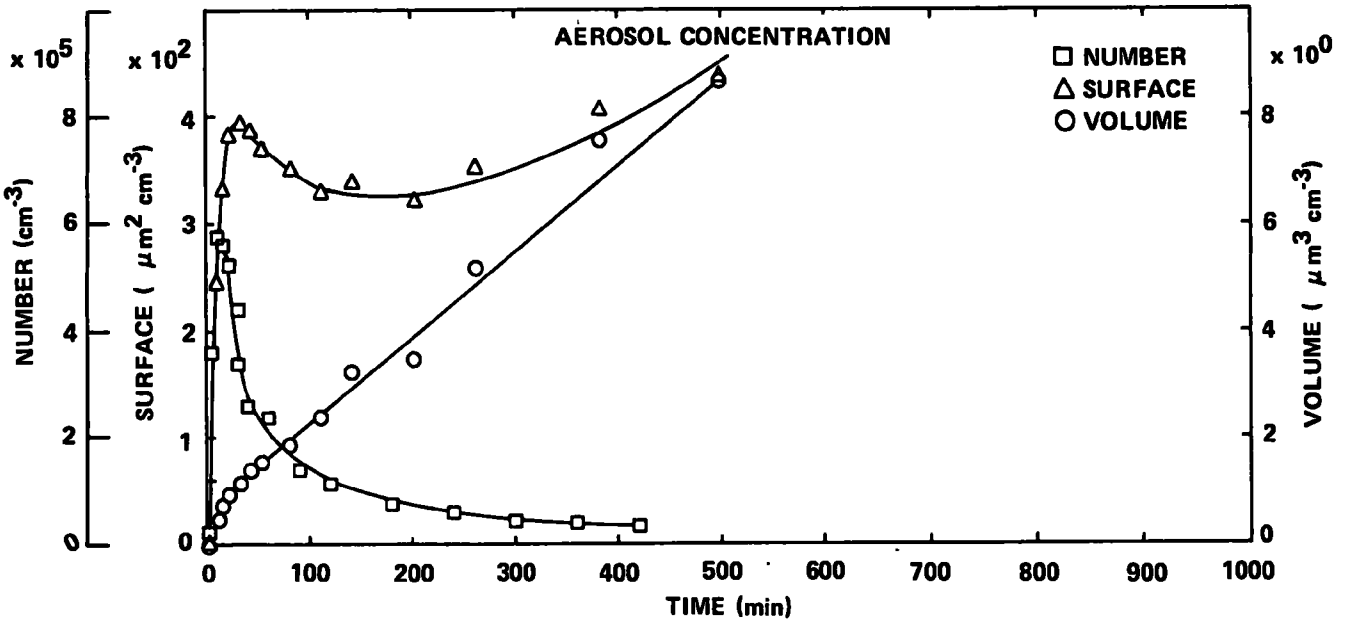

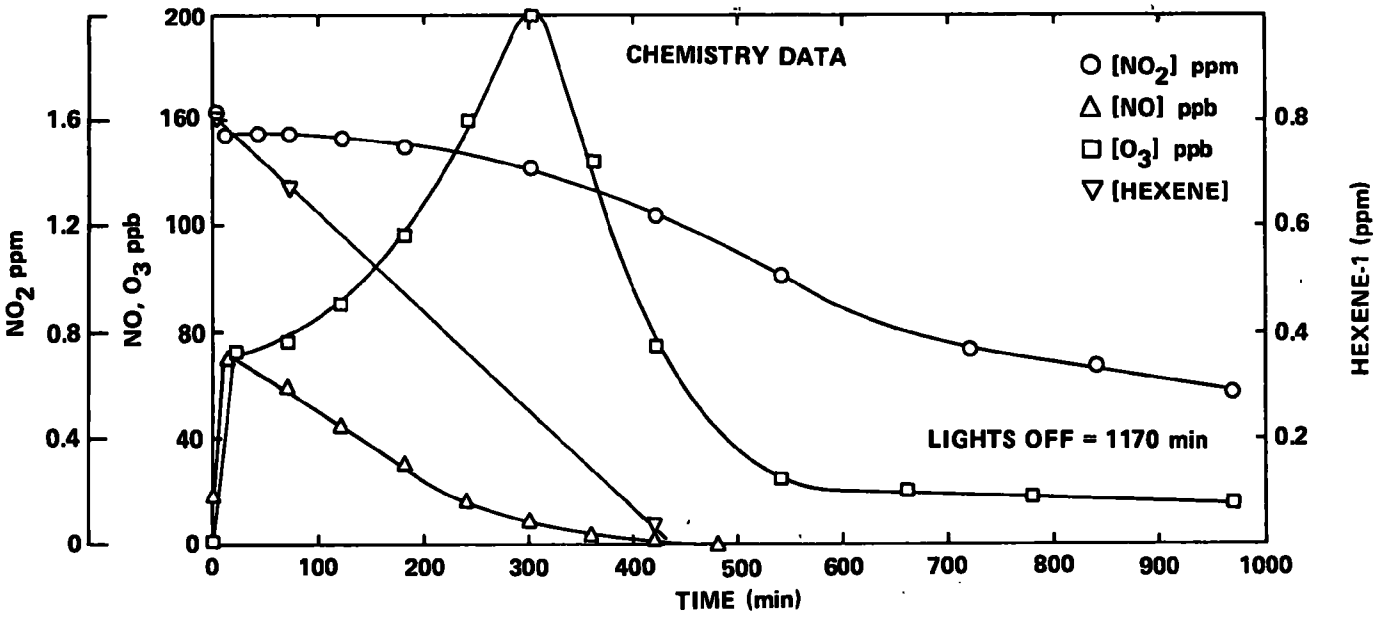

APPENDIX B

AEROSOL AND CHEMISTRY DATA FROM MARCH 1974 WORKSHOP WITH DUPLICATE UNIVERSITY OF MINNESOTA EXPERIMENTS

ORDER OF PRESENTATION:

(1) SO_2 Experiments
(2) Toluene Experiments
(3) Hexene Experiments
(4) M-xylene Experiments
(5) Cyclohexene Experiments
(6) NaCl Experiments

TABLE IX. SUMMARY OF AEROSOL DATA FROM MARCH WORKSHOP

Run No.	System	RH %	N_{max} #-cc^{-1}	SE μm^2-cc^{-1}	$\frac{dv}{dt}(SO_2)$ μm^3-cc^{-1}-hr^{-1}	$\frac{dv}{dt}(HC)$ μm^3-cc^{-1}-hr^{-1}	SO_2 Photox %-hr^{-1}	Comments
6	toluene + NO	30	3.1×10^4	640	--	2.2	--	no vol. first 4 hrs
30	toluene + NO	20	1.3×10^4	750	--	2.6	--	no vol. first 4 hrs
29	toluene + NO + SO_2	30	1.6×10^5	>750	0.78	1.5	0.32	1st 4 hrs*
7	toluene + SO_2	20	2.1×10^5	800	1.17	3.2	0.45	1st 50 min*
5	hexene + NO	40	1.4×10^5	610	--	2.1	--	no vol. first 5 hrs
21	hexene + NO	37	1.2×10^5	215	--	0.5	--	no vol. first 6 hrs
18	hexene + NO + SO_2	37	1.4×10^5	>1500	0.61	5.8	0.16	1st 6 hrs*
20	hexene + SO_2	35	3.6×10^5	950	0.75	3.2	0.25	1st 60 min*
15	m-xylene + NO	38	8.4×10^4	1150	--	14.1	--	no vol. first 60 min.
14	m-xylene + NO + SO_2	29	2.6×10^5	2700	0.92	25.0	0.32	1st 60 min*
17	m-xylene + SO_2	35	2.8×10^5	384	0.84	1.6	0.23	1st 60 min*
10	cyclohexene + NO	38	3.6×10^4	3500	--	110	--	no vol. first 90 min
12	cyclohexene + NO	30	4.2×10^4	2450	--	75	--	no vol. first 3 hrs
9	cyclohexene + NO + SO_2	30	1.7×10^5	4200	0.74	105	0.28	first 2 hrs
13	cyclohexene + SO_2	35	2.7×10^5	1300	1.20	10	0.49	first 30 min
1	0.52 ppm SO_2	25	5.5×10^5	>1450	5.61 10.60	--	0.21 0.39	1st 30 min* 1st 2 hrs
4	0.55 ppm SO_2	30	3.9×10^5	4400	4.49 13.60	--	0.16 0.48	1st 30 min* 1st 2 hrs
2	0.05 SO_2	37	2.3×10^5	>575	0.65 2.35	--	0.23 0.79	1st 30 min* 1st 2 hrs
3	0.05 SO_2	40	2.9×10^5	>675	1.04 2.31	--	0.36 0.79	1st 40 min* 1st 2 hrs

*Time over which aerosol growth rate was used in computing SO_2 photooxidation.

Table X . UNIVERSITY OF MINNESOTA DUPLICATE TESTS SUBSEQUENT TO THE MARCH WORKSHOP:

SUMMARY OF AEROSOL DATA FOR HYDROCARBON EXPERIMENTS

Run No.	System	RH %	N_{max} #-cc^{-1}	SE μm^2-cc^{-1}	$\frac{dv}{dt}$ SO_2 μm^3-cc^{-2}-hr^{-1}	$\frac{1}{SO_2}\frac{dv}{dt}$ μm^3-cc^{-1}-hr^{-1}-ppm^{-1}	$\frac{dv}{dt}$ μm^3-cc^{-1}-hr^{-1}	SO_2 photo oxidation %-hr^{-1}
65	toluene + NO + SO_2	28	185 K	330*	1.23	11.3	same	.23
76	toluene + NO	47	4.2 K	550*	--	--	24.5	---
77	toluene + NO + SO_2	57	170 K	1850	1.17	29.9	27.4	.39
87	toluene + NO	30	10 K	340	--	--	8.6	---
88	toluene + NO + SO_2	24	160 K	1600*	1.22	30.5	16.6	.67
60	hexene + NO + SO_2	28	74 K	1200*	.40	5.7	21.2	.12
78	hexene + NO + SO_2	55	230 K	1530	.53	13.9	19.1	.18
92	hexene + NO	33	8.8 K	31	--	--	.09	---
93	hexene + NO + SO_2	32	150 K	1300	.29	8.5	18.0	.16
81	m-xylene + NO	75	23 K	1600	--	--	73	---
82	m-xylene + NO + SO_2	54	230 K	2800	.49	10.4	67	.14
89	m-xylene + NO	26	21 K	1000*	--	--	38	---
91	m-xylene + NO + SO_2	26	230 K	1600	.46	10.0	31	.21
83	cyclohexene + NO	51	.9 K	320	--	--	50	---
94	cyclohexene + NO	31	2.7 K	510	--	--	65	---
95	cyclohexene + NO	29	1.9 K	620	--	--	190	---
96	cyclohexene + NO + SO_2	28	280 K	5400	.43	9.7	250	.20

*Equilibrium surface not reached.

TABLE XI. SUMMARY OF CHEMISTRY DATA FROM MARCH WORKSHOP

Run No.	System	RH %	HC ppm	SO_{2i} ppm	NO_i ppm	$t(NO_2)_{max}$ min	O_{3m} ppm
6	toluene + NO	30	0.35	--	0.170	400	0.285
30	toluene + NO	20	1.17	--	0.530	480	0.380
29	toluene + NO + SO_2	30	0.35	0.05	0.146	330	> 0.225
7	toluene + SO_2	20	0.35	0.05	b	b	0.047
5	hexene + NO	40	0.33	--	0.150	420	> 0.200
21	hexene + NO	37	0.33	--	0.180	420	0.275
18	hexene + NO + SO_2	37	0.33	0.07	0.178	430	--
20	hexene + SO_2	35	0.33	0.055	b	b	0.052
15	m-xylene + NO	38	0.34	--	0.150	100	0.222
14	m-xylene + NO + SO_2	29	0.34	0.055	0.150	105	0.305
17	m-xylene + SO_2	35	0.34	0.07	b	b	0.030
10	cyclohexene + NO	38	0.33	--	0.138	120	0.190
12	cyclohexene + NO	30	0.33	--	0.140	190	0.192
9	cyclohexene + NO + SO_2	30	0.33	0.05	0.220	180	0.325
13	cyclohexene + SO_2	35	0.33	0.06	b	b	0.011

Table XII. UNIVERSITY OF MINNESOTA DUPLICATE TESTS SUBSEQUENT TO THE MARCH WORKSHOP:

SUMMARY OF CHEMICAL DATA FOR HYDROCARBON EXPERIMENTS

Run No.	System	RH %	HC ppm	SO_{2i} ppm	NO_i ppm	$[NO_2]_{max}$ ppm	$t[NO_2]_{max}$ min	$[O_3]_{max}$ ppm
65	toluene + NO + SO_2	28	.35	.108	.30	.145*	460	.2*
76	toluene + NO	47	.35	--	.152	.095	210	.30
77	toluene + NO + SO_2	57	.38	.039	.155	.115	160	.362
87	toluene + NO	30	.35	--	.155	.140	130	.402
88	toluene + NO + SO_2	24	.35	.040	.17	.122	155	.315*
60	hexene + NO + SO_2	28	.35	.07	.16	.123	395	.162*
78	hexene + NO + SO_2	55	.35	.038	.165	.130	255	.438
92	hexene + NO	33	.35	--	.12	.104	280	.290
93	hexene + NO + SO_2	32	.35	.034	.122	.125	350	.302*
81	m-xylene + NO	75	.35	--	.155	.144	80	.343
82	m-xylene + NO + SO_2	54	.35	.047	.151	.130	94	.361
89	m-xylene + NO	26	.35	--	.132	.142	68	.379
91	m-xylene + NO + SO_2	26	.35	.046	.117	.115	70	.262
83	cyclohexene + NO	51	.35	--	.13	.101	90	.32*
94	cyclohexene + NO	31	.35	--	.103	.108	60	.20
95	cyclohexene + NO	29	.35	--	.124	.128	103	.254
96	cyclohexene + NO + SO_2	28	.35	.045	.133	.130	85	.241

*max not reached by end of irradiation period.

TABLE XIII. UNIVERSITY OF MINNESOTA DUPLICATE TESTS SUBSEQUENT TO THE MARCH WORKSHOP: SUMMARY OF SO_2 EXPERIMENTS

Run No.	Concentration ppm	RH %	N_{max} $\#\text{-cc}^{-1}$	SE_2 $\mu m^2\text{-cc}^{-1}$	$\frac{dv}{dt}_3$ SO_2 $\mu m^3\text{-cc}^{-1}\text{-hr}^{-1}$	$\frac{1}{SO_2}\frac{dv}{dt}$ $\mu m^3\text{-cc}^{-1}\text{-hr}^{-1}\text{-ppm}^{-1}$	SO_2 photox $\%\text{-hr}^{-1}$
45	.59	28	260 K	470	1.9	3.2	.07
46	.59	40	340 K	570	2.2	3.8	.065
49	.59	67	590 K	800	5.6	9.4	.10
52	.56	36	90 K	190	.46	.83	.015
53	.56	30	670 K	2100	20	3.7	.07
54	.56	25	100 K	190	.28	.50	.01
57	.56	12	39 K	210	.78	1.4	.04
66	.61	27	100 K	680*	2.7	4.5	.10
68	.62	39	94 K	310	1.1	1.8	.03
69	.053	40	280 K	270	.84	16	.27
70	.54	57	210 K	400*	1.2	2.2	.03
71	.048	55	95 K	200*	.32	6.6	.09
72	.50	54	220 K	840*	4.2	8.5	.12
79	.038	70	68 K	110*	.21	5.6	.06
80	.40	78	250 K	550	2.2	5.5	.05
85	.38	34	245 K	640	2.5	6.6	.13
86	.051	27	82 K	190	.35	6.8	.14
97	.035	27	100 K	270*	1.1	30	.63

*Equilibrium surface not reached, maximum surface.

(1) SO_2 EXPERIMENTS

CALSPAN

RUN NO. 1 20 FEBRUARY 1974 SO_2 FILTERED AIR SYSTEM R.H. = 25%; SO_2 = 0.52 ppm

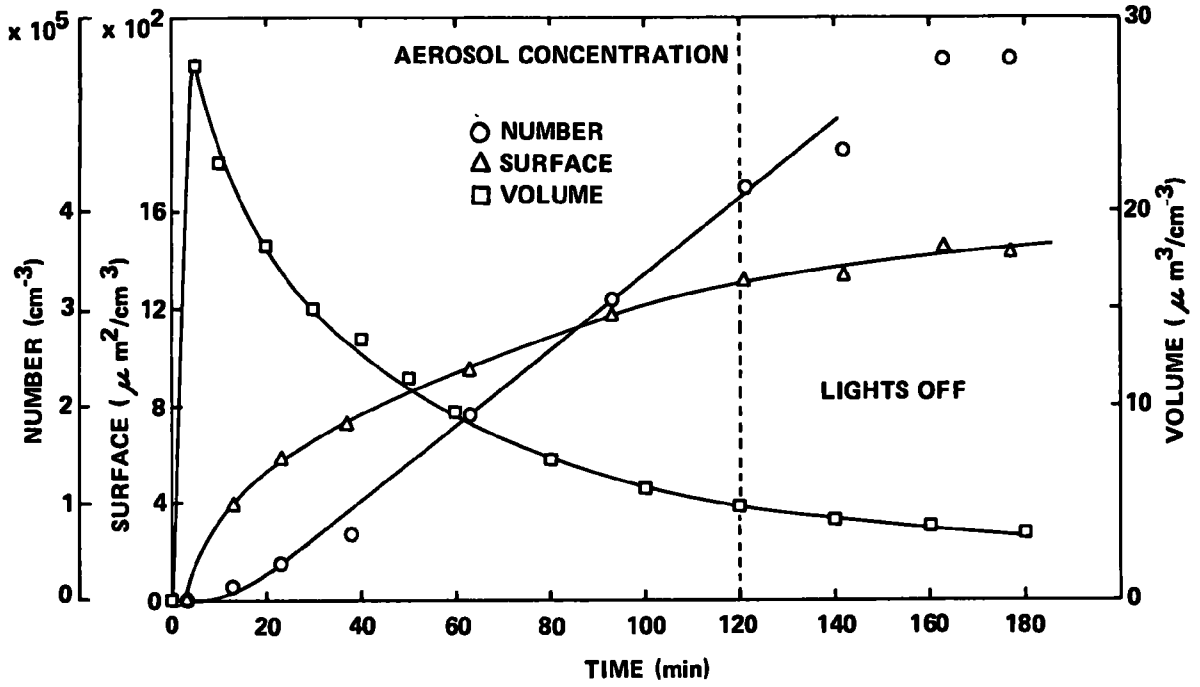

CALSPAN

RUN NO. 4 21 FEBRUARY 1974 SO_2 FILTERED AIR SYSTEM R.H. = 35%; SO_2 = 0.55 ppm; NO = 0.010 ppm; NO_2 = 0.004 ppm

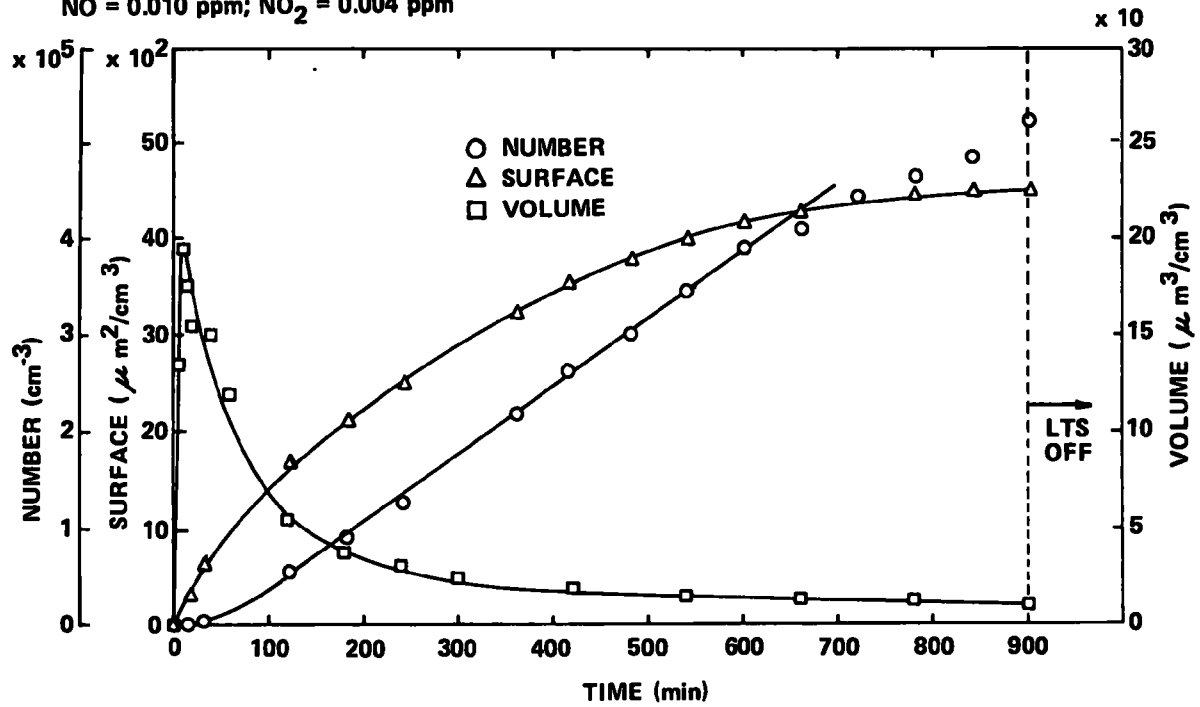

CALSPAN
RUN NO. 2 20 FEBRUARY 1974 SO_2 FILTERED AIR SYSTEM; R.H. = 37%; SO_2 = 0.05 ppm

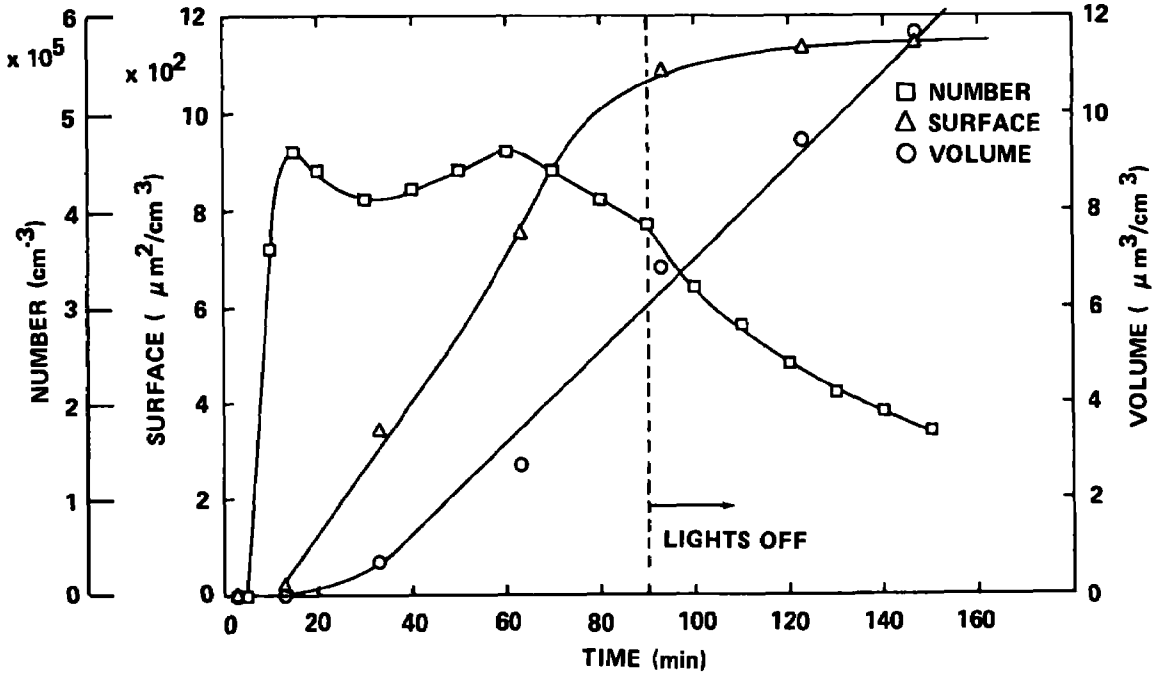

CALSPAN
RUN NO. 3 21 FEBRUARY 1974 SO_2 FILTERED AIR SYSTEM; R.H. = 40%; SO_2 = 0.05 ppm

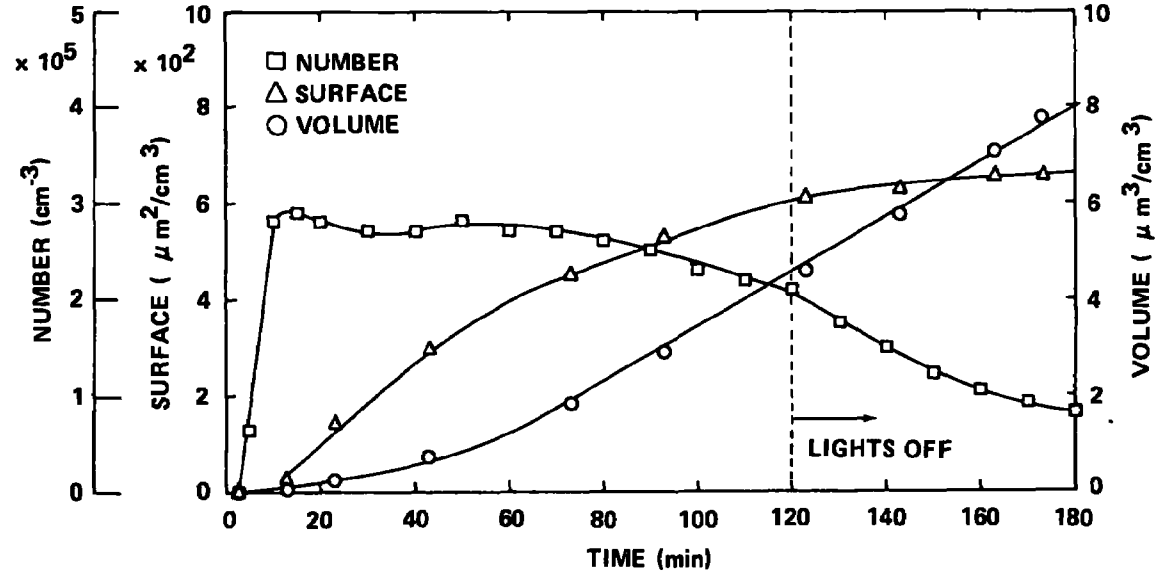

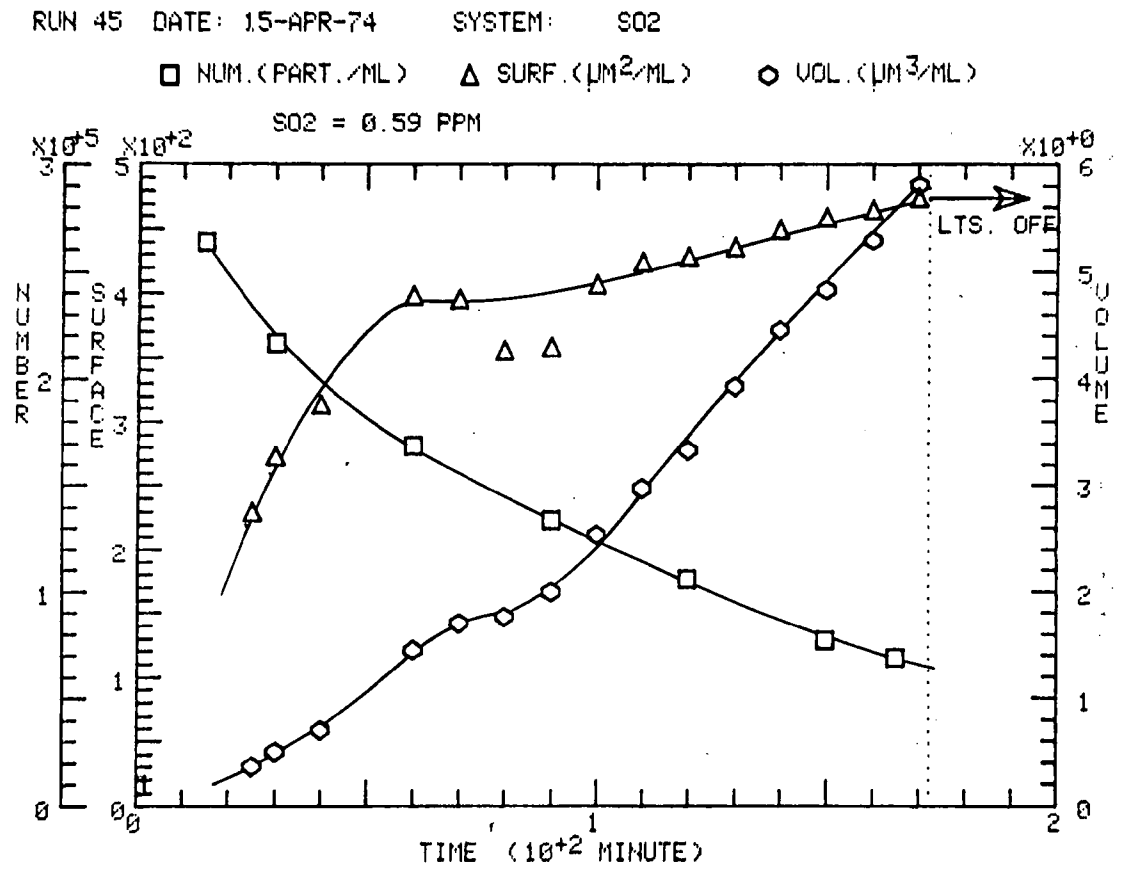
RUN 45 DATE: 15-APR-74 SYSTEM: SO2
NUM.(PART./ML)
SURF.(μM²/ML)
VOL.(μM³/ML)
SO2 = 0.59 PPM
X10+5
X10+2
X10+0
LTS. OFF
NUMBER
SURFACE
VOLUME
TIME (10+2 MINUTE)

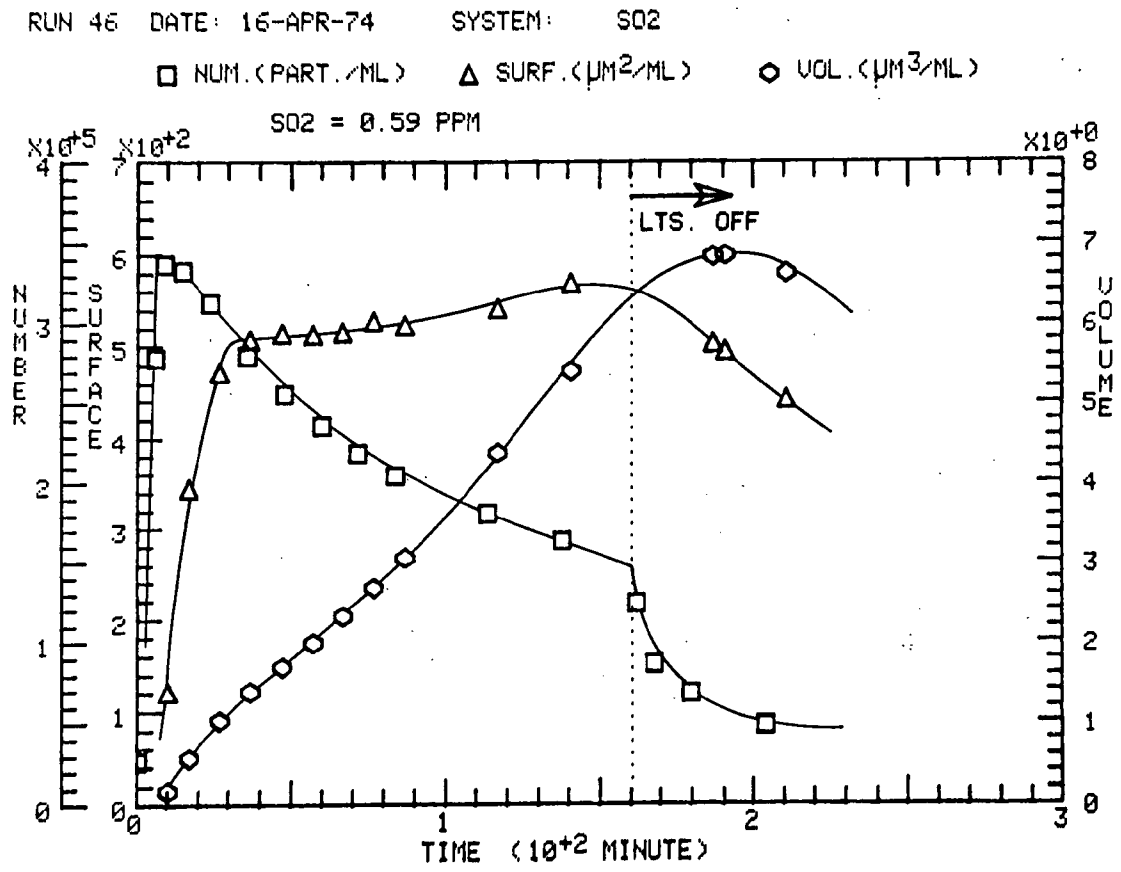
RUN 46 DATE: 16-APR-74 SYSTEM: SO2
NUM.(PART./ML)
SURF.(μM²/ML)
VOL.(μM³/ML)
SO2 = 0.59 PPM
X10+5
X10+2
X10+0
LTS. OFF
NUMBER
SURFACE
VOLUME
TIME (10+2 MINUTE)

RUN 49 DATE: 20-APR-74 SYSTEM: SO2

□ NUM.(PART./ML) △ SURF.(μM^2/ML) ◇ VOL.(μM^3/ML)

SO2 = 0.59 PPM

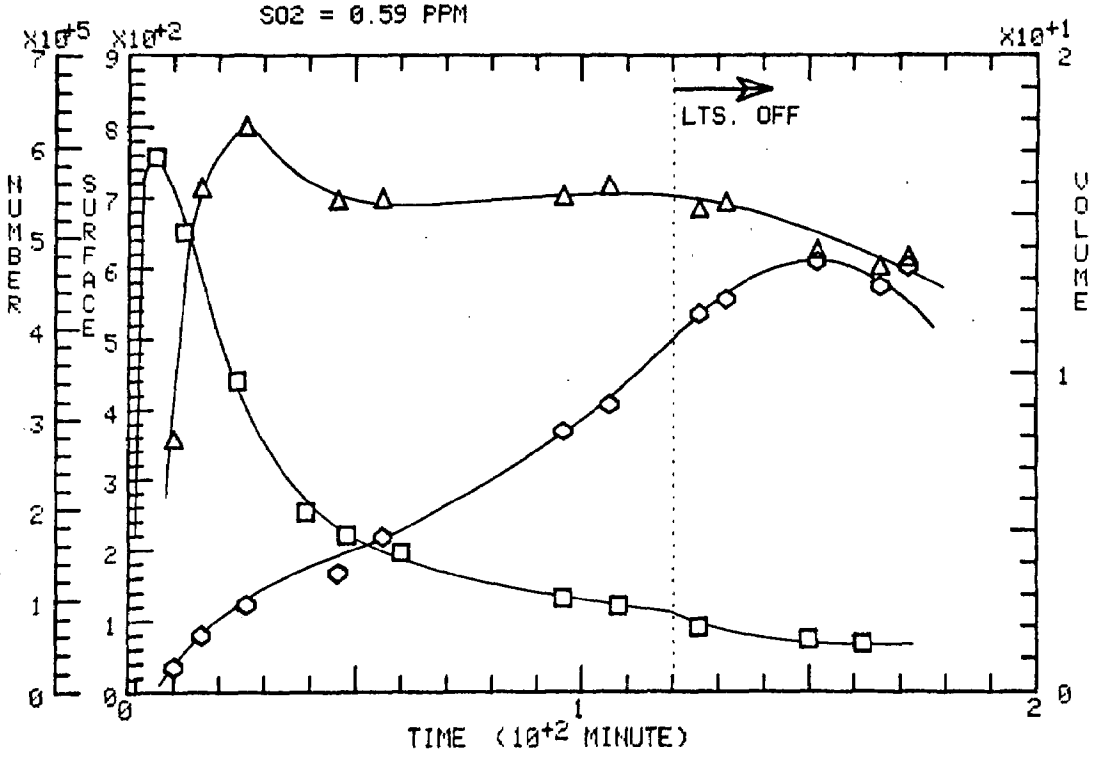

RUN 52 DATE: 30-APR-74 SYSTEM: SO2

□ NUM.(PART./ML) △ SURF.(μM^2/ML) ◇ VOL.(μM^3/ML)

SO2 = 0.56 PPM

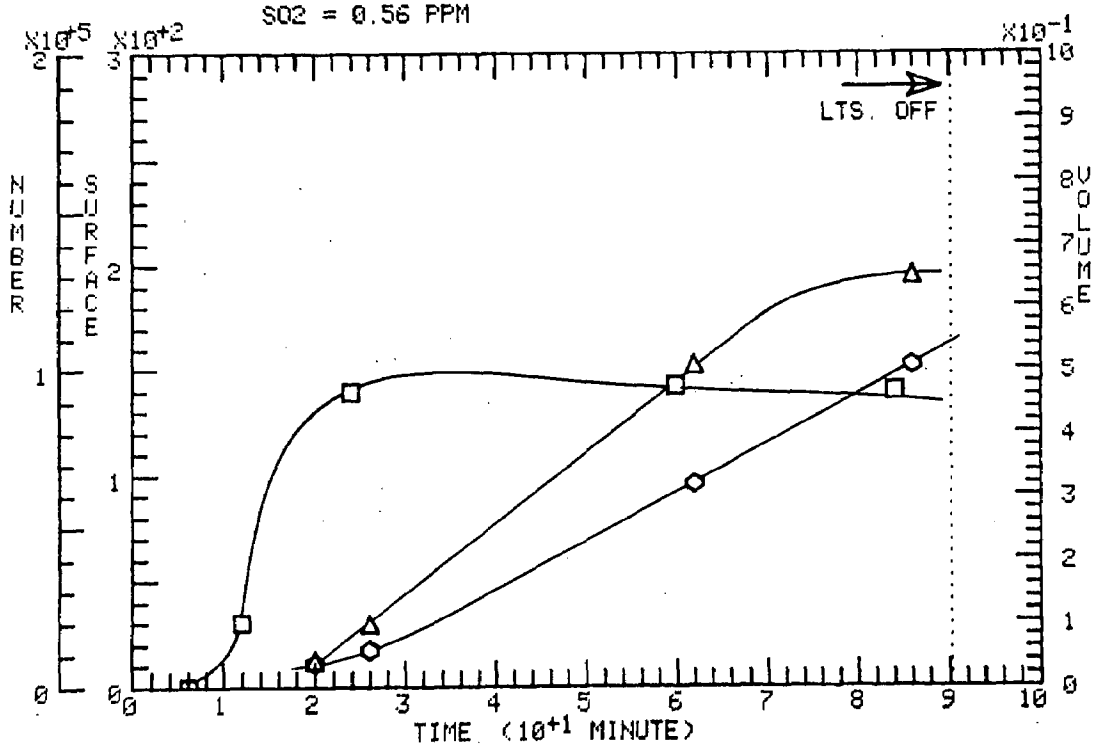

RUN 53 DATE: 1-MAY-74 SYSTEM: SO2

□ NUM.(PART./ML) △ SURF.(μM²/ML) ◇ VOL.(μM³/ML)

SO2 = 5.6 PPM

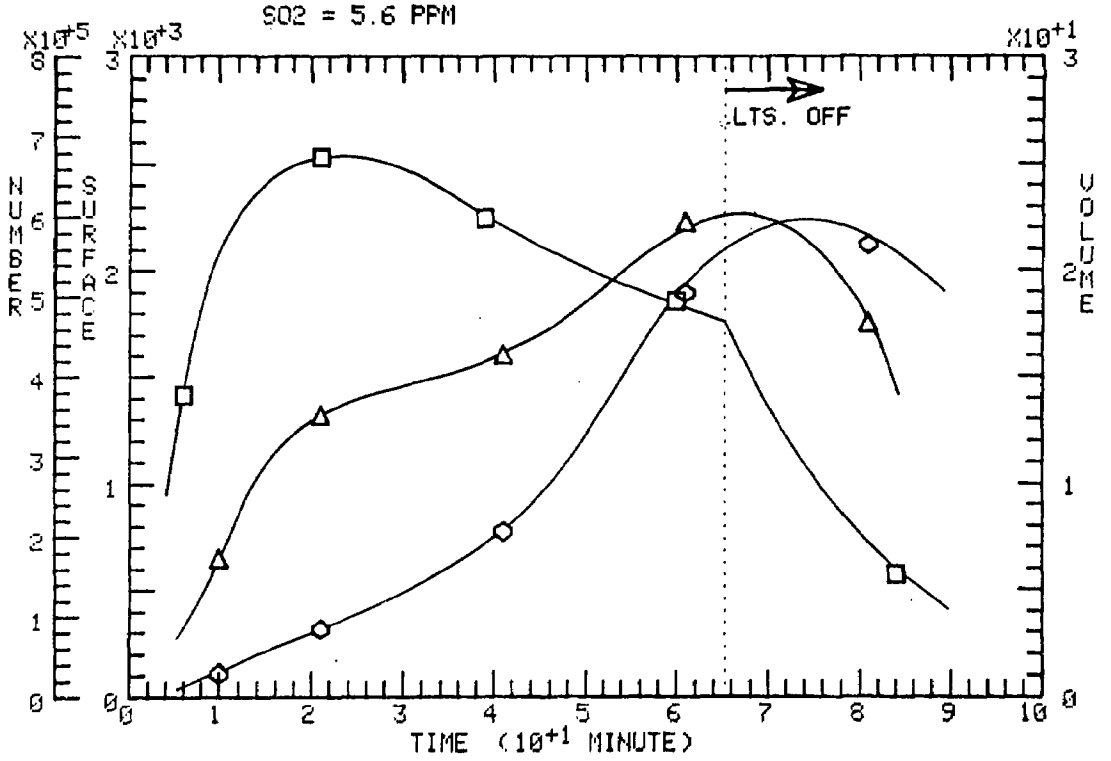

RUN 54 DATE: 3-MAY-74 SYSTEM: SO2

□ NUM.(PART./ML) △ SURF.(μM²/ML) ◇ VOL.(μM³/ML)

SO2 = 0.56 PPM

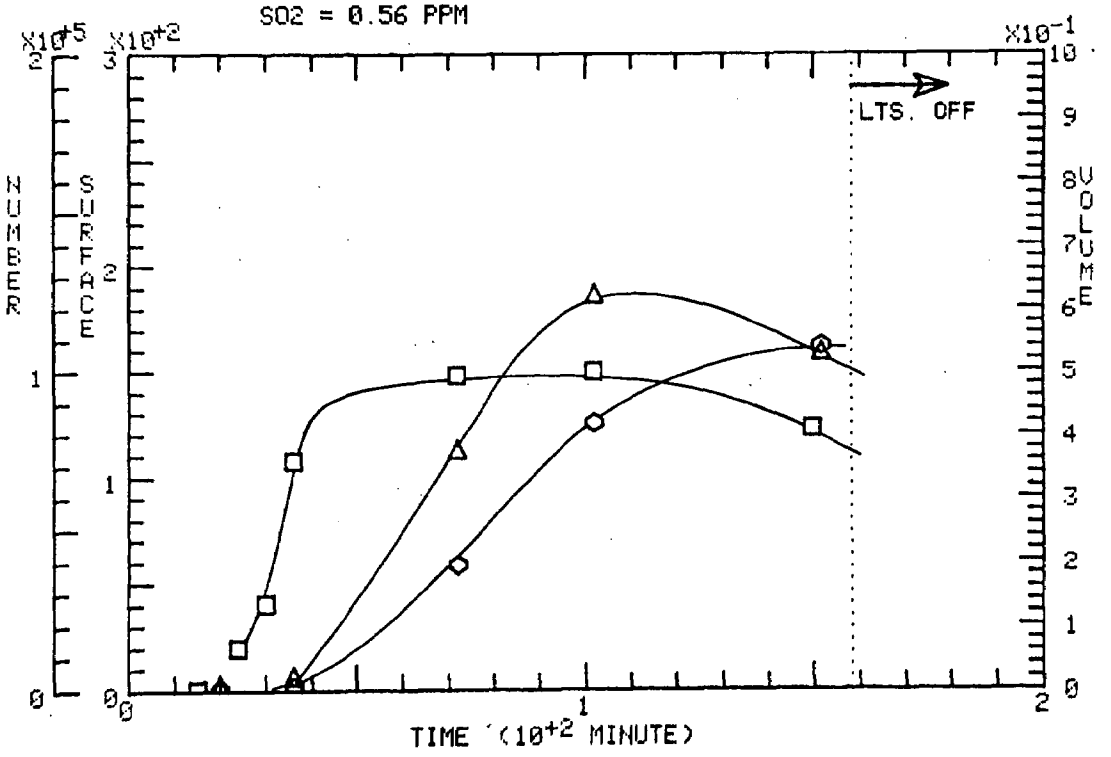

RUN 57 DATE: 8-MAY-74 SYSTEM: SO2

□ NUM.(PART./ML) △ SURF.(μM²/ML) ◇ VOL.(μM³/ML)

SO2 = 0.56 PPM

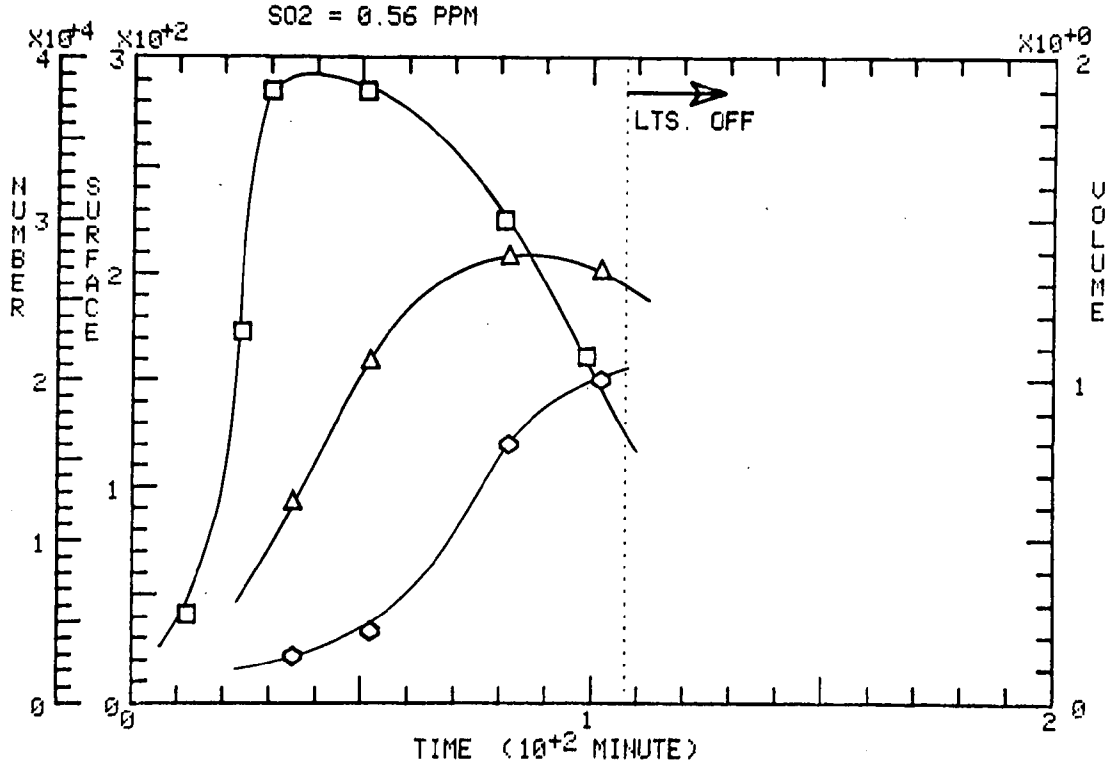

RUN 66 DATE: 23-MAY-74 SYSTEM: SO2

□ NUM.(PART./ML) △ SURF.(μM²/ML) ◇ VOL.(μM³/ML)

SO2 = 0.605 PPM

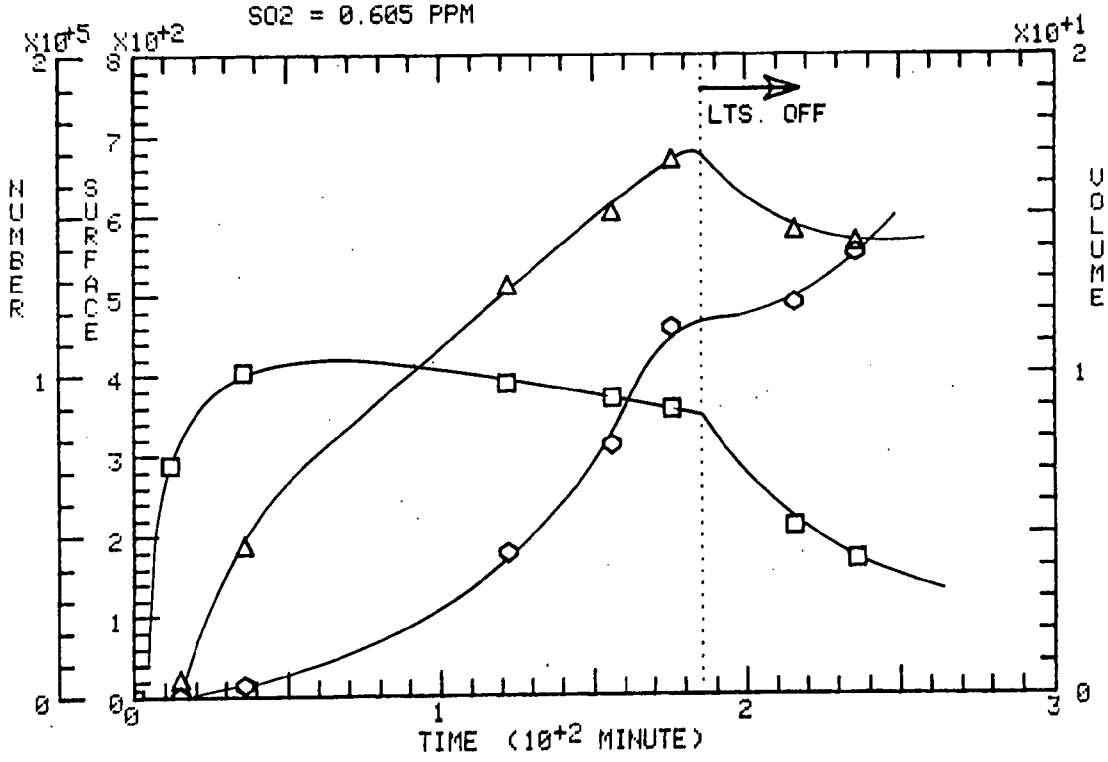

RUN 68 DATE: 25-MAY-74 SYSTEM: SO2

□ NUM.(PART./ML) △ SURF.(μM^2/ML) ○ VOL.(μM^3/ML)

SO2 = 0.62 PPM

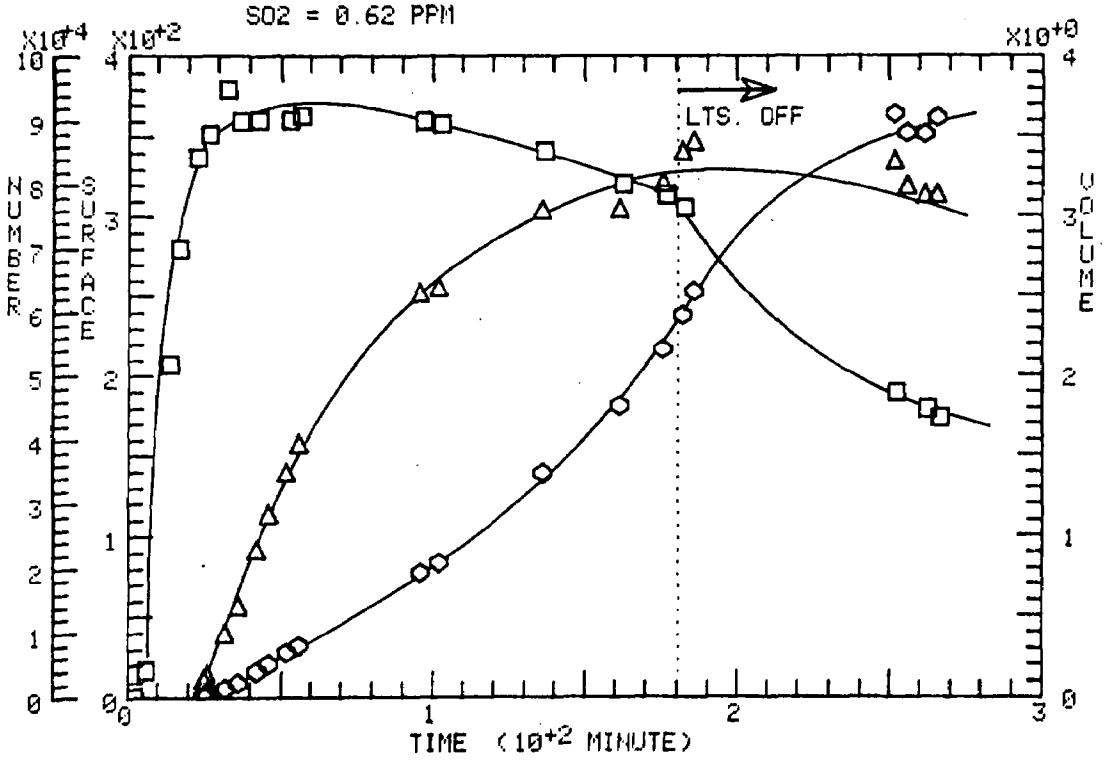

RUN 69 DATE: 3-JUN-74 SYSTEM: SO2

□ NUM.(PART./ML) △ SURF.(μM^2/ML) ○ VOL.(μM^3/ML)

SO2 = 0.053 PPM

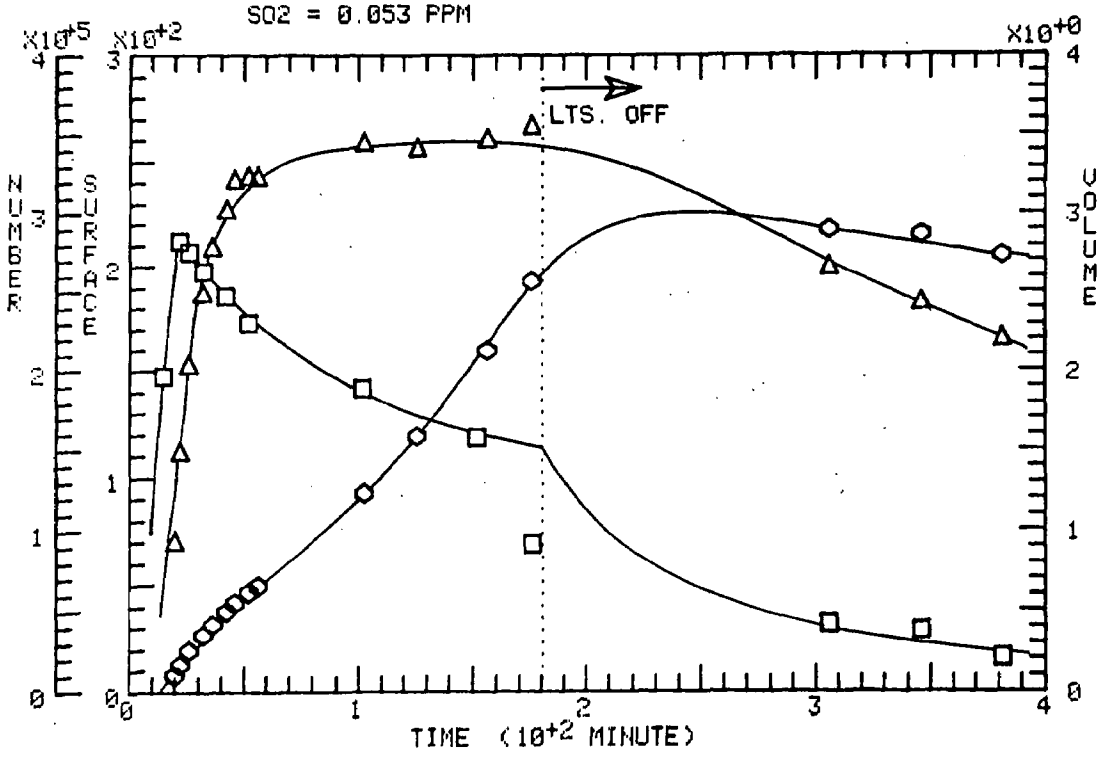

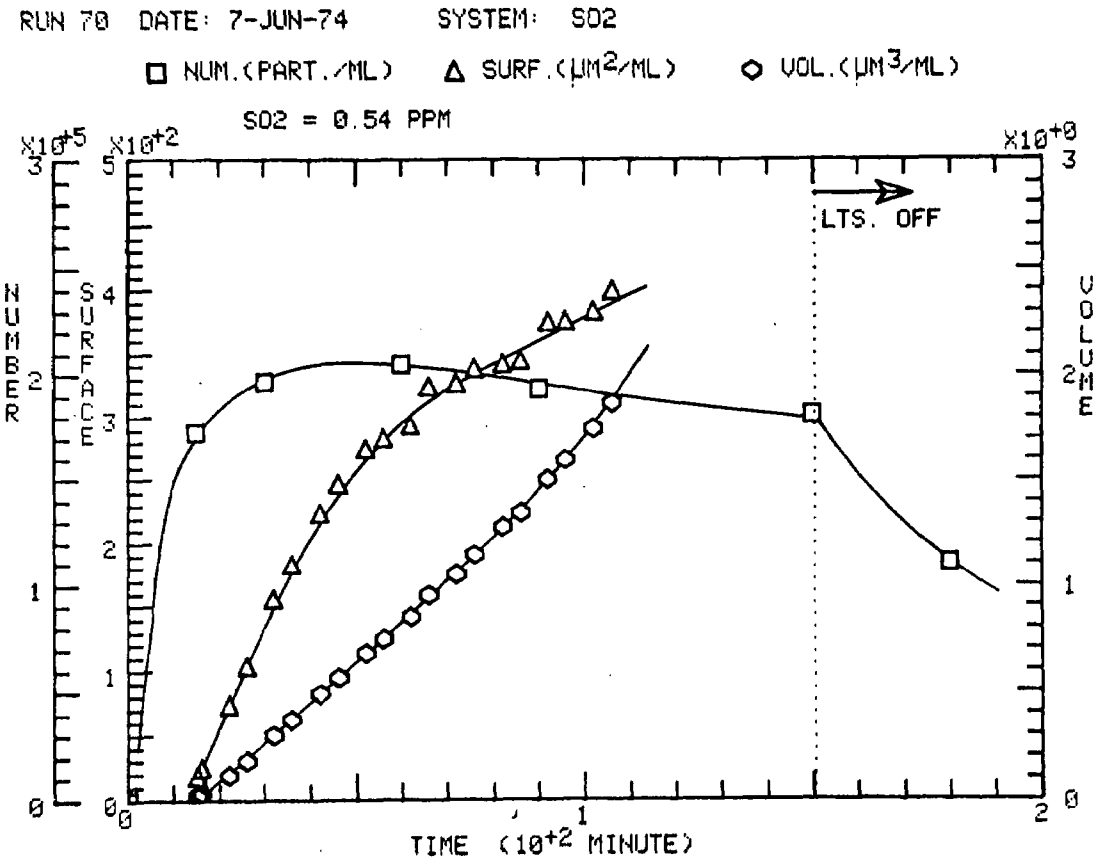
RUN 70 DATE: 7-JUN-74 SYSTEM: SO2
NUM.(PART./ML) SURF.(μM²/ML) VOL.(μM³/ML)
SO2 = 0.54 PPM
X10+5
X10+2
X10+0
LTS. OFF
NUMBER
SURFACE
VOLUME
TIME (10+2 MINUTE)

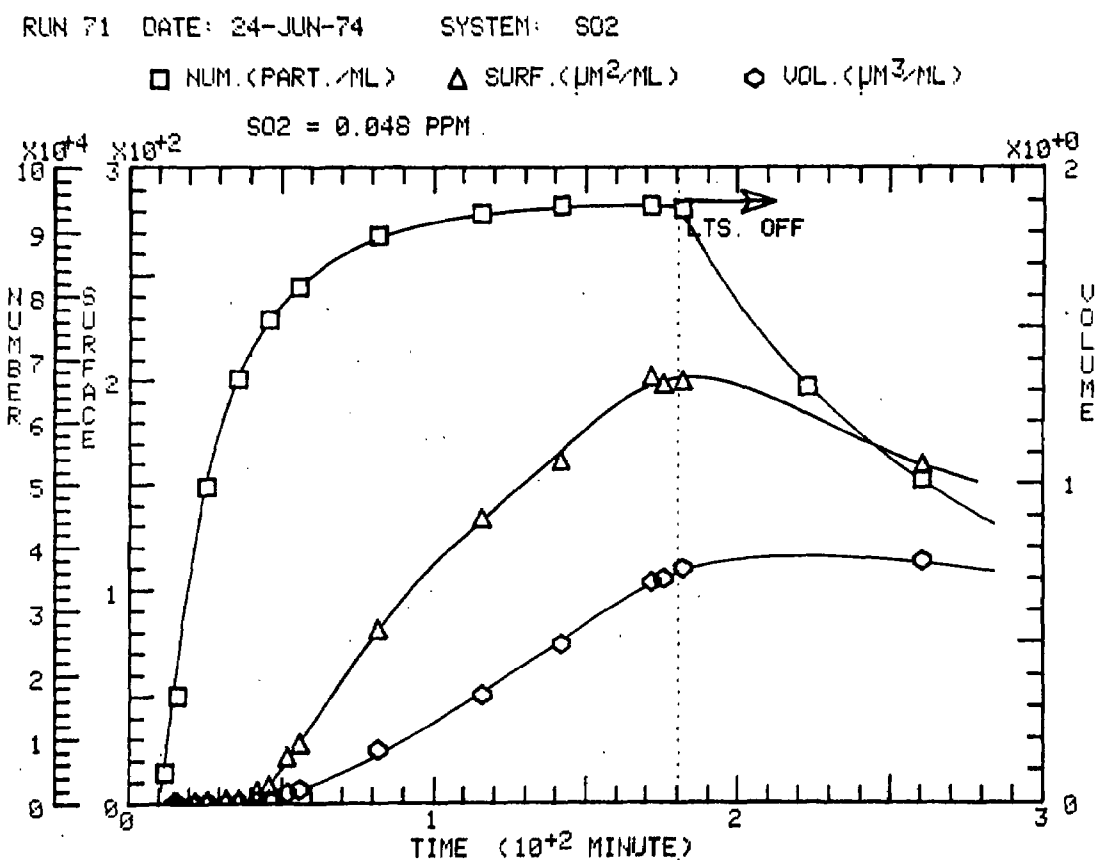
RUN 71 DATE: 24-JUN-74 SYSTEM: SO2
NUM.(PART./ML) SURF.(μM²/ML) VOL.(μM³/ML)
SO2 = 0.048 PPM
X10+4
X10+2
X10+0
LTS. OFF
NUMBER
SURFACE
VOLUME
TIME (10+2 MINUTE)

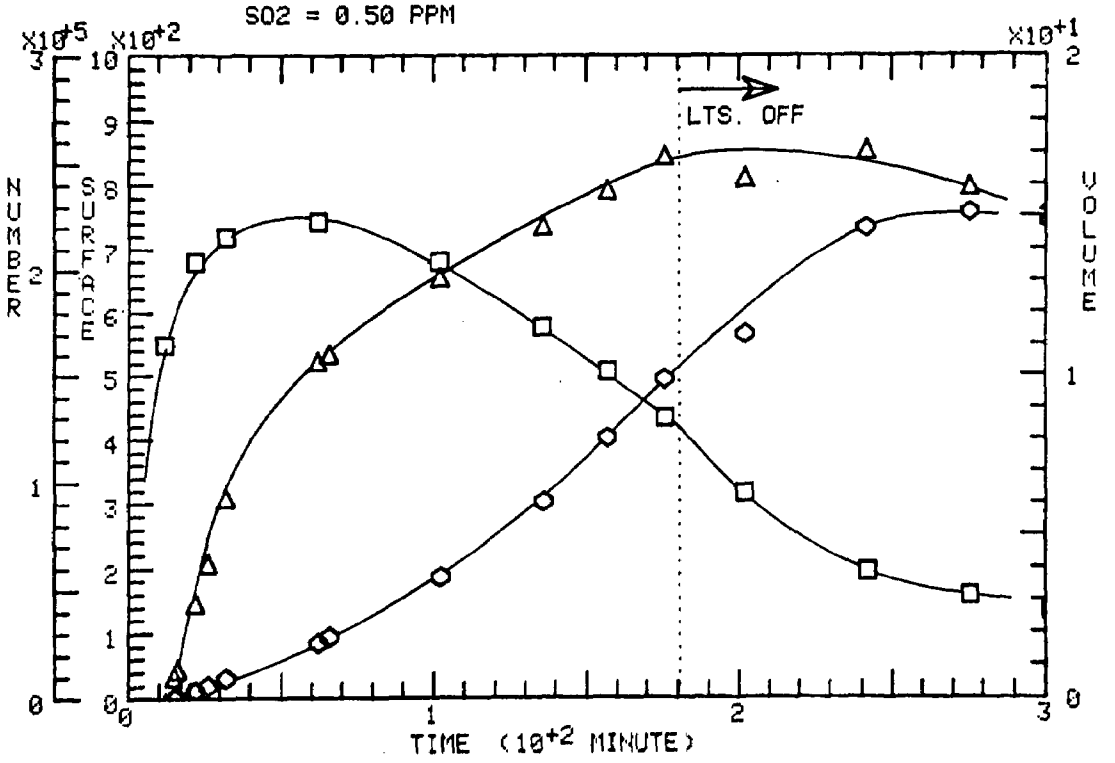
RUN 72 DATE: 25-JUN-74 SYSTEM: SO2
NUM.(PART./ML) SURF.(μM²/ML) VOL.(μM³/ML)
SO2 = 0.50 PPM
X10+5
X10+2
X10+1
LTS. OFF
NUMBER
SURFACE
VOLUME
TIME (10+2 MINUTE)

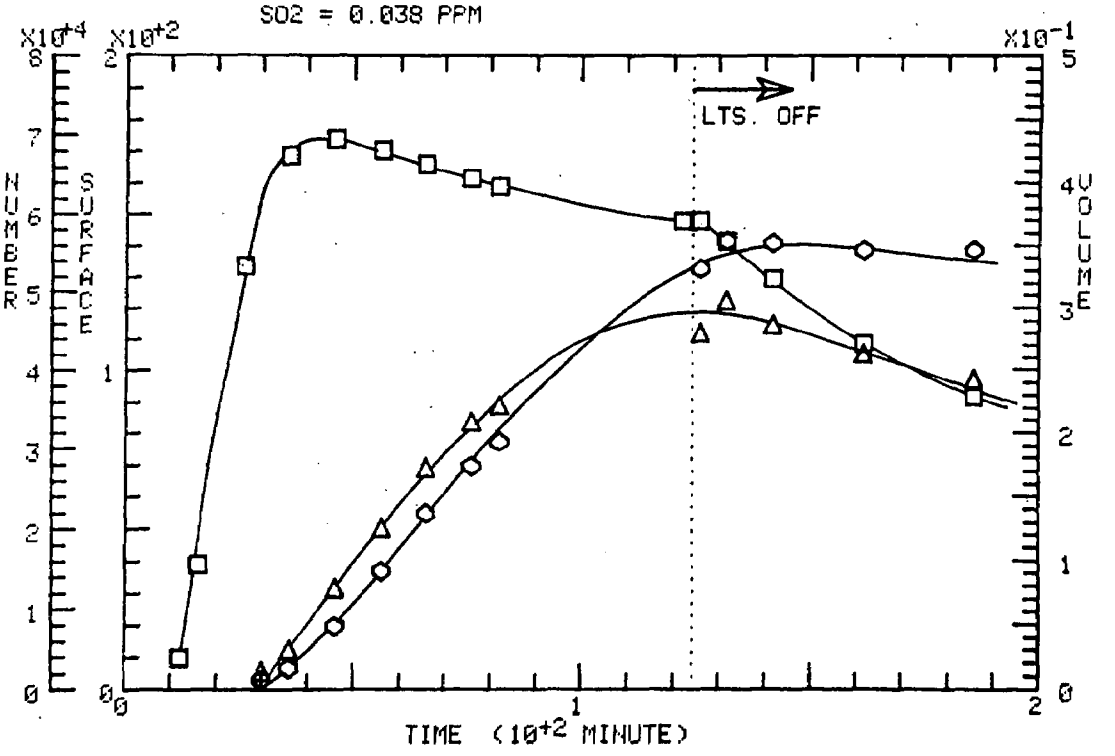
RUN 79 DATE: 2-JUL-74 SYSTEM: SO2
NUM.(PART./ML) SURF.(μM²/ML) VOL.(μM³/ML)
SO2 = 0.038 PPM
X10+4
X10+2
X10-1
LTS. OFF
NUMBER
SURFACE
VOLUME
TIME (10+2 MINUTE)

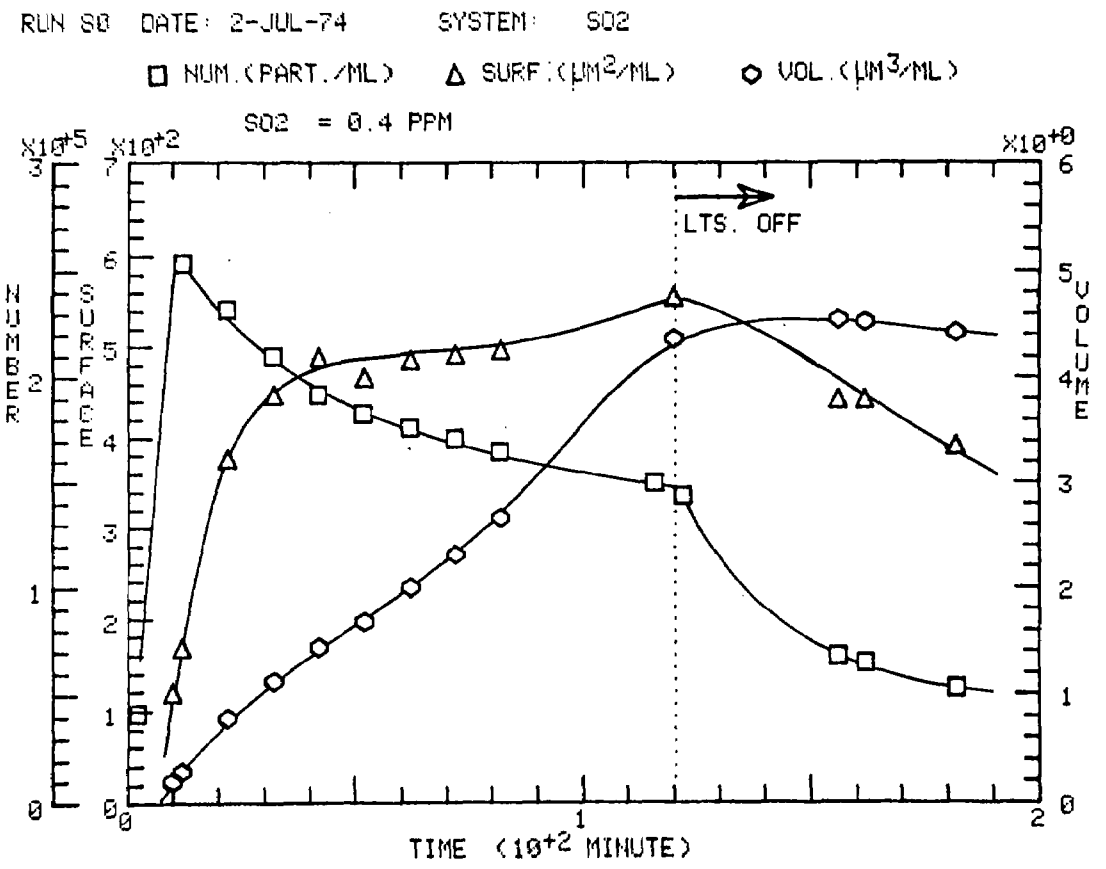
RUN S0 DATE: 2-JUL-74 SYSTEM: SO2
NUM.(PART./ML) SURF.(μM²/ML) VOL.(μM³/ML)
SO2 = 0.4 PPM
X10+5
X10+2
X10+0
LTS. OFF
NUMBER
SURFACE
VOLUME
TIME (10+2 MINUTE)

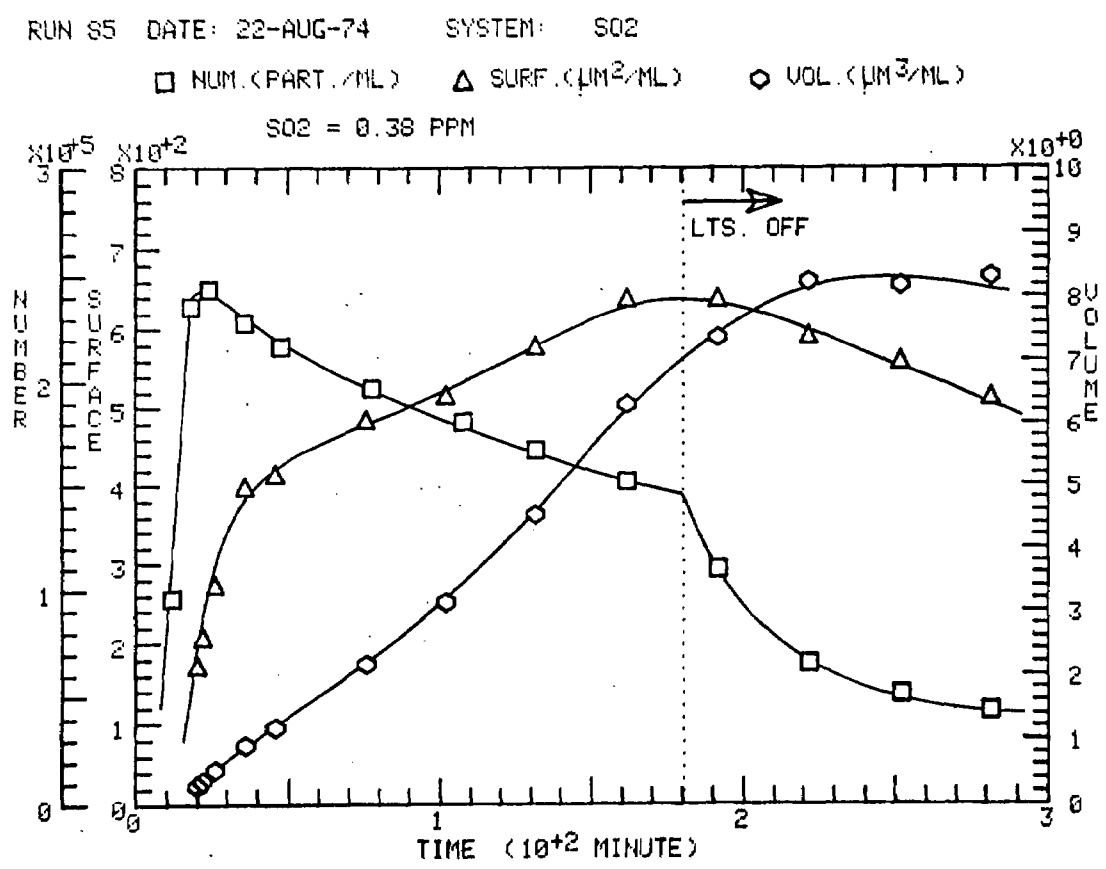
RUN S5 DATE: 22-AUG-74 SYSTEM: SO2
NUM.(PART./ML) SURF.(μM²/ML) VOL.(μM³/ML)
SO2 = 0.38 PPM
X10+5
X10+2
X10+0
LTS. OFF
NUMBER
SURFACE
VOLUME
TIME (10+2 MINUTE)

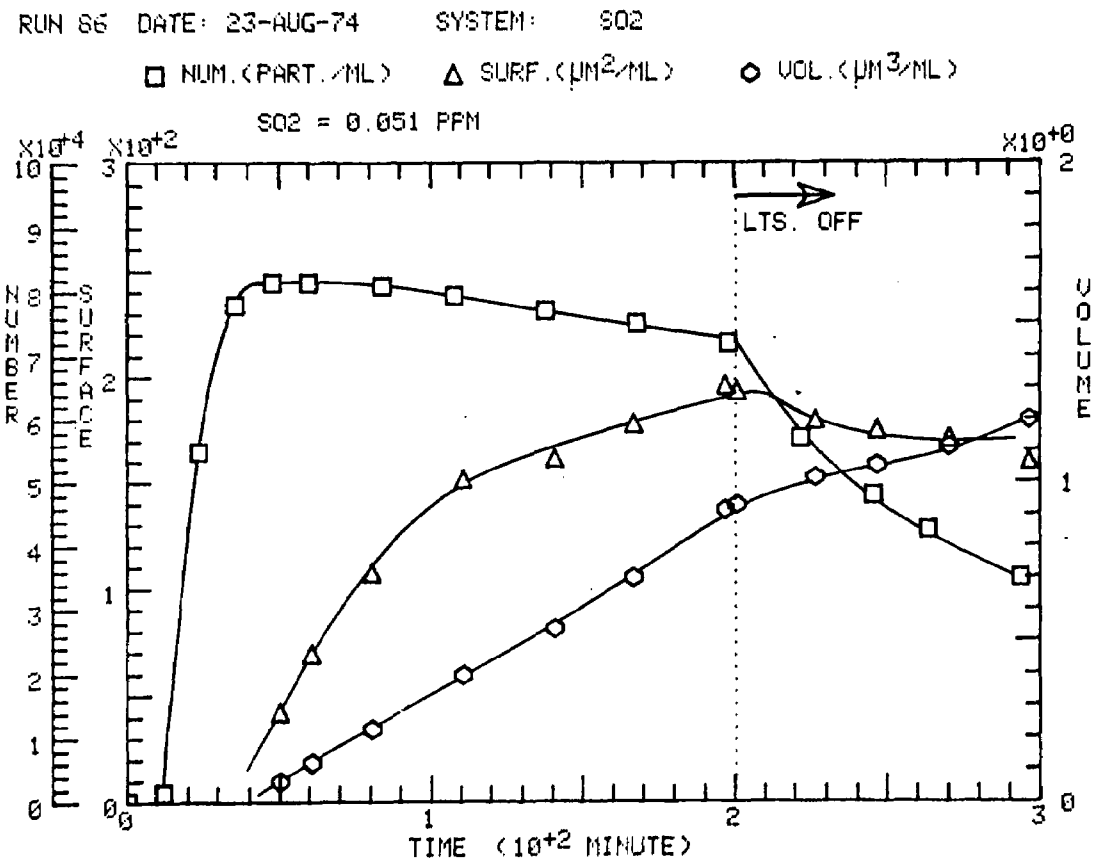
RUN 86 DATE: 23-AUG-74 SYSTEM: SO2
NUM.(PART./ML) SURF.(μM²/ML) VOL.(μM³/ML)
SO2 = 0.051 PPM
X10+4
X10+2
X10+0
LTS. OFF
NUMBER
SURFACE
VOLUME
TIME (10+2 MINUTE)

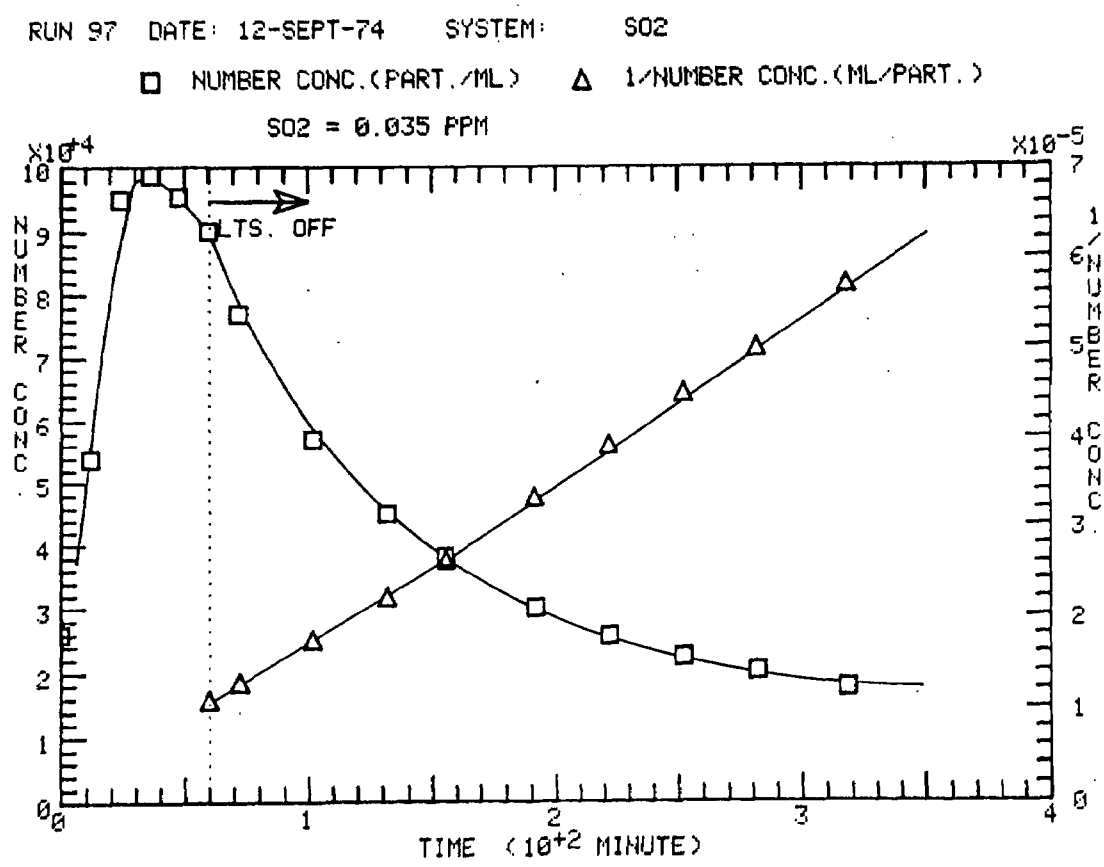
RUN 97 DATE: 12-SEPT-74 SYSTEM: SO2
NUMBER CONC.(PART./ML) 1/NUMBER CONC.(ML/PART.)
SO2 = 0.035 PPM
X10+4
X10-5
LTS. OFF
NUMBER CONC
1/NUMBER CONC
TIME (10+2 MINUTE)

(2) TOLUENE EXPERIMENTS

CALSPAN
RUN NO. 6 24 FEBRUARY 1974 TOLUENE-NO-FILTERED AIR SYSTEM R.H. = 30%;
TOLUENE = 0.35 ppm; NO = 0.170 ppm; NO_2 = 0.01 ppm

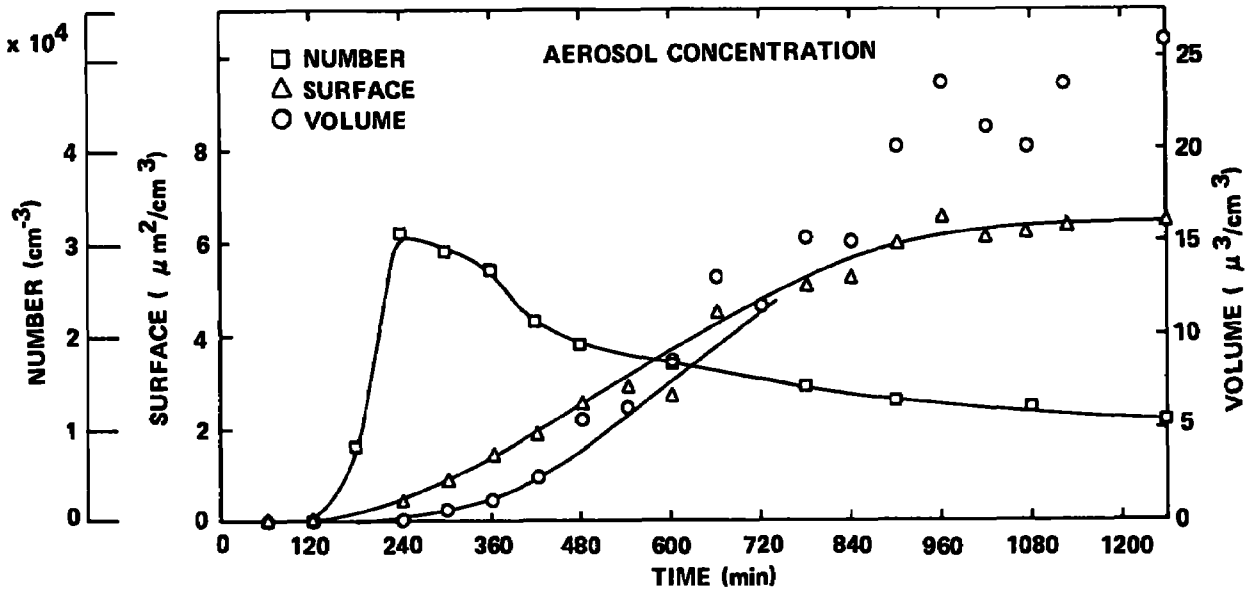

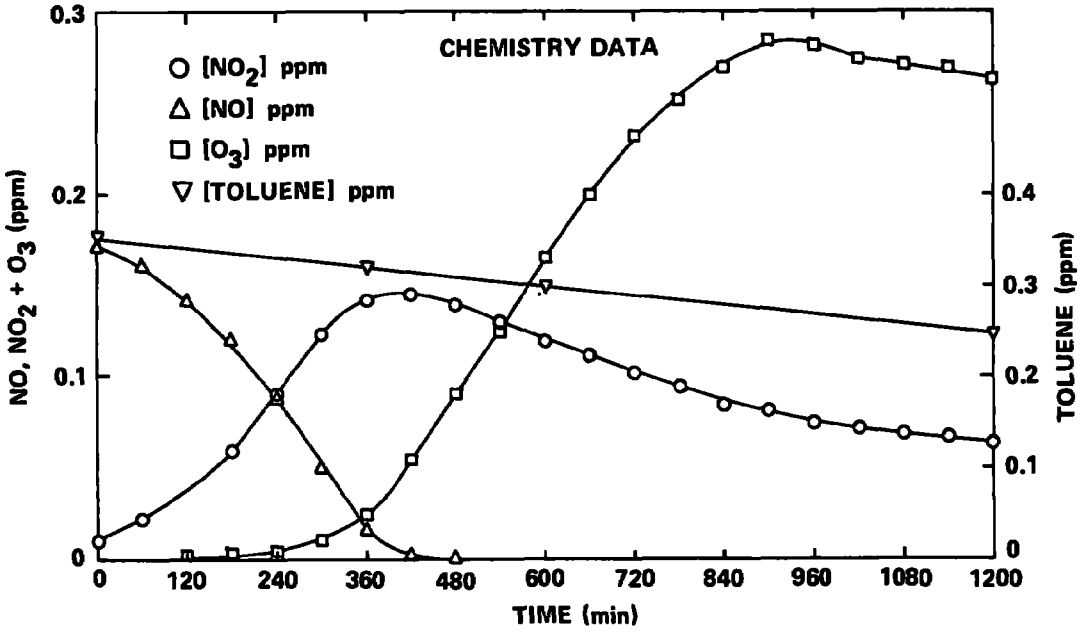

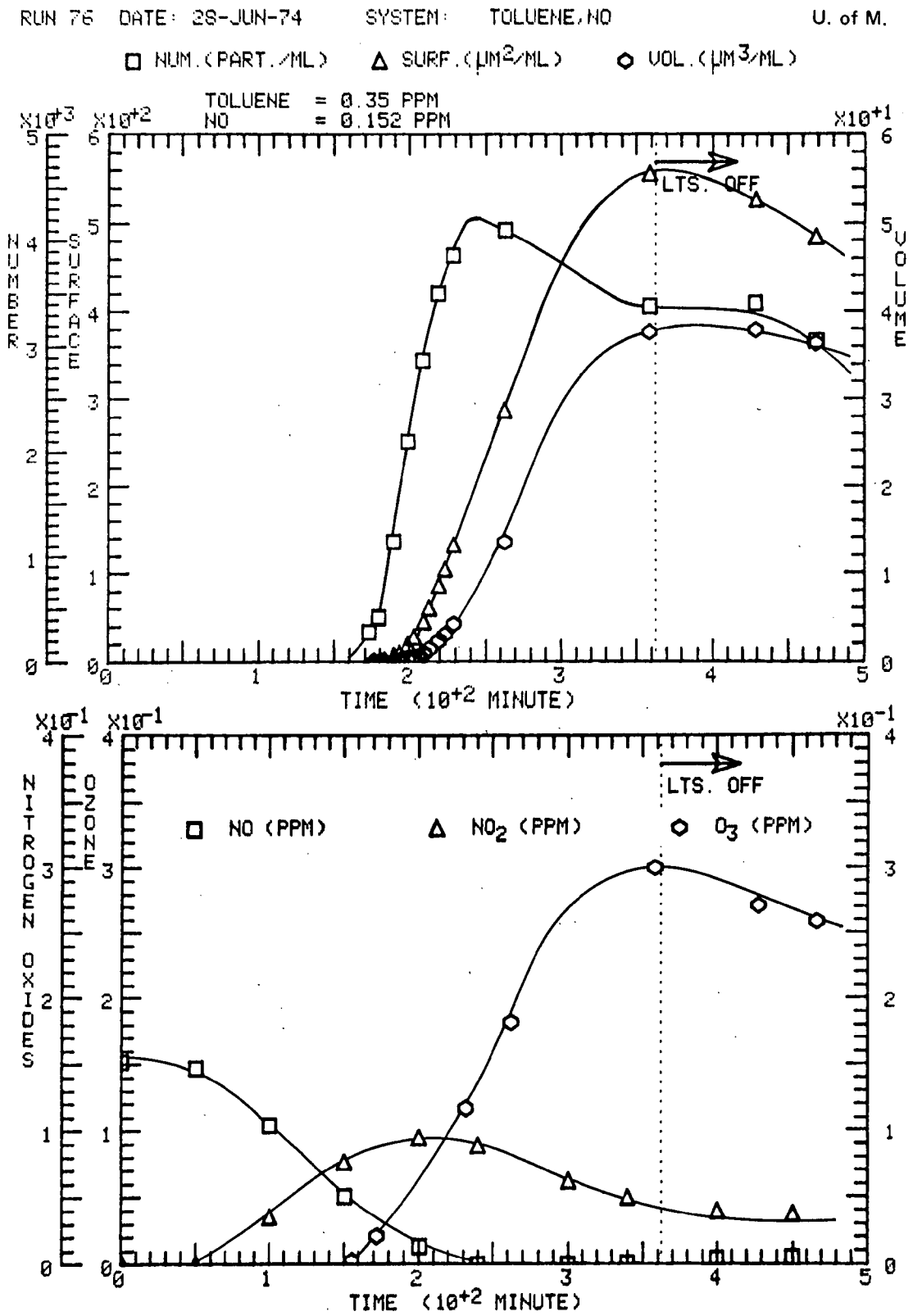
RUN 76 DATE: 28-JUN-74 SYSTEM: TOLUENE/NO U. of M.
NUM.(PART./ML) SURF.(μM²/ML) VOL.(μM³/ML)
TOLUENE = 0.35 PPM
NO = 0.152 PPM
LTS. OFF
NUMBER
SURFACE
VOLUME
TIME (10+2 MINUTE)
NITROGEN OXIDES
OZONE
NO (PPM)
NO2 (PPM)
O3 (PPM)
LTS. OFF
TIME (10+2 MINUTE)

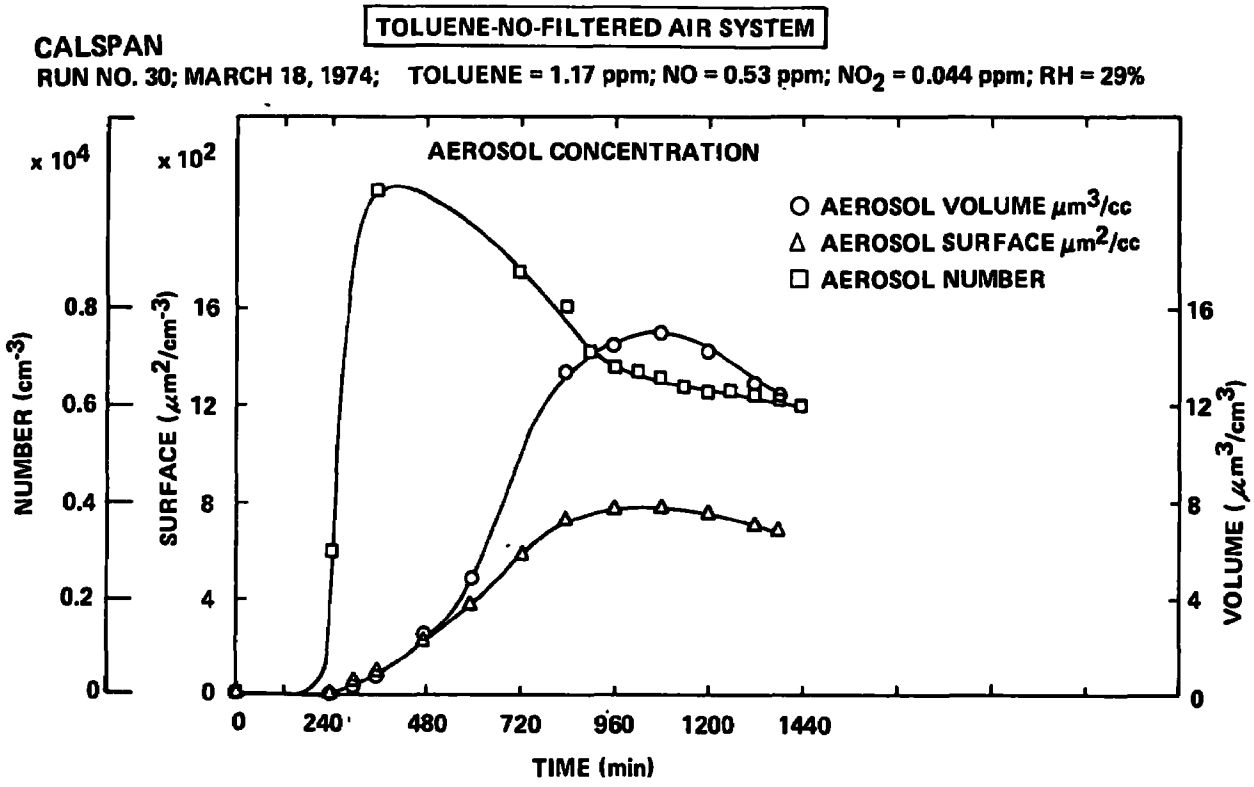
TOLUENE-NO-FILTERED AIR SYSTEM
CALSPAN
RUN NO. 30; MARCH 18, 1974; TOLUENE = 1.17 ppm; NO = 0.53 ppm; NO_2 = 0.044 ppm; RH = 29%
AEROSOL CONCENTRATION
O AEROSOL VOLUME $\mu m^3/cc$
Δ AEROSOL SURFACE $\mu m^2/cc$
□ AEROSOL NUMBER
x 10^4
x 10^2
NUMBER (cm^{-3})
SURFACE ($\mu m^2/cm^{-3}$)
VOLUME ($\mu m^3/cm^3$)
0.8
0.6
0.4
0.2
0
16
12
8
4
0
0
240
480
720
960
1200
1440
TIME (min)

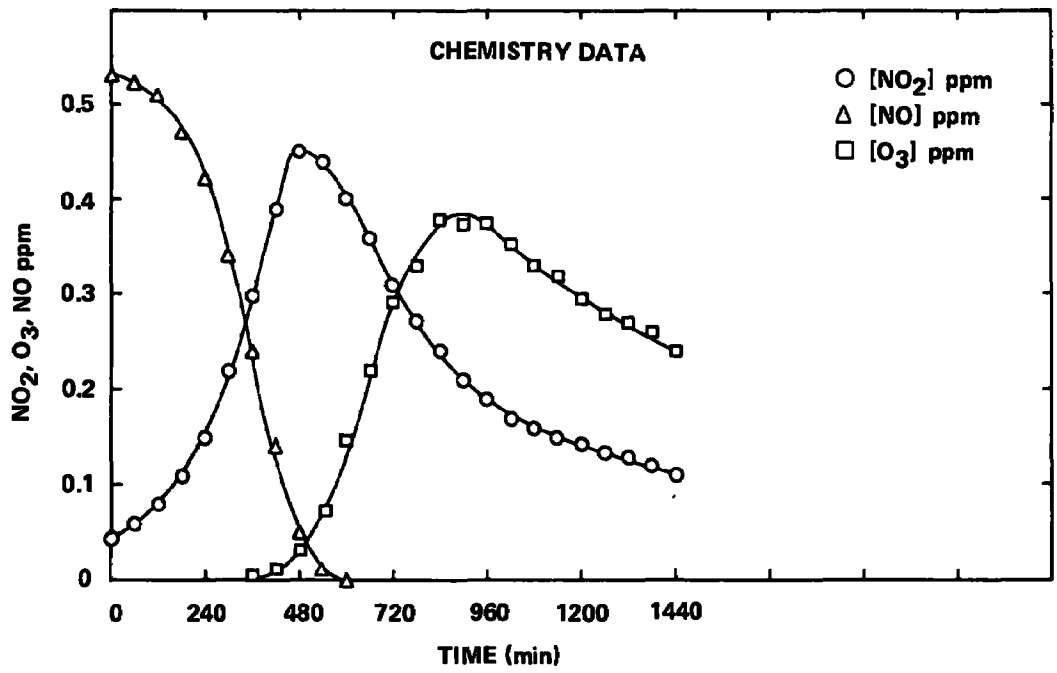
CHEMISTRY DATA
O [NO_2] ppm
Δ [NO] ppm
□ [O_3] ppm
NO_2, O_3, NO ppm
0.5
0.4
0.3
0.2
0.1
0
0
240
480
720
960
1200
1440
TIME (min)

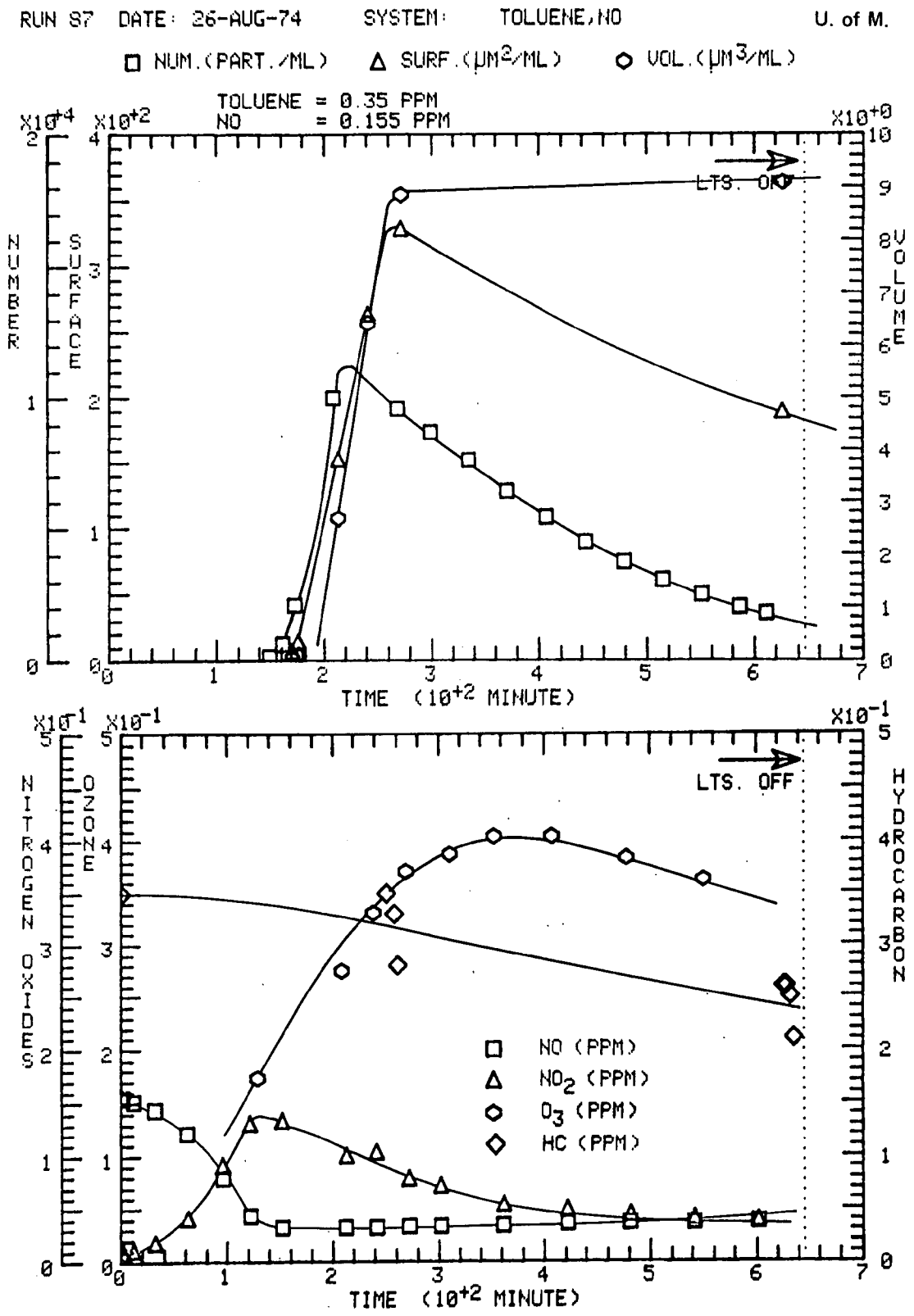
RUN 87 DATE: 26-AUG-74 SYSTEM: TOLUENE/NO U. of M.
NUM.(PART./ML) SURF.(μM²/ML) VOL.(μM³/ML)
TOLUENE = 0.35 PPM
NO = 0.155 PPM
X10+4
X10+2
X10+0
LTS. ON
NUMBER
SURFACE
VOLUME
TIME (10+2 MINUTE)
X10-1
X10-1
X10-1
LTS. OFF
NITROGEN OXIDES
OZONE
HYDROCARBON
NO (PPM)
NO2 (PPM)
O3 (PPM)
HC (PPM)
TIME (10+2 MINUTE)

CALSPAN

RUN NO. 8 26 FEBRUARY 1974 TOLUENE-NO-SO_2-FILTERED AIR SYSTEM; R.H. = 26%;
TOLUENE = 0.35 ppm; NO = 0.138 ppm; NO_2 = 0.01 ppm; SO_2 = 0.055 ppm

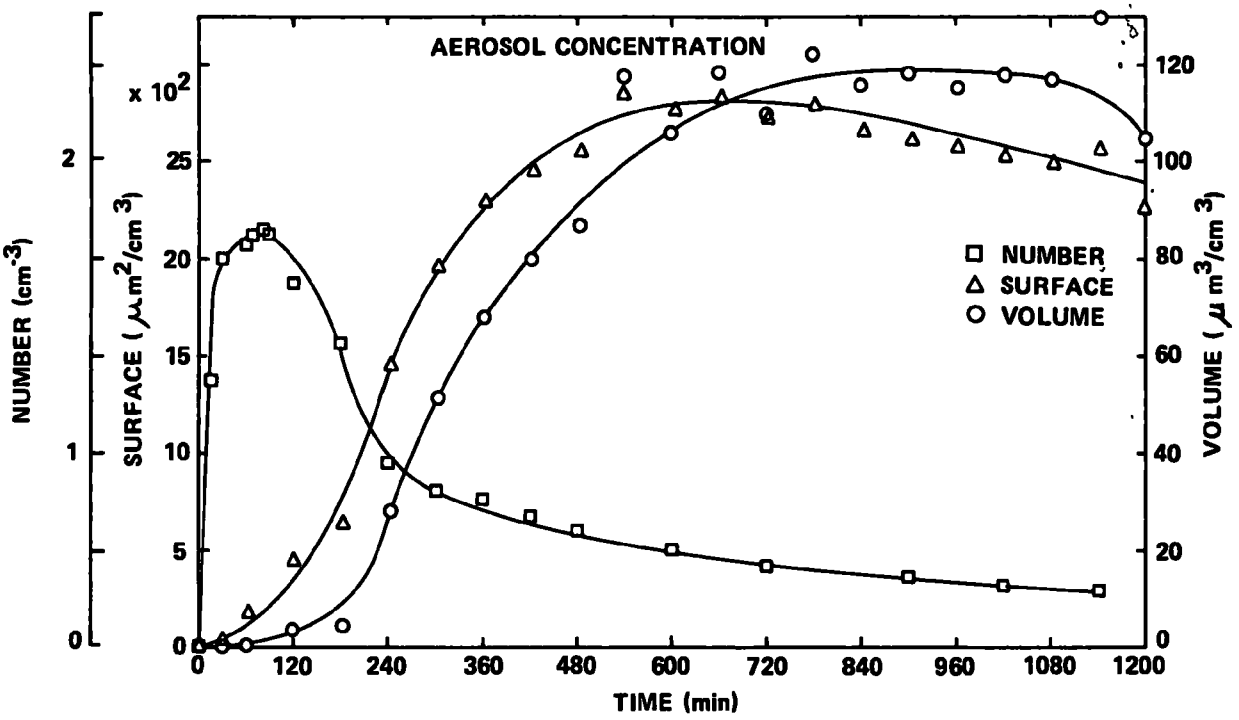

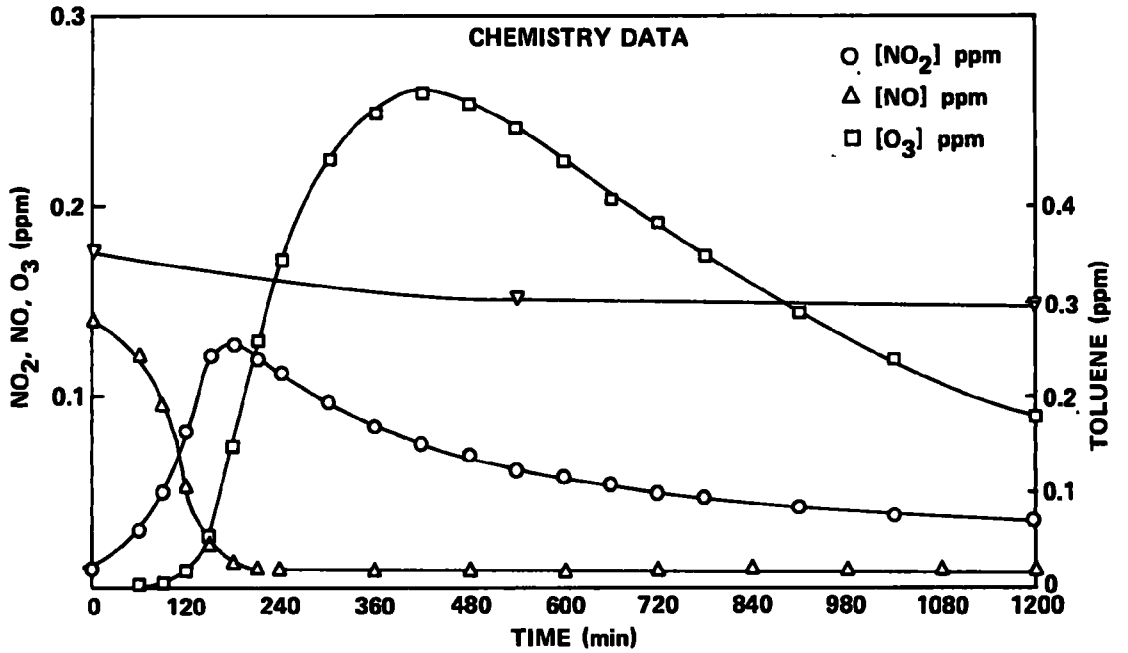

CALSPAN

RUN NO. 29 MARCH 17, 1974

TOLUENE-NO-SO_2-FILTERED AIR SYSTEM

TOLUENE = 0.35 ppm; NO = 0.146 ppm; NO_2 = 0.009 ppm; SO_2 = 0.05 ppm; RH = 30%

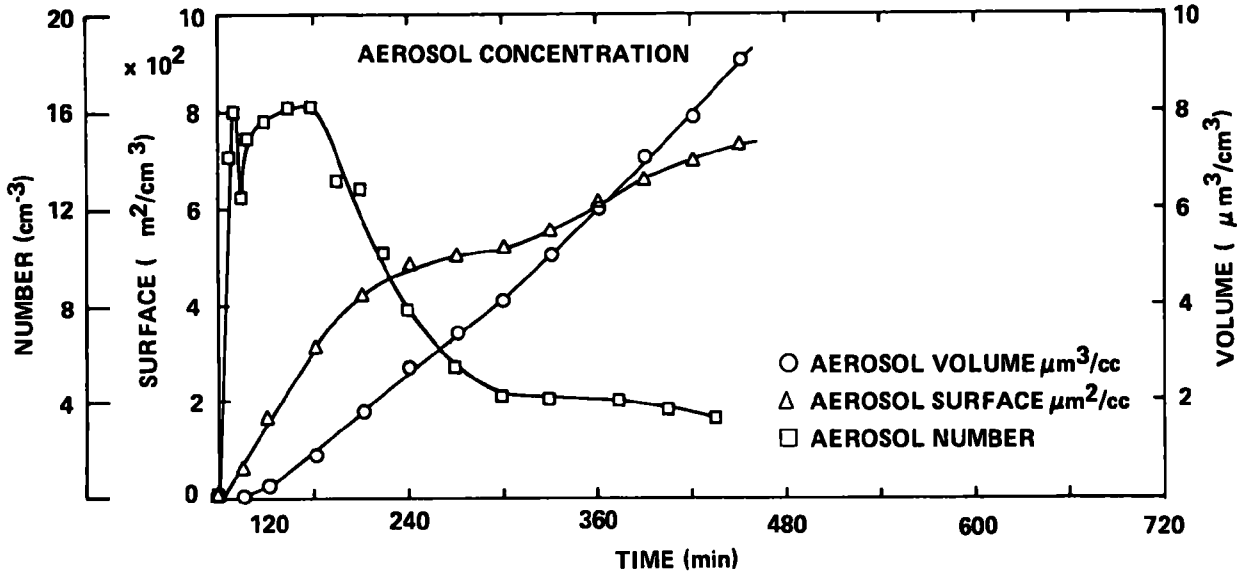

TOLUENE-NO-SO_2 IN FILTERED AIR

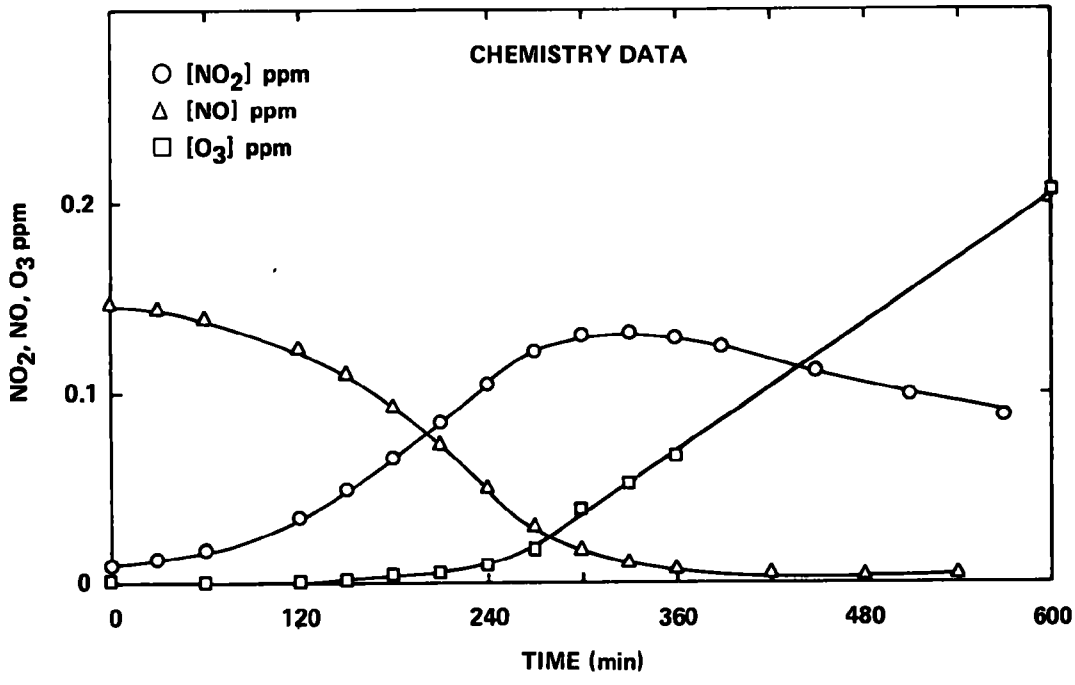

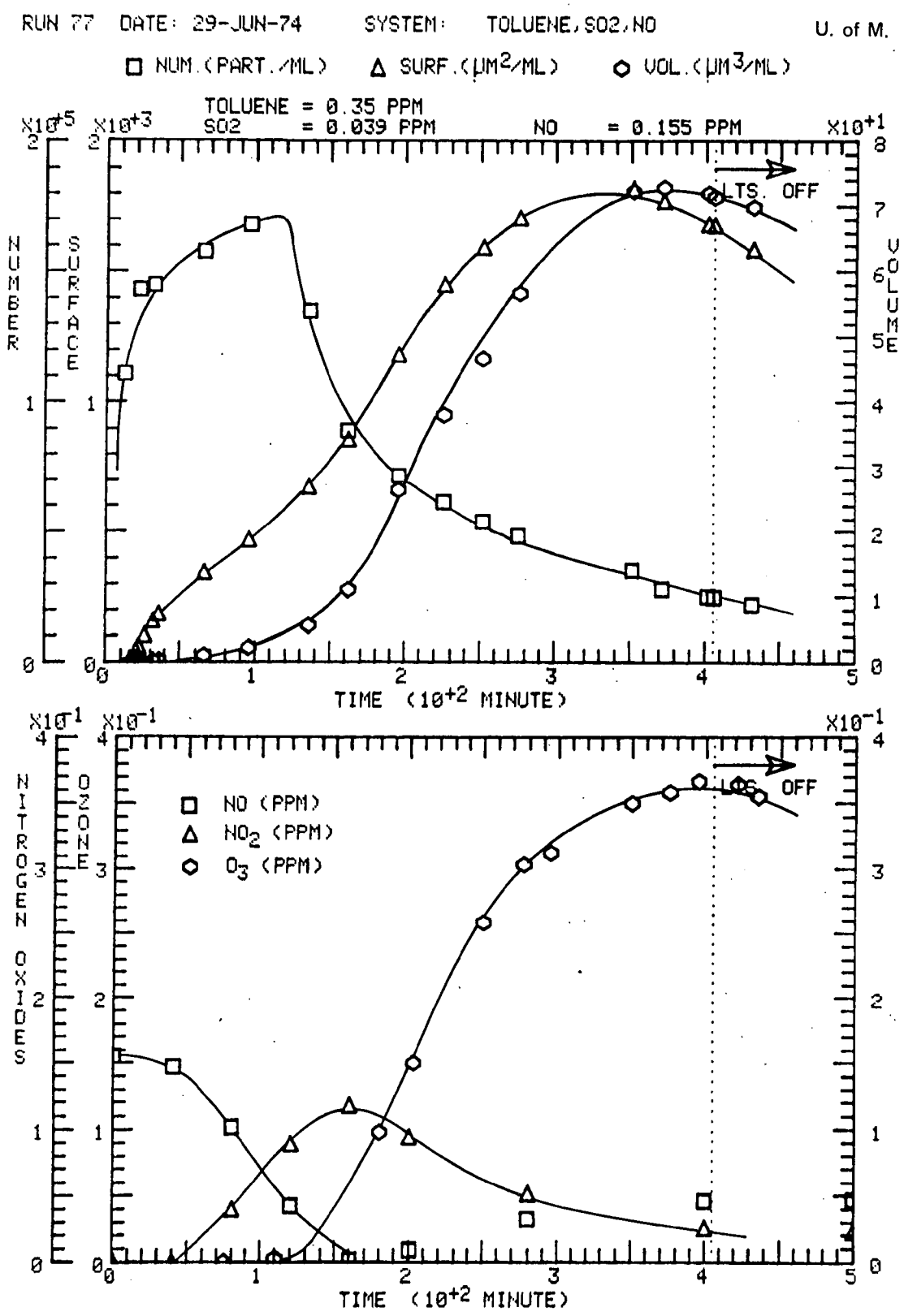
RUN 77 DATE: 29-JUN-74 SYSTEM: TOLUENE, SO2, NO
U. of M.
NUM. (PART./ML)
SURF. (μM²/ML)
VOL. (μM³/ML)
TOLUENE = 0.35 PPM
SO2 = 0.039 PPM
NO = 0.155 PPM
LTS. OFF
NUMBER
SURFACE
VOLUME
TIME (10+2 MINUTE)
NO (PPM)
NO2 (PPM)
O3 (PPM)
NITROGEN OXIDES
OZONE

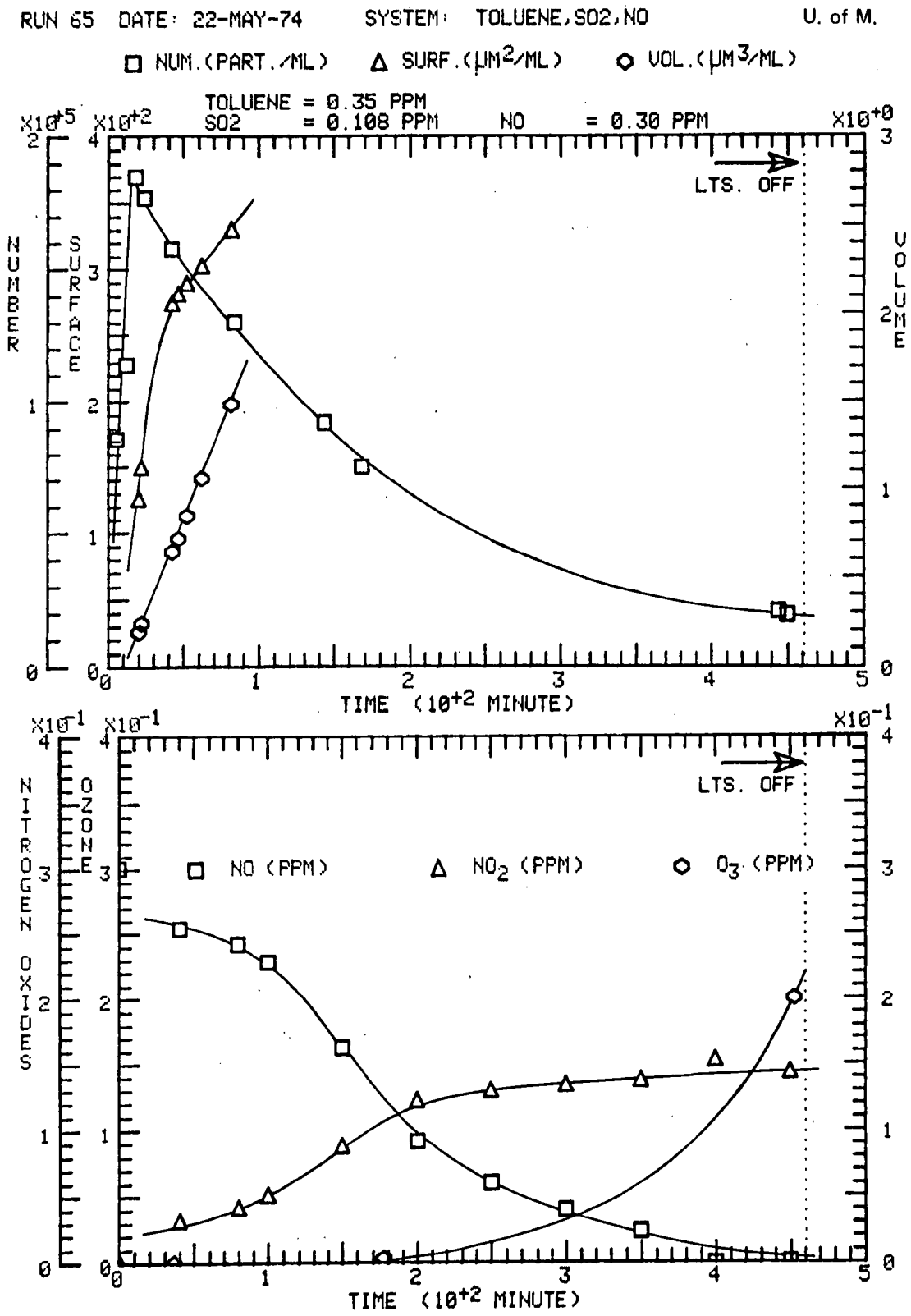
RUN 65 DATE: 22-MAY-74 SYSTEM: TOLUENE, SO2, NO U. of M.
NUM. (PART./ML) SURF. (μM²/ML) VOL. (μM³/ML)
TOLUENE = 0.35 PPM
SO2 = 0.108 PPM
NO = 0.30 PPM
X10+5
X10+2
X10+0
LTS. OFF
NUMBER
SURFACE
VOLUME
TIME (10+2 MINUTE)
X10-1
X10-1
X10-1
LTS. OFF
NITROGEN OXIDES
OZONE
NO (PPM)
NO2 (PPM)
O3 (PPM)
TIME (10+2 MINUTE)

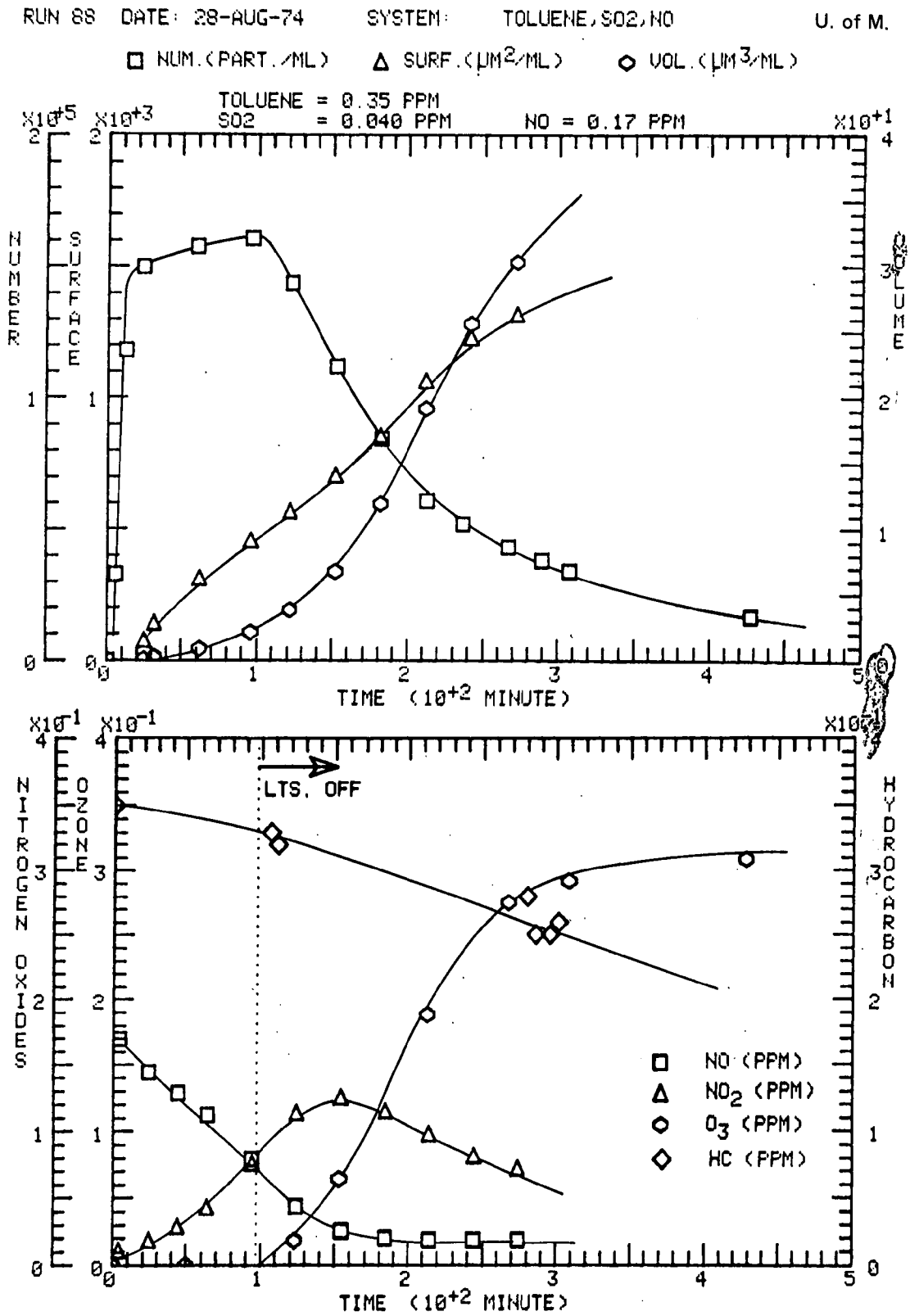
RUN 88 DATE: 28-AUG-74 SYSTEM: TOLUENE/SO2/NO U. of M.
NUM.(PART./ML) SURF.(μM²/ML) VOL.(μM³/ML)
TOLUENE = 0.35 PPM
SO2 = 0.040 PPM NO = 0.17 PPM
X10^+5
X10^+3
X10^+1
NUMBER
SURFACE
VOLUME
TIME (10^+2 MINUTE)
X10^-1
NITROGEN OXIDES
OZONE
HYDROCARBON
LTS. OFF
NO (PPM)
NO2 (PPM)
O3 (PPM)
HC (PPM)
TIME (10^+2 MINUTE)

CALSPAN
RUN NO. 7 25 FEBRUARY 1974 TOLUENE-SO_2-FILTERED AIR SYSTEM R.H. = 33%;
TOLUENE = 0.35 ppm; SO_2 = 0.54 ppm

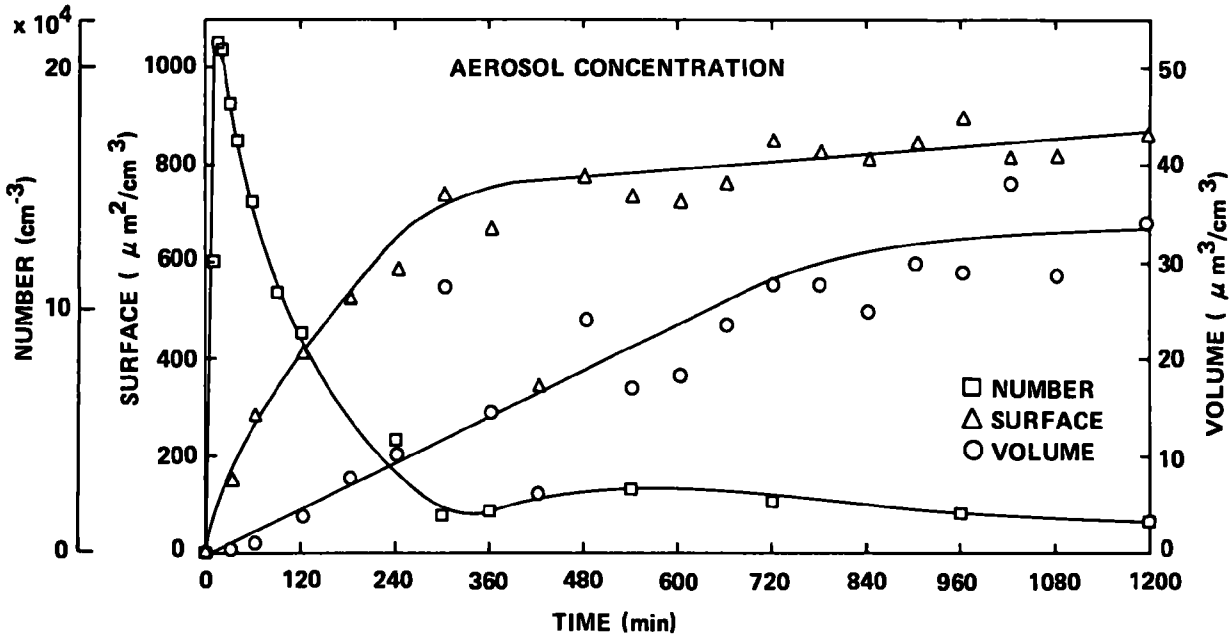

(3) HEXENE EXPERIMENTS

CALSPAN

RUN NO. 5 22 FEBRUARY 1974 HEXENE-1 - NO-FILTERED AIR SYSTEM R.H. = 41%; HEXENE-1 = 0.33 ppm; NO = 0.152 ppm; NO_2 = 0.014 ppm

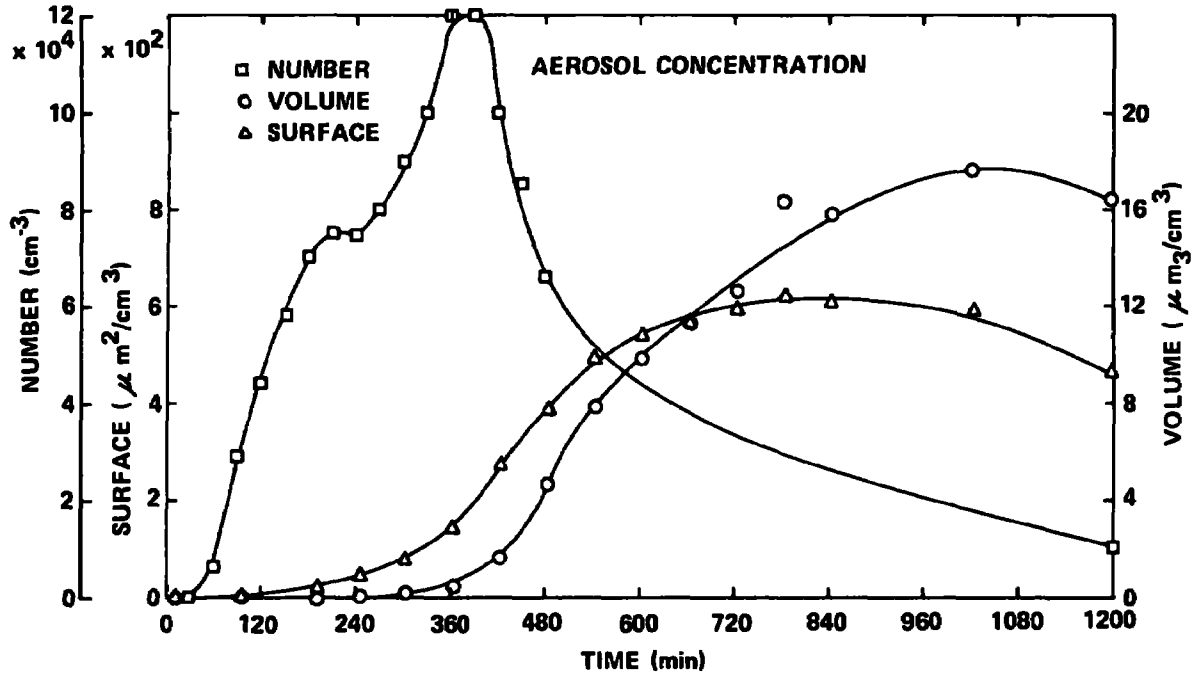

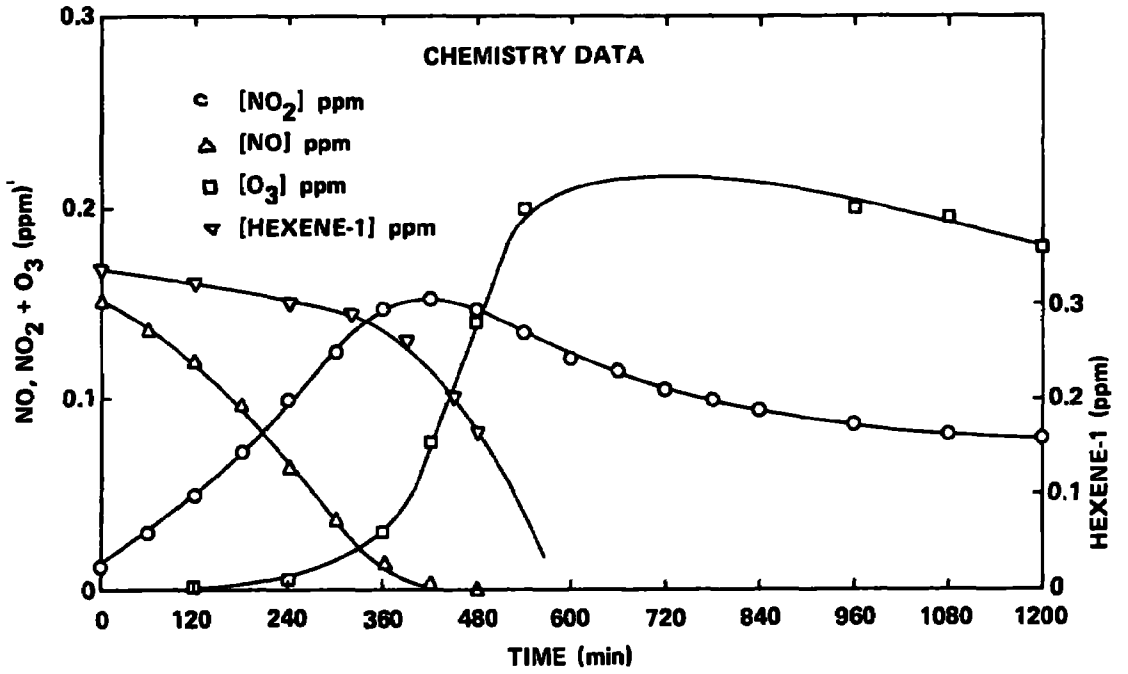

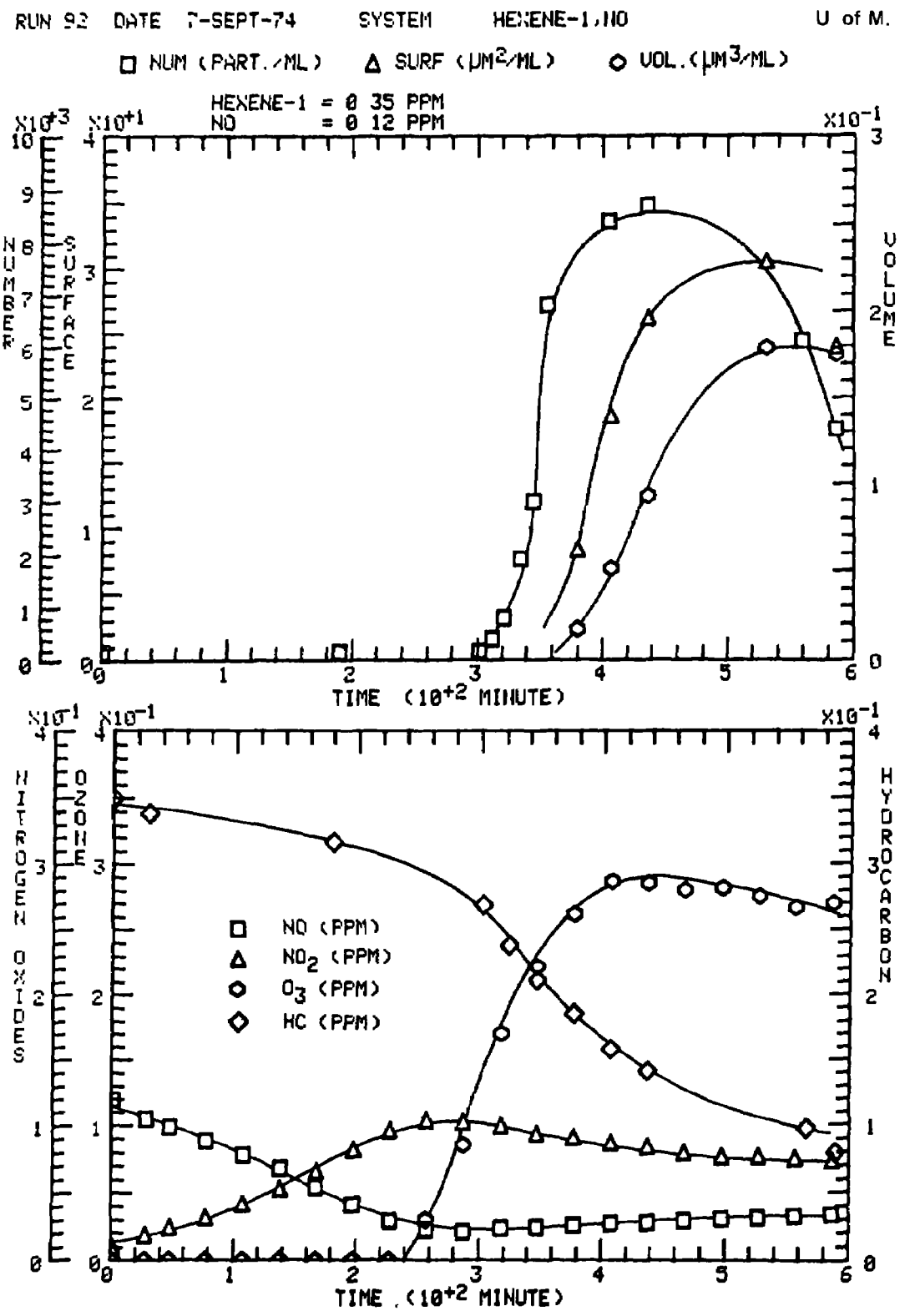
RUN 92 DATE 7-SEPT-74 SYSTEM HEXENE-1/NO U of M.
□ NUM (PART./ML) △ SURF (μM²/ML) ◇ VOL.(μM³/ML)
HEXENE-1 = 0 35 PPM
NO = 0 12 PPM
X10+3
X10+1
X10-1
NUMBER
SURFACE
VOLUME
TIME (10+2 MINUTE)
X10-1
X10-1
X10-1
NITROGEN OXIDES
OZONE
HYDROCARBON
□ NO (PPM)
△ NO2 (PPM)
◇ O3 (PPM)
◇ HC (PPM)
TIME (10+2 MINUTE)

CALSPAN

RUN NO. 21 MARCH 8, 1974 HEXENE-1-NO-FILTERED AIR SYSTEM

HEXENE-1 = 0.33 ppm; NO = 0.180 ppm; NO_2 = 0.010 ppm

RH = 37%

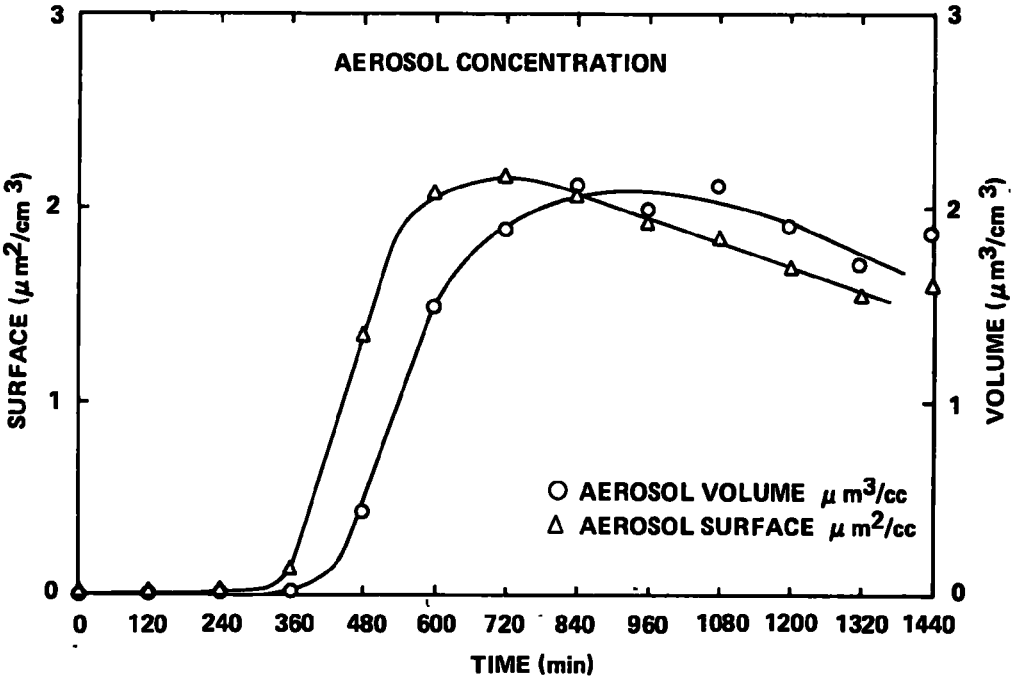

HEXENE-1-NO IN FILTERED AIR

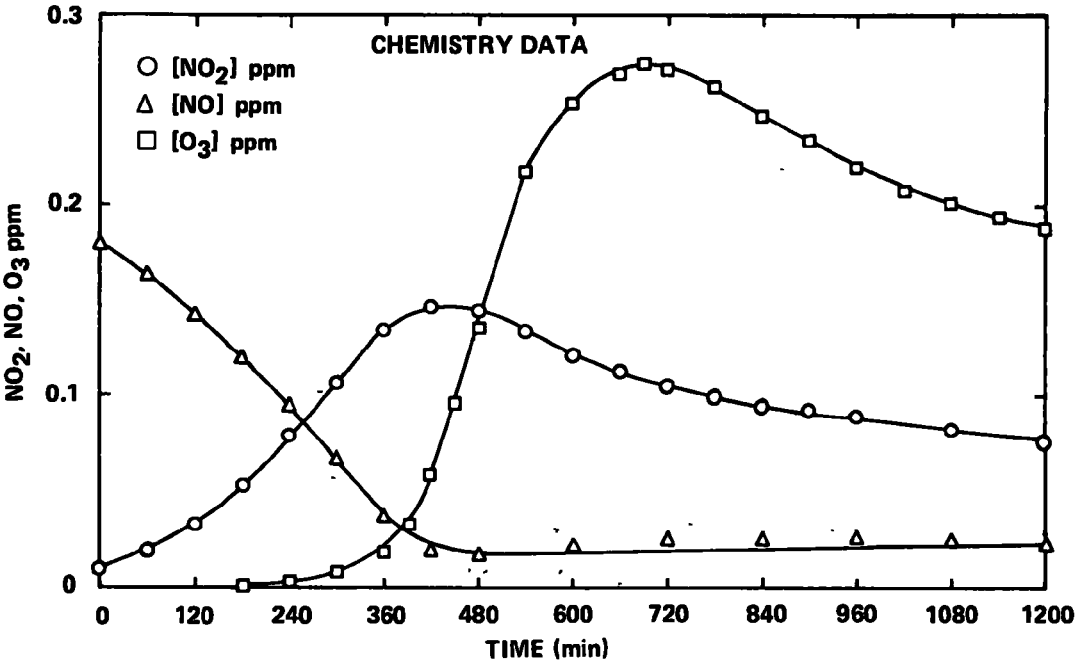

CALSPAN

RUN NO. 18 MARCH 6, 1974 HEXENE-1-SO_2-NO SYSTEM

HEXENE-1 = 0.33 ppm; NO = 0.178 ppm; NO_2 = 0.008 ppm; SO_2 = 0.07 ppm

RH = 37%

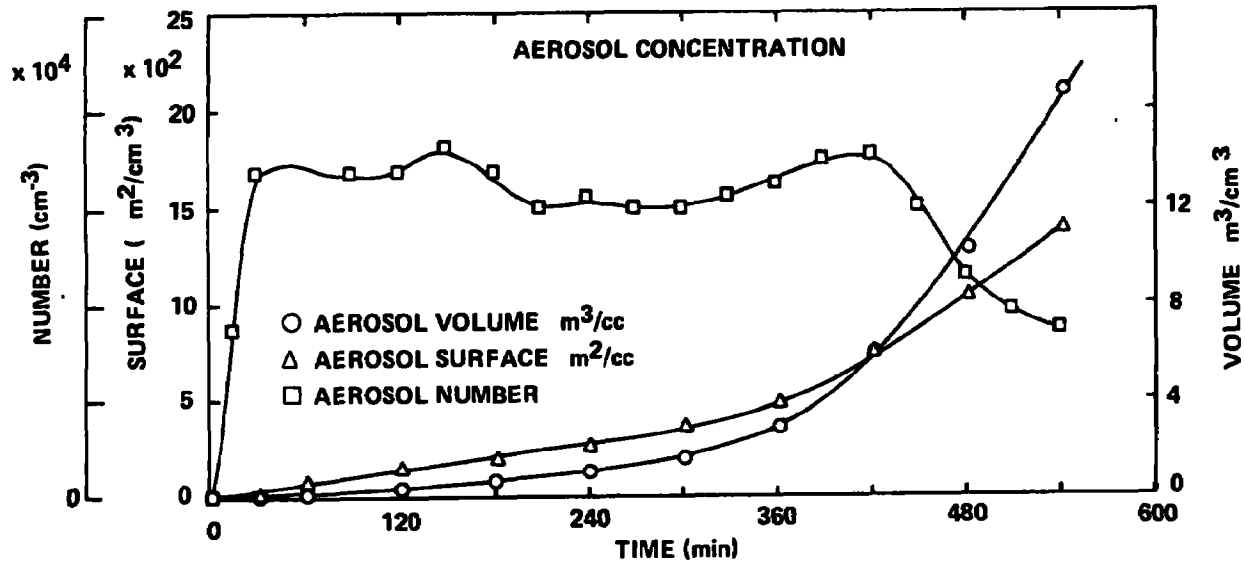

HEXENE-1-SO_2-NO-FILTERED AIR SYSTEM

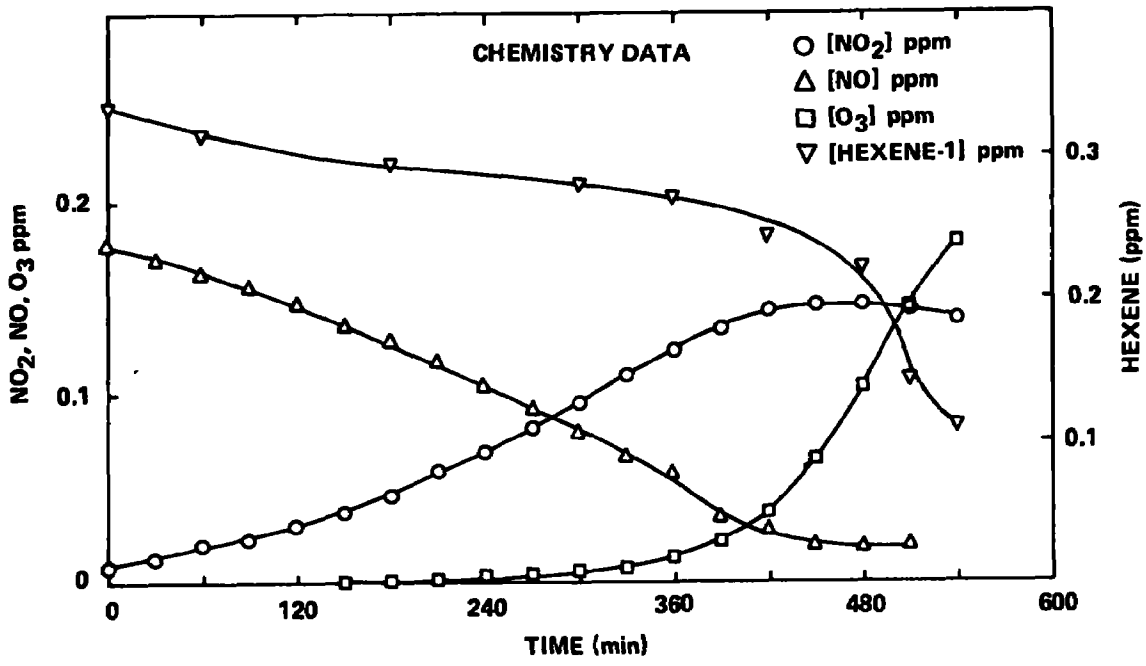

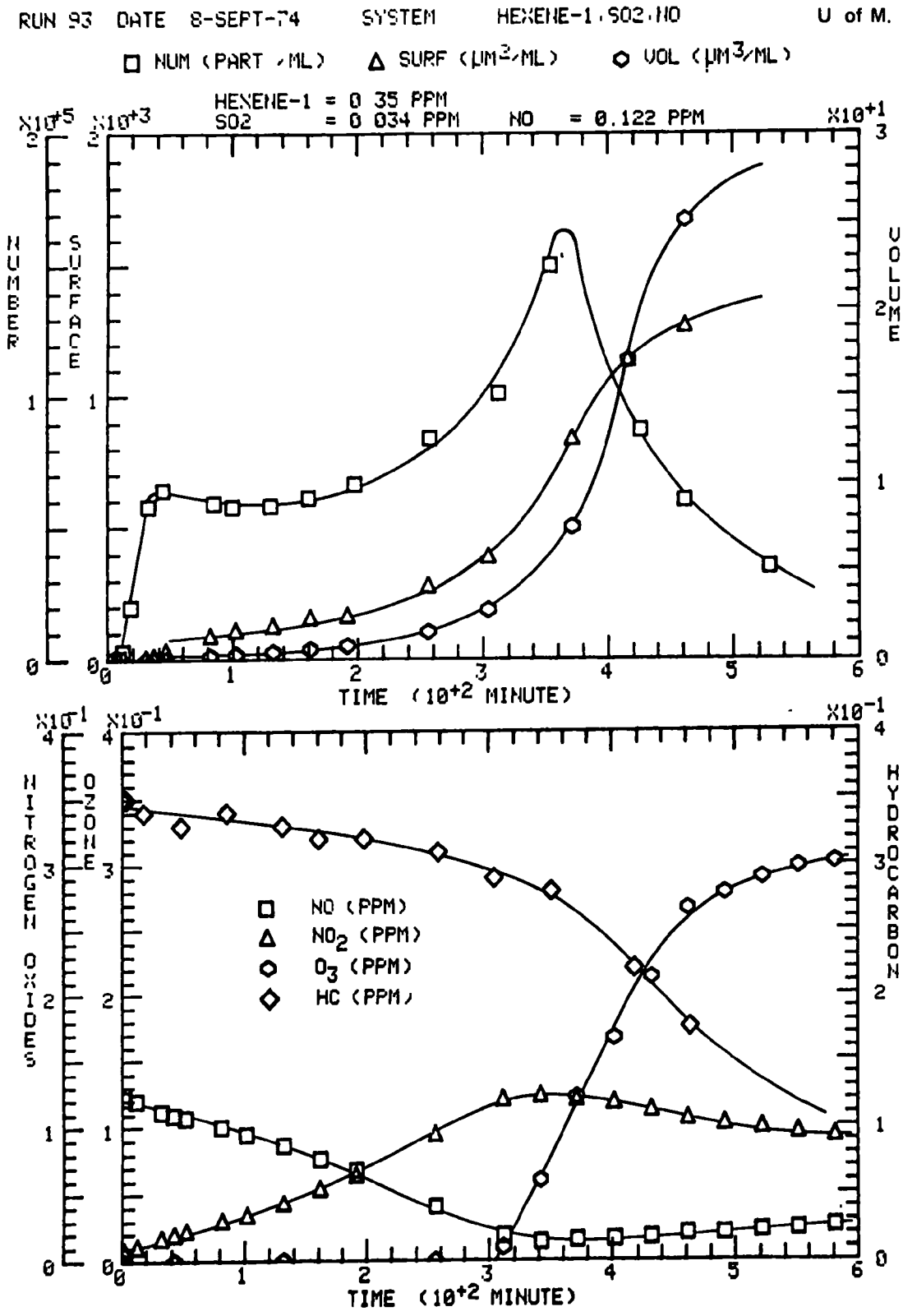
RUN 93 DATE 8-SEPT-74 SYSTEM HEXENE-1,SO2,NO U of M.
NUM (PART/ML) SURF (μM²/ML) VOL (μM³/ML)
HEXENE-1 = 0 35 PPM
SO2 = 0 034 PPM NO = 0.122 PPM
X10+5
X10+3
X10+1
NUMBER
SURFACE
VOLUME
TIME (10+2 MINUTE)
X10-1
X10-1
X10-1
NITROGEN OXIDES
OZONE
HYDROCARBON
NO (PPM)
NO2 (PPM)
O3 (PPM)
HC (PPM)
TIME (10+2 MINUTE)

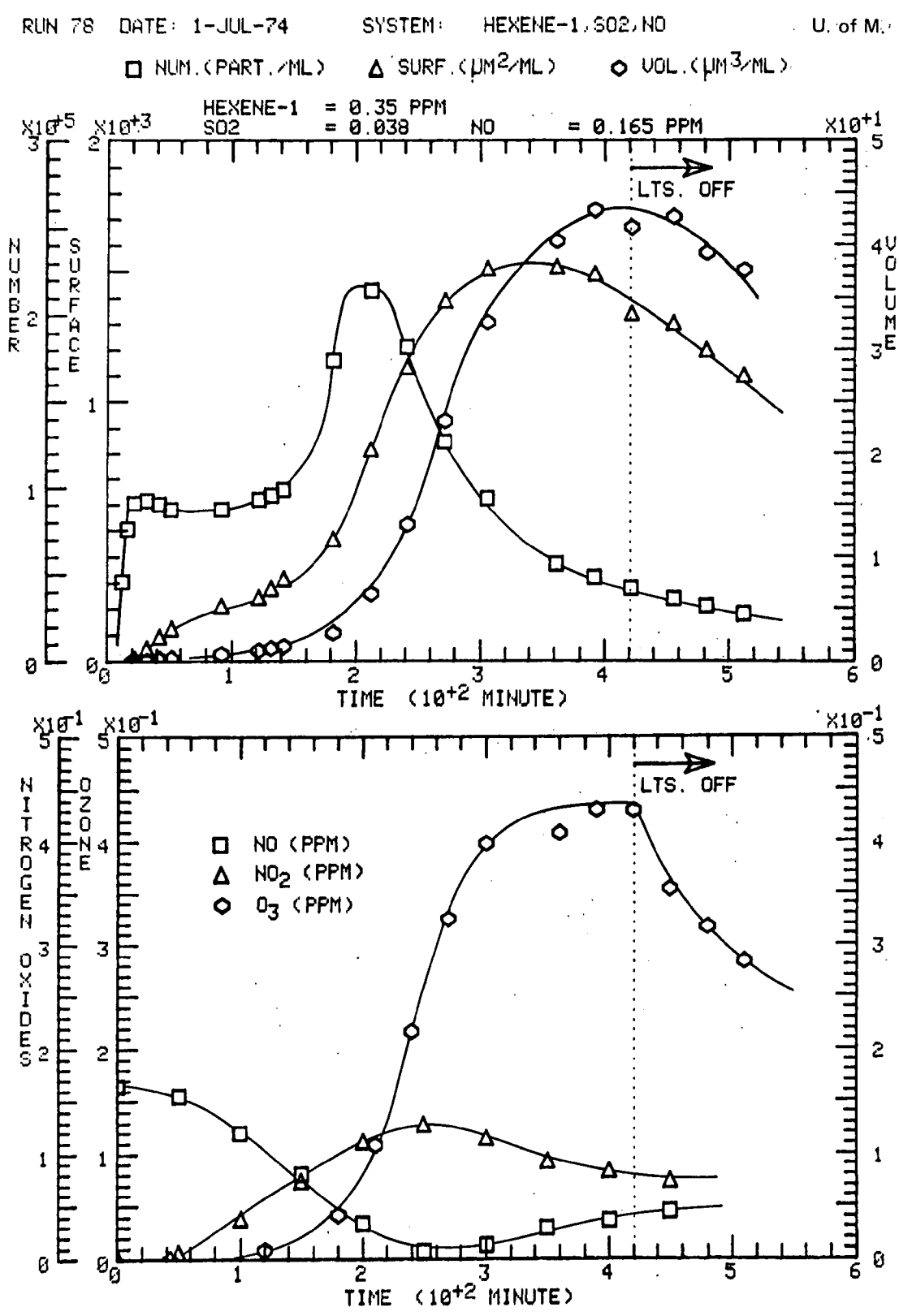
RUN 78 DATE: 1-JUL-74 SYSTEM: HEXENE-1/SO2/NO U. of M.
NUM.(PART./ML) SURF.(μM²/ML) VOL.(μM³/ML)
HEXENE-1 = 0.35 PPM
SO2 = 0.038 NO = 0.165 PPM
X10+5 X10+3 X10+1
NUMBER SURFACE VOLUME
LTS. OFF
TIME (10+2 MINUTE)
X10-1 X10-1 X10-1
NITROGEN OXIDES OZONE
NO (PPM)
NO2 (PPM)
O3 (PPM)
LTS. OFF
TIME (10+2 MINUTE)

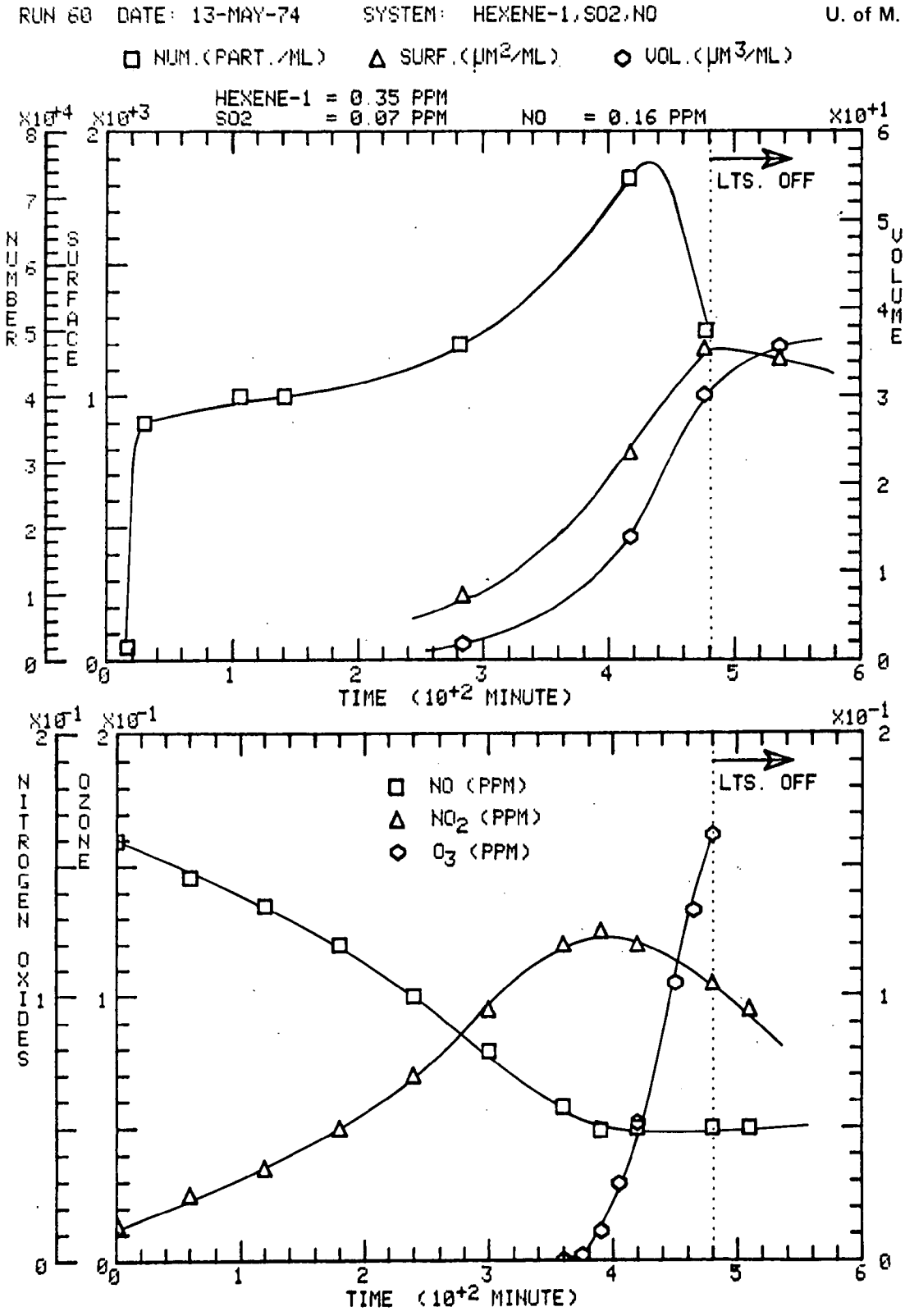
RUN 60 DATE: 13-MAY-74 SYSTEM: HEXENE-1,SO2,NO U. of M.
NUM.(PART./ML) SURF.(μM²/ML) VOL.(μM³/ML)
HEXENE-1 = 0.35 PPM
SO2 = 0.07 PPM
NO = 0.16 PPM
LTS. OFF
NUMBER
SURFACE
VOLUME
TIME (10+2 MINUTE)
NO (PPM)
NO2 (PPM)
O3 (PPM)
NITROGEN OXIDES
OZONE

CALSPAN
RUN NO. 20 MARCH 7, 1974 HEXENE-1-SO_2 SYSTEM HEXENE-1 = 0.33 ppm; SO_2 = 0.055 ppm RH = 40%

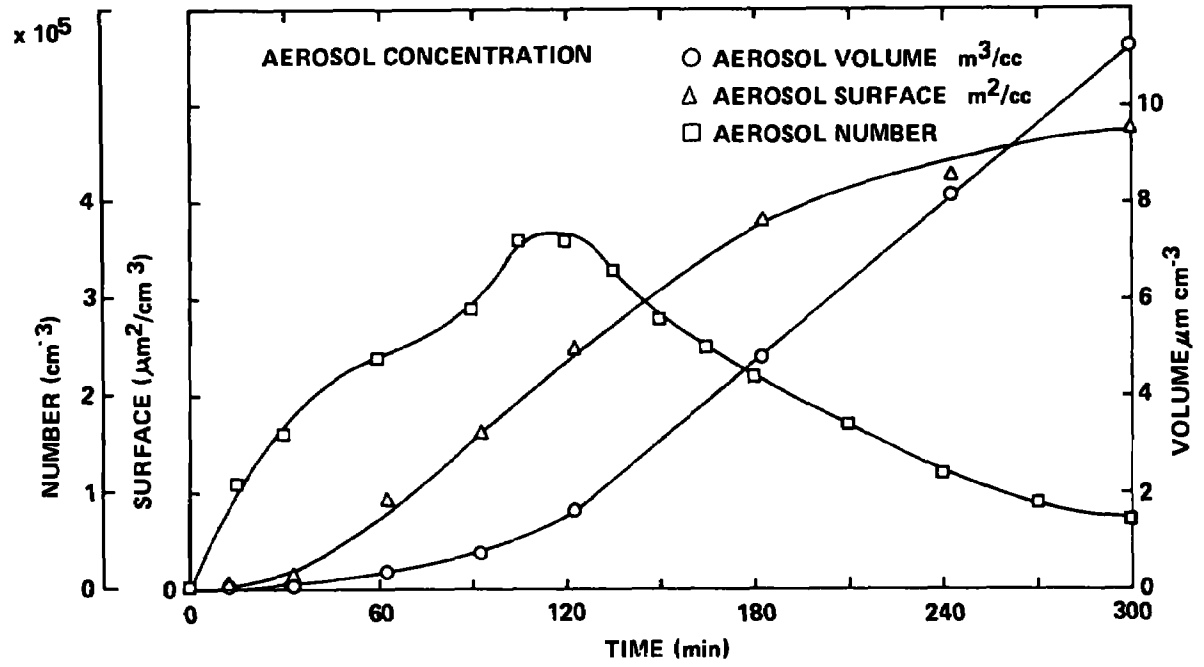

(4) M-XYLENE EXPERIMENTS

CALSPAN

RUN NO. 15 MARCH 4, 1974 **XYLENE-NO-FILTERED AIR SYSTEM**

m-XYLENE = 0.34 ppm; NO = 0.150 ppm; NO_2 = 0.014 ppm; RH = 38%

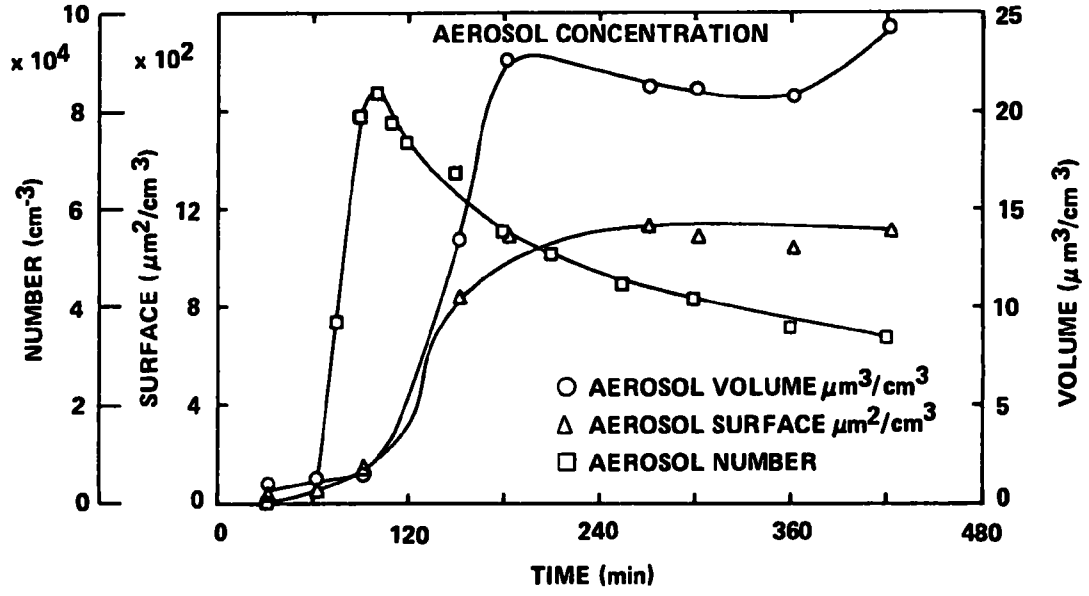

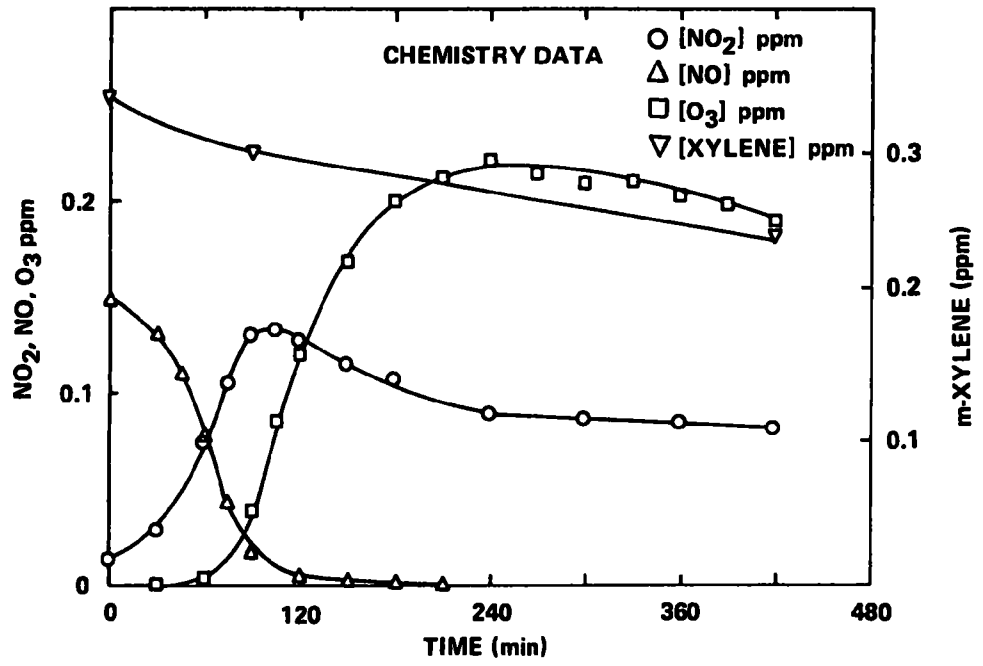

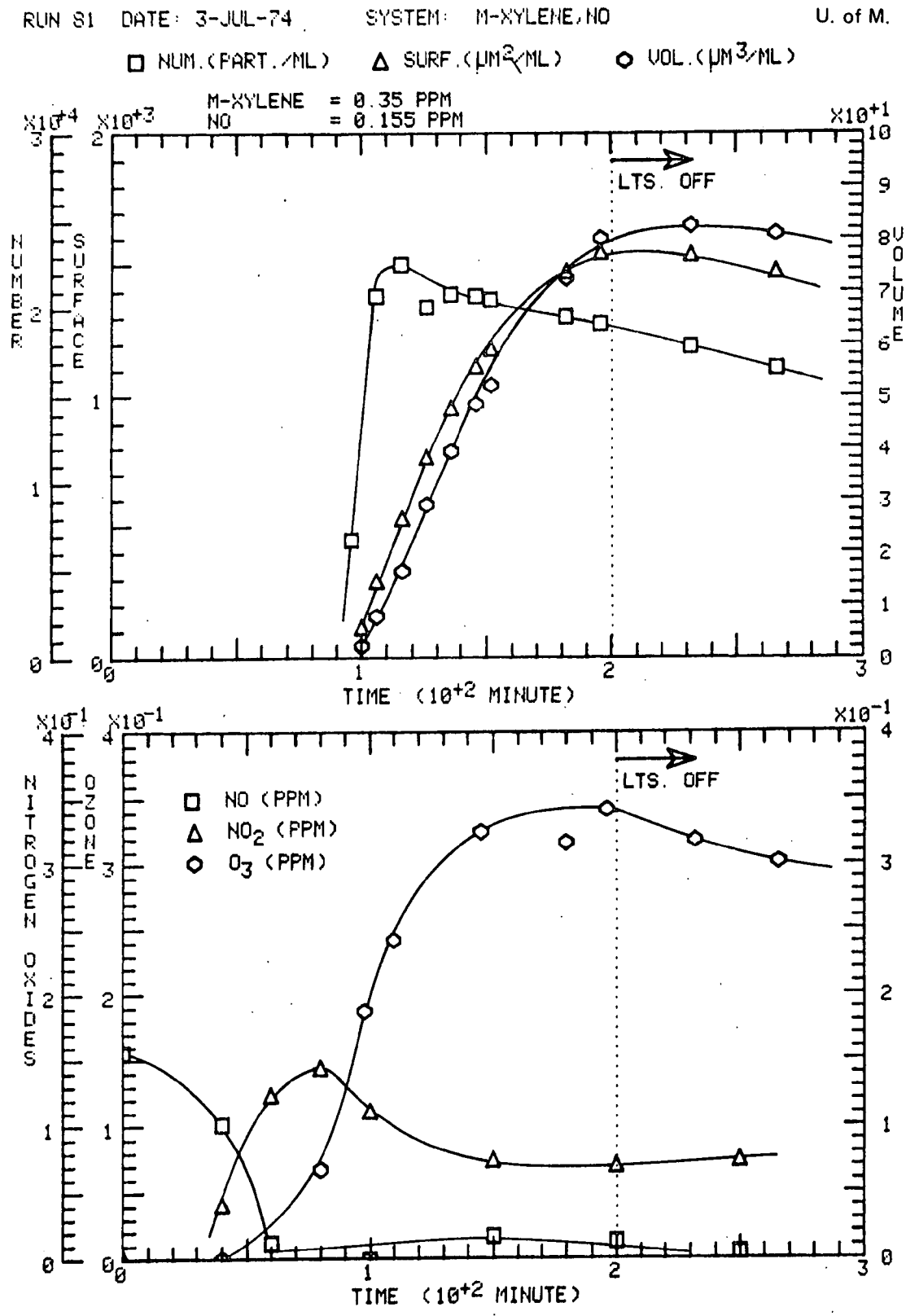
RUN S1 DATE: 3-JUL-74 SYSTEM: M-XYLENE/NO U. of M.
NUM.(PART./ML) SURF.(μM²/ML) VOL.(μM³/ML)
M-XYLENE = 0.35 PPM
NO = 0.155 PPM
X10+4
X10+3
X10+1
NUMBER
SURFACE
VOLUME
LTS. OFF
TIME (10+2 MINUTE)
X10-1
X10-1
X10-1
NITROGEN OXIDES
OZONE
NO (PPM)
NO2 (PPM)
O3 (PPM)
LTS. OFF
TIME (10+2 MINUTE)

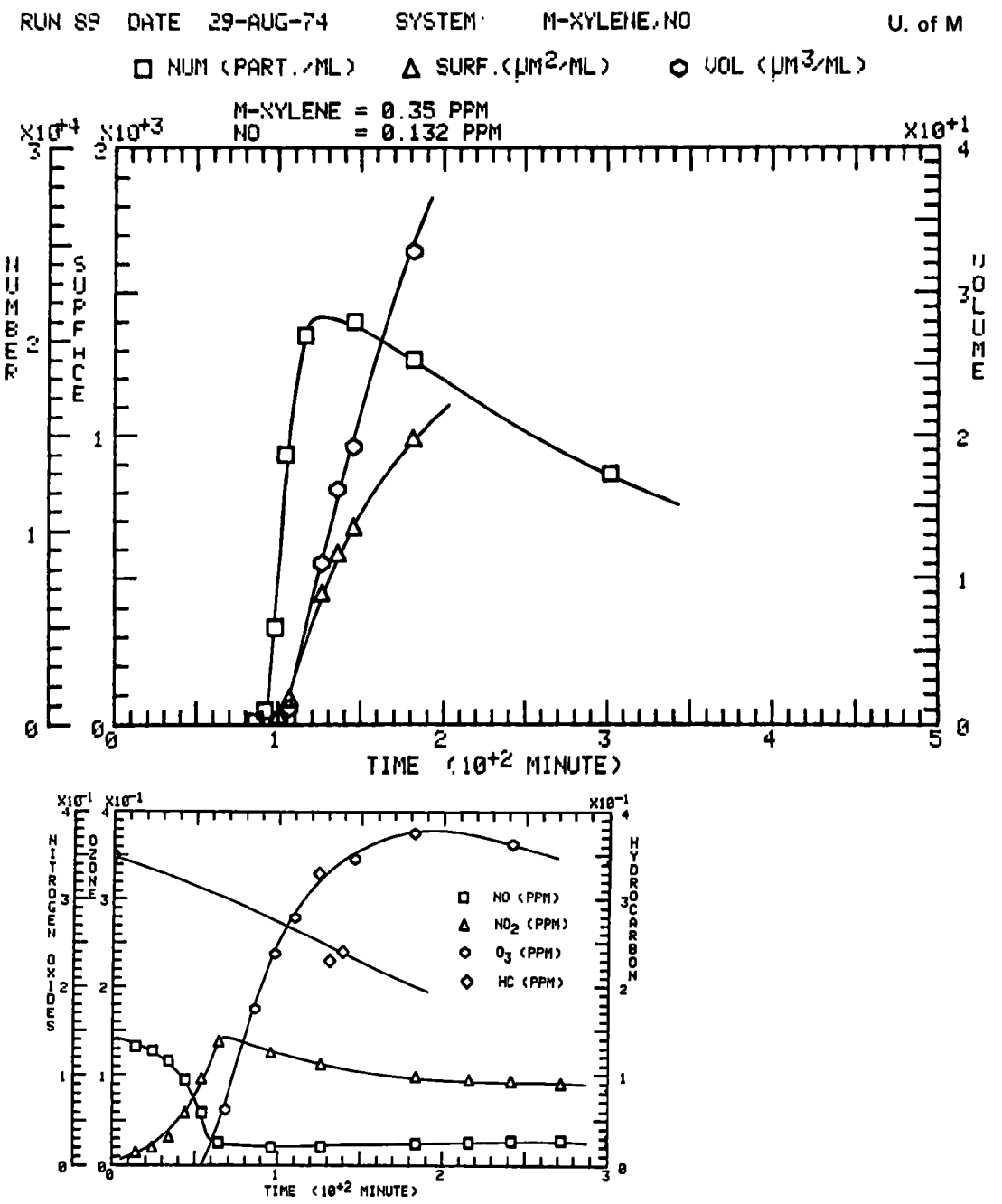
RUN 89 DATE 29-AUG-74 SYSTEM: M-XYLENE/NO U. of M
NUM (PART./ML) SURF.(μM²/ML) VOL (μM³/ML)
M-XYLENE = 0.35 PPM
NO = 0.132 PPM
NUMBER
SURFACE
VOLUME
TIME (10+2 MINUTE)
NITROGEN OXIDES
OZONE
HYDROCARBON
NO (PPM)
NO2 (PPM)
O3 (PPM)
HC (PPM)
TIME (10+2 MINUTE)

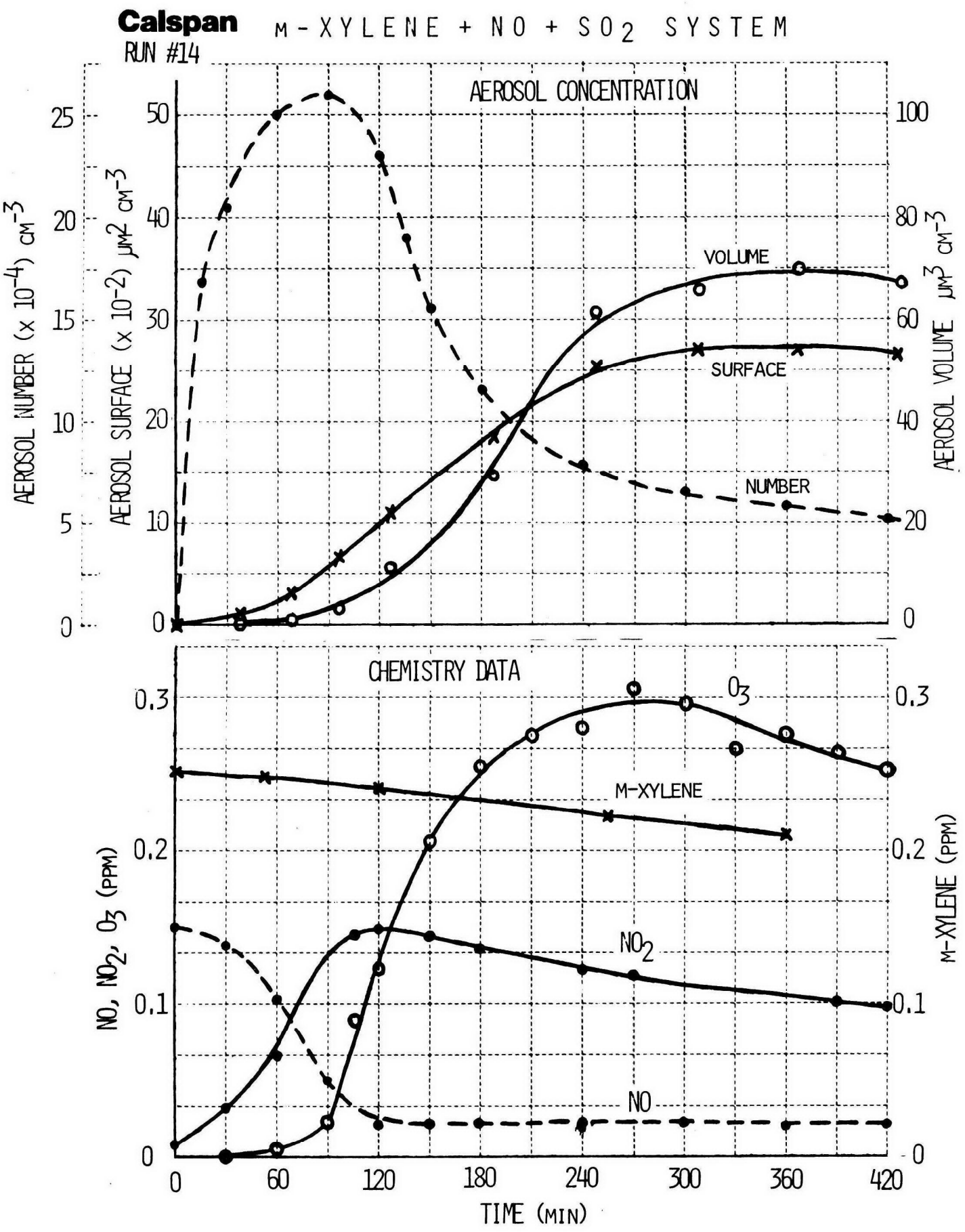
Calspan
M-XYLENE + NO + SO2 SYSTEM
RUN #14
AEROSOL CONCENTRATION
AEROSOL NUMBER (x 10-4) cm-3
AEROSOL SURFACE (x 10-2) µm2 cm-3
AEROSOL VOLUME µm3 cm-3
VOLUME
SURFACE
NUMBER
CHEMISTRY DATA
O3
M-XYLENE
NO2
NO
NO, NO2, O3 (PPM)
M-XYLENE (PPM)
TIME (MIN)

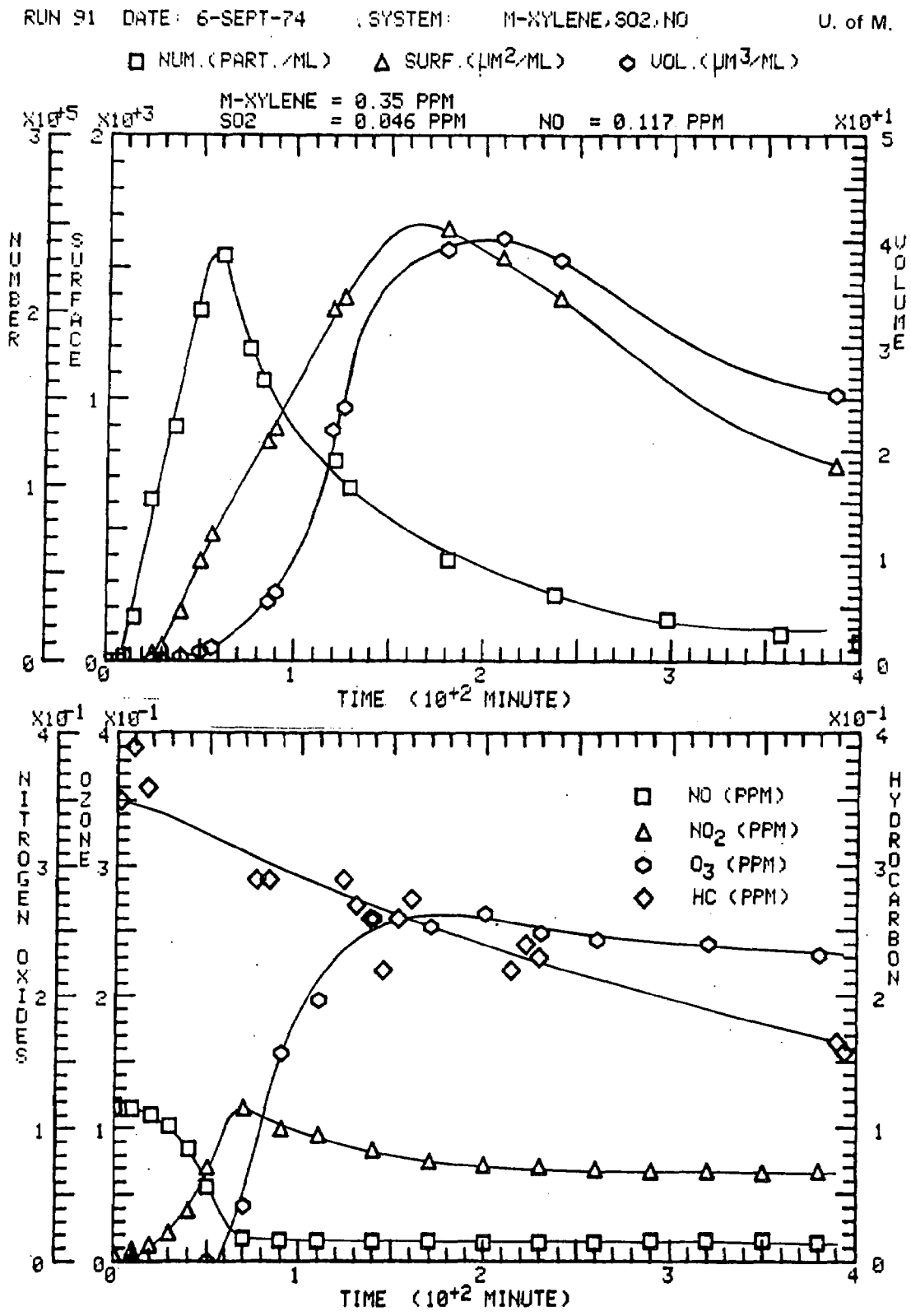
RUN 91 DATE: 6-SEPT-74 SYSTEM: M-XYLENE, SO2, NO U. of M.
□ NUM. (PART./ML) △ SURF. (μM²/ML) ◇ VOL. (μM³/ML)
M-XYLENE = 0.35 PPM
SO2 = 0.046 PPM NO = 0.117 PPM
X10+5
X10+3
X10+1
NUMBER
SURFACE
VOLUME
TIME (10+2 MINUTE)
X10-1
NITROGEN OXIDES
OZONE
HYDROCARBON
□ NO (PPM)
△ NO2 (PPM)
◇ O3 (PPM)
◇ HC (PPM)
TIME (10+2 MINUTE)

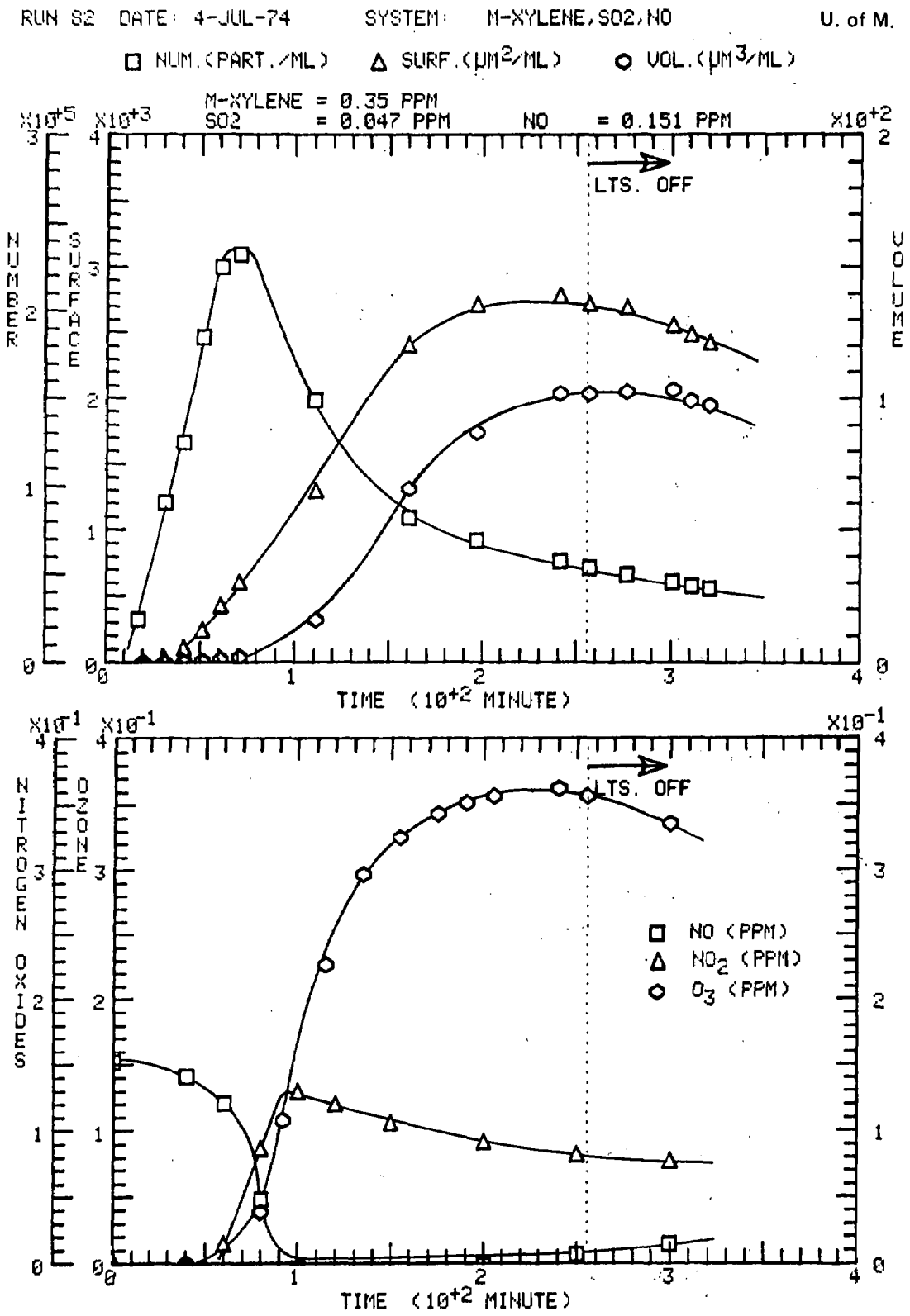
RUN S2 DATE: 4-JUL-74 SYSTEM: M-XYLENE, SO2, NO U. of M.
NUM. (PART./ML) SURF. (μM²/ML) VOL. (μM³/ML)
M-XYLENE = 0.35 PPM
SO2 = 0.047 PPM
NO = 0.151 PPM
LTS. OFF
NUMBER
SURFACE
VOLUME
TIME (10+2 MINUTE)
NITROGEN OXIDES
OZONE
NO (PPM)
NO2 (PPM)
O3 (PPM)

CALSPAN

RUN NO. 17 MARCH 5, 1974 XYLENE-SO_2 SYSTEM XYLENE = 0.34 ppm; SO_2 = 0.07 ppm; RH = 41%

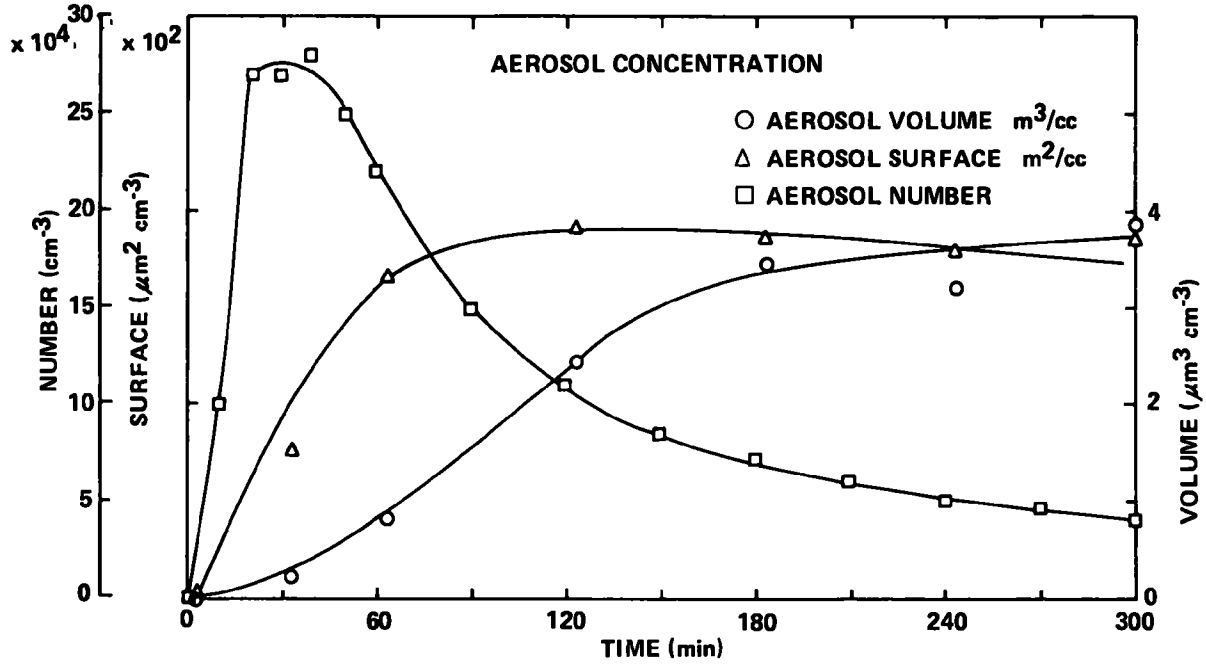

(5) CYCLOHEXENE EXPERIMENTS

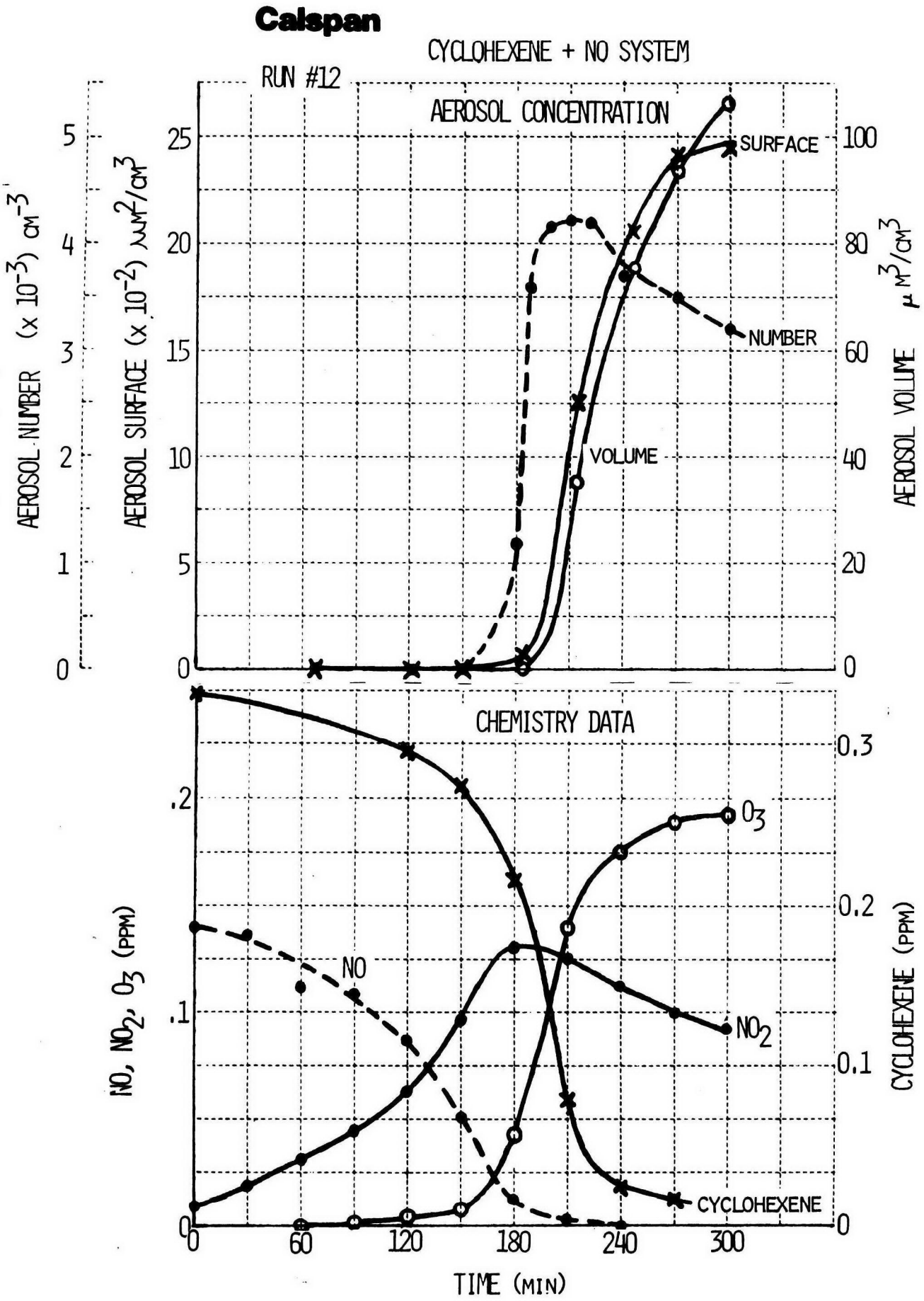
Calspan
CYCLOHEXENE + NO SYSTEM
RUN #12
AEROSOL CONCENTRATION
AEROSOL NUMBER (x 10⁻³) cm⁻³
AEROSOL SURFACE (x 10⁻²) μm²/cm³
AEROSOL VOLUME μm³/cm³
SURFACE
NUMBER
VOLUME
CHEMISTRY DATA
NO, NO₂, O₃ (PPM)
CYCLOHEXENE (PPM)
O₃
NO
NO₂
CYCLOHEXENE
TIME (MIN)

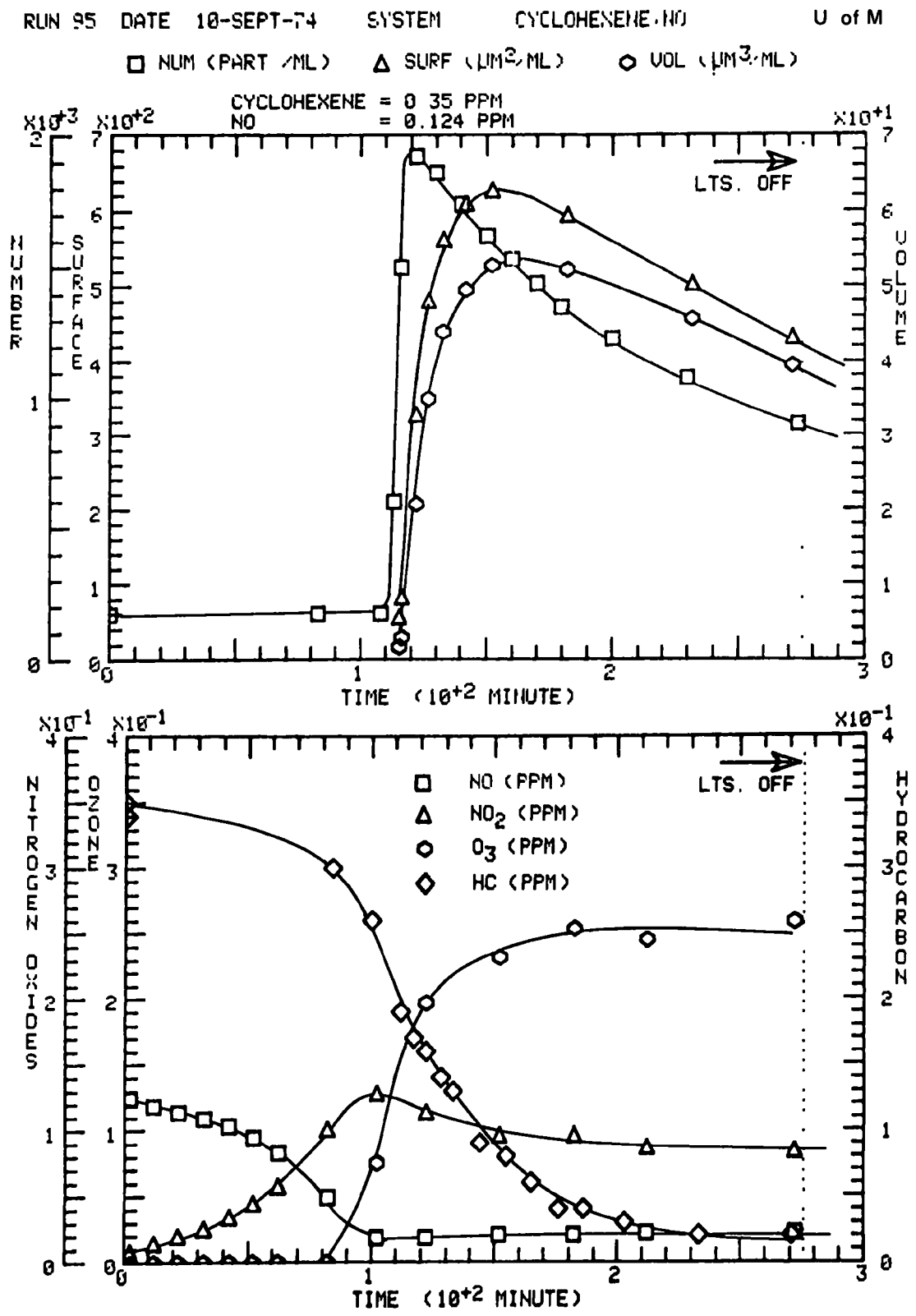
RUN 95 DATE 10-SEPT-74 SYSTEM CYCLOHEXENE-NO U of M
NUM (PART /ML)
SURF (μM²/ML)
VOL (μM³/ML)
CYCLOHEXENE = 0 35 PPM
NO = 0.124 PPM
LTS. OFF
NUMBER
SURFACE
VOLUME
TIME (10+2 MINUTE)
NO (PPM)
NO2 (PPM)
O3 (PPM)
HC (PPM)
NITROGEN OXIDES
OZONE
HYDROCARBON

CALSPAN

RUN NO. 10 28 FEBRUARY 1974 CYCLOHEXENE-NO-FILTERED AIR SYSTEM R.H. = 38%;
CYCLOHEXENE = 0.33 ppm; NO = 0.138 ppm; NO_2 = 0.026 ppm
NO STIRRING

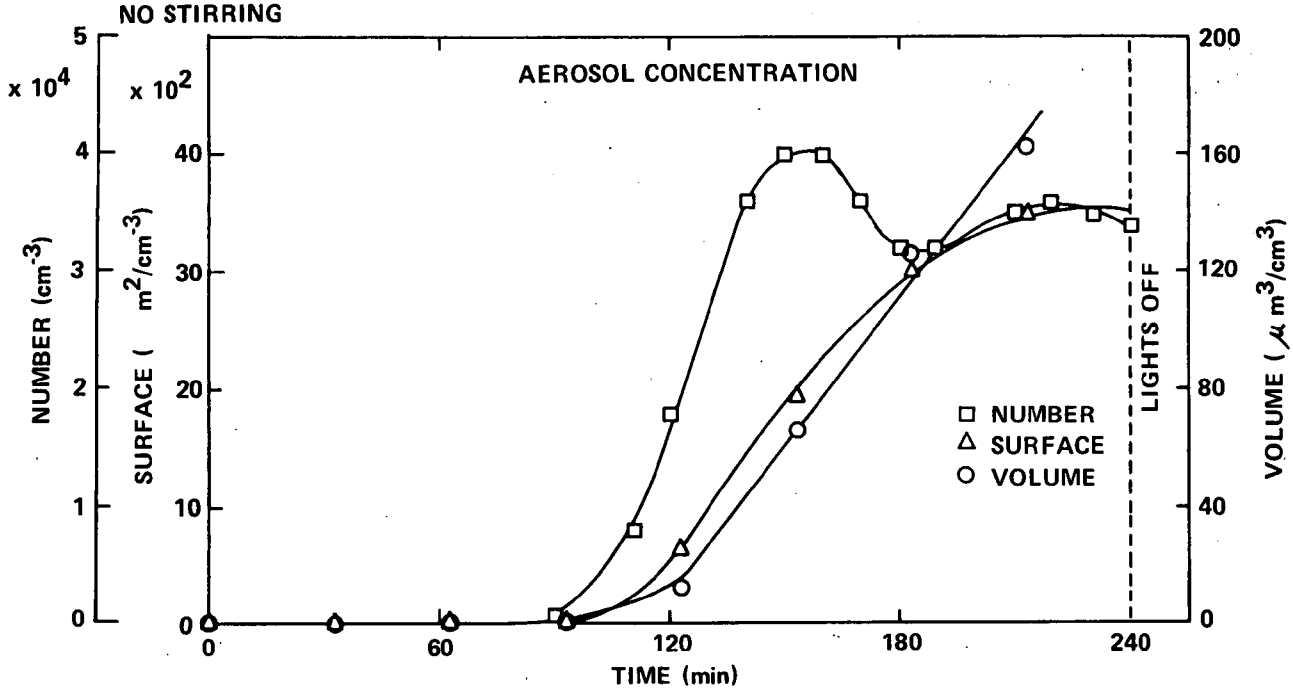

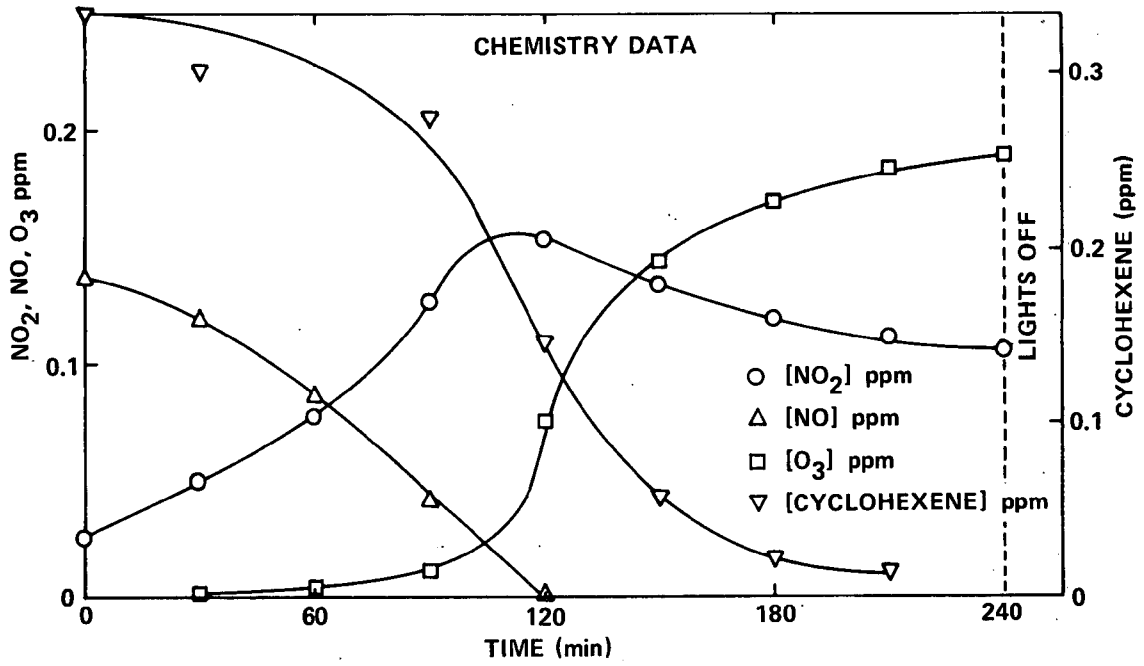

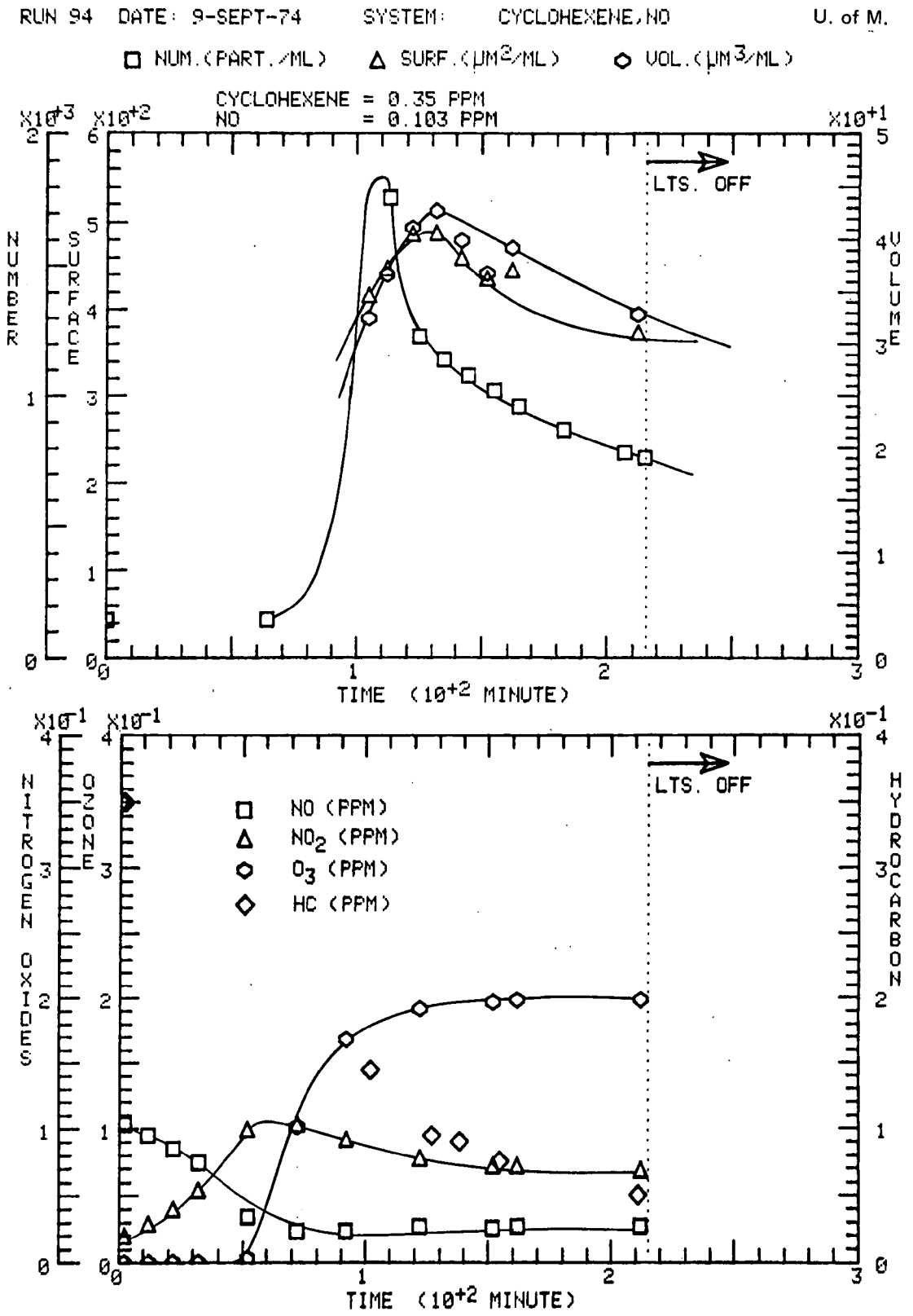
RUN 94 DATE: 9-SEPT-74 SYSTEM: CYCLOHEXENE/NO U. of M.
□ NUM.(PART./ML) △ SURF.(μM²/ML) ◇ VOL.(μM³/ML)
CYCLOHEXENE = 0.35 PPM
NO = 0.103 PPM
X10+3
X10+2
X10+1
NUMBER
SURFACE
VOLUME
LTS. OFF
TIME (10+2 MINUTE)
X10-1
NITROGEN OXIDES
OZONE
HYDROCARBON
□ NO (PPM)
△ NO2 (PPM)
◇ O3 (PPM)
◇ HC (PPM)
LTS. OFF
TIME (10+2 MINUTE)

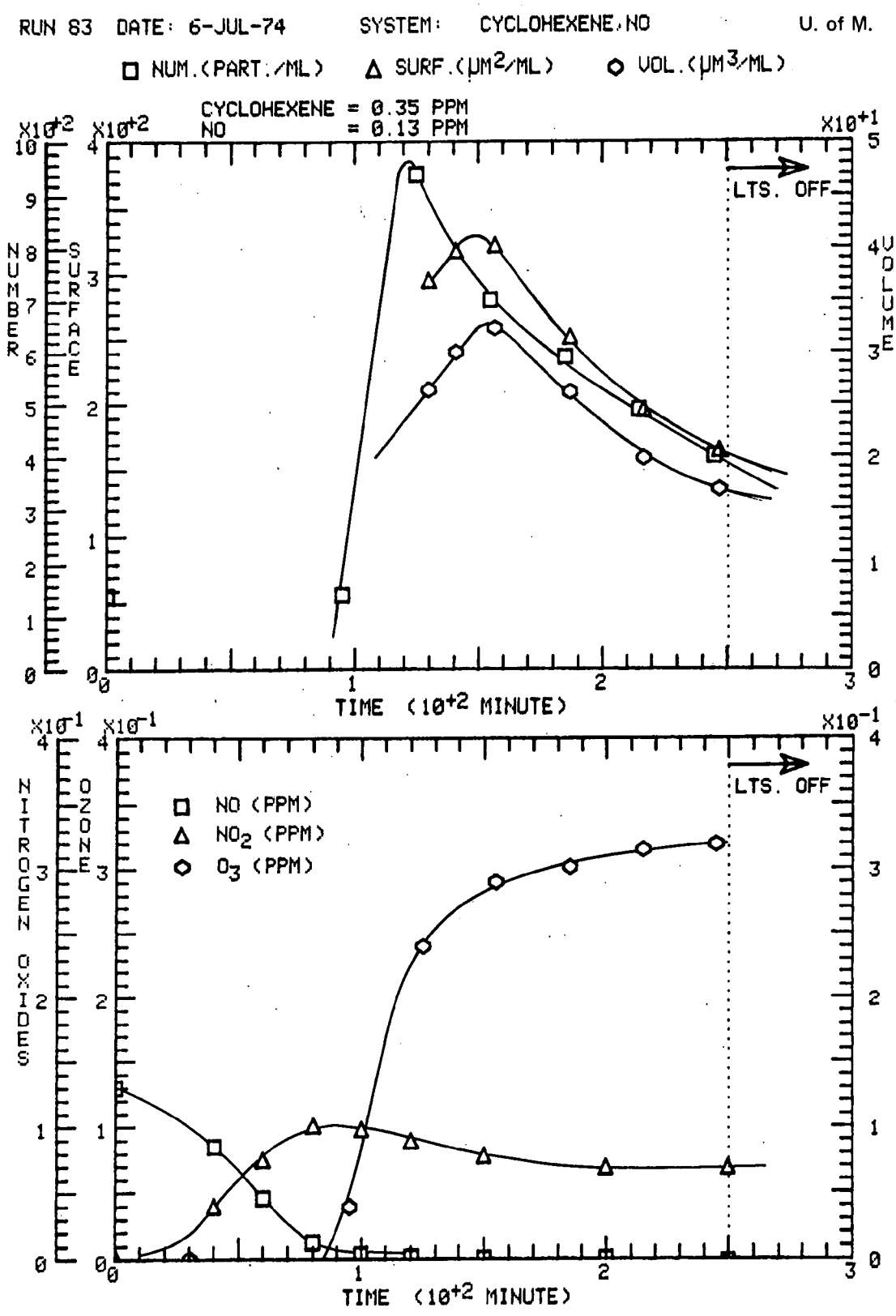
RUN 83 DATE: 6-JUL-74 SYSTEM: CYCLOHEXENE-NO U. of M.
□ NUM.(PART./ML) △ SURF.(μM²/ML) ◇ VOL.(μM³/ML)
CYCLOHEXENE = 0.35 PPM
NO = 0.13 PPM
X10+2
X10+2
X10+1
NUMBER
SURFACE
VOLUME
LTS. OFF
TIME (10+2 MINUTE)
X10-1
X10-1
X10-1
NITROGEN OXIDES
OZONE
□ NO (PPM)
△ NO2 (PPM)
◇ O3 (PPM)
LTS. OFF
TIME (10+2 MINUTE)

CALSPAN

RUN NO. 9 27 FEBRUARY 1974 CYCLOHEXENE-NO-SO_2-FILTERED AIR SYSTEM R.H. = 36%;

CYCLOHEXENE = 0.33 ppm; NO = 0.220 ppm; NO_2 = 0.020 ppm; SO_2 = 0.05 ppm

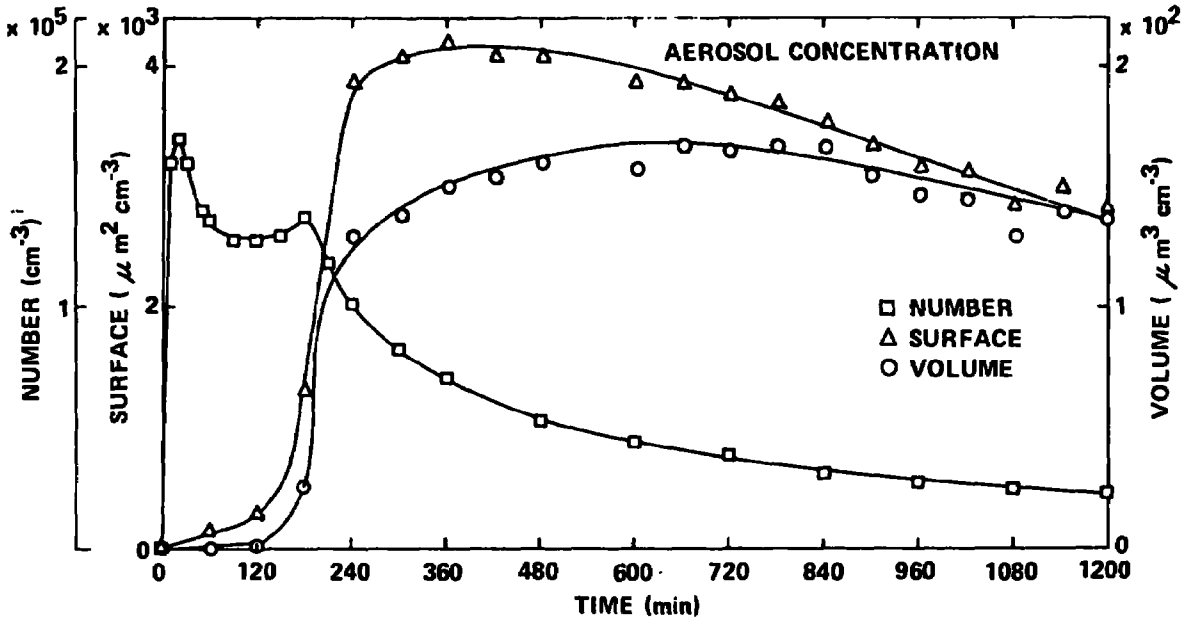

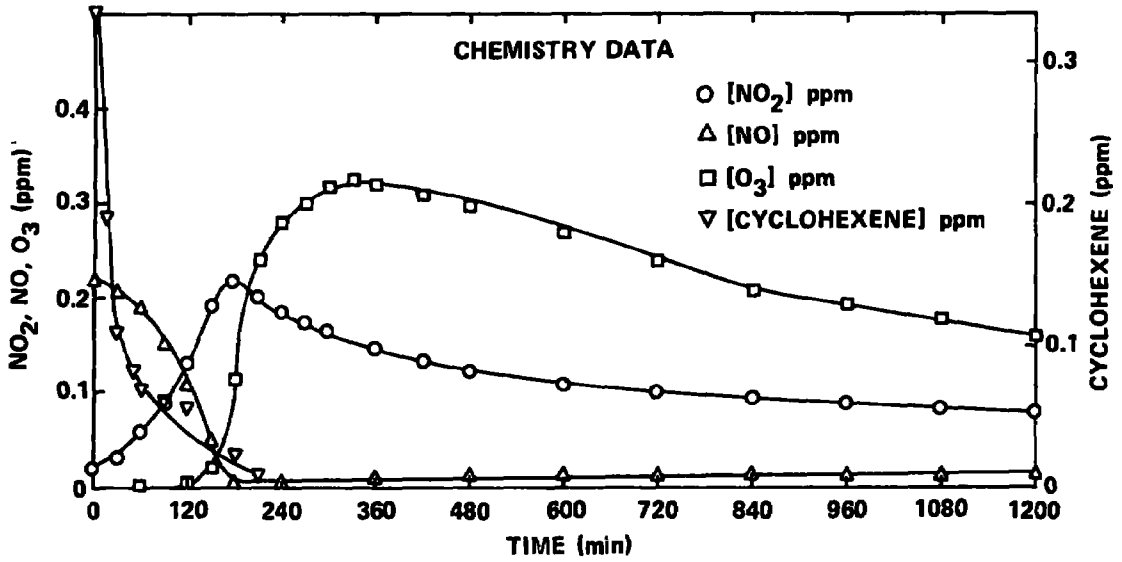

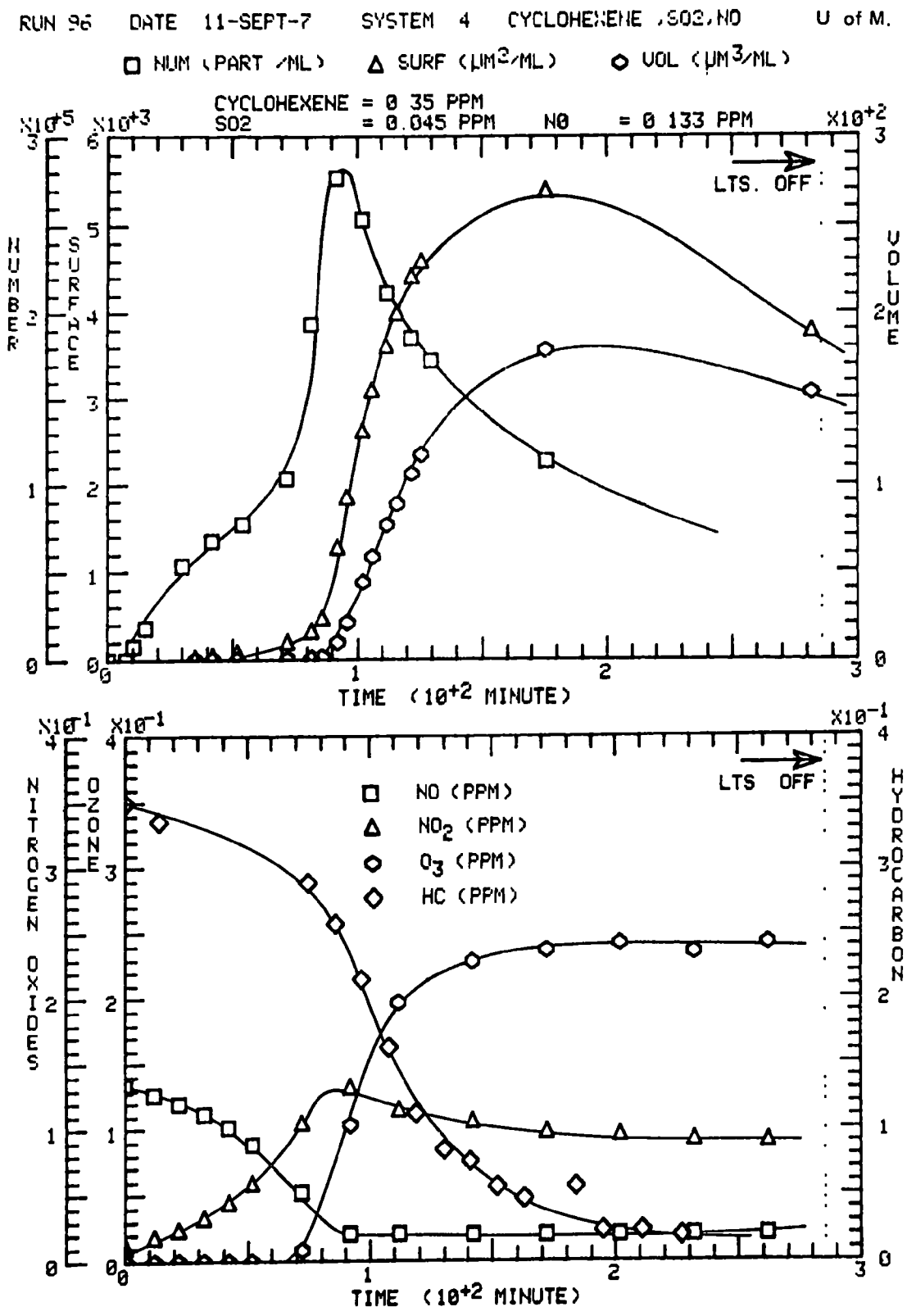
RUN 96 DATE 11-SEPT-7 SYSTEM 4 CYCLOHEXENE /SO2/NO U of M.
NUM (PART /ML) SURF (μM²/ML) VOL (μM³/ML)
CYCLOHEXENE = 0 35 PPM
SO2 = 0.045 PPM NO = 0 133 PPM
X10+5
X10+3
X10+2
NUMBER
SURFACE
VOLUME
LTS. OFF
TIME (10+2 MINUTE)
X10-1
X10-1
X10-1
NITROGEN OXIDES
OZONE
HYDROCARBON
NO (PPM)
NO2 (PPM)
O3 (PPM)
HC (PPM)
LTS OFF
TIME (10+2 MINUTE)

CALSPAN

RUN NO. 13; MARCH 2, 1974 CYCLOHEXENE-SO_2-FILTERED AIR SYSTEM RH = 35%

CYCLOHEXENE = 0.33 ppm; NO = 0.012; NO_2 = 0.003 ppm; SO_2 = 0.06 ppm

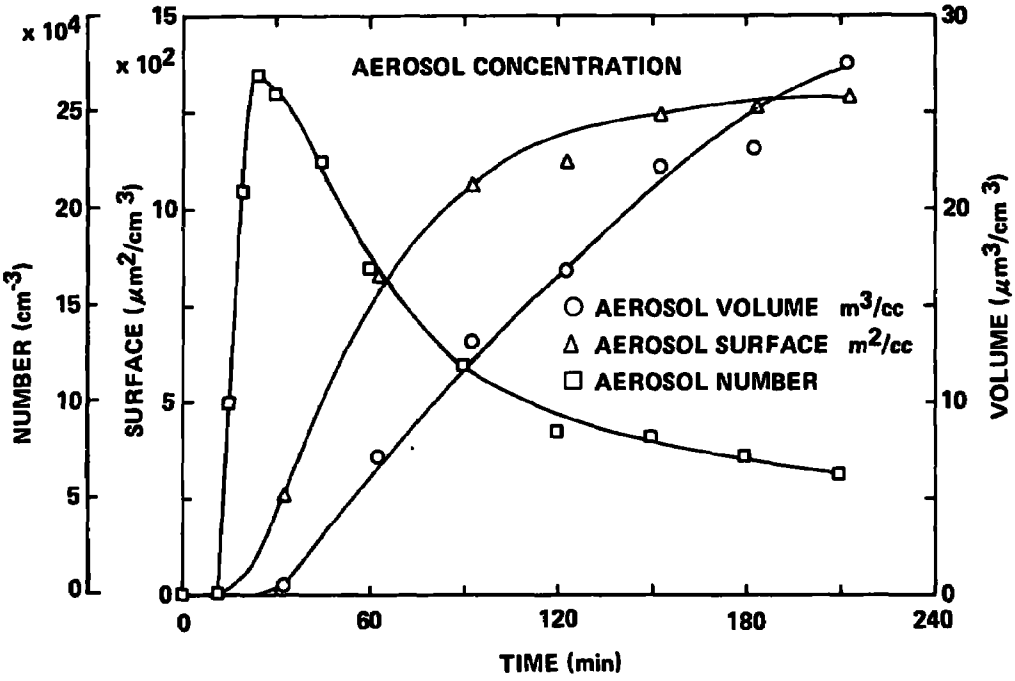

NaCl EXPERIMENTS

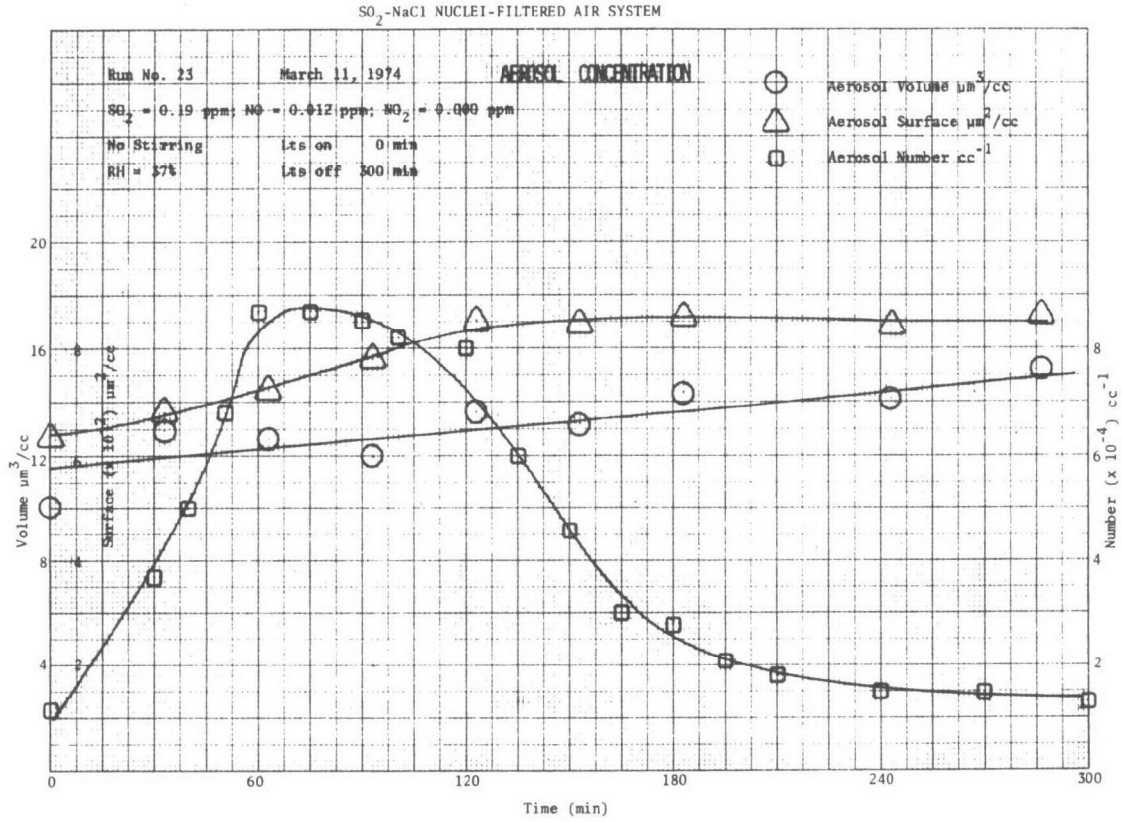
SO_2-NaCl NUCLEI-FILTERED AIR SYSTEM
Run No. 23 March 11, 1974 AEROSOL CONCENTRATION
SO_2 = 0.19 ppm; NO = 0.012 ppm; NO_2 = 0.000 ppm
No Stirring Lts on 0 min
RH = 57% Lts off 300 min
Aerosol Volume $\mu m^3/cc$
Aerosol Surface $\mu m^2/cc$
Aerosol Number cc^{-1}
Volume $\mu m^3/cc$
Surface ($\times 10^{-2}$) $\mu m^2/cc$
Number ($\times 10^{-4}$) cc^{-1}
Time (min)

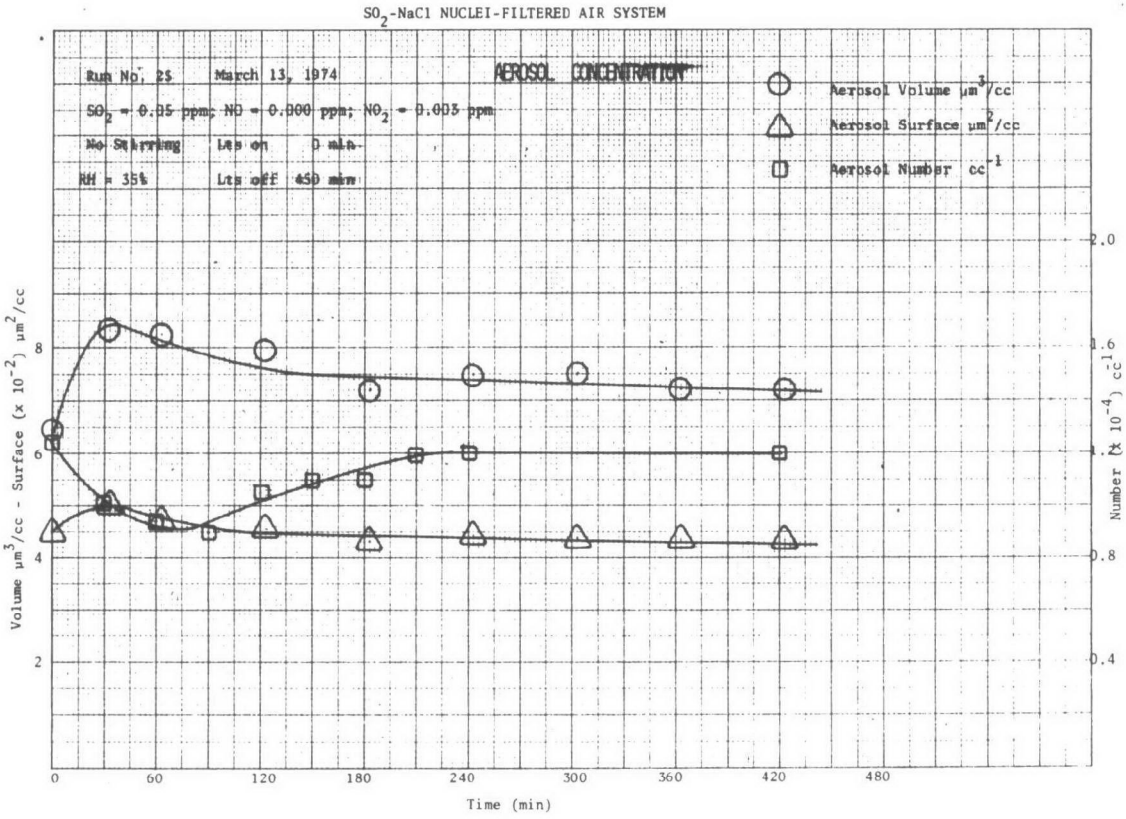
SO_2-NaCl NUCLEI-FILTERED AIR SYSTEM
Run No. 25 March 13, 1974 AEROSOL CONCENTRATION
SO_2 = 0.05 ppm; NO = 0.000 ppm; NO_2 = 0.003 ppm
No Stirring Lts on 0 min
RH = 35% Lts off 450 min
Aerosol Volume $\mu m^3/cc$
Aerosol Surface $\mu m^2/cc$
Aerosol Number cc^{-1}
Volume $\mu m^3/cc$ - Surface ($\times 10^{-2}$) $\mu m^2/cc$
Number ($\times 10^{-4}$) cc^{-1}
Time (min)

XYLENE-NO-SO_2-NaCl NUCLEI-FILTERED AIR SYSTEM

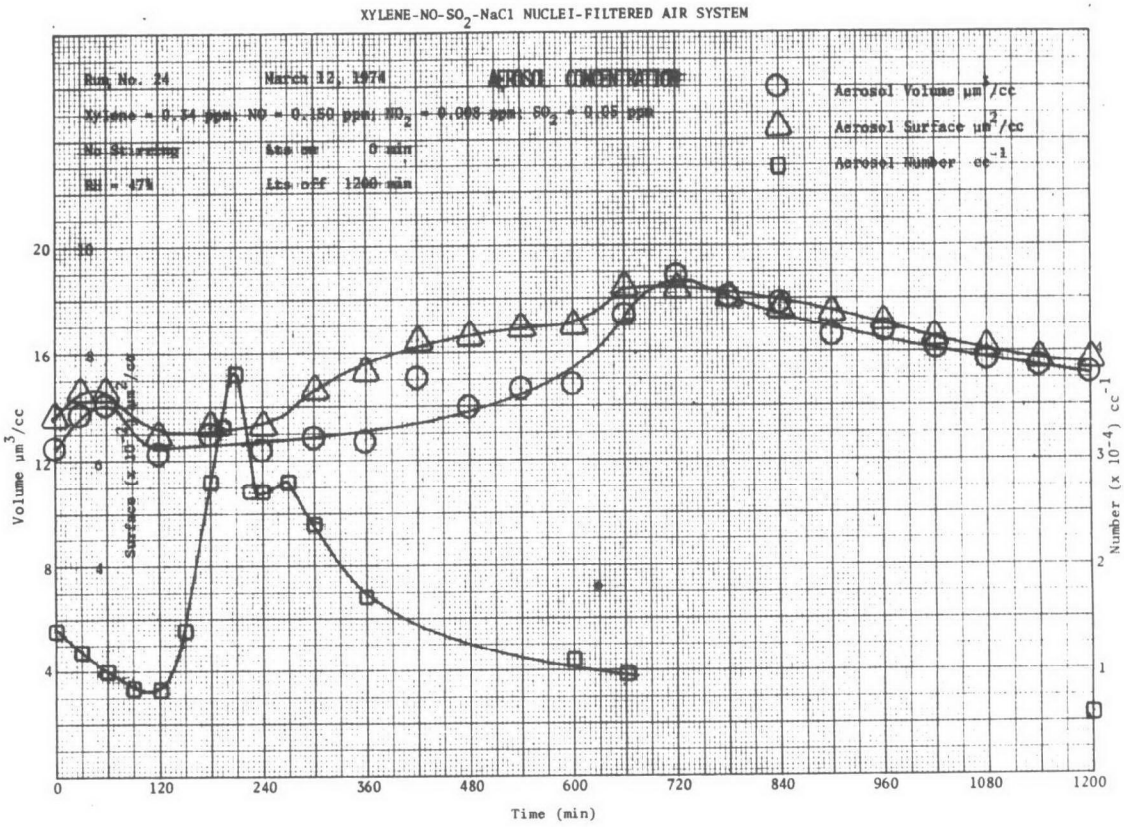

XYLENE-NO-SO_2-NaCl NUCLEI IN FILTERED AIR.

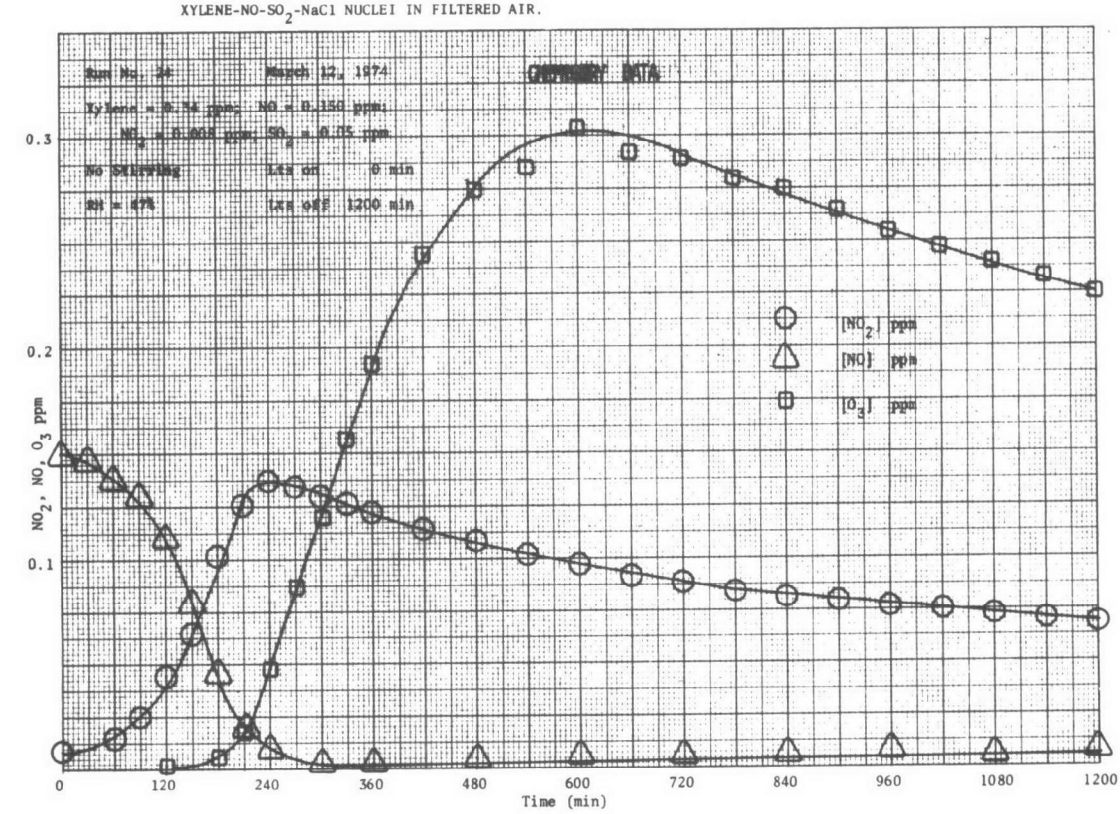

CYCLOHEXENE-NO-SO_2-NaCl NUCLEI-FILTERED AIR SYSTEM

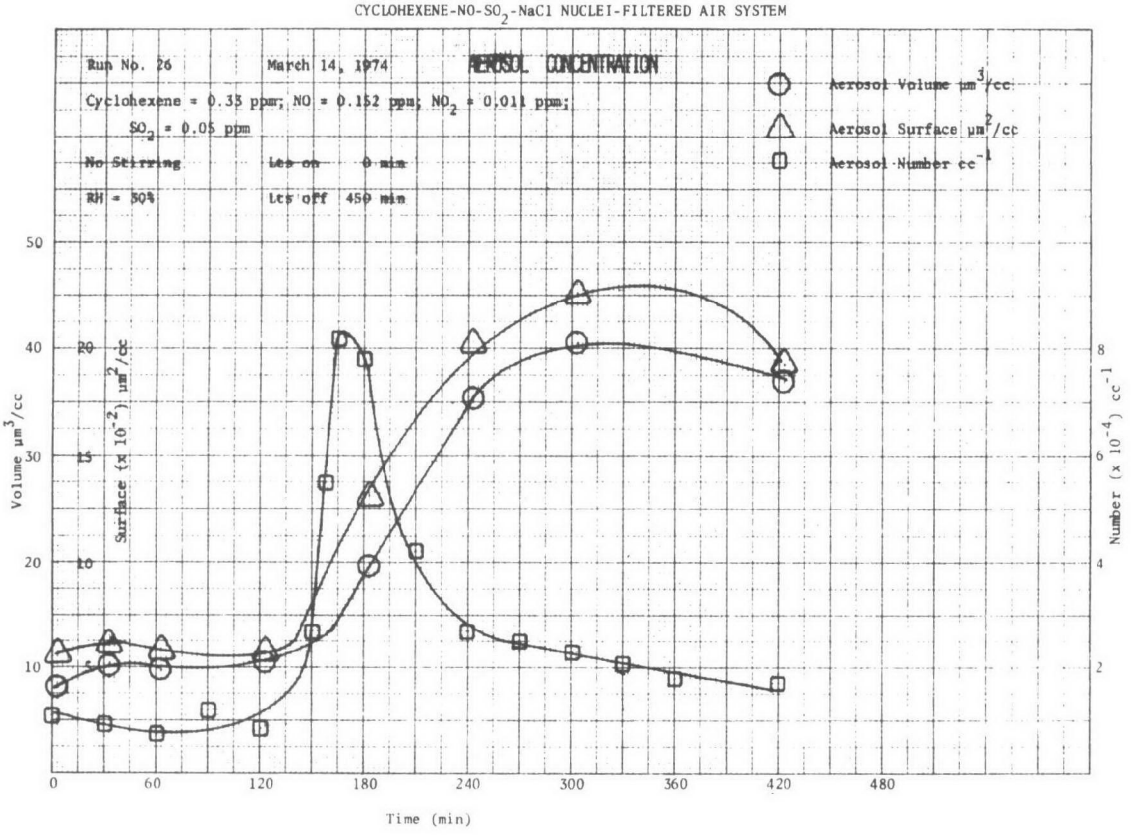

CYCLOHEXENE-NO-SO_2-NaCl NUCLEI IN FILTERED AIR